Integrated Signalling Models: An Interplay between Netrin-1, Cadherins, and Proteoglycans

Stephanie Nicole Harris

Integrated Program in Neuroscience

Montreal Neurological Institute

Faculty of Medicine

McGill University

Montreal, Quebec, Canada

December 2019

A thesis submitted to McGill University in

partial fulfillment of the requirements of the degree of

Doctor of Philosophy in Neuroscience

Abstract

Netrin-1 is a well characterized axon guidance molecule widely expressed in the developing and adult central nervous system (CNS). Along with its receptor deleted in colorectal cancer (DCC), netrin-1 has been extensively studied for its role in commissural axon guidance and, more recently, synaptic plasticity. While the interaction between netrin-1 and DCC is well understood, how these molecules interact with other proteins and signalling pathways in neurons and with the extracellular matrix (ECM) remains largely unknown. In this thesis we explore the interplay between the netrin-1/DCC axon guidance pathway, the cadherin cell adhesion pathway, and proteoglycans in the ECM both during development and in the adult nervous system.

This thesis examines an interaction between the netrin-1/DCC signalling complex and the cadherin/catenin cell adhesion complex. We report that DCC and cadherin 12 (CDH12) interact in the developing spinal cord and that this interaction influences commissural axon growth. We also show that netrin-1 signalling leads to the phosphorylation of β-catenin at two separate residues, S675 and Y142, which influences cytoskeletal dynamics and filopodia formation at the leading edge of the growth cone. This interaction between DCC and CDH12 persists in the postnatal brain where netrin-1 mediates distribution and co-localization of these two proteins within the plasma membrane. We also investigate an interaction between netrin-1 and proteoglycans in the ECM. We identify a previously unknown function for the netrin-1 C-domain in glycosaminoglycan (GAG) binding and show that interactions between netrin-1 and GAG chains influences commissural axon growth. Further, we show that netrin-1 binding to GAGs can alter the physical properties of GAG films and that netrin-1 localizes to perineuronal nets (PNNs) in the adult brain. We demonstrate that netrin-1 binds PNN GAGs and we speculate that this contributes to synaptic plasticity. The results presented in this thesis provide new insight into how molecular signalling pathways integrate with one another to regulate complex neuronal

processes and we suggest new models for how they contribute to commissural axon guidance and synapse function.

Résumé

La netrin-1 est une molécule bien caractérisée, impliquée dans le guidage axonal et largement exprimée dans le système nerveux central (CNS) en développement et adulte. Tout comme son récepteur deleted in colorectal cancer (DCC), la netrin-1 a été largement étudiée dans le cadre de son rôle dans le guidage des axones commissuraux et, plus récemment, dans la plasticité synaptique. Bien que l'interaction entre la netrin-1 et DCC soit bien comprise, leurs interactions avec d'autres protéines et voies de signalisation neuronales ainsi qu'avec la matrice extracellulaire (MEC) restent largement inconnus. Cette thèse examine l'interaction entre la voie de guidage axonale netrin-1/DCC, la voie d'adhésion cellulaire dépendant des cadherines et les protéoglycans de la MEC, à la fois durant le développement et dans le système nerveux adulte.

Cette thèse examine une interaction entre le complexe de signalisation netrin-1/DCC et le complexe d'adhésion cellulaire cadherin/catenin. Nous rapportons ici que DCC et la cadherin 12 (CDH12) interagissent dans le développement de la moelle épinière et que cette interaction influence la croissance des axones commissuraux. Nous montrons également que la signalisation de la netrin-1 conduit à la phosphorylation de la β-catenin à deux résidus distincts, S675 et Y142, qui influence la dynamique du cytosquelette et la formation de filopodes au front des cônes de croissance. L'interaction entre DCC et le CDH12 persiste dans le cerveau postnatal où la netrin-1 assure la distribution et la co-localisation de ces deux protéines au sein de la membrane plasmique. Nous étudions également ici une interaction entre la netrin-1 et les protéoglycans de la MEC. Nous identifions une fonction jusque-là inconnue pour le domaine C de la netrin-1 dans la liaison du glycosaminoglycane (GAG) et montrons que les interactions entre la netrin-1 et les

chaînes du GAG influencent la croissance des axones commissuraux. De plus, nous montrons que la liaison de la netrin-1 aux GAG peut altérer les propriétés physiques des couches de GAG et que la netrin-1 se localise dans les maillages périneuronaux (PNN) dans le cerveau adulte. Nous démontrons que la netrin-1 se lie aux GAG PNN et nous supposons que cela contribue à la plasticité synaptique. Les résultats présentés dans cette thèse fournissent un nouvel aperçu de la façon dont les voies de signalisation moléculaire s'intègrent les unes aux autres pour réguler les processus neuronaux complexes et nous suggérons de nouveaux modèles expliquant la façon dont ils contribuent au guidage des axones commissuraux et à la fonction des synapses.

Table of Contents

Abstract……..…..**2**

Résumé……**3**

Table of Contents……...**5**

Acknowledgements……..….**11**

List of Figures and Tables……...……**13**

List of Abbreviations……...……**15**

Contributions of Authors……...…..…**18**

Introduction

Preface……..….**22**

Chapter 1: Literature Review I: Neuronal Development……..……...**23**

I. Axon Guidance…….…**23**

i. Commissural Neuron Guidance……...**25**

II. Netrins and Netrin Receptors……...……**29**

i. Netrin Family of Proteins…….**31**

ii. Netrin Receptors……...……...…**32**

a. DCC…….**33**

iii. Netrin-1 and DCC signalling…….……..……...….**34**

iv. Netrin-1 Function…….…**36**

III. Synaptic Development……...……...**39**

IV. Cadherins……...**40**

i. Classical cadherins……**41**

a. Cadherin 12……..**44**

ii. Cadherin Function in the Nervous System……...……..**45**

V. Catenins…….....**49**

VI. Concluding Remarks…….....**50**

Preface……...…….**52**

Chapter 2: Literature Review II: Neuronal Extracellular Matrix……..……..…….**53**

I. Proteoglycans……**53**
i. Heparan sulfate proteoglycans……**56**
a. Glypicans……**57**
b. Syndecans……**59**
ii. Chondroitin sulfate proteoglycans……**60**
a. Lecticans……**61**
II. Extracellular Matrix……**62**
i. Function in the Nervous System……**64**
a. Axon Guidance……**64**
b. Synaptic Function……**67**
III. Perineuronal Nets……**67**
i. Structure and function……**69**
IV. Concluding Remarks……**71**

Research Rational and Objectives……**72**

Results

Preface……**74**

Chapter 3: Cadherin 12 interacts with DCC to modulate commissural axon guidance in the developing rodent spinal cord……**75**

I. Abstract……**76**
II. Introduction……**77**
III. Methods……**79**
i. Animals……**79**
ii. Antibodies and reagents……**79**
iii. 2-dimentional liquid chromatography mass spectrometry……**80**
iv. Cell culture……**81**
v. Growth cone expansion assay……**82**
vi. β-catenin phosphorylation assay……**82**
vii. Co-immunoprecipitation……**82**
viii. Western blot analysis……**84**

ix. Immunohistochemistry……..**84**
x. Cell surface binding assay……..…..**85**
xi. Immunocytochemistry…….……..**85**
xii. Embryonic dorsal spinal cord explants…….……**86**
xiii. Open book preparations……...……**86**
IV. Results……..……**87**
i. Characterisation of the CDH12 monoclonal antibody……..……**87**
ii. Identifying novel DCC binding partners……**89**
iii. Cadherin 12 co-immunoprecipitates with DCC…….…**89**
iv. Expression of cadherin 12 in the developing spinal cord…….….**90**
v. Netrin-1 does not bind cadherin 12…….…..**91**
vi. Cadherin 12 provides a permissive environment for spinal commissural neuron growth……...….**92**
vii. Netrin-1 induces phosphorylation of β-catenin……**93**
viii. DCC expression does not alter β-catenin expression…….....**95**
ix. Cadherin 12 increases netrin-1 induced commissural axon outgrowth……...…**96**
x. Cadherin 12 function is required for commissural axon turning.……**96**
V. Discussion……..……..……**97**
VI. Figures……...….**102**

Preface……**116**

Chapter 4: DCC interacts with CDH12 in the rat brain and may influence synaptic function..**117**

I. Abstract……..**118**
II. Introduction……**119**
III. Methods……..……**121**
i. Animals……...……**121**
ii. Antibodies and reagents……...…**121**
iii. Immunohistochemistry ……..……**122**
iv. Western blot analysis…….……..……**122**
v. Cell culture…….…….……**122**
vi. Immunocytochemistry ……**123**

vii. Subcellular fractionation……..…**123**
viii. ICCS……...…….**124**
ix. Biotinylation of surface proteins……..……**125**
x. Co-Immunoprecipitation……..**125**
xi. Mass spectrometry……...**126**
xii. Electrophysiological recordings……...……**126**
IV. Results……**127**
i. Cadherin 12 protein distribution in the brain……..….**127**
ii. Subcellular localization of Cadherin 12……...……**128**
iii. Netrin-1 promotes aggregation and co-localization of CDH12 and DCC……...**129**
iv. Netrin-1 increases cell surface CDH12 and DCC……...….**131**
v. DCC Co-IPs with CDH12……..……..**131**
vi. Functional significance of cadherin 12 in cortical neurons……**133**
V. Discussion…….…….**134**
i. CDH12 expression in the brain……**134**
ii. DCC interacts with CDH12 and Dlg5 which may regulate function……...**135**
VI. Figures……..…..**137**

Preface…….……**144**

Chapter 5: Proteoglycan binding regulates the distribution and function of netrin-1 in the embryonic spinal cord: identification of a GAG binding site in the netrin-1 C-terminal domain……....**145**
I. Abstract……..**146**
II. Introduction……...…….**147**
III. Methods……..…**149**
i. Animals……**149**
ii. Antibodies and reagents……..…….**149**
iii. Generation of recombinant netrin-1 C terminal domain protein fragments…....**150**
iv. Heparin batch binding assay……..…..**151**
v. Cell surface binding assay…….……..**151**
vi. Immunocytochemistry…….…**152**
vii. Immunohistochemistry……**152**

viii. Glycan isolation from embryonic neural tissue……**153**
ix. Biotinylation of isolated GAGs……**154**
x. GAG ELISA assay……**155**
xi. Embryonic dorsal spinal cord explants……**155**
xii. Surface plasmon resonance……**155**
xiii. Chick *in ovo* electroporation……**156**
IV. Results……**156**
i. The netrin-1 NTR-like C-domain contains GAG binding sequences……**156**
ii. HSPGs and CSPGs in embryonic spinal cord……**158**
iii. Netrin-1 C-domain mediates GAG binding……**158**
iv. Netrin-1 binds GAGs expressed in the embryonic CNS……**159**
v. HSPGs are required for netrin-1 induced axon outgrowth……**161**
vi. Netrin-1 binds glypicans and syndecans……**163**
vii. Glypican modulates netrin-1 induced axon outgrowth……**164**
V. Discussion……**166**
i. Netrin-1 interacts with GAGs via C-domain interactions……**166**
ii. Multimerization of netrin-1 activates DCC……**167**
iii. Structural specificity of GAG function……**169**
iv. Netrin synergizing activity……**170**
v. Conserved heparin binding function of the NTR domain……**171**
VI. Figures……**173**

Preface……**187**
Chapter 6: Netrin-1 is associated with perineuronal nets in the adult rodent brain……**188**
I. Abstract……**189**
II. Introduction……**190**
III. Methods……**191**
i. Animals……**191**
ii. Antibodies and reagents……**192**
iii. Immunohistochemistry……**192**
iv. Biochemical fractionation of whole brain……**193**
v. Isolation of glycans from fractions……**193**

vi. Biotinylation of isolated GAGs……..……**194**
vii. GAG ELISA assay…….……..**195**
viii. Western blot analysis…….……**195**
ix. Surface plasmon resonance……**196**
x. Quartz crystal microbalance with dissipation monitoring…….……**196**
IV. Results……...….**197**
i. Netrin-1 associates with PNNs……...…….**197**
ii. Netrin-1 binds PNN GAGs……...……**198**
iii. Netrin-1 softens CS GAG films……...……**202**
V. Discussion……..**203**
VI. Figures……....……**206**

Discussion

Preface……**214**
Chapter 7: General Discussion and Concluding Remarks……...……..**215**

I. Integrated Model of Commissural Axon Guidance.…….…….**215**
II. Integrated Model for Synapse Function……..……...……**218**
III. Concluding Remarks……..……**222**

Bibliography

Publications……**224**

References……...……**225**

Acknowledgments

They say it takes a village to raise a child and I think the same can be said for completing a PhD. While I like to think of myself as being fiercely independent, I could not have done this without the support of the many individuals around me. Its difficult to know where to start so I will start with the obvious. Thank you to my supervisor, Dr. Timothy Kennedy. Thank you for taking me on as undergraduate student for a summer project and then letting me stick around and continue to annoy you. Thank you for giving me the opportunity to learn and become the scientist I am today. Thank you for also supporting me outside of the lab, especially for allowing me to chase my athletic goals. For never making me feel guilty about taking time off to compete in Olympic trials or national championships and for putting up with my many, many injuries (I can almost straighten my finger!). I am so grateful that you supported both my academic and non-academic pursuits in life.

Thank you to my committee members, Dr. Ed Ruthazer and Dr. JF Cloutier for their guidance throughout my graduate studies. Thank you to Dr. James Fawcett and Dr. Jessica Kwok for teaching me everything I know about GAGs. Thank you for welcoming me into your laboratories and making the second half of this thesis possible. Without your guidance I would be lost in the world of sugars. Thank you also to the MNI-Cambridge collaboration and the Don Baxter Collaborative Travel Award. These funding sources made it possible for me to travel to England and work in these labs.

Thank you to all current and former lab members for making the TEK lab an amazing place to be part of, and for teaching me everything I know. Special shout-outs to Karen, Jenea, Katie, Ilana, Greta, Diane, Anais, Jeanne, Celina, and Nat. You have all had lasting impacts on my life and I

continue to value your friendship outside of the lab. To Camille Juzwik, my lab wife, for being unwaveringly supportive of everything I do. Thank you for sharing lunch with me, letting me wear your slippers, and taking the time to talk to me when I was feeling sad. Thank you for being you! I also want to acknowledge everyone else at the MNI and say how unbelievably lucky I feel to have worked in such a unique and special place.

I also want to thank all the people outside of science who have had such a huge impact on my life during my PhD. To my tripod, Denny and Anni for our silly group chats and for always being supportive even though you have no idea what I am doing. Thank you Anni for reading my thesis even though it melted your brain! The McGill Track and Field Team and the Westmount Rugby Club. When I was not at the lab you very likely could find me either at the track or on the rugby pitch. You all keep me sane. A special thanks to Abby, who took me in these past few months when I ended up at the end of my lease with no where to live. I never thought I wanted to live with a roommate, but it turns out I was so very wrong! Thank you for dinners, art projects, trips to Walmart/Canadian Tire/Michael's, country music, and wine! I love our little family and the fur babies.

And last, but most important, my family. My mom Debbie, my dad Greg, and my sister Jackie. Thank you for loving me and supporting me through all these years of school. There will never be enough words for me to express everything you mean to me or to thank you for everything you have done. I love you three so so so much!

List of Figures and Tables

Figure 1.1 – Commissural axon guidance molecules in the developing spinal cord

Figure 1.2 – Netrin and netrin receptors

Figure 1.3 – DCC signalling mechanisms

Figure 1.4 – Classical cadherin structure and orientation

Figure 2.1 – Proteoglycan structure

Figure 2.2 – Chondroitin sulfate subunits

Figure 3.1 – Cadherin 12 antibody validation

Figure 3.2 – CDH12 is a possible DCC interacting protein

Figure 3.3 – Immunohistochemical distribution of CDH12 in E10.5, E12.5, and E14.5 mouse spinal cord

Figure 3.4 – Distribution of CDH12 protein in embryonic rat spinal cord *in vivo* and embryonic spinal commissural neurons *in vitro*

Figure 3.5 – CDH12 does not bind netrin-1

Figure 3.6 – CDH12 substrate enhances netrin-1 induced filopodia formation

Figure 3.7 – Increased phosphorylation of β-catenin following netrin-1 treatment

Figure 3.8 – Unaltered β-catenin expression in DCC null embryonic mouse spinal cord

Figure 3.9 – CDH12-Fc potentiates netrin-1 induced commissural axon outgrowth

Figure 3.10 – Competing CDH12-CDH12 binding with CDH12-Fc disrupts commissural axon guidance at the ventral midline

Figure 3.11 – Model for cadherin function in commissural axon guidance

Figure 4.1 – Characterization of CDH12 protein in rat brain

Figure 4.2 – CDH12 distribution in cultured rat neurons

Figure 4.3 – Subcellular fractionation to address the distribution of DCC and CDH12

Figure 4.4 – ICCS supports interaction of DCC and CDH12 in cortical neurons

Figure 4.5 – DCC, CDH12, and β-catenin co-IP

Figure 4.6 – Electrophysiological recordings from 14 DIV cortical neuron cultures

Figure 5.1 – Netrin-1 C-domain alignment and HEK cell binding

Figure 5.2 – Distribution of HS and CS in rat E13/14 rat spinal cord

Figure 5.3 – Heparin batch binding assay

Figure 5.4 – ELISA assay of netrin-1 binding to GAGs isolated from embryonic rat CNS

Figure 5.5 – Dorsal spinal explant assay with heparin and synthetic polymers

Figure 5.6 – Glypican and syndecan ELISA and SPR

Figure 5.7 – Glypican induced axon outgrowth

Figure 5.8 – Glypican-1 electroporated chick spinal cords

Figure 5.9 – Model of HSPG multimerization of netrin-1 and DCC

Figure 6.1 – PNN staining in the adult rat brain

Figure 6.2 – Adult GAG binding to netrin-1

Figure 6.3 – CS subunit structure and netrin-1 binding

Figure 6.4 – SPR measurements for the interaction between CS and netrin-1

Figure 6.5 – QCM-D data for netrin-1

Figure 7.1 – Integrated model for commissural axon guidance

Figure 7.2 – Integrated model for synapse function

Table 3.1 – Cadherin family homology

Table 3.2 – Mass spectrometry band analysis for CDH12

Table 4.1 – Mass spectrometry band analysis for Dlg5

Table 5.1 – K_D Measurements for netrin-1 binding to HS

Table 6.1 - K_D Measurements for netrin-1 binding to CS

List of Abbreviations

AMPA: α-amino-3-hydroxy-5-methyl-4-isoxazolepropionic acid
BMP: bone morphogenic protein
Boc: brother of CDO
BSA: bovine serum albumin
C4ST: chondroitin 4-sulfotransferase
C6ST: chondroitin 6-sulfotransferase
CAM: cell adhesion molecule
CD: cluster density
CDC42: cell division control protein 42
CDH: cadherin
CDH12: cadherin 12
CNS: central nervous system
Comm: commissureless
CS: chondroitin sulfate
CSPG: chondroitin sulfate proteoglycan
DA: degree of aggregation
DCC: deleted in colorectal cancer
DG: dentate gyrus
DS: dermatan sulfate
DSCAM: down syndrome cell adhesion molecule
E11: embryonic day 11
E13: embryonic day 13
E17: embryonic day 17
EC: extracellular
ECM: extracellular matrix
EDTA: ethylenediaminetetraacetic acid
EGF: epidermal growth factor
EMT: endothelial mesenchymal transition
EPSC: excitatory post synaptic current
ER: endoplasmic reticulum
EXT: exostosin
FAK: focal adhesion kinase
FAT: focal adhesion targeting
FGF: fibroblast growth factor
FRET: fluorescence resonance energy transfer
GABA: gamma-Aminobutyric acid
GalNAc: acetyl-D-galactosamine
GAG: glycosaminoglycan

GDF: growth differentiation factor
GlcA: D-glucuronic acid
GlcNAc: N-acetyl-D-glucosamine
GPI: glycosylphosphatidylinositol
HA: Hyaluronic acid
HAS: hyaluronan synthase
HAPLN: hyaluronan and proteoglycan link protein
HEPES: 4-(2-hydroxyethyl)-1-piperazineethanesulfonic acid
Hhip: hedgehog interacting protein
HI-FBS: heat inactivated fetal bovine serum
HI-HS: heat inactivated horse serum
HRP: horse radish peroxidase
HS: heparan sulfate
HSPG: heparan sulfate proteoglycans
ICCS: image cross correlation spectroscopy
IdoA: L-iduronic acid
Ig: immunoglobulin
IgG: immunoglobulin G
KS: Keratan sulfate
LTP: long term potentiation
MS: multiple sclerosis
NaCl: sodium chloride
NFM: neurofilament M
NGL: netrin-G ligand
NMDA: N-methyl-D-aspartic acid
NrCAM: neuronal cell adhesion molecule
NTR: netrin-like
N-WASP: neural Wiskott-Aldrich syndrome protein
Pak: p21-activating kinase
PBS: phosphate buffered saline
PBST: Phosphate buffered saline with Triton X-100
PCR: polymerase chain reaction
PCPE: procollagen C-endopeptidase enhancer
PDL: poly-D-lysine
PFA: paraformaldehyde
PG: Proteoglycan
PKA: protein kinase A
PMSF: phenylmethylsulfonyl fluoride
PNN: perineuronal net
PSD-95: post-synaptic density 95

PVA: parvalbumin
QCM-D: Quartz crystal microbalance with dissipation monitoring
RGC: retinal ganglion cell
Robo: roundabout
RT-PCR: reverse transcription polymerase chain reaction
SDS: sodium dodecyl sulfate
Sema: semaphorin
SFK: Src family kinase
Sfrp: secreted frizzled related protein
SGBS: Simpson-Golabi-Behmel syndrome
Shh: sonic hedgehog
Smo: smoothened
SNARE: Snap Receptor
SPR: Surface plasmon resonance
TAG-1: transient axonal glycoprotein-1
TCA: Trichloroacetic acid
TIRF: total internal reflection fluorescence
TBS: Tris buffered saline
TBST: Tris buffered saline with Tween 20

Contributions of Authors

Chapter 1: Literature Review I – Neuronal Development

- **Stephanie N. Harris:** Wrote the chapter and drew the figures
- **Timothy E. Kennedy:** Edited the text

Chapter 2: Literature Review II – Proteoglycans and neuronal extracellular Matrix

- **Stephanie N. Harris:** Wrote the chapter and drew the figures
- **Timothy E. Kennedy:** Edited the text

Chapter 3: Cadherin 12 interacts with DCC to modulate commissural axon guidance in the developing rodent spinal cord

- **Stephanie N. Harris:** Designed and performed experiments and analysis for figures 1, 2, 3, 4, 6, 7, 8, 9, 10, and 11, assembled all figures, and wrote the manuscript
- **Ian V. Beamish:** Performed netrin binding assay for figure 5, ran whole spinal cord DCC IP for figure 2B, and cultured dorsal spinal explants for figure 9.
- **Sonia Rodrigues:** Performed DCC IP and mass spectrometry analysis from commissural neurons for figure 2A.
- **Timothy E. Kennedy:** Designed experiments and edited the text

Chapter 4: DCC interacts with CDH12 in the rat brain and may influence synaptic function

- **Stephanie N. Harris:** Designed and performed experiments and analysis for all figures, assembled all figures, and wrote the manuscript
- **Katherine E. Horn:** Performed PSD fractionation in figure 4C, assisted with fractionation in figure 4B and ran DCC, PSD95, and synaptophysin western blots.
- **Angelica Gopal:** Performed ICCS analysis in figure 5 A-D.
- **Stephen D. Glasgow:** Performed electrophysiology on cultured cortical neurons in figure 7.
- **Paul Wiseman:** Assisted with experimental design for figure 5.
- **Timothy E. Kennedy:** Designed experiments and edited the text.

Chapter 5: Proteoglycan binding regulates the distribution and function of netrin-1 in the embryonic spinal cord: identification of a GAG binding site in the netrin-1 C-terminal domain

- **Stephanie N. Harris:** Designed and performed experiments and analysis for figures 1, 2, 4, 5, 6, 7, 8, and 9, assembled all figures, and wrote the manuscript
- **Ian V. Beamish, Nathalie Marcal, Daryan Chitsaz, Simon Moore:** Performed dorsal spinal cord explant dissections for figure 5 and figure 7.
- **Celina Cheung:** Generated netrin C-domain constructs and performed heparin batch binding assay for figure 3. Performed spinal cord staining in figure 2 and figure 7H.
- **Lynda Djerbal:** Performed SPR analysis in figure 6C.
- **Mahmoud Moussa, K. Adam Baker:** Analysed a portion of the dorsal explant outgrowth in Figure 5B and figure 7.
- **Chao Chang:** Performed chick electroporation for figure 8.
- **Michael J. Landry:** Generated sulphonated polystyrene used in figure 5.
- **Christopher Barret:** Assisted Michael J. Landry with experimental design for figure 5.
- **Claire Y. Benard:** Provided glypican-1 protein for figure 7A, provided valuable insight.
- **Artur Kania:** Assisted Chao Chang with experimental design for figure 8.
- **Ralf Richter:** Assisted Lynda Djerbal with experimental design for figure 6C.
- **Jessica Kwok:** Assisted with experimental design, provided guidance and valuable insight.
- **Timothy E. Kennedy:** Designed experiments and edited the text.

Chapter 6: Netrin-1 is associated with perineuronal nets in the adult rodent brain

- **Stephanie N. Harris:** Designed and performed experiments and analysis for figures 1, 2, and 3, assembled all figures, and wrote the manuscript
- **Lynda Djerbal:** Performed SPR in figure 4 and QCM-D in figure 5.
- **Heleen M. van't Spijker:** Assisted with performing ELISA assays in figure 2D, provided biotinylated GAGs for brain fraction ELISAs in figure 2D and 2E. Provided biotinylated CS subunits for figure 3F.
- **Ralf Richter:** Assisted Lynda Djerbal with experimental design for figures 4 and 5.
- **James Fawcett:** Assisted with experimental design, provided guidance and valuable insight

- **Jessica Kwok:** Assisted with experimental design, provided guidance and valuable insight
- **Timothy E. Kennedy:** Designed experiments and edited the text.

Chapter 7: General discussion and concluding remarks

- **Stephanie N. Harris:** Wrote the chapter and drew the figures
- **Timothy E. Kennedy:** Edited the text

INTRODUCTION

Preface

The formation of the central nervous system (CNS) requires the execution of many precise and complex processes in order for correct neuronal migration, axon growth, and synaptic connections to occur. First, there must be appropriate expression and regulation of the molecules involved in guiding neuronal migration and axon extension. As axons reach their targets, specific signalling is required for the proper formation and maintenance of synaptic connections. These precise and targeted processes are essential for the proper development and function of the CNS. This introductory chapter provides an overview of commissural axon guidance, synaptogenesis, and the role of cell adhesion molecules in each of these processes.

Chapter 1

Literature Review I – Neuronal Development

I. Axon Guidance

During development, axons extend over long distances through a complex neural environment to reach precise targets and form synapses. To achieve this targeted growth, environmental guidance cues break down the long complex growth trajectory into shorter intermediate steps providing axons with pathfinding information as they grow. Guidance cues originate from guidepost cells localized in specialized regions of the nervous system, such as floor plate cells of the spinal cord (Tessier-Lavigne & Goodman, 1996). Molecular signals in the environment are detected and integrated by the growth cone of developing neurons to determine the appropriate direction of growth. Growth cones are highly motile structures located in the tip of growing axons. They contain actin-rich regions at the leading edge, which can be arranged into sheet like structures called lamellipodia, or rod-like structures called filopodia. The actin cytoskeleton is reorganized within the growth cones in response to guidance cues causing either expansion or collapse (Dent, Gupton, & Gertler, 2011). When a growth cone encounters an attractive cue it will expand, adding new membrane at its leading edge and, in contrast, encountering a repulsive cue will lead to a retraction of the membrane at the leading-edge causing collapse. This regulated expansion and collapse results in directional growth of the axonal process (Bashaw & Klein, 2010). In the absence of environmental guidance cues, developing axons are often mistargeted leading to severe, and sometimes lethal, defects in the nervous system (Evans & Bashaw, 2010; Tessier-Lavigne & Goodman, 1996).

There are two classifications of guidance cues: permissive and instructive. Permissive cues allow or prevent growth of the axon without giving directional information. Instructive cues provide the required directional information and can either attract or repel a growing axon (Tessier-Lavigne & Goodman, 1996). Instructive guidance cues can be further classified as short range or long range, both of which can be tethered to cells or freely diffusible. Short range cues stay closely associated with the cells that produce them, whereas long range cues can be found up to several cell diameters away from their source (Tessier-Lavigne & Goodman, 1996). To convey information to the growing axons, guidance cues are often present in a gradient within neuronal tissue. Gradients can be formed through differential expression of guidance cues by cells within the tissue or through the diffusion of the cues away from their source. Multiple gradients of different cues can overlap to encode additional and more complex information to growing axons (Kennedy, Serafini, de la Torre, & Tessier-Lavigne, 1994; Sloan, Qasaimeh, Juncker, Yam, & Charron, 2015). Gradients of axon guidance cues have been shown to be important for the development of various structures, including the ventral spinal commissure, which is most relevant to the work presented in this thesis and will be covered in more detail in the following sections (Erskine & Herrera, 2007; Kennedy et al., 1994).

Tessier-Lavigne *et. al* (1988) provided one of the first demonstrations of chemotropic axon guidance. They showed that a floor plate derived cue, later identified as netrin-1, could influence commissural axon outgrowth from a dorsal spinal explant over a distance of approximately 200 μm (Kennedy et al., 1994; Serafini et al., 1994; Tessier-Lavigne, Placzek, Lumsden, Dodd, & Jessell, 1988). Many families of axon guidance cues have since been identified and implicated in the guidance of commissural axons in the developing spinal cord.

I.i. Commissural Neuron Guidance

In the mammalian CNS, commissural axon tracts carry information from one side of the organism to the other to achieve appropriate and coordinated function. The ventral spinal commissure is formed by sensory interneurons that originate in the dorsal region of the spinal cord, project ventrally, and then cross the midline. In the developing rat spinal cord, commissural neurons originate between embryonic day (E) 9.5 and E12.5 and midline crossing is complete by E14 (Helms & Johnson, 2003; Pignata, Ducuing, & Castellani, 2016). After crossing, the axons make a rostral turn and project toward the brain, extending within the ventral funiculus (Figure 1.1) (Bovolenta & Dodd, 1990).

Providing directional guidance to commissural axons in the spinal cord requires a coordinated and cooperative effort of repulsive guidance cues derived from the roof plate and attractive guidance cues derived from the floor plate. The first step requires guiding axons to the ventral midline. The primary chemo-repulsive molecules involved are bone morphogenic protein (BMP)-7, growth differentiation factor (GDF)-7, and draxin. Both BMP-7 and GDF-7 are secreted by the roof plate and drive the initial projection of commissural neurons ventrally (Augsburger, Schuchardt, Hoskins, Dodd, & Butler, 1999; Butler & Dodd, 2003; Yamauchi, Varadarajan, Li, & Butler, 2013). Draxin repels neurite outgrowth in the dorsal spinal cord and draxin-null mice show de-fasciculation defects in the descending commissural axon tracts (Islam et al., 2009).

The primary chemo-attractive molecules involved in guiding axons to the ventral midline are netrin-1 and sonic hedgehog (Shh). Netrin-1 and its receptor, deleted in colorectal cancer (DCC), are essential for the proper guidance of commissural axons. Loss of netrin-1 or DCC results in the failure of commissural neurons to reach the ventral midline, leading to the absence

of the ventral commissure (Bin et al., 2015; Fazeli et al., 1997; Serafini et al., 1996). The function of both netrin-1 and its receptors will be covered in more detail in the following sections.

Shh is a morphogen secreted from the floor plate that functions in co-operation with netrin-1 to mediate commissural axon turning (Charron, Stein, Jeong, McMahon, & Tessier-Lavigne, 2003). Shh is not able to stimulate commissural axon outgrowth on its own but works in concert with netrin-1 to properly orient developing axons through the ventral spinal cord to the midline (Charron et al., 2003). Commissural neuron growth cones express smoothened (Smo) and bi-regional Cdon-binding protein (Boc), both of which are receptors for Shh and mediate commissural axon turning (Charron et al., 2003; Okada et al., 2006).

Once axons reach the ventral midline, several cues are required to guide them across to the contralateral side. Attractive cues mediate the entry of neurons into the midline; however, in order to exit the midline, they must lose sensitivity to the attractive cues and gain sensitivity to repulsive cues. Repulsive cues drive commissural neurons out of the midline and prevent re-entry and re-crossing of post-crossing neurons (Evans & Bashaw, 2010). Netrin-1 is the major attractive cue at the midline of the spinal cord. In *Xenopus laevis,* activation of the receptor roundabout (Robo) -1 via slits leads to Robo-1 binding to the cytoplasmic tail of DCC, which in turn silences the growth cones response to netrin-1 (Stein & Tessier-Lavigne, 2001). Along with inactivation of the netrin-1/DCC response, neurons become sensitive to slits and semaphorins, which help drive them out of the midline to the contralateral side of the spinal cord.

Slits are a family of repulsive guidance molecules expressed by the floor plate in the spinal cord that prevent ipsilateral neurons from crossing the midline, and also prevent post-crossing contralateral neurons from re-crossing (Kidd, Bland, & Goodman, 1999; Long et al., 2004;

Rajagopalan, Vivancos, Nicolas, & Dickson, 2000; Simpson, Bland, Fetter, & Goodman, 2000). Vertebrates express three slits, -1, -2, and -3 and four slit receptors, Robo -1 through -4 (Blockus & Chedotal, 2016; Brose et al., 1999). Fine tuning commissural neuron sensitivity to slits occurs through controlling the presentation of Robo on growth cones (Long et al., 2004; Simpson et al., 2000). In *Drosophila melanogaster,* Robo expression is regulated post-translationally by a protein called commissureless (comm) which targets Robo for degradation in pre-crossing neurons (Keleman et al., 2002). As axons cross the midline, comm expression is downregulated, allowing Robo to appear on the surface of commissural growth cones (Kidd et al., 1998). Once on the surface of commissural neurons, Robo sensitizes growth cones to the repulsive function of slits pushing them out of the midline to the contralateral side and preventing re-crossing (Kidd et al., 1998). Possible orthologues of comm that regulate Robo trafficking in mammals have been recently identified (Gorla et al., 2019). However, the major focus of the regulation of slit/Robo trafficking in mammals to date has instead studied the significance of alternative splicing of Robo mRNA (Z. Chen, Gore, Long, Ma, & Tessier-Lavigne, 2008; Sabatier et al., 2004). Rig-1/Robo3 has been identified as a protein which may function in a similar manner to comm by suppressing repulsion in pre-crossing neurons (Sabatier et al., 2004). Alternative splicing of Robo3 in neurons pre- and post-crossing can account for functional differences in the protein, providing the switch from attraction to repulsion. Pre-crossing neurons express the splice variant Robo-3.1, which suppresses the function of other Robo receptors, thus preventing repulsion. Post-crossing neurons express the splice variant Robo-3.2, which functions in concert with other Robo receptors to enhance repulsion (Z. Chen et al., 2008).

Another family of repulsive cues involved in guiding axons across the midline to the contralateral side is the Semaphorins (Semas), which function to prevent commissural neurons

from re-crossing the midline. Sema3B is expressed by floor plate cells and binds to its receptors neuropilin-2 and plexinA1 (Pignata et al., 2016). Pre-crossing commissural axons are insensitive to semaphorins due to calpain-1 mediated degradation of plexinA1 (Nawabi et al., 2010). Expression of neuronal cell adhesion molecule (NrCAM) at the midline inhibits calpain-1, allowing for accumulation of plexinA1 on the membrane. In turn, growth cones become responsive to Sema3B repulsion, forcing them out of the midline and subsequently preventing re-crossing (Nawabi et al., 2010).

Following midline crossing, commissural neurons make a rostral turn and extend longitudinally towards the brain in the white matter tracts of the ventral funiculus. This turn is directed by gradients of Wnts and Shh along the anterior-posterior axis (Sakai et al., 2012). Wnt4 is present in a graded distribution that is high anteriorly and low posteriorly, attracting post-crossing commissural axons through the function of its receptor frizzled 3 (Lyuksyutova et al., 2003). In addition to this, Shh acts to repel axons along the same axis through an opposing gradient that is high posteriorly and low anteriorly acting through the receptor hedgehog-interacting protein (Hhip) (Bourikas et al., 2005). Shh also helps to regulate a gradient of Wnt5a and Wnt7a by inducing the expression of Secreted frizzled-related protein 1 (Sfrp1) (Domanitskaya et al., 2010). Wnt5a and 7a are not localized in a graded distribution. However, Sfrp1 is a Wnt antagonist and the induction of Sfrp1 by Shh leads to a functional Wnt gradient that is high anteriorly, further assisting the attraction of post-crossing commissural neurons longitudinally up the spinal cord (Domanitskaya et al., 2010). Collectively, these signals work together to ensure proper guidance of commissural axons to the midline, across the midline, and turning rostrally post-crossing (Figure 1.1).

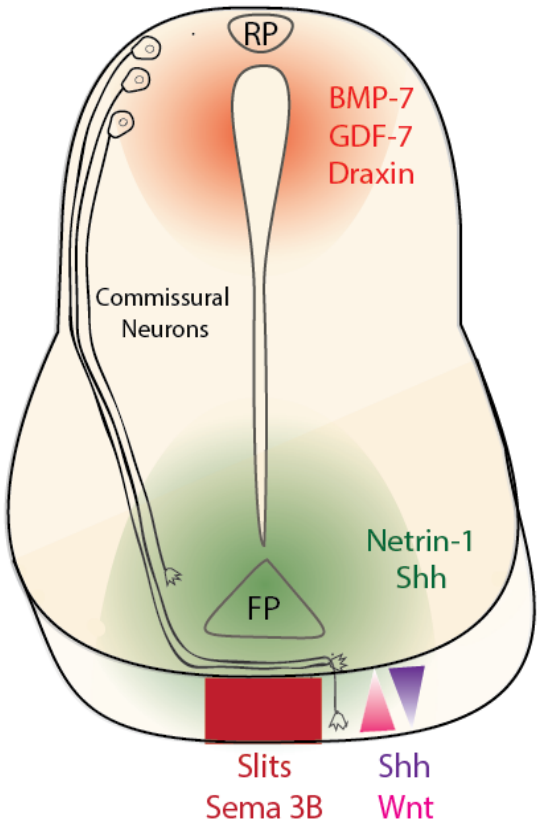

Figure 1.1: Commissural axon guidance in the developing spinal cord

BMP-7, GDF-7, and Draxin repel commissural growth cones from the dorsal spinal cord towards the ventral spinal cord. Netrin-1 and Shh attract growth cones towards the ventral region of the spinal cord. While crossing the midline, neurons become sensitive to slits and semaphorin 3B, and insensitive to netrin-1. This forces axons out of the midline and prevents post-crossing neurons from re-crossing back to the ipsilateral side. Shh and Wnt are present in complimentary anterior-posterior gradients to mediate the rostral turn and longitudinal growth of post-crossing commissural neurons.

(RP, roof plate; FP, floor plate)

II. Netrins and Netrin Receptors

Netrins are a highly conserved family of laminin-related proteins that were originally isolated and characterized based on their chemotropic axon guidance ability (Kennedy et al., 1994; Serafini et al., 1994). Since their discovery, research has shown that the netrins can mediate a wide variety of functions in the nervous system and in many other tissues including vasculature, lung, pancreas, mammary gland, and muscle (reviewed in (Lai Wing Sun, Correia, & Kennedy,

2011)). Netrins are secreted extracellular proteins that can function both as a chemoattractant or a chemorepellent depending on the receptors expressed by the responding cell. Netrin receptors include: the DCC/neogenin family; Unc5 homologs; Down syndrome cell adhesion molecule (DSCAM); and Netrin-G ligands (NGL) (Figure 1.2) (Lai Wing Sun et al., 2011).

Figure 1.2: Netrin and netrin receptors

A) Netrin structure. Netrins -1, -2, and -3 share a similar domain structure with domains VI and V being homologous to the γ chain of laminins. Netrin -5 is similar but lacks domain VI and one EGF repeat of domain V. Netrin-4 and the netrin-Gs have similar domain structure, minus the c-domain, but are most similar to the β chain of laminin.

B) Structure of common netrin receptors. Receptors shown are single-pass transmembrane proteins and all are members of the Ig superfamily of proteins. Receptors include deleted in colorectal cancer (DCC); the DCC paralog neogenin; the UNC5 homologs; down syndrome cell adhesion molecule (DSCAM); and netrin-G ligands (NGL). DCC is the most studied netrin receptor.

Abbreviations: Ig: Immunoglobulin domain; FNIII: fibronectin type III domain; P1, P2, and P3: conserved cytoplasmic tail regions of DCC; TSP: thrombospondin domain; ZU5: zona occludens 5 domain; DB: DCC binding domain; DD: death domain; LRR: leucine rich repeat.

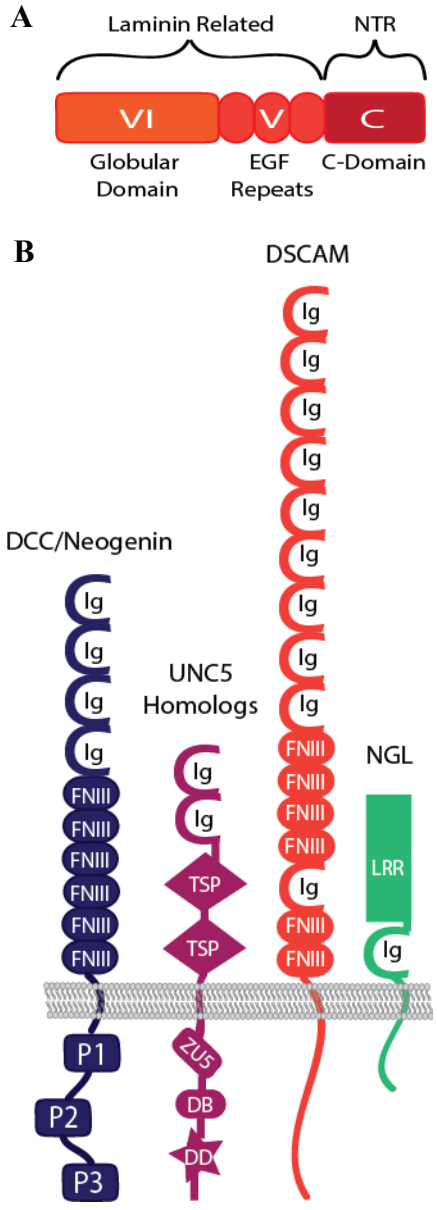

II.i. Netrin Family of Proteins

Netrins were first isolated from embryonic chick brain based on their ability to promote commissural axon outgrowth (Kennedy et al., 1994; Serafini et al., 1994). Netrins are highly conserved among vertebrates and many invertebrates, and netrin orthologs include Netrin A and B in *Drosophila melanogaster* (R. Harris, Sabatelli, & Seeger, 1996) and UNC-6 in *Caenorhabditis elegans* (Ishii, Wadsworth, Stern, Culotti, & Hedgecock, 1992). To date, seven members of the netrin family have been identified in vertebrates. Netrins -1 through -5 make up the secreted netrins while netrins -G1 and -G2 are glycophosphatidyl inositol (GPI)-linked membrane-bound netrins (Lai Wing Sun et al., 2011; Yamagishi et al., 2015). Nearly all netrins are expressed in mammals with the exception of netrin-2, which is expressed exclusively in birds and fish (Lai Wing Sun et al., 2011). The N-terminal domain of netrins are homologous to laminins with netrins -1 and -3 being most similar to the laminin γ1 chain while netrin-4 and netrins G1 and G2 share the most similarity with the laminin β1 chain (Rajasekharan & Kennedy, 2009). The secreted netrins are comprised of ~ 600 amino acids, resulting in a protein approximately 75 kDa in size with three structural domains, domain VI and domain V, which are homologous to laminins, as well as a C-terminal netrin-like (NTR) domain (Figure 1.2) (Kennedy, 2000). Netrin-G proteins and netrin-4 contain domains VI and V but lack the NTR C-domain. Despite all netrins being similar in structure, the secreted and GPI-linked netrins are functionally distinct due to the engagement of different netrin receptors.

Netrin-1 is the most studied netrin and is critical for commissural axon guidance. The significance of netrin-1 function is highlighted by the severity of defects seen in knockout animals. Mice that are hypomorphic for netrin-1 protein die at birth and have severe axon guidance defects including the complete absence of the ventral spinal commissure (Serafini et

al., 1996). Full netrin-1 nulls do not live past E14.5, showing a much more severe phenotype than the hypomorphs, with death likely due to defects in heart or vasculature formation (Bin et al., 2015). Domains VI and V are required for receptor binding while the function of the C-domain remains unknown (Finci et al., 2014; K. Xu et al., 2014). A 2010 study (Weiss et al., 2010) demonstrated that another NTR containing protein, procollagen C-proteinase enhancer-1 (PCPE-1), binds to the heparan sulfate proteoglycan (HSPG) family of proteins through its NTR domain. Netrin-1 has been shown to have high affinity for heparin, which is an HSPG family member; and the NTR C-domain may be involved in binding to HSPG proteins, a function which will be further addressed in this thesis.

II.ii. Netrin Receptors

Multiple families of netrin receptors are expressed in vertebrates that mediate the various functions of netrins. As mentioned above, netrin receptors include DCC/neogenin, UNC5 A-D, DSCAM, and NGLs (Figure 1.2). Most known netrin receptors are single-pass transmembrane proteins and members of the IgG superfamily of proteins (Lai Wing Sun et al., 2011). DCC and the UNC5 homologues are the most-studied and well characterized netrin receptors and are expressed in many different cell types both in the nervous system and in other tissues (Lai Wing Sun et al., 2011). The attractive or repulsive response to netrin-1 is determined by the receptors expressed by a responding cell. DCC is involved in both attractive and repulsive responses to netrin-1 while the UNC5 homologues mediate the repulsive response to netrin-1. Based on this model, a cell that expresses only DCC is predicted to have an attractive response to netrin-1, while a cell that expresses both DCC and UNC5 will have a repulsive response (Lai Wing Sun et al., 2011). The work done in this thesis focuses on protein interactions with DCC.

II.ii.a. DCC

DCC was originally identified as a candidate tumor suppressor gene in humans due to its frequent loss of heterozygosity in colorectal tumors (Fearon et al., 1990; Keino-Masu et al., 1996). While the original DCC-null knockout analyses showed no differences in tumorigenesis, researchers identified a major neural-developmental phenotype that included dysregulated axon guidance and identified DCC as a receptor for netrin-1 (Fazeli et al., 1997). Mice lacking DCC have severe commissural axon guidance defects, with the majority of commissural axons failing to cross the midline, phenocopying the netrin-1 deficient mice (Fazeli et al., 1997; Serafini et al., 1996). The DCC family of receptors includes DCC and neogenin in mammals (Cho et al., 1994; Vielmetter et al., 1997); Unc 40 in *C. elegans* (Chan et al., 1996); and Frazzled in *D. melanogaster* (Kolodziej et al., 1996). DCC and neogenin are structurally similar members of the immunoglobulin (Ig) superfamily of proteins and contain four Ig repeats, six fibronectin type 3 domains, a transmembrane domain, and an intracellular domain comprised of three conserved domains, P1, P2 and P3 (Figure 1.2) (Keino-Masu et al., 1996). Neogenin is not as well characterized as DCC; however, there is evidence that it mediates attractive responses when bound to netrin-1 and repulsive responses when bound to repulsive guidance molecule (RGM) (De Vries & Cooper, 2008). Additionally, it is believed neogenin can functionally substitute for DCC in organisms that do not express DCC, such as birds (Phan et al., 2011). In rodent spinal cord, DCC is highly expressed in commissural neurons starting at E11 and expression in the nervous system continues into the adult (Horn et al., 2013; Keino-Masu et al., 1996). Homodimers of DCC have been proposed to mediate the attractive response of neurons to netrins, while heterodimers of DCC and UNC-5 mediate the repulsive response to netrins (Hong et al., 1999).

II.iii. Netrin-1 and DCC Signalling

Crystal structures indicate that netrin-1 binds DCC at the fourth and fifth fibronectin type III (FNIII) repeats leading to receptor multimerization (Figure 1.3) (Finci et al., 2014; K. Xu et al., 2014). The intracellular domain of DCC is constitutively bound to Nck-1 and focal adhesion kinase (FAK) and these interactions are independent of netrin-1 binding to DCC (Li et al., 2004; Ren et al., 2004). Netrin-1 binding to DCC initiates several downstream signalling cascades starting with DCC phosphorylation, a step critical for appropriate commissural axon guidance (Lai Wing Sun et al., 2011). Signalling is proposed to initiate with the homodimerization of the P3 domain of DCC, which leads to the clustering of FAK and a helix 1 swap of the focal adhesion targeting domains (FAT) of FAK (Stein, Zou, Poo, & Tessier-Lavigne, 2001; S. Xu et al., 2018). Netrin-1 is thought to stabilize this interaction by clustering DCC on the surface which brings the FAT domains into close proximity to each other. This allows for the helix swap to occur and initiates an influx of calcium ions that further stabilizes the helix swap confirmation of the FAT domains (S. Xu et al., 2018). Clustering of FAK and interaction with phosphatidylinositol 4,5-bisphosphate (PIP2) at the membrane leads to the release of FAK autoinhibition, autophosphorylation of FAK, and initiation of signalling downstream of DCC (S. Xu et al., 2018). Phosphorylated FAK then recruits and activates src family kinases (SFKs), specifically Fyn, and both FAK and SFKs phosphorylate DCC.

Netrin-1 binding DCC also leads to the recruitment and activation of P21 activated kinase (Pak) 1, cell division control protein 42 (CDC42), and Rac1, all of which are required for growth cone expansion. Pak1 is recruited to the receptor complex through interactions with Nck-1, while SFKs regulate the recruitment and activation of Rho GTPase family members CDC42 and Rac1 (Shekarabi & Kennedy, 2002; Shekarabi et al., 2005). Evidence has been obtained that these

proteins, along with neural Wiskott-Aldrich syndrome protein (N-WASP), are recruited into a complex with the DCC receptor when it is bound to netrin-1 (Shekarabi et al., 2005). The Rho GTPases, including CDC42 and Rac1, play key roles mediating the organization of the actin cytoskeleton within the growth cone. Specifically, CDC42 regulates the formation of filopodia and Rac1 regulates the formation of lamellipodia (Ridley, 2001).

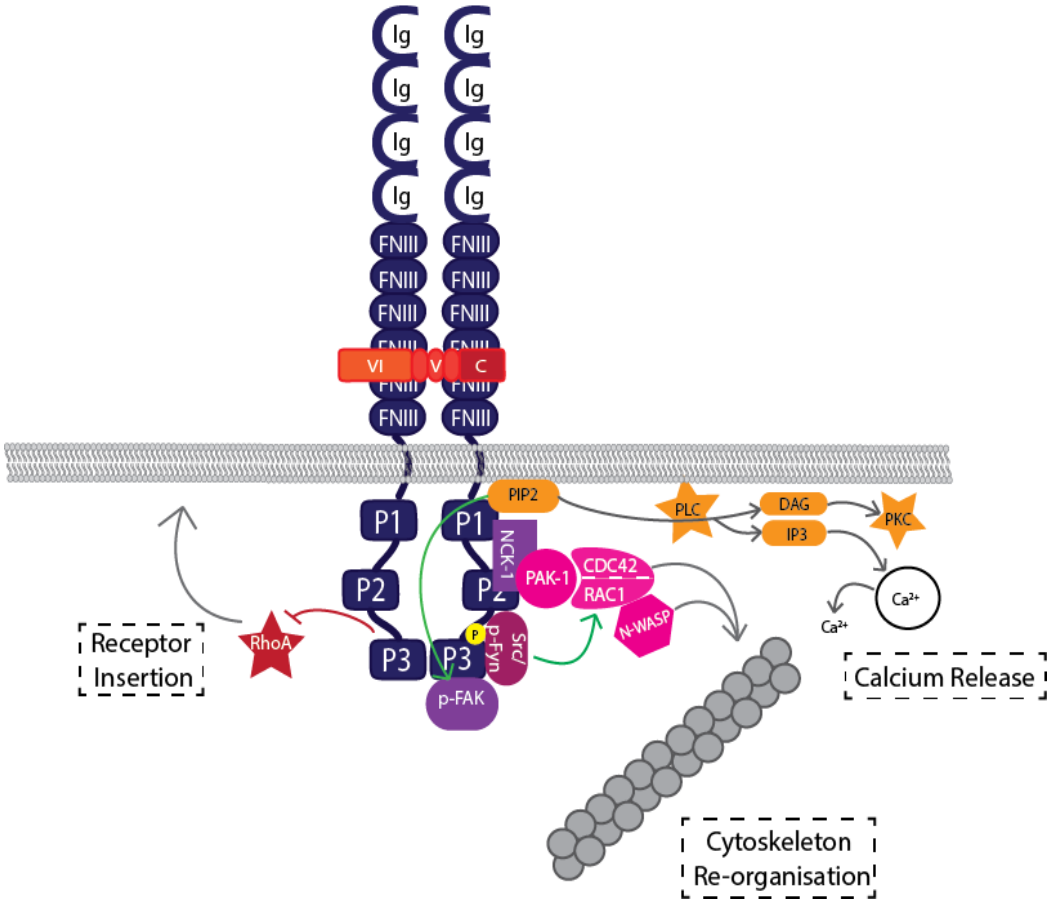

Figure 1.3: DCC signalling mechanisms

NCK-1 and FAK are constitutively bound to DCC. Netrin-1 binding leads to clustering of DCC, autophosphorylation of FAK, recruitment of SFKs and Pak1, and activation of CDC42 and RAC1. This signalling then leads to reorganization of the actin cytoskeleton. Downstream inhibition of RhoA increases DCC receptor insertion, and activation of PIP2 synthesis promotes release of calcium from intracellular stores.

The localization of DCC to the plasma membrane can also be regulated by netrin-1 signalling. Netrin-1 binding to DCC inhibits RhoA, which leads to an increase in growth cone expansion and increases the amount of DCC localized to the plasma membrane (Moore et al., 2008). This creates a positive feedback loop where DCC signaling increases its own surface expression to enhance commissural axon guidance (Moore et al., 2008). Protein kinase A (PKA) activation also leads to the insertion of DCC on the plasma membrane from intracellular vesicular pools, thus increasing growth cone sensitivity to netrin-1. Moreover, in cortical neurons, depolarization of the cell also leads to an increase in plasma membrane DCC expression (Bouchard, Horn, Stroh, & Kennedy, 2008; Bouchard et al., 2004). The regulation of DCC surface expression and the downstream signalling cascade initiated through netrin-1 binding mediate a number of cellular processes as outlined above (Figure 1.3).

II.iv. Netrin-1 Function

Netrin-1 is most characterized for its role guiding developing commissural neurons toward the floor plate and across the ventral midline. Netrin-1 also has a number of diverse functions in addition to axon guidance. In the nervous system, netrin-1 regulates cell migration; axon branching; synaptogenesis; synapse function and long-term potentiation (LTP); oligodendrocyte development; and myelin maintenance (Lai Wing Sun et al., 2011). Outside the nervous system, netrins have been demonstrated to regulate cell adhesion in the developing mammary gland and pancreas, and branching in the lung and vasculature system (Baker, Moore, Jarjour, & Kennedy, 2006). For the purposes of this thesis, the function of netrin-1 in the nervous system, specifically in axon guidance and synapse formation, will be covered in detail.

In the CNS, netrin-1 can function both as a short-range cue, adhering to the surface of a cell that produced it to exert local effects; or as a long-range secreted cue, diffusing through the

extracellular matrix (ECM) and affecting cells up to several cell diameters away. In the developing spinal cord, netrin-1 is secreted by floor plate cells and creates a gradient of netrin-1 that is high ventrally and low dorsally (Kennedy et al., 1994). This gradient of netrin-1 directs growing commissural axons towards the ventral midline of the spinal cord (Kennedy, Wang, Marshall, & Tessier-Lavigne, 2006). Axon turning assays have demonstrated that netrin-1 functions as a long range directional cue causing commissural growth cone turning at a distance from the netrin-1 source (de la Torre et al., 1997; Kennedy et al., 1994; Ming et al., 1997). Cultured retinal ganglion cells (RGC) and spinal neurons from *Xenopus laevis* were shown to turn towards a local source of soluble netrin-1 puffed into culture from a micropipette. Further, this turning was demonstrated to depend on DCC (de la Torre et al., 1997; Ming et al., 1997). Additionally, culturing floor plate cells or netrin-1 expressing COS cells parallel to the normal direction of axon extension in embryonic spinal cord was sufficient to cause a deflection in the trajectory of axon growth. For DCC expressing commissural axons, this deflection in growth is towards the netrin-1 expressing cells and can occur at a distance up to several hundred micrometers away (Fazeli et al., 1997; Kennedy et al., 1994). These experiments provided strong evidence that netrin-1 functions as a long-range chemotropic guidance cue.

Recently, controversy arose regarding the capacity of netrin-1 to function as a long-range chemotropic guidance cue. A series of papers argued that netrin-1 does not form a gradient and functions only as a short-range permissive cue (Dominici et al., 2017; Varadarajan et al., 2017; Yamauchi et al., 2017). These papers questioned the significance of netrin-1 being secreted by floor plate cells by demonstration that netrin-1 originating from neural progenitor cells of the ventricular zone is important for commissural axon guidance, a source that had largely been ignored (Dominici et al., 2017; Varadarajan et al., 2017; Yamauchi et al., 2017). However,

further investigation showed that selective deletion of netrin-1 from floor plate cells in embryonic mouse spinal cord does cause a disruption in commissural axon trajectories, supporting a role for floor plate derived netrin-1 (Moreno-Bravo, Roig Puiggros, Mehlen, & Chedotal, 2019; Wu et al., 2019). Although the relative significance of long-range vs short-range functions can still be debated, it is absolutely clear that netrin-1 is critical for proper development of the spinal cord.

Netrins also function in the adult animal, and many of these functions appear to depend on short-range actions, including roles at synapses and in myelination. Manitt *et al.* (2009) showed that through a DCC-mediated pathway, netrin-1 modulates RGC axon branching during innervation of the tectum in *Xenopus laevis*. Blocking DCC function in RGC axons reduced the formation of new synapses and decreased netrin-1 induced axonal branching; however, this had no effect on the stability of already formed synapses (Manitt, Nikolakopoulou, Almario, Nguyen, & Cohen-Cory, 2009). In the rat, netrin-1 promotes the formation of excitatory synapses in the cortex during early development (Goldman et al., 2013). Netrin-1 increases the formation of filopodia along axons and dendrites, and netrin-1 coated beads promote adhesion and recruit synaptic proteins to the site of bead contact (Goldman et al., 2013). DCC is enriched in dendritic spines and regulate synapse function and plasticity in hippocampal neurons (Horn et al., 2013). Conditional knockout of DCC at post-natal day 14 leads to a decrease in the size of dendritic spines and impaired N-methyl-D-aspartate receptor (NMDAR) dependant LTP (Horn et al., 2013). Conditional knockout of either netrin-1 or DCC from mature forebrain glutamatergic neurons in mice results in reduced frequency but not amplitude of miniature excitatory post synaptic currents (mEPSCs), and addition of exogenous netrin-1 to hippocampal slices is sufficient to induce a prolonged increase in mEPSCs in CA1 hippocampal neurons (Glasgow et

al., 2018; Goldman et al., 2013). Activity-dependant release of netrin-1 from dendritic spines has also been shown to be required for LTP in hippocampal neurons (Glasgow et al., 2018). These results indicate that netrin-1 and DCC may play a role both in stabilizing synaptic contacts during development, and in the maintenance and function of synapses in the adult organism.

III. Synaptic Development

Synapses are specialized adhesive junctions that link one neuron to another and allow for directional communication between cells. The term synapse was first coined by Charles Sherrington and comes from the Greek roots "syn" meaning together and "haptein" meaning to clasp (Foster & Sherrington, 1897). Synapses are comprised of closely opposed pre- and post-synaptic boutons with a small space, the synaptic cleft, between the two membranes. The pre-synapse is defined by the accumulation of synaptic vesicles near the membrane surface of the active zone, while the post-synapse is defined by a dense scaffold of molecules known as the post-synaptic density (PSD) (Garner, Zhai, Gundelfinger, & Ziv, 2002). Synapses can be chemical or electrical in nature. In a chemical synapse, neurotransmitters are released from vesicles in the active zone of the pre-synaptic membrane, diffuse across the cleft, and bind to receptors on the post-synaptic membrane (Sudhof, 2018). In excitatory neurons, binding of the neurotransmitter to the post-synaptic receptors triggers an influx of ions that depolarizes the cell and initiates an action potential (Sudhof, 2018). Glial cells surround the synapse and can modulate neurotransmitter availability through impacts on neurotransmitter re-uptake and degradation (Araque, Parpura, Sanzgiri, & Haydon, 1999). The pre- and post-synaptic membranes along with the glial cell process is known as the "tripartite" synapse (Araque et al., 1999).

When an axon or pre-synaptic filopodium reaches its postsynaptic target, a series of events must occur in order for this contact to develop into a functional synapse. The initial contact is stabilized by synaptic adhesion proteins, leading to a change in membrane structure on both sides of the synaptic contact. Pre- and post-synaptic proteins are then recruited to the site of contact, forming an immature synapse that will either mature into a functional synapse or be pruned away (Sudhof, 2018).

The pre- and post-synaptic membranes must be anchored in close proximity to one another through the engagement of cell adhesion molecules (CAMs). Cadherins, in particular, a large family of calcium dependent adhesion molecules, have been proposed to provide a code to help neurons find their appropriate synaptic partners (Price, De Marco Garcia, Ranscht, & Jessell, 2002). The role of cadherins in synapse formation is discussed in detail in the section below. In addition to cadherins, multiple other cell adhesion molecules and signalling molecules are enriched at synapses to regulate formation and function, including netrin-1 and DCC, as described above.

IV. Cadherins

Cadherins are a large superfamily of calcium-dependant CAMs, many of which are expressed in the nervous system. The cadherin superfamily of proteins can be subdivided into many smaller families including classical cadherins, protocadherins, desmosomal cadherins, fat-like cadherins, seven pass transmembrane cadherins, and cadherin related molecules such as ret (Yagi & Takeichi, 2000). All cadherin superfamily members have an extracellular domain comprised of a conserved structure called a cadherin repeat, but vary greatly in their intracellular domains, which likely accounts for differences in signalling and function. Some of the main functions of

the cadherin superfamily of proteins include cell-cell adhesion and cell sorting; and as a consequence of those functions, they also play an important role in regulating tissue morphology (Takeichi, 1991).

IV.i. Classical Cadherins

Classical cadherins are a major transmembrane component of adherence junctions and are important regulators of cell-cell adhesion (Shapiro & Weis, 2009). Mammalian classical cadherins consist of an extracellular domain comprised of five extracellular cadherin repeats, a transmembrane domain, and an intracellular domain (Figure 1.4) (Shapiro & Weis, 2009). Classical cadherins can be further subdivided into type I and II classical cadherins based on the presence or absence, respectively, of the HAV tripeptide motif in the first extracellular cadherin repeat (Patel, Chen, Bahna, Honig, & Shapiro, 2003). Type I classical cadherins include: E-cadherin, N-cadherin, P-cadherin, R-cadherin and M-cadherin; while type II includes: CDH 5-12, 18-22, and 24 (Gul, Hulpiau, Saeys, & van Roy, 2017). The extracellular (EC) domain mediates calcium binding to cadherins as well as cadherin-cadherin binding; while the intracellular domain is important for binding to the catenin family of proteins, and for cell signalling and cadherin function (S. T. Suzuki, 1996). Cadherins form clusters on the cell surface and bind *in trans,* often exhibiting homophilic specificity, to cadherins present on opposing cells, promoting strong cell-cell adhesion (Weis, 1995). Some instances of heterophilic cadherin binding have also been demonstrated, though these interactions tend to be weaker than homophilic binding interactions (Shimoyama, Tsujimoto, Kitajima, & Natori, 2000).

Without calcium present, cadherins are globular and unable to bind to each other *in trans* (Weis, 1995). When calcium binds to the EC of cadherins they become rigid and undergo a conformational change that allows cadherin-cadherin binding (Weis, 1995). Evidence from

crystal structures suggests that the EC domain of calcium-bound cadherins is curved resulting in EC1 and EC5 being at nearly right angles to each other (Shapiro & Weis, 2009). This curved confirmation results in the EC1 domain of the two *trans*-oriented cadherins being parallel to one another, which is crucial for adhesive function and likely mediates binding specificity (Figure 1.4A) (Shapiro & Weis, 2009). The force across a *trans* dimer of cadherins is relatively low given their need to regulate adhesion. The formation of a strand dimer increases binding strength, as the forces across multiple cadherin complexes add up to a much higher adhesive strength (Zhang, Sivasankar, Nelson, & Chu, 2009). Early evidence suggested that molecules of N cadherin form a strand dimer through *cis*-binding, resulting in the formation of a "cadherin zipper"; however, *cis* dimers have been found to only form under conditions of low calcium, which in turn would prevent *trans* binding (Shapiro & Weis, 2009; Weis, 1995; Zhang et al., 2009). Attempting to resolve this cadherin binding conundrum, Zhang *et al.* (2009) used fluorescence resonance energy transfer (FRET) analysis to determine binding orientations. They found that cadherins only bind in *trans* through their EC1 domain and that binding initiates lateral clustering of cadherins that then results in an increase in the number of cadherin dimers in the adhesive complex (Zhang et al., 2009). Thus, cadherin clustering and not *cis*-binding is important for adhesive strength across the membrane.

The intracellular domain of classical cadherins links to the actin cytoskeleton and other signalling pathways through the binding of catenins (Shapiro & Weis, 2009). P120 catenin and β-catenin can bind directly to the cytoplasmic tail of cadherins, while α-catenin binds to β-catenin but does not directly interact with the cadherin tail. Catenins are important regulators of actin dynamics within the cell and participate in Wnt signalling pathways to regulate gene expression. Engagement of cadherins also regulates the Rho family of GTPases and, similar to

DCC, cadherins interact with CDC42, Rac1, and RhoA (Noren, Niessen, Gumbiner, & Burridge, 2001).

Epithelial or E-cadherin is found in all tissue outside the nervous system while neural, or N-cadherin, is the main cadherin found inside the nervous system. The differential expression of these two cadherins is crucial for cell sorting in early embryonic development. Cells that initiate expression of N-cadherin will become neural tissue, while cells that express E-cadherin will persist as ectoderm and form all of the tissue outside the nervous system (Takeichi, 1991). The ability of cells to selectively adhere to cells of like type; e.g., neural to neural; is critical to sort cells as a prelude to proper tissue development and the formation of neuronal connections. The differential expression of different cadherins is critical for many cell types at different stages of development to find and adhere to their proper cellular partners (Takeichi, 1991). It has been proposed that cadherins are also involved in regulating the organization of neurons into circuits based on specific cadherin expression in different brain regions. For example, expression of CDH6 is important for correct formation of auditory tracts, while CDH9 regulates synaptic sorting between dentate gyrus and CA3 hippocampal neurons (Suzuki et al., 2011). Type II classical cadherins in particular have been suggested to play a role in neuron sorting and synapse specificity (Price et al., 2002). A portion of the work done in this thesis focuses on the type II classical cadherin, cadherin 12.

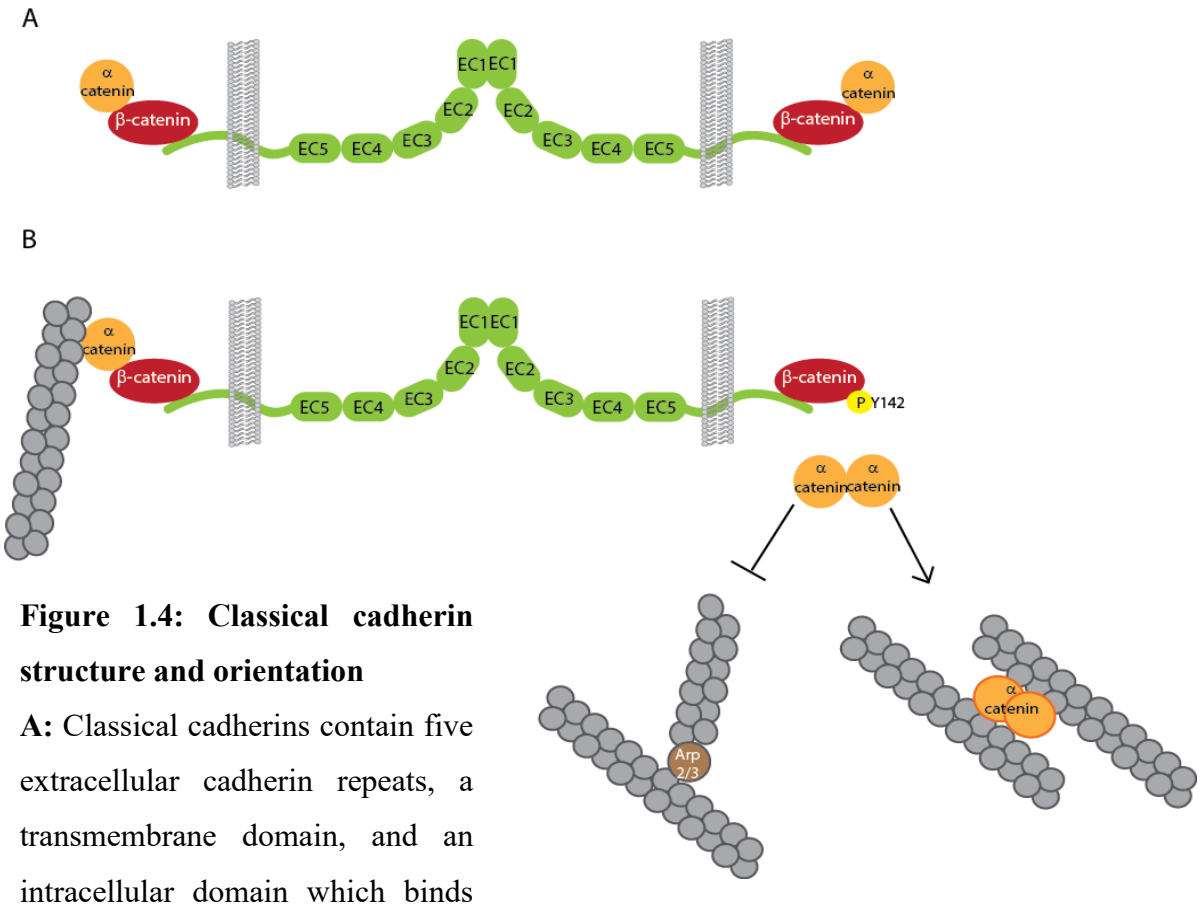

Figure 1.4: Classical cadherin structure and orientation

A: Classical cadherins contain five extracellular cadherin repeats, a transmembrane domain, and an intracellular domain which binds to catenins.

B: Left: Textbook model of cadherin, catenin, actin interaction. **Right:** mutually exclusive model of cadherin, catenin, actin interaction.

IV.i.a. Cadherin 12

Cadherin 12 (CDH12), also termed brain cadherin or N-cadherin-2, is a type II classical cadherin expressed in the central nervous system (Mayer, Bercsenyi, Geczi, Szabo, & Lele, 2010). Tanihara *et al.* (1994) were the first to clone CDH12 and showed that it has two unique amino acid additions: one amino acid addition near the N-terminus and a short sequence of amino acids near the C-terminus (Tanihara, Sano, Heimark, St John, & Suzuki, 1994). The role of CDH12 has been investigated primarily in cancer cell metastasis (J. F. Wang et al., 2011; Zhao et al.,

2013). In both colorectal cancer and salivary adenoid cystic carcinoma, CDH12 expression was increased in cancer tissue compared to normal tissue (J. F. Wang et al., 2011; Zhao et al., 2013). Increased CDH12 expression was also correlated with an increase in migration and tissue invasion indicating a role in cancer cell metastasis. Furthermore, CDH12 has been shown to promote the epithelial to mesenchymal transition (EMT) in colorectal cancer cells, further enhancing cancer cell migration and invasion (Ma et al., 2016). Although the function of CDH12 has mainly been studied in cancer cells, its expression in the CNS has been briefly described. CDH12 was initially described in both human and mouse brain under the name "brain cadherin" and was found to be present in the grey matter of both species using northern blot analysis (Selig, Lidov, Bruno, Segal, & Kunkel, 1997). To further characterise the expression of CDH12 in the developing and adult mouse, Mayer *et. al* (2010) used *in situ* hybridization and RT-PCR to detail CDH12 mRNA expression in different brain areas. Expression of CDH12 mRNA begins at ~E12.5 and continues into the adult, with expression peaking at approximately post natal day 7 (P7) (Mayer et al., 2010). CDH12 mRNA is expressed throughout the brain, including in many cortical and subcortical regions and in the hippocampus; however, very little work has been done to describe the function of CDH12 in the nervous system (Mayer et al., 2010).

IV.ii. Cadherin Function in the Nervous System

Cadherins play a critical role in cell-cell adhesion and cell sorting. In the nervous system this can be extended to functions in synapse formation, cell migration, and axon guidance. Cadherin proteins have been found to be enriched at synapses in the CNS and evidence suggests that cadherins also play a role in synaptogenesis (Arikkath & Reichardt, 2008; Fannon & Colman, 1996). N-cadherin is highly expressed at central synapses and has been shown to be one of the first molecules to become enriched at developing synapses (Shapiro & Colman, 1999). Cadherins

are important for stabilizing dendritic spines and for spine maturation, and without cadherin accumulation the initial synaptic contact falls apart (Bamji, 2005). Overexpression of dominant negative N-cadherin prevents spine head maturation as well as the accumulation of synaptic vesicles at the site of synaptic contact (Takeichi & Abe, 2005). N-cadherin knockouts have defects in synaptic transmission, synaptic vesicle recycling, and LTP, demonstrating the important role for N-cadherin in synaptic function (Bozdagi, Shan, Tanaka, Benson, & Huntley, 2000; Bozdagi, Valcin, Poskanzer, Tanaka, & Benson, 2004; Jungling et al., 2006; Saglietti et al., 2007). Pre-treating neuronal cultures with an antibody against the extracellular domain of N-cadherin does not change basal synaptic transmission, but does significantly impair LTP (Tang, Hung, & Schuman, 1998). Interestingly, cadherin 11 knockout cultures have enhanced LTP with no effect on basal synaptic transmission (Manabe et al., 2000). These differential effects on synaptic function highlight the diversity of cadherin function within the same protein family, though the effects of other cadherin family members on synaptic function still need to be investigated in greater detail.

The main described synaptic function for cadherins is adhesion. They regulate synaptic stability by holding the pre- and post-synapse together through *trans*-binding across the synaptic cleft. Electrical activity at the synapse leads to dimerization of N-cadherin into a protease resistant complex, stabilizing the nascent synapse (Salinas & Price, 2005). While N-cadherin is important for synapse formation and maintenance, the widespread expression of N-cadherin throughout all neuronal tissue makes it a poor candidate for regulating synaptic sorting. Type II classical cadherins, however, are much less ubiquitously expressed and combinatorial expression of these cadherins could provide a cadherin code for synapse and circuit formation (Redies & Takeichi, 1996). Subsets of cadherins are expressed on specific cells, and cells which express the

same combination of cadherins will synapse with each other creating a role for cadherins in mediating synaptic specificity (Fannon & Colman, 1996; Redies, 1995). Cadherin 9 (CDH9) has been shown to regulate circuit formation in the hippocampus where both dentate gyrus (DG) and CA3 neurons express CDH9, while CA1 neurons do not, leading to targeted synapse formation (Williams et al., 2011). Additionally, DG neurons in culture will avoid CA1 neurons while specifically synapsing with CA3 neurons, a process which is dependant on cadherin expression (Williams et al., 2011). In the retina, CDH8 and CDH9 are expressed by distinct classes of bipolar cells and regulate synaptic specificity and circuit formation (Duan, Krishnaswamy, De la Huerta, & Sanes, 2014). Combinatorial expression of cadherins -6, -8, and -11, are important for defining specific circuits in the forebrain (S. C. Suzuki et al., 1997); and in the spinal cord combinatorial expression of MN-cadherin, T-cadherin, and cadherins -6, -7, -8, and -10 regulate the sorting of motor neuron pools (Price et al., 2002). Differential and combinatorial expression of cadherins throughout the nervous system is hypothesized to function as a "cadherin code" for appropriate synapse and circuit formation, ultimately contributing to the appropriate development of the organism.

In addition to synapse functions, cadherins have also been shown to make functional contributions to axon guidance during neural development. Two separate studies found that extending axons will follow a layer of cells that express complimentary cadherins (Matsunaga, Hatta, Nagafuchi, & Takeichi, 1988; Redies, Inuzuka, & Takeichi, 1992). Axons expressing N-cadherin grow specifically along a path of cells that has been transfected to express N-cadherin while avoiding non-expressing cells (Matsunaga et al., 1988; Redies et al., 1992). This suggests that cadherins contribute to axon guidance by creating a permissive cellular path for axons to adhere to and follow until they reach their target.

N-cadherin also interacts with Robo during commissural axon guidance acting to properly sort post crossing commissural axons into the ventral and lateral funiculi (Sakai et al., 2012). High Robo expression on intermediate longitudinal commissural neurons inhibits N-cadherin mediated adhesion, allowing these axons to join the lateral funiculus tract (Sakai et al., 2012). In the absence of Robo expression, or with overexpression of N-cadherin, commissural neurons are not properly sorted. High levels of N-cadherin expression results in all commissural neurons targeting the ventral funiculus tract, thereby preventing the formation of the lateral funiculus (Sakai et al., 2012). N-cadherin has also been shown to play a role in commissural axon guidance in chick embryos by regulating β-catenin protein localization (Yang et al., 2016). N-cadherin knockdown leads to an accumulation of β-catenin in the nucleus of neurons, while overexpression results in accumulation at the plasma membrane (Yang et al., 2016). Additionally, either N-cadherin overexpression or knockdown leads to a reduced number of commissural neurons reaching the contralateral side of the spinal cord. Those that do make it stay within the ventral funiculus, and in turn the lateral funiculus fails to form (Yang et al., 2016).

Interestingly, DCC also influences the mRNA expression and protein levels of N-cadherin in neuroblastoma cells. While increased Robo leads to a decrease in N-cadherin, DCC appears to have the opposite effect with overexpression of full length DCC leading to a slight increase in N-cadherin and β-catenin mRNA expression (Reyes-Mugica et al., 2001). Expression of a truncated DCC lacking the cytoplasmic tail causes a significant decrease in N-cadherin, β-catenin, and α-catenin mRNA expression and protein levels (Reyes-Mugica et al., 2001). This indicates that the cytoplasmic tail of DCC is important in regulating cadherin and catenin expression, although the function of this remains unknown (Reyes-Mugica et al., 2001).

Together, these studies show that cadherins play an important role in axon guidance, specifically commissural axon guidance, along with their well-established roles at the synapse and in cellular adhesion. The work in this thesis aims to further elucidate mechanisms for cadherin function in axon guidance.

V. Catenins

Cadherin engagement leads to the activation of catenins which are important downstream signalling molecules that regulate cadherin function. The catenin family of proteins are well studied cadherin binding partners that link the intracellular domain of cadherins to the actin cytoskeleton. Catenin family members include α-catenin, β-catenin, and P120 catenin (McCrea & Gu, 2010). While α-catenin and P120 catenin are primarily involved in cadherin signalling, β-catenin functions as a critical mediator of both cadherin adhesion and Wnt signalling as a transcription factor to directly regulate gene expression (McCrea & Gu, 2010). The textbook model of cadherin/catenin function consists of cadherin bound to β-catenin, β-catenin bound to α-catenin, and α-catenin bound to F-actin, creating a chain-like linkage to the cytoskeleton (Figure 1.4B) (Drees, Pokutta, Yamada, Nelson, & Weis, 2005). However, recently studies have revealed that reconstituting this binding *in vitro* is problematic, as α-catenin will only bind one of β-catenin or F-actin at a time, and the binding is mutually exclusive (Figure 1.4B) (Drees et al., 2005). This modification to the model contains no physical link between cadherins and the F-actin cytoskeleton, and indicates that α-catenin needs to be released from the β-catenin/cadherin complex in order to mediate actin polymerization (Drees et al., 2005). Phosphorylation of β-catenin at Y142 regulates the binding of α-catenin to β-catenin (Piedra et al., 2003). When Y142 is phosphorylated, β-catenin can no longer bind to α-catenin, releasing α-catenin into the cytosol.

Released α-catenin exists as a homodimer that binds actin filaments and inhibits the Arp2/3 complex, shifting actin polymerization from branched sheets to linear bundles, a process required for filopodia formation (Figure 1.4B) (Drees et al., 2005). Phosphorylation of serine and threonine residues in the N-terminal region of β-catenin targets it for degradation while phosphorylation of serine and threonine residues in the middle of the protein promotes its stability (Valenta, Hausmann, & Basler, 2012). Tyrosine phosphorylation at several residues throughout the protein regulates β-catenin signalling and its association with cadherin proteins (Valenta et al., 2012). Thus, kinase dependent signaling can balance β-catenin association with cadherins and regulate its participation in canonical Wnt signalling. To participate in Wnt signalling, β-catenin must first be released from the cadherin adhesion complex, and this is regulated by phosphorylation of β-catenin at a number of residues (Daugherty & Gottardi, 2007; Verheyen & Gottardi, 2010). Activation of Wnt signaling inhibits the β-catenin destruction complex, leading to β-catenin accumulation in the cytosol and subsequent translocation to the nucleus where it acts as a transcription factor that regulates the expression of Wnt targeted genes (Stamos & Weis, 2013). The vast repertoire of β-catenin interactions regulates multiple different cellular processes including synaptic vesicle accumulation, dendritic spine morphology, axon guidance, axon regeneration, and gene transcription (Bamji et al., 2003; Okuda, Yu, Cingolani, Kemler, & Goda, 2007).

VI. Concluding Remarks

The coordinated response of neurons to many cues in the nervous system is required for proper growth, guidance, and synapse formation. The interplay between cell adhesion molecules and axon guidance cues is proving to be an interesting field of study as both molecules play an

important role in developmental processes in the nervous system. The regulation of adhesion is important for many cellular processes. Targeted cell-cell adhesion is required for axon guidance and synapse formation. Cells must regulate the degree of adhesion in order to migrate in the proper direction and make the appropriate connections. Understanding how axon guidance cues may help regulate the function of cell adhesion molecules will provide critical insights into the complex development of the nervous system. In turn, knowing how these initial growth pathways function will allow them to be isolated as therapeutic targets and perhaps manipulated to promote recovery of functions that have been lost following injury or disease in the adult.

Preface

Individual cells within the CNS are supported in their environment by a complex mix of extracellular proteins and glycosaminoglycans (GAGs) which form a structure known as the extracellular matrix (ECM). The ECM has a multitude of functions including, but not limited to providing structural support for cells; anchoring and sequestering secreted molecules; and acting in a complex with secreted and membrane-bound proteins to regulate their function (Frantz, Stewart, & Weaver, 2010).

The composition of the ECM determines tissue strength and elasticity, which in turn can regulate cell migration, growth, and differentiation (Frantz et al., 2010). The structure and function of the ECM not only varies throughout development but also across brain regions, leading to a large degree of local diversity and the opportunity to affect multiple cellular functions. Given the potential of the ECM to influence neuronal function, it is important to understand how the ECM interacts with various proteins during development and in the adult CNS. This introductory section provides an overview of the structure and functions of the ECM in the nervous system and will address perineuronal nets (PNNs), a highly specialized ECM structure.

.

Chapter 2

Literature Review II – Proteoglycans and Neuronal Extracellular Matrix

I. Proteoglycans

Proteoglycans (PGs) are a diverse group of macromolecules made up of a core protein decorated with one or more long unbranched glycosaminoglycan (GAG) side chain (Couchman & Pataki, 2012). PGs are classified into four sub families: chondroitin sulfate/dermatan sulfate (CS/DS), heparan sulfate (HS), keratan sulfate (KS), and hyaluronic acid (HA). Classification is based on the repeating sugar unit of the GAG chain (Figure 2.1 B-D) (Schaefer & Schaefer, 2009). GAG side chains are attached to a serine residue within the core protein via a tetra-saccharide linker, with the exception of HA which is not attached to a core protein and exists only as a GAG chain (Figure 2.1 A) (Schaefer & Schaefer, 2009). This linker region consists of a xylose-galactose-galactose-glucuronic acid, where the xylose is attached to the serine residue in the core protein and the glucuronic acid is attached to the GAG side chain (Kearns, Vertel, & Schwartz, 1993). Following core protein synthesis, PGs are translocated through the endoplasmic reticulum (ER) and Golgi apparatus where glycosylation occurs (Kearns et al., 1993). In the ER, xylose is added to the core protein serine residues by xylose transferase. The protein is then delivered to the Golgi apparatus where the remaining linker residues are sequentially added by Gal I, Gal II, and GlcA I transferases (Kearns et al., 1993; Silbert & Sugumaran, 2002). The sugar composition of the GAG side chain determines which PG family the core protein belongs to and is conferred by the first residue added following the linker region. For example, addition of N-acetyl-D-glucosamine (GlcNAc) will designate an HS chain, while addition of N-acetyl-D-galactosamine

(GalNAc) will designate a CS chain (Bulow & Hobert, 2006). Repeating disaccharide units are added by the appropriate transferases creating an elongated GAG chain and sulfotransferases, epimerases, and sulfatases found in the Golgi apparatus can then sulfate and further modify the GAG chain. The finished protein is then exocytosed and integrated into the ECM (Bulow & Hobert, 2006).

Proteoglycans are extremely heterogenous and diverse as there can be variations not only in the core protein, but also in the GAG chain length, type, sulfation pattern, and the number of chains attached to any given core protein (Ruoslahti, 1988). PGs in the ECM can passively bind and regulate the function of other proteins by increasing their local concentration. PGs do so by tethering and accumulating the proteins of interest within a specific area or by increasing a proteins stability, allowing it to remain active longer (Fuerer, Habib, & Nusse, 2010). PGs can also play an active role in molecular signalling by cross-linking ligands to their receptors or by acting as a co-receptor in regulating ligand-receptor interactions to initiate downstream signalling (Holt & Dickson, 2005). Heparan sulfate proteoglycans (HSPGs) and chondroitin sulfate proteoglycans (CSPGs) interact with a variety of proteins in the developing and adult CNS. Understanding how PGs interact with other proteins will provide important insights into their function regulating axon growth and guidance and synapse formation and function in the CNS.

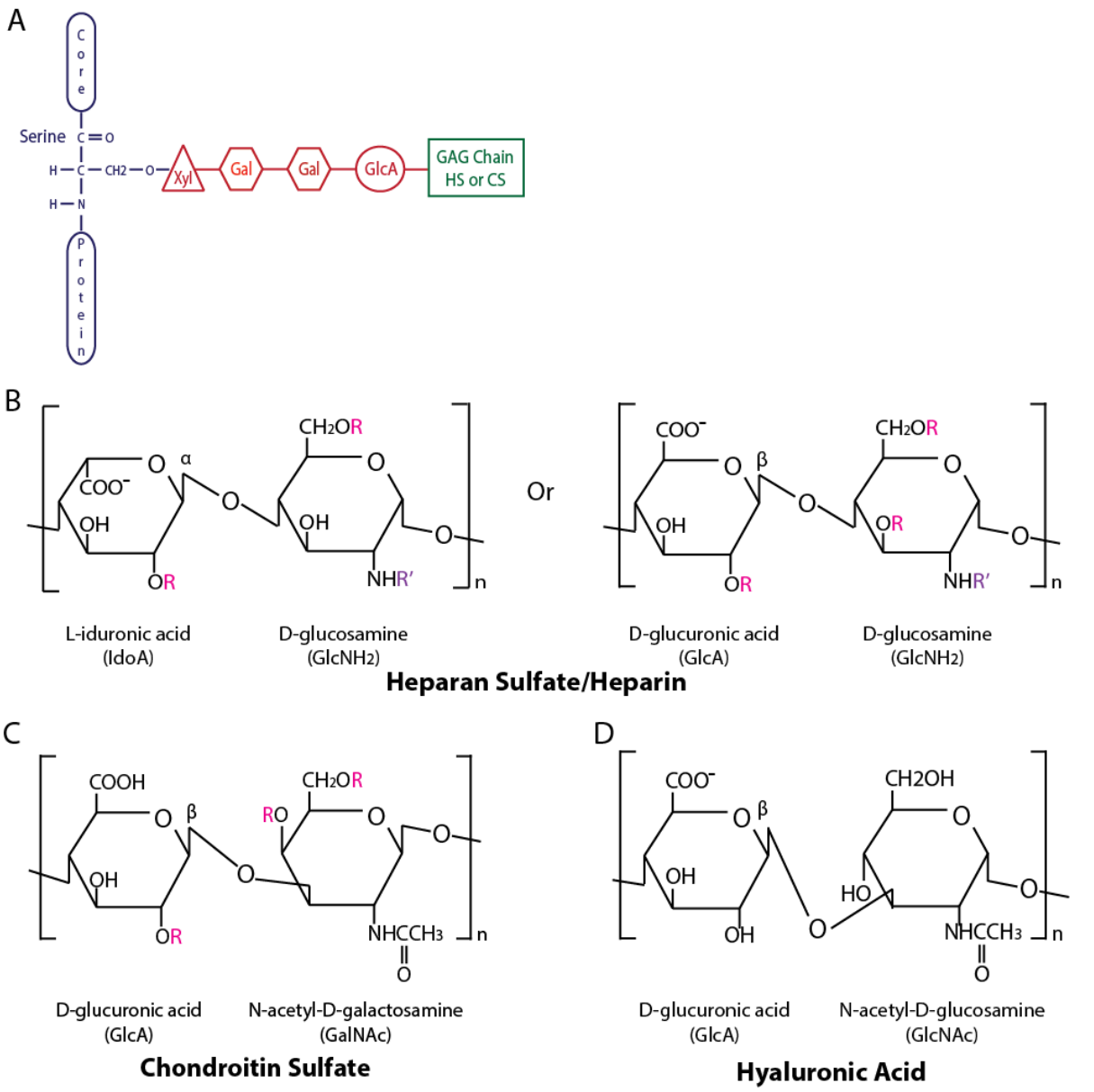

Figure 2.1: Proteoglycan structure. A: GAG chains are linked to the core proteins at serine residues through a tetra saccharide linker of xylose-galactose-galactose-glucuronic acid. **B:** Disaccharide structure of heparan sulphate and heparin proteoglycans. **C:** Disaccharide structure of chondroitin sulfate proteoglycans. **D:** Disaccharide structure of hyaluronic acid. Pink R represents sites of possible sulfation (HS and CS) and purple R' represents sites of possible acetylation (HS).

I.i. Heparan Sulfate Proteoglycans

HS GAG chains are comprised of a repeating disaccharide unit of D-glucuronic acid (GlcA) – GlcNAc. The GlcA can be epimerized into L-iduronic acid (IdoA) resulting in two possible configurations of the repeating sugar unit (Figure 2.1 B) (Holt & Dickson, 2005). Heparin is a heavily sulfated form of heparan sulfate that is primarily produced in mast cells (Rönnberg, Melo, & Pejler, 2012). HS GAG chain elongation is carried out by the exostosin (EXT) family of glycosyl transferases. Sulfation is regulated through N-deacetylases/N-sulfotransferases which replace acyl groups with sulfate groups and O-sulfotransferases which add sulfate groups to the 3-O-, 2-O-, or 6-O- residue (Holt & Dickson, 2005). HS chain modification creates discrete domains of similarly modified residues within the GAG chain and these domains are important for mediating ligand binding (Turnbull, Powell, & Guimond, 2001). S domains are regions of heavily sulfated residues, while N domains contain very few sulfations on the sugar residues (Turnbull et al. 2001). There is no template for the modification of heparan sulfate side chains leading to immense diversity within the protein family. Distinct tissues will differentially express epimerases and sulfotransferases leading to GAG chains with varying structure based on their tissue of origin (Bülow & Hobert, 2004; Turnbull et al., 2001). Further, an evolutionarily conserved 6-O-endosulfatase has been shown to be expressed on the cell surface which can de-sulfate residues on the HS chain after it has been exocytosed in response to signalling from various molecules (Dhoot et al., 2001; S. Wang et al., 2004). The varying composition of the chain and its ability to be modified creates a large degree of diversity and allows a vast quantity of information to be encoded into a single protein family.

Within the HSPG family there are four major core protein groups: glypicans, syndecans, perlecans, and agrins (Holt & Dickson, 2005). Glypicans and syndecans are associated with the

cell membrane while perlecans and agrins are secreted into the ECM (Sarrazin, Lamanna, & Esko, 2011).

I.i.a. Glypicans

Glypicans are GPI linked members of the HSPG family that have a variety of functions in the neuronal ECM (Filmus, Capurro, & Rast, 2008). Mammals have six glypicans, named 1-6, flies have two, *dally* and *dally-like,* while *C. elegans* has only have one, *lon-2* (Filmus et al., 2008). Mammalian glypicans can be further subdivided into two broad groups with glypicans 1, 2, 4, and 6 forming one group, and glypicans 3 and 5 forming the other (Filmus et al., 2008). While primary sequence similarity across all glypicans is low, only ~25%, there is a highly conserved region of 14 cysteine residues that are important for protein folding (Filmus et al., 2008; Svensson, Awad, Hakansson, Mani, & Logan, 2012). Despite having only the glypican-1 crystal structure solved, it is known that the conserved cysteine residues are crucial for the formation of a stable alpha helical domain and it is predicted that the structure of all glypicans will be relatively similar (Svensson et al., 2012). Disruption of this alpha helical domain in glypican-1 leads to the addition of CS chains instead of HS chains further highlighting the importance of this highly conserved structural domain (Svensson et al., 2012). Glypicans also contain a conserved HS chain addition site near the region of membrane attachment (Filmus et al., 2008). The proximity of this conserved attachment site to the cell membrane places the GAG chains in an ideal position to interact with membrane-associated proteins and regulate cell function (Filmus et al., 2008).

All six mammalian glypicans are expressed in the nervous system in varying patterns. Glypican-1 is expressed in the developing nervous system by both neurons and neuroepithelial cells and Glypican-1 protein is enriched along axons and at synapses in the adult (Litwack et al.,

1998). Glypican-1 interacts with proteins such as fibroblast growth factor (FGF) and slits to regulate brain size and cell survival (Jen, Musacchio, & Lander, 2009; Ronca, Andersen, Paech, & Margolis, 2001). Glypican-2, also called cerebroglycan, is expressed almost exclusively in the developing nervous system, specifically in post-mitotic neurons (Ivins, Litwack, Kumbasar, Stipp, & Lander, 1997). Glypican-2 is distributed along axons and highly expressed during periods of axon extension, with enrichment in growth cones throughout the developing brain and spinal cord, including in commissural neurons and at the ventral commissure (Ivins et al., 1997). Once axons reach their target, glypican-2 expression is down-regulated, which is consistent with a role for glypican-2 in axon guidance (Ivins et al., 1997). Glypican-3 is expressed in spinal cord neurons and dorsal root ganglia, and acts as a regulator of the cell cycle (Iglesias et al., 2008). Glypican-3 loss-of-function results in Simpson-Golabi-Behmel syndrome (SGBS), an X-linked disease in humans characterized by severe malformations and general overgrowth including an increase in height, weight, and head circumference (Iglesias et al., 2008). Glypican-4, formerly called k-glypican, is expressed in neuronal precursor cells during development and interacts with FGF2 to regulate neurogenesis in the brain (Hagihara, Watanabe, Chun, & Yamaguchi, 2000). Glypican-4 is also expressed by astrocytes and localized release of glypican-4 leads to AMPA receptor clustering and synapse formation (Allen et al., 2012). Glypican-5 is expressed by neurons throughout the CNS in both developing and adult mammals and has been shown to associate with sonic hedgehog in cerebellar granule cell precursors to promote proliferation (Saunders, Paine-Saunders, & Lander, 1997; Witt et al., 2013). A single nucleotide polymorphism in the glypican-5 gene is associated with multiple sclerosis (MS) in human patients (Lorentzen et al., 2010). Glypican-6 is expressed in astrocytes and functions with glypican-4 to regulate AMPA receptor recruitment and synapse formation (Allen et al., 2012).

I.i.b. Syndecans

Syndecans are transmembrane proteins in the HSPG family. There are 4 mammalian syndecans, 1- 4, all of which are expressed in the nervous system (Hartmann & Maurer, 2001). *C. elgans* and *Drosophila* each have one syndecan, SDN-1 and SDC, respectively (Rhiner, Gysi, Fröhli, Hengartner, & Hajnal, 2005; Spring, Paine-Saunders, Hynes, & Bernfield, 1994). Syndecans have a highly conserved intracellular domain that interacts with the cytoskeleton, allowing extracellular molecules to modulate cell growth dynamics (Hartmann & Maurer, 2001). The ectodomain of syndecans are highly divergent across the family and bind to a variety of growth factors and soluble molecules in the ECM (Hartmann & Maurer, 2001). Syndecan-1 is the only syndecan family member that is a hybrid HSPG and CSPG, bearing GAG chains from both subfamilies (Hartmann & Maurer, 2001).

The mammalian syndecans are expressed in the nervous system in varying patterns. Syndecan-1 is widely expressed in the embryonic brain and spinal cord with expression decreasing in the later embryonic and postnatal stages (Nakanishi et al., 1997). Despite being down-regulated in adulthood, syndecan-1 plays an important role in neuronal regeneration. Following nerve injury, syndecan-1 is upregulated in a sub-population of spinal cord neurons and is speculated to promote neurite outgrowth during regeneration (Murakami, Tanaka, Bando, & Yoshida, 2015). Syndecan-2 is expressed in mature hippocampal neurons and plays a role in dendritic spine maturation (Ethell & Yamaguchi, 1999). Syndecan-3, also known as N-syndecan, is highly expressed in the embryonic brain and spinal cord, with levels peaking at postnatal day 7 and then reduced in adulthood (Carey, 1997; Nakanishi et al., 1997). Syndecan-3 knockout animals exhibit enhanced levels of LTP in the CA1 region of the hippocampus (Kaksonen et al., 2002). Syndecan-3 and syndecan-4 are both expressed in Schwann cells and are enriched at

paranodes in the peripheral nervous system (Goutebroze, Carnaud, Denisenko, Boutterin, & Girault, 2003).

I.ii. Chondroitin Sulfate Proteoglycans

Chondroitin sulfate sugar chains are made up of repeating GlcA – GalNAc disaccharides which are differentially sulfated to create distinct subunits termed CS-A, CS-B, CS-C, CS-D, and CS-E (Figure 2.2) (Sugahara et al., 2003). CS-A and CS-C are mono-sulfated; while CS-B, CS-D, and CS-E are di-sulfated. CS-B is also known as DS and the GlcA residue of the disaccharide is epimerized to IdoA (Sugahara et al., 2003). CS-A and CS-C, also referred to as chondroitin 4- and 6- sulfates, respectively, are the two most abundant CS subunits, with CS-C being the most abundant during embryogenesis and CS-A being the most abundant in the adult animal (Foscarin, Raha-Chowdhury, Fawcett, & Kwok, 2017). CS chain elongation is carried out by two enzymes, N-acetylgalactosaminyl transferase and glucuronyl transferase, which alternate to add the GalNAc and GlcA sugar residues (Silbert & Sugumaran, 2002). Sulfation of the CS chain occurs during chain synthesis through the action of chondroitin 6-sulfotransferase (C6ST) in the medial Golgi and chondroitin 4-sulfotransferase (C4ST) in the trans Golgi (Silbert & Sugumaran, 2002). Uronyl 2-sulfotransferase can sulfate both the IdoA and GlcA residues though at a much lower frequency than C6ST and C4ST sulfate the GalNAc residues (Silbert & Sugumaran, 2002). Unlike HS chains, which have discrete regions of sulfation within the same chain, CS chains are sulfated in an all-or-none fashion with the majority of CS chains being fully sulfated and a small number of chains remaining unsulfated (Silbert & Sugumaran, 2002).

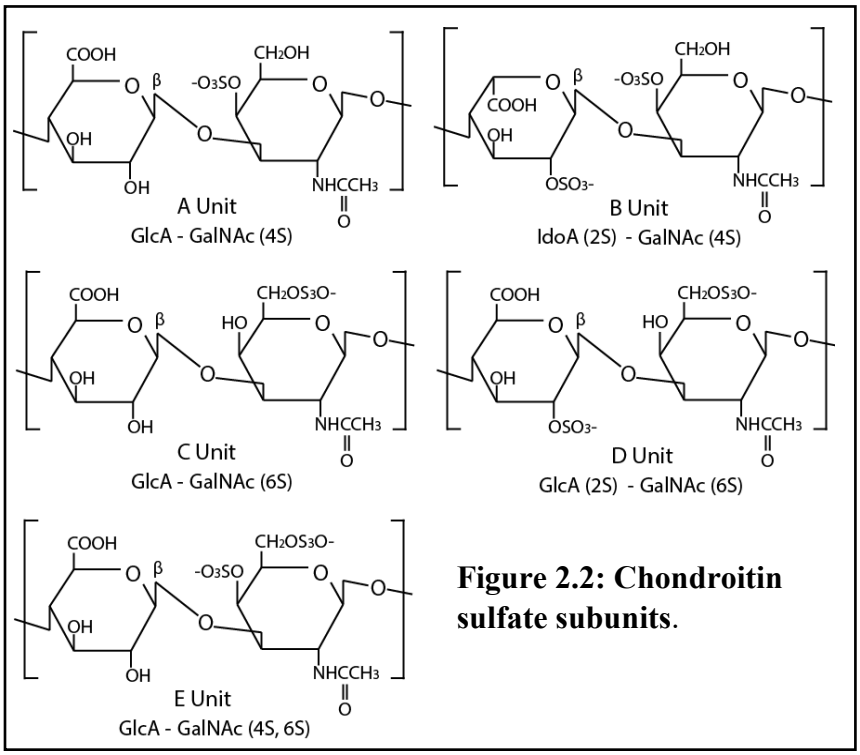

Figure 2.2: Chondroitin sulfate subunits.

I.ii.a. Lecticans

Lecticans are a family of HA-binding CSPGs that include aggrecan, versican, neurocan, and brevican (Hartmann & Maurer, 2001). All lectican core proteins share specific structural domains including the N-terminal HA-binding domain, the C-terminal epidermal growth factor (EGF)-like domain, and the c-type lectin-like domain. The gene structure of lecticans is also highly conserved among family members (Bandtlow & Zimmermann, 2000; Hartmann & Maurer, 2001). Many isoforms of each lectican form due to alternative mRNA splicing; post-translational modification of the core protein; or cleavage events which create secreted active fragments (Bandtlow & Zimmermann, 2000; Hartmann & Maurer, 2001). Lecticans bind to tenascins via the c-type lectin-like domain to help form specific structures in the ECM such as PNNs (Hartmann & Maurer, 2001). All lecticans are expressed in the CNS and largely mediate inhibitory functions. Aggrecan, neurocan, brevican, and versican have all been shown to limit

neurite extension of various neuron populations (Dutt et al., 2011; Hartmann & Maurer, 2001). Aggrecan inhibits retinal and sensory neurite extension and prevents neural crest cell migration (Hartmann & Maurer, 2001). Neurocan blocks both neurite outgrowth and cell adhesion; and is upregulated by astrocytes following injury, contributing to the inhibitory nature of the glial scar (Hartmann & Maurer, 2001). Brevican inhibits neurite outgrowth and cell adhesion in cerebellar granule cells and is upregulated in highly invasive glial tumors (Hartmann & Maurer, 2001). Versican causes growth cone collapse and neurite retraction of developing peripheral nervous system axons (Dutt et al., 2011). Interestingly, single lectican knockout animals show very few defects in the nervous system suggesting some redundancy among the proteins. Neurocan and brevican knockouts have no obvious phenotypes while aggrecan and versican knockouts are embryonically lethal due to respiratory and heart defects, respectively, with no noted defects in the nervous system (Dutt et al., 2011; Hartmann & Maurer, 2001). While knockouts of the individual proteins have little effect, treatment with chondroitinase ABC to degrade the CS chains of CSPGs has widespread effects in the CNS, promoting axon growth and regeneration after injury, as well as reopening critical periods and promoting synaptic plasticity (Lensjo, Lepperod, Dick, Hafting, & Fyhn, 2017; Moon, Asher, Rhodes, & Fawcett, 2001; Pizzorusso et al., 2002).

II. Extracellular Matrix

The ECM is a non cellular 3-dimensional matrix that is present in all tissues of the body and is largely composed of proteoglycans, along with water and other proteins (Lodish et al., 2004). The precise composition of proteins and proteoglycans within the ECM varies drastically between tissues leading to a heterogenous matrix that mediates a wide range of functions (Frantz

et al., 2010). Some of the functions mediated by the ECM include providing scaffolding and support for cells, mediating strength and elasticity of tissues, controlling diffusion of molecules to maintain homeostasis and bioavailability, and binding and interacting with extracellular molecules to mediate cell signaling (Frantz et al., 2010). Components of the ECM are synthesized intracellularly by resident cells in the tissue and then secreted into the extracellular space. The protein components of the ECM can be integrated into the cell membrane as a transmembrane protein, linked to the cell surface by GPI-protein coupling, or they can be soluble and integrated into the matrix without cellular contact (Frantz et al., 2010). Main ECM components include the proteins collagen, elastin, fibronectin, and laminin, along with the proteoglycans HS, CS, DS, KS, and HA (Lodish et al., 2004).

The ECM of the nervous system is highly specialized and unique in its composition compared to the ECM of non-nervous system tissues. While collagen, elastin, fibronectin and laminin are major components of ECM throughout the body, they are expressed only at low levels, if at all, in the CNS (Happel & Frischknecht, 2016). ECM in the CNS is dominated by the expression of PGs along with their binding proteins including tenascins and link proteins (Happel & Frischknecht, 2016). CNS ECM can also be further subdivided into three types: loose ECM, membrane tethered ECM, and PNN ECM (Sorg et al., 2016). Loose ECM is largely composed of HA and fills in the majority of the extracellular space acting as a reservoir for various soluble molecules, including axon guidance cues and growth factors, acting to help regulate their function (Happel & Frischknecht, 2016). Membrane-tethered ECM is linked to cell membranes either through trans-membrane proteins or a glycosylphosphatidylinositol (GPI) link. Membrane-tethered ECM interacts with cellular proteins to modulate their signalling and may be readily remodelled in response to activity and injury (Bozzelli, Alaiyed, Kim, Villapol, &

Conant, 2018). PNNs are a highly specialized form of ECM only present in the adult nervous system which forms a mesh-like structure around cell bodies and proximal dendrites of specific types of neurons throughout the brain (Bozzelli et al., 2018; Celio & Blumcke, 1994). PNNs are key regulators of synaptic plasticity and interact with various molecules to influence synaptic function (Bozzelli et al., 2018; Fawcett, 2009; Galtrey, Asher, Nothias, & Fawcett, 2007; N. G. Harris, Nogueira, Verley, & Sutton, 2013; Romberg et al., 2013; D. Wang, Ichiyama, Zhao, Andrews, & Fawcett, 2011)

II.i. Function in the Nervous System

Within the nervous system the ECM mediates many cellular processes including neuronal survival, cellular migration, axon growth and guidance, synapse formation, and glial cell function; in addition to providing overall structural support (Reichardt & Tomaselli, 1991). HSPGs and CSPGs are widely expressed in the ECM of the mammalian nervous system and can interact with a wide range of molecules. As a result, PGs in the CNS ECM can modulate and regulate many molecular processes, both in the developing and adult nervous system.

II.i.a. Axon Guidance

HSPGs and CSPGs have been shown to interact with and regulate the function of secreted axon guidance cues in the developing organism (Holt & Dickson, 2005). Bulow and Hobert (2004) first proposed the idea of a sugar code for developing axons following studies performed in *C. elegans*, where they found that individually knocking out the different HSPG sulfotransferases caused differing axon guidance defects (Bülow & Hobert, 2004). This led them to conclude that differential modifications of the sugar chain could regulate different guidance responses in specific neurons. In mice, knocking out EXT-1 in the CNS, which prevents HS-chain elongation, causes severe CNS defects and results in death shortly after birth (Inatani, Irie, Plump, Tessier-

Lavigne, & Yamaguchi, 2003). EXT-1 knockout animals completely lack olfactory bulbs, have an abnormally small cerebral cortex, malformations in the midbrain and cerebellum, and fail to form commissural axon tracts (Inatani et al., 2003). Some of these malformation and size differences can be attributed to aberrant FGF-signalling, a process known to be dependent on HSPGs cross linking FGF to the FGF receptor (Ornitz et al., 1992; Rapraeger, Krufka, & Olwin, 1991; Spivak-Kroizman et al., 1994; Yayon, Klagsbrun, Esko, Leder, & Ornitz, 1991). However, other defects cannot be explained by deficient FGF signalling (Inatani et al., 2003). Notably, in terms of axon guidance, these mice fail to form the corpus collosum, the hippocampal commissure and the anterior commissure which are three main commissures of the forebrain. Commissure formation is known to be independent from FGF signalling and indicates an important role for HSPGs in guidance at the midline (Inatani et al., 2003). Knocking out only one of HS 6-O-sulfonotransferase (HS6ST) or 2-O-sulfonotransferase (HS2ST) leads to differential axon guidance defects in the optic chiasm (Pratt, Conway, Tian, Price, & Mason, 2006). Mice lacking the HS6ST enzyme show defects in retinal innervation while the HS2ST mutants show disorganisation in the optic chiasm (Pratt et al., 2006). These results fit with the idea of a sugar code to regulate axon guidance, where the pattern of chain modification and sulfation can regulate different axon guidance pathways and interactions with different molecules. While these discoveries reveal the critical importance of HSPGs for axon guidance, the mechanisms underlying HSPG function have just begun to be elucidated. Netrins, semaphorins, and slits are all families of axon guidance cues that have been shown to interact with HSPGs in the context of axon guidance in the developing CNS (Blanchette, Perrat, Thackeray, & Bénard, 2015; Chanana, Steigemann, Jäckle, & Vorbrüggen, 2009; Johnson et al.,

2004; Kantor et al., 2004; Kastenhuber et al., 2009; Matsumoto, Irie, Inatani, Tessier-Lavigne, & Yamaguchi, 2007; Steigemann, Molitor, Fellert, Jäckle, & Vorbrüggen, 2004).

While the ability of Netrin-1 to bind heparin has been known since its discovery, the functional implications of this interaction have not been fully studied (Serafini et al., 1994). In 2007, Matsumoto and colleagues showed that cell autonomous expression of HSPGs in commissural neurons are required for proper commissural axon guidance in the spinal cord and that this was dependant on netrin-1/DCC signalling (Matsumoto et al., 2007). However, the mechanism of action was never determined. More recently, it was shown that the *C. elegans* HSPG, lon-2 (glypican), modulates unc6 (netrin) mediated axon guidance (Blanchette et al., 2015). Interestingly, this was found to be through a direct interaction between the core protein of the *C. elegans* glypican lon-2 and the netrin receptor unc40 (DCC), as opposed to an interaction with the sugar chains, as shown in the EXT-1 knockout animals (Blanchette et al., 2015).

CSPGs have also been shown to regulate axon guidance during development, although they are less studied than HSPGs, and mainly have inhibitory effects. In *Xenopus*, bath application of CS led to a widening of optic tracts throughout the brain and mistargeting of retinal ganglion cell axons (Walz, Anderson, Irie, Chien, & Holt, 2002). These neurons also show altered growth patterns with an increased likely hood of stalling and failing to make forward progress (Walz et al., 2002). Studies have also looked at the effects of individual CS subunits on axon guidance and outgrowth which found varying responses that are specific to the sulfation pattern of the subunits. CS-A is found to repel axon growth by cerebellar granule neurons, while CS-C has no effect (H. Wang et al., 2008). Conversely, CS-D and CS-E have both been identified as growth-promoting. Cultured E18 rat hippocampal neurons have significantly increased outgrowth on CS-D and CS-E substrates compared to control substrates;

while CS-A, CS-B, and CS-C substrates had no effect (Clement et al., 1998; Clement, Sugahara, & Faissner, 1999). CSPGs also interact with other axon guidance cues to regulate their function. Semaphorin 5A is an axon guidance molecule that is regulated by an interaction with GAG proteins. When bound to HSPGs, semaphorin 5A is an attractive cue; however, when interacting with CSPGs it is a repulsive cue (Kantor et al., 2004). The differential effect of PGs on axon guidance cues provides an additional level of functional regulation beyond ligand receptor interaction and allows the environment to alter axon guidance responses. The specific presence of HSPGs or CSPGs in the environment can determine whether a neuron will be attracted or repelled by specific axon guidance cues, and the regulated expression of PGs is important for proper development of the nervous system.

II.i.b. Synaptic Function

Proteoglycans have demonstrated roles in both synapse formation and synaptic plasticity. One of the first demonstrations of the importance of proteoglycans to synapse formation was the study of the HSPG agrin at cholinergic synapses (Herbst & Burden, 2000). Agrin expression precedes synapse formation and induces clustering of the acetylcholinesterase receptor (Herbst & Burden, 2000). CSPGs play an important role in regulating synaptic plasticity as the CNS matures and are a main component of PNNs, a structure known to be important for regulating synaptic plasticity in the adult (Fawcett, 2009; Galtrey et al., 2007; N. G. Harris et al., 2013; Romberg et al., 2013; D. Wang et al., 2011).

III. Perineuronal Nets

PNNs are highly specialized ECM structures in the adult CNS which surround the cell bodies and proximal dendrites of a subset of neurons. PNNs have been shown to be present throughout

many brain structures, including the cortex, hippocampus, cerebellum, and spinal cord (Bozzelli et al., 2018). The majority of PNNs surround parvalbumin (PVA) positive GABAergic interneurons, but have also been shown to surround glutamatergic neurons in the hippocampus (Lensjø, Christensen, Tennøe, Fyhn, & Hafting, 2017). PNNs are now widely accepted as a structure critically important in mediating plasticity throughout the brain, yet, their initial discovery was met with scepticism. Camillo Golgi first described PNNs in 1893 as a thin covering for neurons that enveloped cell bodies and their branches (Celio, Spreafico, De Biasi, & Vitellaro-Zuccarello, 1998; Spreafico, De Biasi, & Vitellaro-Zuccarello, 1999; Vitellaro-Zuccarello, De Biasi, & Spreafico, 1998). At the time of this initial discovery, Golgi and Ramon y Cajal were caught in a feud over whether the "reticular theory" or the "neuron doctrine" accurately described how the nervous system functioned (Celio et al., 1998; Spreafico et al., 1999; Vitellaro-Zuccarello et al., 1998). The "reticular theory" postulated that all the cells in the nervous system are connected in a single continuous network, while the "neuron doctrine" states that the nervous system is made up of individual discontinuous cells (Glickstein, 2006). When first describing PNNs, Golgi called them a reticular structure and used PNNs as evidence to support the "reticular theory", which he strongly supported (Spreafico et al., 1999). Cajal, however, advocated for the "neuron doctrine", and therefore argued that a reticular structure such as PNNs should not exist (Celio et al., 1998). Cajal therefore rejected the existence of the PNN suggesting it was merely an artifact of the staining process. Cajals' rejection resulted in very few scientists pursuing the structure of the PNN and it disappeared from the forefront of scientific research until a resurfacing in the 1980s (Spreafico et al., 1999). Advances in histochemical staining techniques have since confirmed the existence of PNNs, with the last few decades providing tremendous new insight into the importance of PNNs and how they affect neuronal

function. PNNs appear as a honeycomb mesh around neurons with small holes in which inputting neurons can make synaptic contacts (Celio & Blumcke, 1994). PNN composition is heterogeneous, and neurons are surrounded by PNNs of slightly varying composition depending on location and function of the neuron (C. Lander, Kind, Maleski, & Hockfield, 1997; Cynthia Lander, Zhang, & Hockfield, 1998; Maleski & Hockfield, 1997). The molecular components of the PNN are synthesized by both the neurons and the surrounding glia cells. Their appearance in the brain marks the closure of critical periods of neuronal plasticity (Bozzelli et al., 2018; C. Lander et al., 1997; Cynthia Lander et al., 1998; Maleski & Hockfield, 1997). Enzymatic digestion of PNNs can re-open critical periods and enhance synaptic plasticity in older animals (Lensjo et al., 2017; Moon et al., 2001; Pizzorusso et al., 2002). PNNs function to regulate synaptic plasticity (Brakebusch et al., 2002; Carstens, Phillips, Pozzo-Miller, Weinberg, & Dudek, 2016; Hylin, Orsi, Moore, & Dash, 2013), create a physical barrier to prevent neurotransmitter receptor diffusion (Frischknecht et al., 2009), buffer ions across the membrane (Tsien, 2013), and bind to molecules to regulate their access to the neuron (van 't Spijker & Kwok, 2017)

III.i. Structure and Function

PNNs are composed of proteoglycans (CSPGs and HA), link proteins, and tenascins (Kwok, Dick, Wang, & Fawcett, 2011). Hyaluronan synthase (HAS) on the neuronal cell surface synthesizes and excretes hyaluronan into the extracellular space. CSPGs then bind to HA, the interaction stabilized through the binding of link proteins, creating an aggregate of proteoglycans in the extracellular space. Tenascins, specifically tenascin-R, can bind to the C-termini of three CSPG core proteins, leading to a high degree of organisation and the creation of a lattice-like structure characteristic of PNNs (Kwok et al., 2011). HAS is also responsible for anchoring the

PNN to the cell (Kwok et al., 2011). The CSPGs in the PNN are all part of the lectican family. Aggrecan, versican, neurocan, and brevican, have all been shown to be present in PNNs; however, only aggrecan is specifically required for PNN formation (Kwok et al., 2011). The composition of CSPGs affects how compact the PNN is, as some bind to tenascins with higher affinity, leading to a greater degree of cross linking and a more compact PNN. Additionally, the size of the protein and degree of glycosylation can also affect the compactness of the PNN (Kwok et al., 2011). The composition of CSPGs in the PNN is affected by the brain region and its neuronal diversity, such that the activity within that specific brain region will determine differences in PNN composition (Bozzelli et al., 2018). The link proteins hyaluronan and proteoglycan-binding link protein (HAPLN) 1 and 2 are both found in the PNN. They are important in stabilizing the interaction between HA and CSPGs, and without them the PNN fails to condense (Kwok, Carulli, & Fawcett, 2010).

The appearance of PNNs coincide with the closure of critical periods of plasticity in the CNS and the PNN is believed to “lock in” neuronal circuits. PNNs regulate synapse formation and plasticity, lateral movement of proteins within the neuronal membrane, ion balance in the environment surrounding neurons, binding and access of molecules to neurons, and protect neurons from oxidative stress and bioactive proteins (Bozzelli et al., 2018; Kwok et al., 2011; van 't Spijker & Kwok, 2017). Digestion of the PNN causes an increase in the number of synapses; however, the sensitivity of these synapses to glutamate is decreased and the synapses show reduced function (Pyka et al., 2011; van 't Spijker & Kwok, 2017). Digestion of PNNs leads to increased lateral mobility of AMPA receptor subunits on the cell membrane, causing them to move away from the region of synaptic contact which may account for the reduction in glutamate sensitivity (Frischknecht et al., 2009). CSPGs in the PNN are also binding partners for

many other molecules in the CNS and can bind and link these molecules to neurons to mediate function. One example is semaphorin 3a, which preferentially binds to CS-E subunits of CSPGs, localizing it into the PNN rather than loose ECM (van 't Spijker & Kwok, 2017). Semaphorin 3a is known to be a non-permissive axon guidance cue that also plays a role in synapse function (Bouzioukh et al., 2006). While the function of semaphorin 3a in the PNN has not yet been fully elucidated it is possible that PNNs may present semaphorin 3a to approaching neurons and given its function as a repulsive molecule this would likely limit new synaptic contact (van 't Spijker & Kwok, 2017).

IV. Concluding Remarks

The ECM in the nervous system, and specifically the proteoglycans which comprise it, plays an important role in regulating neuronal function. The complexity and extreme variability of PG structure within the neuronal ECM allows for a vast amount of information to be encoded within a single protein family. Small changes in sulfation pattern can lead to large changes in cell signalling and function. Further, changes in protein expression within individual cells can affect the composition of the ECM. Understanding how the ECM interacts with neurons in the CNS and how these interactions affect both cell function and matrix composition will provide valuable insight into nervous system function. The ECM is an important regulator of cellular processes such as axon guidance, synapse formation, and synaptic plasticity. Specialized ECM within the nervous system has important roles in defining neuronal functions. Specifically, PNNs regulate the closing of critical periods and a shutting down of neuronal plasticity. Understanding the role of the ECM in CNS function and the capacity to alter or regulate the ECM could provide a valuable method to modulate neuronal function.

Research Rationale and Objectives

Rationale:

Neurons in the CNS are not isolated cells but rely on interactions with other cells and the extracellular environment in order to properly function. Research tends to focus on a specific mechanism within a single signalling pathway rather than looking at how two (or more) signalling pathways may integrate to regulate specific cellular functions. In this thesis we aim to determine how multiple signalling pathways interact to regulate neuronal function. Specifically, we aim to determine how the netrin-1/DCC axon guidance pathway interacts with the cadherin/catenin cell adhesion pathway to regulate commissural axon guidance and synapse formation (Chapter 3 and Chapter 4). We aim to determine the function of the netrin-1 C-domain and to characterize an interaction between netrin-1 and ECM proteoglycans (Chapter 5). Finally, we aim to determine a function for interaction between netrin-1 and PNNs, a specialized form of ECM, and to gain insight into how this may regulate synaptic plasticity in the adult nervous system (Chapter 6). Understanding how multiple signalling pathways integrate and regulate specific cellular functions will help us to better understand the nervous system as a whole rather than as isolated signaling pathways.

RESULTS

Preface

The interaction of the axon guidance cue netrin-1 with its receptor DCC, and their function in commissural axon guidance, are well characterized; however, little is known regarding interactions of this signalling complex with other transmembrane proteins during axon guidance. In this chapter we investigate an interaction between the netrin-1 receptor DCC and the cell adhesion molecule CDH12. We provide evidence for an interaction between DCC and CDH12 in commissural neurons and that this interaction influences commissural axon growth. We also show that netrin-1 alters the phosphorylation state of β-catenin, a key downstream signalling molecule in the cadherin cell adhesion complex. A manuscript corresponding to this chapter is in preparation for publication.

Chapter 3

Cadherin 12 interacts with DCC to modulate commissural axon guidance in the developing rodent spinal cord

Stephanie N. Harris*, Ian V. Beamish*, Sonia Rodrigues*, Timothy E. Kennedy*

*Department of Neurology and Neurosurgery, Montreal Neurological Institute, McGill University, Montreal, Quebec, Canada, H3A 2B4

I. ABSTRACT

Cadherins are a large family of calcium dependent cell adhesion molecules that are widely expressed throughout the nervous system. The role of cadherins in cell-cell adhesion has been extensively studied, however it is now becoming clear that they also play an important role in axon guidance and circuit formation. The axon guidance cue netrin-1 and its receptor DCC are well studied for their role in commissural axon guidance in the developing spinal cord. Here we provide evidence that the netrin-1/DCC axon guidance pathway and the cadherin/catenin cell adhesion complex converge to regulate commissural axon guidance. We identified a type two classical cadherin, CDH12, as a putative DCC binding partner in commissural neurons. CDH12 is a relatively understudied type II classical cadherin that is expressed in the embryonic spinal cord by neuroepithelial cells and commissural neurons. Further, we demonstrate that netrin-1 regulates phosphorylation of β-catenin, a key downstream signalling partner of cadherins. Netrin-1 induces phosphorylation of β-catenin at two sites, Y142 and S675, both of which are phosphorylated by kinases activated by DCC. We also show that disruption of CDH12 binding in the spinal cord disrupts commissural neuron growth. These results demonstrate that netrin-1/DCC signalling and cadherin/catenin signalling function together in the developing spinal cord during commissural axon extension.

II. INTRODUCTION

Cadherins are calcium dependant cell adhesion molecules with more than one hundred members in the cadherin superfamily. Of those, just over twenty are members of the classical cadherin subfamily, many of which are expressed in the nervous system. Classical cadherins are transmembrane proteins comprised of five extracellular cadherin repeats, a transmembrane domain, and an intracellular signaling domain. Classical cadherins are classified as either type I or type II, where type II classical cadherins lack the characteristic HAV tripeptide motif present in the first extracellular cadherin repeat of type I classical cadherins (Patel et al., 2003). While N-cadherin is widely expressed in the developing nervous system, there is a growing body of literature that demonstrates more selective effects of type II cadherins in circuit formation during the development of the central nervous system (CNS) (Price et al., 2002; S. C. Suzuki et al., 1997; Williams et al., 2011). The intracellular domain of cadherins engage the catenin family of proteins which participate in intracellular signaling cascades regulating an array of cellular functions, including F-actin dynamics and wnt signaling (Shapiro & Weis, 2009). While cadherins have been extensively studied for their role in cell-cell adhesion, their role in axon guidance and circuit formation during the development of the nervous system is becoming more apparent. Two groups have shown that neurons expressing N-cadherin will follow underlying cells that also express N-cadherin while avoiding cells that do not (Matsunaga et al., 1988; Redies et al., 1992). Additionally, the level of N-cadherin, which can be regulated by Robo, is important for sorting post crossing commissural neurons into their appropriate longitudinal axon tracts (Sakai et al., 2012). Over expression of N-cadherin or loss of Robo both resulted in the loss of the intermediate longitudinal projection (ILC) with all neurons projecting in the medial longitudinal projection (MLC) (Sakai et al., 2012). Targeted shRNA disruption of N-cadherin

expression in chick embryos resulted in defects in commissural axons crossing the ventral midline, and while the mechanism underlying this remains unknown, the authors hypothesized this was due to altered β-catenin expression (Yang et al., 2016). β-catenin functions downstream from cadherins in cell adhesion and is also a critical regulator of wnt signaling in commissural neurons (Aviles & Stoeckli, 2016). β-catenin knockdown leads to commissural neurons stalling in the commissure and failing to make the rostral turn on the contralateral side of the spinal cord (Aviles & Stoeckli, 2016). Additionally, β-catenin has been shown to be required for anteroposterior axon guidance in *C. elegans*, further highlighting the potential importance of this signaling molecule in axon guidance (Maro, Klassen, & Shen, 2009).

Netrin-1 and DCC are critical for commissural axon guidance in the developing spinal cord and knocking out either protein leads to a total loss of the ventral spinal commissure (Bin et al., 2015; Keino-Masu et al., 1996; Kennedy et al., 1994; Serafini et al., 1996). Ectopic expression of DCC has been shown to modulate levels of N-cadherin, α-catenin, and β-catenin in neuroblastoma cells. Expressing a truncated DCC, which lacks the cytoplasmic tail, results in reduced expression of N-cadherin, α-catenin and β-catenin at both the mRNA and protein levels (Reyes-Mugica et al., 2001). Additionally, netrin-1 is known to be important for the growth of thalamic axons and the application of ectopic netrin-1 causes an increase in immunocytochemical fluorescence staining intensity of β-catenin in thalamic growth cones (Braisted et al., 2000; Pratt et al., 2012). Despite increasing evidence that axon guidance and cell adhesion pathways converge to mediate axon growth, the mechanism and functional significance of possible interplay between netrin-1/DCC signalling and cadherins is not yet understood.

Using an unbiased screen for DCC interacting proteins we identified cadherin-12 (CDH12) as a putative binding partner. We obtained independent evidence supporting this

interaction in primary commissural neurons and determined that CDH12 contributes to commissural axon guidance in the embryonic spinal cord. CDH12 is a relatively understudied type II classical cadherin with expression in the developing and adult rodent brain. Functional studies have focused on the role of CDH12 in colorectal cancer, largely leaving its function in the nervous system yet to be determined (Ma et al., 2016; Zhao et al., 2013). Here we provide evidence for an interaction between the netrin-1/DCC axon guidance pathway and the cadherin/catenin cell adhesion complex. We report that DCC interacts with the type II classical cadherin, CDH12, and that this interaction regulates β-catenin phosphorylation, which contributes to commissural axon guidance in the developing spinal cord.

III. METHODS

III.i. Animals

All procedures were performed in accordance with the Canadian Council on Animal Care guidelines for the use of animals in research and approved by the Montreal Neurological Institute Animal Care Committee and the McGill Animal Compliance Office. Sprague-Dawley rats were obtained from Charles Rivers Laboratory at various developmental stages (St-Constant, QC, Canada) (vaginal plug = E0). Wild type C57/Bl6 mice were bred in house at the Montreal Neurological Institute Animal Care Facility.

III.ii. Antibodies and reagents

Antibodies: Rabbit anti CDH12 (abcam, EPR1792), mouse anti N-cadherin (BD transduction laboratories, 610920), rabbit anti N-cadherin (abcam, EPR1791-4), rabbit anti E-cadherin (Cell Signaling, 24E10), mouse anti β-catenin (BD transduction laboratories, 610153), rabbit anti

phosphorylated S675 β-catenin (abcam, ab58615), rabbit anti phosphorylated Y142 β-catenin (abcam, ab27798), mouse anti DCCin (BD pharmingen, 554223), mouse anti DCC AF5 (Calbiochem, OP45), rabbit anti netrin-1 (abcam, EPR5428), rabbit anti GAPDH (santa cruz biotechnology, sc-25778), hamster anti mouse CD29 (BD Biosciences, 562219), mouse anti V5 (Abcam, ab27671), alexa fluor Phalloidin (Thermo Fisher, A12379), Hoechst 33258 (Life Technologies), mouse IgG (Jackson Immuno Research, 015-000-003), peroxidase-conjugated donkey anti mouse IgG (Jackson Immuno Research, 715-035-150), peroxidase-conjugated donkey anti rabbit (Jackson Immuno Research, 711-035-152), alexa fluor donkey anti rabbit (molecular probes, A31572 & A21206), alexa fluor goat anti mouse (molecular probes, A-11003 & A-11001), Cell Tracker CM DiI (Thermo Fisher, C7000).

Pharmacological Inhibitors: IPA3 (Tocris), PIR3.5 (Tocris), PP2 (abcam), PP3 (abcam).

Protein and DNA constructs: CDH12-Fc (R&D Systems 2240-CA-050), CDH12-GFP (Ori Gene RC208156L2), DCC-GFP (generated in house); UNC5B-GFP (generated in house); SltTrk-GFP (Generated as described (Beaubien, Raja, Kennedy, Fournier, & Cloutier, 2016)).

III.iii. 2-dimensional liquid chromatography mass spectrometry

Protein isolation and sequencing was carried out as described (Rodrigues, 2011). Briefly, proteins were separated using SDS-PAGE, bands cut from the gel, and digested using trypsin. A Quadrupole Time-Of-Flight micro instrument (QTOF; Waters Corporation, Milford, MA) was used for mass spectrometry analysis. Peak lists were generated using Mascot Distiller 2.0.0 software (Matrixscience, Boston, MA) and peptide identification carried out through a non-redundant search on the National Center for Biotechnology Information database (NCBInr; ftp://ftp.ncbi.nih.gov/blast/db/FASTA/nr.gz). CellMapBase, a program developed in house, was

used to generate a list of identified proteins and only those with $p<0.05$ were analysed. Proteins were considered a positive hit if they were detected in 2 of 3 samples tested.

III.iv. Cell culture

Commissural Neurons: Dorsal spinal cords were micro dissected from embryonic day 13 (E13) rat embryos (Charles River, Quebec) and dissociated as previously described (Moore & Kennedy, 2008). Neurons were plated on plasma treated coverslips coated with 10 µg/ml of poly-d-lysine (PDL) or 2 µg/ml PDL for GC expansion experiments. PDL coating was carried out for 1 hr at rt using a volume of 500 µl PDL per coverslip. PDL coated coverslips were then washed 3 times with ddH_2O and allowed to air dry. Neurons were grown in neurobasal (Thermo Fisher) supplemented with 10% heat inactivated fetal bovine serum (FBS), 1% penicillin - streptomycin (P/S) (Thermo Fisher), and 1% GlutaMAX (Thermo Fisher). After 24 hr media was changed to neurobasal supplemented with 2% B-27 (Thermo Fisher), 1% P/S and 1% GlutaMAX and cells were cultured for an additional 24 hr. Cells were cultured at 37^{o} C with 5% CO_2. Cells were then fixed using 4% para formaldehyde (PFA) in 20% sucrose for 20 min at rt, or lysed in 3% Triton X-100 buffer (50 mM HEPES [pH 7.4], 150 mM NaCl, 2 mM EGTA [pH 8], 15mM $MgCl_2$, 0.1% glycerol, 3% Triton X-100), or lysed in radio immunoprecipitation assay (RIPA) buffer (10 mM phosphate buffer [pH 7.2], 150 mM NaCl, 1% NP-40, 0.5% sodium deoxycholate, and 0.1% SDS) depending on the assay in which cells were being used.

HEK293T Cells: Cells were grown on plasma treated coverslips coated with 10 µg/ml of PDL. PDL coating was carried out for 1 hr at room temp using a volume of 500 µl PDL per coverslip. PDL coated coverslips were then washed 3 times with ddH_2O and allowed to air dry. Cells were grown in DMEM (Thermo Fisher) supplemented with 10% heat inactivated FBS, and

1% P/S. Cells were cultured at 37° C with 5% CO_2. Cells were fixed on ice in 4% PFA for 20 min.

III.v. Growth cone expansion assay

Commissural neurons were cultured for 2 days prior to treatment as described above. Neurons were stimulated with 200 ng/ml of purified recombinant netrin-1 for 15 min and then fixed with 4% PFA in 20% sucrose for 20 min at rt. Immunostaining was carried out as described below.

III.vi. β-catenin phosphorylation assay

Commissural neurons were cultured for 2 days prior to treatment with 200 ng/ml of netrin-1 for 15 min. For inhibitor experiments, neurons were treated for 20 min with 10 μM of indicated inhibitor prior to stimulation with 200 ng/ml of netrin-1 for 15 min. After netrin-1 stimulation cells were lysed in RIPA buffer on ice and phosphorylation assayed via western blot.

III.vii. Co-Immunoprecipitation

Commissural neurons were cultured for 2 days prior to treatment. Neurons were treated with 200 ng/ml netrin-1 for 15 min and were then lysed in ice-cold 1% Triton X-100 lysis buffer (50 mM HEPES [pH 7.4], 150 mM NaCl, 2 mM EGTA [pH 8], 15mM $MgCl_2$, 0.1% glycerol, 1% Triton X-100) for mass spectrometry analysis or 3% Triton X-100 lysis buffer for DCC immunoprecipitation (IP), both buffers were supplemented with protease inhibitors; Aprotinin 2 μg/ml, Leupeptin 5 μg/ml, EDTA 5 mM, PMSF 1 mM, sodium orthovanadate 1 mM, and sodium fluoride 10 mM. Cells were lysed in 1 ml of buffer and the whole cell homogenate collected into pre-chilled tubes and placed on ice for 20 min. The samples were then spun at 13793 RCF at 4° C for 15 min (Eppendorf 5415 C centrifuge). The supernatant was used for IP

and the pellet discarded. Prior to IP the supernatant was pre-cleared for 30 min using 30 µl of protein A/G beads to remove nonspecific binding. Samples were then spun at 1000 RCF (Eppendorf 5415 C centrifuge) for 2 min and supernatant transferred to a new tube for IP. IPs were performed using 1 µg of mouse anti-DCC_{in} for mass spectrometry or 2 µg of mouse anti-DCC_{in} for CDH12 co-IP. DCC_{in} was incubated with the cell lysate at 4° C for 1 hr. Protein A/G beads (Santa Cruz Biotechnology) were then added and incubated for an additional 1 hr at 4^{o} C. Beads were then pelleted and washed three times in ice cold lysis buffer with protease inhibitors as described above. Proteins associated with the beads were eluted using Laemmli buffer (Laemmli, 1970) and characterized using western blot analysis

From whole spinal cord: Whole spinal cords from E13 rats were homogenized in a buffer composed of 1% NP-40, 0.5% sodium deoxycholate, and 5% bovine serum albumin (BSA) in PBS supplemented with protease inhibitors; Aprotinin 2 µg/ml, Leupeptin 5 µg/ml, EDTA 5 mM, PMSF 1 mM, sodium orthovanadate 1 mM, and sodium fluoride 10 mM. Cords were homogenized in 0.5 ml of buffer and collected into pre-chilled tubes and placed rotating at 4^{o}C for 10 min. The samples were then spun at 13793 RCF at 4^{o} C for 10 min (Eppendorf 5415 C centrifuge). The supernatant was used for IP and the pellet discarded. Prior to IP the supernatant was pre-cleared for 30 min using 60 µl of 50:50 slurry of protein A/G bead and PBS to remove nonspecific binding. Samples were then spun at 1000 x RCF (Eppendorf 5415 C centrifuge) for 2 min and supernatant transferred to a new tube for IP. IPs were performed using 3 µg of DCC AF5 and 3 µg DCC_{in} or 6 µg of mouse anti V5 as a control. Antibody was incubated with the cell lysate at 4° C for 1 hr. A 50:50 slurry of Protein A/G beads and PBS pre blocked in 5% BSA (Santa Cruz Biotechnology) were then added and incubated for an additional 1 hr at 4^{o} C. Beads were then pelleted and washed four times in ice cold lysis buffer with protease inhibitors as

described above. Proteins associated with the beads were eluted using Laemmli buffer (Laemmli, 1970) and characterized using western blot analysis

III.viii. Western blot analysis

Proteins were separated on an 8% poly acrylamide gel and then transferred by electroblotting onto nitrocellulose using a 350 mA current for 1 hr and 15 min. Nitrocellulose membranes were blocked in 5% skim milk powder or 3% BSA in TBST for 1 hr. Primary antibodies were diluted in blocking buffer and incubated at 4^{o} C overnight. Membranes were then washed in blocking buffer 3 x 10 min. Secondary antibodies were diluted in blocking buffer and incubated for 1 hr at rt. Membranes were then washed 2 x 10 min in TBST and 2 x 10 min in TBS. The membrane was then incubated with Western Lightning ECL pro (Perkin-Elmer Inc.) and exposed to film.

III.ix. Immunohistochemistry

Embryos (ages indicated in figure legends) were isolated by dissection and fixed by submersion in Carnoy's solution, 60% ethanol, 10% acetic acid, and 30% chloroform, for 2 hr at rt. Embryos were then washed twice with 100% ethanol for 20 min and cleared in toluene for 1 hr before being embedded in paraffin (Fisher Scientific). Sections, 10 μm thick, were cut with a microtome and mounted on SuperFrost Plus Slides (Fisher Scientific). Tissue sections were dewaxed and rehydrated prior to staining as follows. Excess wax was melted in an oven at 50^{o} C. Sections were then moved through Xylene, 100% ethanol, 95% ethanol, 70% ethanol, and PBS, each 2 x 3 min for rehydration. Sections underwent an antigen retrieval step by boiling in 10 mM citrate buffer pH 6 for 20 min in a microwave. Slides were cooled in buffer for an additional 15 min before being washed 2 x 5 min in PBS. Slides were then blocked and permeabilized in 0.25% Triton-X 100 and 3% heat inactivated horse serum (hiHS) in PBS. Primary antibodies were

diluted in a buffer of 0.1% Triton-X 100 and 1% hiHS in PBS and incubated overnight at 4^{o} C. Sections were then washed in PBS 3 x 10 min with rocking. Secondary antibodies were diluted in 1% hiHS in PBS for 2 hr at rt and then washed 3 x 10 min in PBS. Slides were then rinsed briefly in water and cover slipped using Fluoro-Gel with tris buffer (Electron Microscopy Sciences).

III.x. Cell surface binding assay

HEK293T cells were transfected with designated DNA constructs using Lipofectamine 2000 (Thermo Fisher). One µg of DNA was mixed with 25 µl of Opti-MEM (Gibco) to create solution A and 1 µl of lipofectamine was mixed with 25 µl of Opti-MEM to create solution B. Solutions A and B were incubated separately at rt for 5 min and then mixed together and incubated at rt for 15 min. The combined solution was then added dropwise to the well and cells were grown in culture for 24 hr in DMEM supplemented with 10% FBS to allow protein expression. Cells were incubated at rt with 1 µg/ml netrin-1 in PBS supplemented with 10% hiHS, 0.1% sodium azide, and 3 µg/ml heparin for 90 min. Cells were washed 3 times with PBS to remove any unbound protein and fixed in 4% PFA on ice for 20 min.

III.xi. Immunocytochemistry

Cells were blocked and permeabilized in 0.25% Triton-X 100 and 3% hiHS in PBS. Primary antibodies were diluted in a buffer of 0.1% Trition-X 100 and 1% hiHS in PBS and incubated overnight at 4^{o} C. Cells were then washed in a buffer of 0.1% Triton-X 100 and 1% hiHS in PBS 3 x 10 min with rocking. Secondary antibodies were diluted in 1% hiHS in PBS for 2 hr at rt and then washed 3 x 10 min in PBS. Cells were then rinsed once briefly in water and mounted on slides using Fluoro-Gel with tris buffer (Electron Micoroscopy Sciences).

III.xii. Embryonic dorsal spinal cord explants

Brachial spinal cord segments were micro dissected from E13 rat embryos and dorsal explants, ~200 μm x ~200 μm, embedded in a 3D collagen matrix as described (Moore & Kennedy, 2008). Immediately following embedding, explants were treated as described in the figure legends. Sixteen hr after treatment explants were fixed in 4% PFA for 1 hr on ice. Explants were imaged using bright field phase contrast microscopy (Zeiss Axiovert S100TV, 20x objective, MagnaFire CCD camera and MagnaFire 4.1C imaging software (Optronics, Goleta, USA).

III.xiii. Open book preparations

Spinal cords were micro dissected from E11 rat embryos and embedded in a 3D collagen matrix as described (Moore & Kennedy, 2008). Immediately following embedding, open book explants were treated as described in the figure legends. Forty-eight hr after treatment open book spinal cord explants were fixed in 4% PFA for 1 hr on ice and were injected with DiI to visualize axon projections.

DiI injection: Cell tracker red DiI was diluted in DMSO at a concentration of 1 mg/ml. DiI injection was done using a pulled glass micropipette with a broken tip. DiI was injected along the dorsal edge of the spinal cord in the region containing commissural neuron cell bodies. The PBS in the dish was changed for fresh PBS after injection to remove any DiI that was not injected into the tissue. DiI was then allowed to diffuse for 4 days at 4^{o} C before confocal imaging (Leica TCS SP8).

IV. RESULTS

IV.i. Characterisation of the CDH12 monoclonal antibody

In order to study CDH12 in the central nervous system we first characterised the specificity of a commercially available rabbit monoclonal antibody, EPR1792Y (Abcam), raised against the C-terminal domain of human CDH12. CDH12, also known as Brain Cadherin or N-cadherin 2, shares ~37% amino acid sequence identity with N-cadherin and up to 62% amino acid sequence identity with other members of the cadherin family (Table 3.1) (uniprot.org). Within the C-terminal domain the amino acid sequence identity of CDH12 increases to 46% when compared to N-cadherin and 49% when compared to E-cadherin. The overall sequence identity shared between CDH12 compared to all classical cadherin family members, type I and type II, is shown in table 3.1. To validate that the EPR1792Y monoclonal antibody binds CDH12 we transfected HEK293T cells with either a cDNA encoding full length human CDH12 with a C-terminal GFP tag (Origene) or mock transfected cells with no DNA and then immunostained using the EPR1792 monoclonal antibody (Figure 3.1A). Immunolabelling colocalized with CDH12-GFP transfected cells and not mock transfected cells, demonstrating that EPR1792Y binds to CDH12 protein. We then addressed the specificity of EPR1792Y to ensure it was binding only CDH12 and not other cadherins. HEK293T cells are reported to express cadherins -1 (E-cadherin), -2 (N-cadherin), -3, -7, -11, 17, 23 and -24 (www.proteinatlas.org), however HEK293T cells were blank when immunolabelled with the EPR1792Y antibody (Figure 3.1A). To specifically address possible cross reactivity with N-cadherin, which is highly expressed in the CNS, hippocampal homogenates were obtained from adult wild type and hippocampal conditional N-cadherin knockout mice and analysed via western blot (Kostetskii et al., 2005). The EPR1792Y monoclonal detected an ~ 140 kDa band in hippocampal homogenates of wildtype and N-

cadherin knockouts at approximately equal levels, while an antibody specific for N-cadherin (abcam, EPR1791-4) detected a band only in wild type homogenate. This finding provides evidence that the EPR1792Y monoclonal antibody does not bind N cadherin protein (Figure 3.1B). We also examined PC12 cells, which are derived from neural crest cells and can be differentiated into neuron-like cells by incubating them with nerve growth factor (NGF). We detected both N-cadherin and E-cadherin on western blots of PC12 cell lysate, however, no EPR1792Y antibody immunoreactivity was detected, indicating that it does not bind N-cadherin or E-cadherin protein (Figure 3.1C). These findings support the conclusion that the EPR1792Y monoclonal antibody specifically binds CDH12.

Table 3.1

Protein	Identity to CDH12 (%)	Classical Cadherin Family
Cadherin 1 (E-Cadherin)	34	Type I
Cadherin 2 (N-Cadherin)	37	Type I
Cadherin 3	32	Type I
Cadherin 4	36	Type I
Cadherin 5	39	Type II
Cadherin 6	62	Type II
Cadherin 7	61	Type II
Cadherin 8	56	Type II
Cadherin 9	58	Type II
Cadherin 10	62	Type II
Cadherin 11	56	Type II
Cadherin 14	60	Type I
Cadherin 15	35	Type I
Cadherin 19	47	Type II
Cadherin 20	56	Type II
Cadherin 22	51	Type II
Cadherin 24	49	Type II

IV.ii. Identifying novel DCC binding partners

To determine potential DCC binding partners we used an unbiased mass spectrometry approach to identify candidate proteins that co-immunoprecipitate with DCC. Commissural neurons were cultured for 2 DIV and treated with 200 ng/ml of netrin-1 for 15 min prior to being collected and lysed in 1% Triton X-100 buffer. Cell lysates were immunoprecipitated using the DCC_{in} monoclonal antibody (BD Pharmingen) or with protein A/G beads alone as a control. Proteins that co-immunoprecipitated with DCC were separated on a polyacrylamide gel and visualized using Coomassie blue. Six well-defined bands selectively enriched in the DCC_{in} lane were excised and analysed using 2-dimensional liquid chromatography mass spectroscopy (Figure 3.2A). These bands contained multiple previously identified DCC interacting effector proteins including the MAPKK MEK2, TUBB3, and 14-3-3, along with novel candidate interacting proteins (Forcet et al., 2002; Kent et al., 2010; Qu et al., 2013). In particular, band number 3 produced two peptide sequences matching CDH12 (Table 3.2). The sequences obtained were specific to CDH12 and did not overlap with any other cadherins within the cadherin superfamily. These results identified CDH12 as a possible novel DCC interacting protein and led us to further investigate a putative interaction between DCC and CDH12.

Table 3.2

Protein Description	Mass spec peptide sequence	Band Number	CDH12 sequence	Amino Acid Range
Brain Cadherin (Cadherin 12)	VDASNLHLDHR	3	VDASNLHLDHR	124-134
	DTLMTSKEDIR	3	DTLMTSKEDIR	420-430

IV.iii. Cadherin 12 co-immunoprecipitates with DCC

To further validate CDH12 as a potential DCC interacting protein, we carried out additional co-immunoprecipitation (co-IP) experiments using embryonic spinal cord homogenates and cultured

embryonic spinal commissural neuron lysates. Whole spinal cords from E13 rats were homogenized and DCC immunoprecipitated using the DCC_{in} monoclonal antibody. Western blot analysis of co-immunoprecipitated proteins revealed an ~140 kDa CDH12 immunoreactive band in the DCC IP sample, but not in IgG controls. This finding supports the mass spectrometry results identifying CDH12 as a protein that can be co-immunoprecipitated with DCC from embryonic spinal cord (Figure 3.2B). We also probed for β-catenin, a critical down stream signaling partner of the cadherins. A β-catenin immunoreactive band was detected in DCC IP samples but not the control IgG IP samples, demonstrating co-IP of β-catenin with DCC from spinal cord homogenates. We then examined if netrin-1 might influence the interaction of DCC and CDH12. Cultured 2 DIV embryonic spinal commissural neurons were either treated with 200 ng/ml of netrin-1 for 15 min prior to lysis or left untreated as control. IgG control samples were not treated with netrin-1. CDH12 was detected in the DCC IP samples from whole cell homogenates and netrin-1 treatment did not influence the amount of CDH12 associated with DCC. No CDH12 immunoreactive band was detected in the IgG IP control (Figure 3.2C). We were unable to examine possible β-catenin co-IP in these samples as a non-specific mouse antibody reactive band ran just under 100 kDa in the cultured commissural neuron samples. β-catenin runs at ~90kDa and was obscured by the nonspecific band. Taken together, these results support the conclusion that CDH12 is a novel DCC interacting partner and that CDH12 and β-catenin co-IP with DCC from embryonic spinal cord.

IV.iv. Expression of cadherin 12 in the developing spinal cord

To visualize the distribution of CDH12 protein in the developing spinal cord we used paraffin sections from E10.5, E12.5, and E14.5 wild type mice (Figure 3.3). Commissural neurons are born in the dorsal brachial spinal cord in mouse between E9.5 and E12.5 and have crossed the

ventral midline by E14 (Helms & Johnson, 2003; Pignata et al., 2016). Therefore, these time points allowed us to examine the distribution of CDH12 throughout commissural axon extension to the ventral midline. CDH12 immunoreactive cells were detected throughout the neuroepithelium and ventricular zone of the embryonic spinal cord at all stages examined. Commissural axons extending from the dorsal spinal cord to the floor plate were also CDH12 immunopositive and CDH12 immunostaining was particularly concentrated in the ventral commissure formed by commissural axons crossing the ventral midline (Figure 3.3). Western blot analysis of homogenates of embryonic CNS confirmed expression of CDH12 protein in E13 and E17 rat spinal cord (Figure 3.4A). Since subsequent experiments were carried out using rat tissue, we also examined the distribution of CDH12 in E13 rat spinal cords and detected CDH12 distributed along descending commissural axons and expressed by neuroepithelial cells. This distribution is essentially identical to the distribution detected in the developing mouse spinal cord (Figure 3.4B). We then examined the cellular distribution of CDH12 in spinal commissural neurons isolated from E13 rat embryos cultured for 2DIV. CDH12 was detected in the cell body, along the shaft of the extending axon, and in commissural neuron growth cones (Figure 3.4 C). Co-labeling for DCC and CDH12 revealed that both are present in commissural neuron growth cones, with a partially overlapping distribution.

IV.v. Netrin-1 does not bind cadherin 12

Netrin-1 is a well characterized DCC ligand; however, it was not known if netrin-1 might also bind to cadherins (Finci et al., 2014; Keino-Masu et al., 1996; K. Xu et al., 2014). We used a HEK293T cell surface binding assay to test the possibility that netrin-1 may be binding to CDH12 and mediating the interaction with DCC. HEK293T cells do not express DCC or CDH12 and express very low levels of netrin-1 and the netrin-1 receptors UNC5B, UNC5C, and UNC5D

(www.proteinatlas.org/cell) (Shekarabi & Kennedy, 2002). To asses binding, HEK293T cells were transfected with plasmids encoding full length CDH12, DCC, UNC5B, or Slitrk1 and grown for 48 hr to allow for protein expression. Recombinant netrin-1 protein was then added at rt in a buffer containing 10 % hiHS and 2 ug/ml heparin to block nonspecific binding, and 0.1 % sodium azide to prevent receptor endocytosis. After a 90 min incubation netrin-1 was washed from the cells and surface binding measured using immunofluorescence. DCC and UNC5B are known netrin-1 receptors and were used as positive binding controls, while the transmembrane protein Slitrk1 was used as a negative control (Keino-Masu et al., 1996; Ko, 2012; Leonardo et al., 1997). Netrin-1 immunofluorescence was clearly visible on cells expressing DCC or UNC5B, but not on cells expressing Slitrk1 or CDH12 providing evidence that CDH12 does not bind netrin-1 (Figure 3.5). These results, along with the IP results, indicate that the CDH12 is interacting with DCC in a netrin-1 independent manner.

IV.vi. Cadherin 12 provides a permissive environment for spinal commissural neuron growth

Cadherins are thought to function in axon guidance by providing a permissive substrate that paves the way for axon extension through complementary cadherin expression. This mechanism predicts that cells expressing one type of cadherin will follow the underlying neuroepithelium expressing the same cadherin (Matsunaga et al., 1988; Redies et al., 1992). The expression of CDH12 by both neurons and neuroepithelial cells in the developing spinals cord suggests that CDH12 may function to provide a permissive, guiding, substrate for commissural axon extension. Growth cones of spinal commissural neurons respond to netrin-1 and *in vitro* application of netrin-1 to commissural neurons triggers a rapid increase in both the area and the number of filipodia per growth cone (Shekarabi et al., 2005). To test whether CDH12 effects this

phenomenon we cultured spinal commissural neurons on glass cover slips coated with recombinant CDH12-Fc to mimic CDH12 expression by neuroepithelial cells. Neurons were cultured both on CDH12-Fc and standard PDL surfaces and treated with 200 ng/ml of netrin-1 for 15 min prior to fixation and immunostaining. Cells were immunostained with fluorescent phalloidin to visualize F-actin and Hoechst to visualize cell nuclei. We then compared neurons grown on a CDH12-Fc surface to those grown on PDL across 5 measures; the number of cells adhered to the surface, the length of the longest neuronal process, the number of filopodia per cell, the number of filopodia per growth cone, and the area of the growth cone (Figure 3.6). All conditions were pooled for the cell count measure as the short duration of the netrin-1 treatment should not affect the number of neurons adhered to the surface. Compared to PDL, the CDH12-Fc surface had no affect on the cell count or the length of the longest process (Figure 3.6). On both the CDH12-Fc and PDL surfaces the number of filopodia per growth cone and the growth cone area was significantly increased following treatment with netrin-1. Interestingly, neurons grown on the CDH12-Fc surface had a significant increase in the total number of filopodia per cell following netrin-1 treatment, but no effect was seen in neurons cultured on PDL (Figure 3.6). The addition of soluble CDH12-Fc had no effect compared to control on either surface for any measure. The difference in the number of filopodia per cell following netrin-1 treatment provides evidence that CDH12 is providing a more permissive substrate for the effect of netrin-1 than PDL alone.

IV.vii. Netrin-1 induces phosphorylation of β-catenin

β-catenin signals downstream of cadherins and functions to regulate various cellular processes including actin dynamics and filament formation (McCrea & Gu, 2010). A number of kinases phosphorylate β-catenin on various residues and this phosphorylation regulates protein stability

and signaling (Valenta et al., 2012). Phosphorylation of β-catenin modulates its ability to bind to other proteins, including cadherins and α-catenin (Valenta et al., 2012). Since netrin-1 induces cell-wide filopodia formation on a CDH12-Fc substrate, beyond just the growth cone as seen on PDL alone, we hypothesized that this may be due to β-catenin signaling enhancing netrin-1 function to promote a more general increase in actin filament formation. To determine if netrin-1 might influence β-catenin phosphorylation we assayed two β-catenin residues known to be phosphorylated by kinases downstream of DCC. Serine 675 (S675) is phosphorylated by P21 activated kinase 1 (Pak1) and Tyrosine 142 (Y142) is phosphorylated by the src family tyrosine kinases (SFKs) Fer/Fyn (Piedra et al., 2003; Zhu et al., 2012). To assess phosphorylation downstream of netrin-1, commissural neurons cultured for 2DIV were treated with 200 ng/ml netrin-1 for 15 min prior to lysis and proteins were then separated on a polyacrylamide gel for western blot analysis (Figure 3.7). Treatment with netrin-1 did not alter the total level of β-catenin protein in commissural neurons; however, significant increases in β-catenin phosphorylation were detected at both S675 and Y142 residues (Figure 3.7A & B). To determine which kinases phosphorylate β-catenin downstream of netrin-1 we used pharmacological inhibitors. To investigate phosphorylation at S675 we used IPA3 which selectively inhibits Pak1 and also its inactive analog PIR3.5 (Deacon et al., 2008). Application of 10 μM IPA3 to cultured 2 DIV commissural neuron for 20 min prior to the addition of 200 ng/ml netrin-1 prevented phosphorylation of β-catenin at S675, while pre-treatment with PIR3.5 had no effect. This provides evidence that netrin-1 promotes phosphorylation of S675 through a Pak1 mediated mechanism (Figure 3.7C). To assess phosphorylation at Y142 we used PP2 which inhibits SFKs, and its inactive analog PP3 (Hanke et al., 1996). Application of 10 μM of both PP2 and PP3 caused an unexpected increase in baseline phosphorylation without netrin-1 present (Figure

3.7D). This result suggested that an off-target effect of PP2 and PP3 may influence phosphorylation of Y142. Intriguingly, casein kinase 1 delta (CK1δ) is a non-SFK target inhibited by both PP2 and PP3 (Bain, McLauchlan, Elliott, & Cohen, 2003). CK1δ functions in the wnt signalling pathway regulating the phosphorylation of various wnt pathway components which are upstream of β-catenin function (Cruciat, 2014). Inhibition of CK1δ by PP2 and PP3 would therefore alter the phosphorylation state of β-catenin as we see in figure 3.7D.

IV.viii. DCC expression does not alter β-catenin expression

Previous studies have shown that netrin-1 and DCC can alter the expression of cadherins and catenins in different neuronal cells *in vitro* (Pratt et al., 2012; Reyes-Mugica et al., 2001). In the growth cones of thalamic neurons, treatment with netrin-1 altered β-catenin fluorescence intensity over a short period of time with levels returning to normal after 24 hr (Pratt et al., 2012). In neuroblastoma cells, disrupting DCC function via ectopic expression of a truncated DCC that lacks the intracellular domain, resulted in reduced expression of N-cadherin and β-catenin (Reyes-Mugica et al., 2001). Considering this evidence along with our finding that netrin-1 signaling promotes β-catenin phosphorylation, we investigated if total levels of β-catenin protein were altered in conventional DCC null knockout mice (Fazeli et al., 1997). Western blot analysis of E14 spinal cord homogenates revealed no significant difference in the protein levels of β-catenin between DCC knockouts and wild type or heterozygous litter mates (Figure 3.8). This indicates that, although DCC regulates β-catenin phosphorylation, a persistent lack of DCC expression does not affect the overall expression of β-catenin in the developing spinal cord.

IV.ix. Cadherin 12 increases netrin-1 induced commissural axon outgrowth

Netrin-1 evokes DCC dependent commissural axon outgrowth from explants of E13 dorsal spinal cord (Kennedy et al., 1994). To determine if CDH12 influences netrin-1 mediated embryonic spinal commissural axon outgrowth we cut ~200 μm x 200 μm explants of dorsal spinal cord and embedded them in a three-dimension collagen gel. After 16 hr in culture total outgrowth was assessed (Figure 3.9). In control conditions with nothing added, and conditions with 200 ng/ml CDH12-Fc, or 50 ng/ml netrin-1 added, only a small amount of outgrowth was detected. In contrast, treatment with 200 ng/ml of netrin-1 evoked a significant increase in axon outgrowth from the explant into the collagen matrix. Notably, the addition of 200 ng/ml of CDH12-Fc with 50ng/ml of netrin-1 evoked axon outgrowth similar to the levels seen with 200 ng/ml of netrin-1 alone. This finding provides evidence that the co-application of CDH12-Fc potentiates the response to netrin-1, despite having no effect on outgrowth on its own (Figure 3.9).

IV.x. Cadherin 12 function is required for commissural axon turning

Cadherin and catenins have previously been demonstrated to alter the trajectory of spinal commissural neurons (Aviles & Stoeckli, 2016; Yang et al., 2016). Commissural axons normally project from the dorsal spinal cord to the floor plate at the ventral midline, cross to the contralateral side, and then turn rostrally to project anteriorly towards the brain. To determine if CDH12 influences commissural axon extension within the neuroepithelium, we used open book explant preparations derived from E11 rat spinal cords and visualized axon trajectories by injecting DiI along the dorsal edge of the spinal cord (Figure 3.10). Open book explants were treated with CDH12-Fc to compete endogenous CDH12-CDH12 interactions. A function

blocking β-1 integrin antibody (CD29) was used as a control to account for non-specific effects of applying the Fc receptor-body (Rajasekharan et al., 2009).

After 48 hr *in vitro*, we determined the effect of disrupting CHD12 interactions on commissural axon turning, examining both initial attraction toward the midline and contralateral turns after crossing the midline. Defects in ipsilateral attraction toward the midline were not detected as a result of including either 10 µg/ml of the CD29 antibody as a control, or 200 ng/ml of the CDH12-Fc. Untreated open books and those treated with the CD29 antibody had no defects and commissural axon turning can be clearly visualized in control conditions as indicated by the white arrow heads in figure 3.10 A-C. Commissural axons in open book explants treated with CDH12-Fc fail to make the rostral turn and either stall after crossing or continue to extend perpendicular to the floor plate into the contralateral neuroepithelium (Figure 3.10 D-F). These results compliment previous studies that showing that loss of β-catenin results in commissural axon stalling and failing to make the rostral turn (Aviles & Stoeckli, 2016).

V. DISCUSSION

Results obtained from a mass spectrometry screen for proteins that co-IP with DCC from embryonic rat spinal commissural neurons led us to investigate a possible interaction between DCC and CDH12. CDH12 is a relatively understudied type II classical cadherin and we provide evidence here that it is widely expressed in the developing spinal cord and influences commissural axon guidance. Further, our finding supports the conclusion that DCC forms a complex with CDH12 and its signaling partner β-catenin, and that netrin-1 signaling through DCC promotes β-catenin phosphorylation.

CDH12 is widely expressed in the developing spinal cord and CDH12 protein is associated with neuroepithelial cells, commissural neuron cell bodies, axons, growth cones, and particularly concentrated in the embryonic spinal ventral commissure. This distribution suggested that CDH12 might play a role in commissural axon guidance. We demonstrate that both CDH12 and its downstream signaling partner β-catenin co-IP with DCC from homogenates of whole embryonic spinal cord and cultured commissural neurons. We also tested the possibility that netrin-1 might bind CDH12 but found no evidence that CDH12 functions directly as a receptor for netrin-1, suggesting that netrin-1 binds to a heteromeric complex of DCC and CDH12 which in turn activates β-catenin signaling.

DCC has previously been shown to regulate cadherin and catenin expression in neuroblastoma cells and netrin-1 to modulate β-catenin expression in thalamic neurons (Pratt et al., 2012; Reyes-Mugica et al., 2001). Ectopic expression of a truncated DCC protein lacking the intracellular domain in neuroblastoma cells resulted in decreased N-cadherin, β-catenin, and α-catenin protein, suggesting that the truncated DCC destabilizes N-cadherin based junctions (Reyes-Mugica et al., 2001). In thalamic neurons, treatment with netrin-1 caused a transient and localized increase in β-catenin fluorescence intensity in growth cones that then decreased below starting levels before returning to baseline (Pratt et al., 2012). These two results suggest a possible convergence of the netrin-1/DCC and cadherin/catenin signaling pathways. While we did not detect any significant difference in β-catenin protein levels in DCC knockout mice, we did determine that netrin-1 increases β-catenin phosphorylation at two residues, Y142 and S675 (Figure 3.7). Both residues are phosphorylated by kinases known to be activated downstream of DCC.

Traditional models of cadherin cell adhesion function have been based on the notion that the intracellular domain of cadherins binds directly to β-catenin, which then binds α-catenin to form a signaling complex that in turn binds to and regulates the local organization of F-actin within the cell (Drees et al., 2005). This model provides a direct physical link between extracellular cadherin – cadherin binding and the intracellular cytoskeleton via a catenin bridge. In contrast, more recent evidence argues against this model. These studies indicate that α-catenin cannot bind both β-catenin and F-actin at the same time, but rather these interactions are mutually exclusive (Drees et al., 2005). Therefore, in order for cadherins to influence actin polymerization in the cell α-catenin must be released from the cadherin catenin adhesion complex. The Y142 residue of β-catenin regulates binding of α- and β-catenin. When Y142 is phosphorylated β-catenin can no longer bind to α-catenin and α-catenin is released into the cytosol where it can then mediate actin polymerization (Aberle, Schwartz, Hoschuetzky, & Kemler, 1996). Once α-catenin is released into the cytosol it forms homodimers which bind to actin filaments and inhibit the Arp2/3 complex. This shifts actin polymerization from branched sheets to linear bundles, a process which is required for filopodia formation (Drees et al., 2005).

Using a phospho-specific antibody we have found that netrin-1 also increases β-catenin phosphorylation at the Y142 residue. Y142 is downstream of fyn kinase *in vitro* and fak kinase *in vivo*, both of which are activated in response to netrin-1 binding DCC (X. L. Chen et al., 2012; Piedra et al., 2003). Netrin-1 signaling through DCC has previously been shown to promote filopodia formation and growth cone expansion in commissural neurons (Shekarabi & Kennedy, 2002; Shekarabi et al., 2005). Our findings provide evidence that netrin-1 binding to DCC causes phosphorylation of β-catenin on Y142 which would result in the release of α-catenin into the cytosol. Once in the cytosol α-catenin homodimers then mediate filopodia formation through

inhibition of Arp 2/3 (Figure 3.11). Consistent with this, we found that commissural neurons grown on a substrate of CDH12 exhibited a significant increase in the number of filopodia in response to treatment with netrin-1 (Figure 3.6). Further, addition of CDH12-Fc to dorsal embryonic spinal cord explants did not influence outgrowth itself, but significantly potentiated axon outgrowth evoked by the 50 ng/ml submaximal concentration of netrin-1. The addition of soluble CDH12-Fc to embryonic dorsal spinal cord explants may cluster or stabilize endogenous CDH12 on the plasma membrane. Increased plasma membrane cadherin is predicted to increase the local concentration of α-catenin which would then in turn promote the polymerization of linear actin filaments as described above leading to increased filipodia formation and axon outgrowth.

Once across the midline, the trajectory of commissural axon growth is regulated through a number of mechanisms, including wnt signalling (Aviles & Stoeckli, 2016). β-catenin is a key downstream effector of canonical wnt signaling and loss of β-catenin leads to stalling of commissural neuron growth cones in the floor plate and a failure to complete the rostral turn (Aviles & Stoeckli, 2016). This phenotype is very similar to what we detect in the current study following the addition of CDH12-Fc to open book explant cultures (Figure 3.10). In order to participate in wnt signalling β-catenin must be released from the cadherin adhesion complex and be stabilized within the cytoplasmic pool. Cadherin internalization is one mechanism that regulates β-catenin release (Kam & Quaranta, 2009; Le, Yap, & Stow, 1999). Exogenous CDH12-Fc added to open book explants is expected to bind endogenous CDH12 expressed by commissural neurons, possibly trapping it on the cell surface. This predicts that binding to CDH12-Fc would antagonize internalization and thereby hinder the release of β-catenin. CDH12-Fc binding would mask cell-cell CDH12 binding and trap CDH12 on the surface. This

would disrupt both CDH12 adhesion and signalling and prevent β-catenin release, accounting for the commissural neuron phenotypes detected in CHD12-Fc treated open book explants (Figure 3.10). Once released, cytosolic β-catenin must be phosphorylated to prevent its inclusion in the β-catenin Destruction Complex and promote its involvement in wnt signalling (Zhao et al., 2013). The S675 residue is one site in particular that has been shown to stabilize β-catenin and promote its transcriptional activity downstream of Rac1 and Pak1 activation (Zhu et al., 2012). Here we show netrin-1 mediates β-catenin phosphorylation at site S675 and that this is dependant on Pak1, a kinase known to be activated downstream of DCC (Shekarabi et al., 2005).

Until now, the interplay between netrin-1/DCC and cadherin/catenin signalling has not been extensively studied. Here we demonstrate the convergence of these two signalling pathways to mediate commissural axon growth in the developing spinal cord. While the specific details underlying the mechanism of action have yet to be determined, our findings support the conclusion that DCC and CDH12 form a heteromeric complex through which netrin-1 regulates β-catenin phosphorylation state and function.

VI. FIGURES

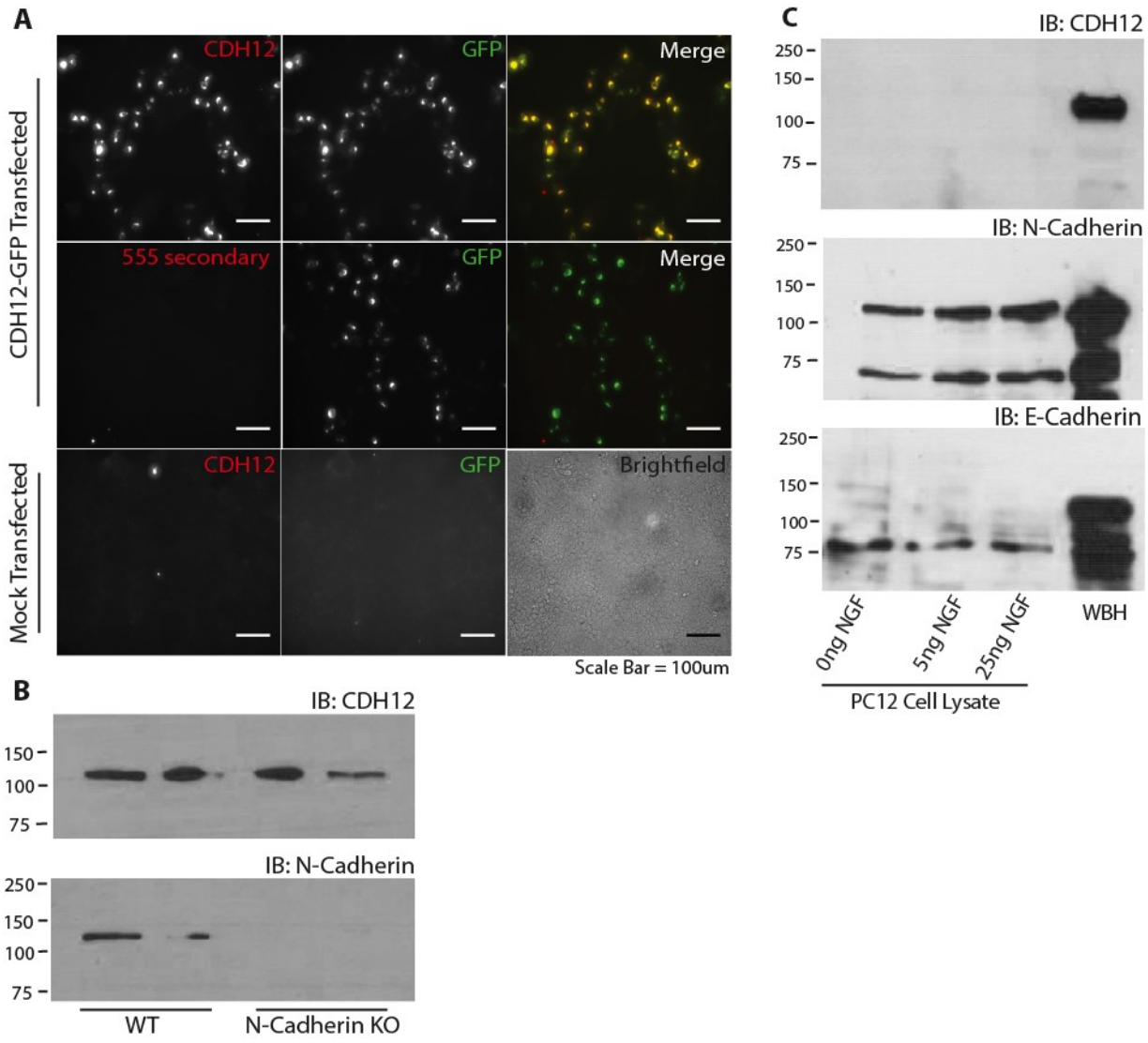

3.1: Cadherin 12 antibody validation. A: HEK293T cells transfected with a cDNA encoding CDH12-GFP or mock transfected (no DNA). Cells were then immunolabelled with the CDH12 antibody or secondary antibody only. Only CDH12-GFP transfected cells were immunopositive for CDH12. **B:** Western blot analysis of hippocampal homogenates from the CA1 region of N-cadherin knockout mice tests the specificity of the CDH12 antibody. Western blots probed for N-cadherin detect an immunopositive band in the wild type (WT) but not the knockout (KO) animals, while blots probed for CDH12 show approximately equal levels of protein in both the

WT and KO homogenates. **C:** Western blot analysis of lysates of PC12 cells differentiated with NGF. Adult rat whole brain homogenate (WBH) was used as control. A CDH12 immunoreactive band, at the predicted molecular weight (~140 kDa), was only detected in WBH. In contrast, antibodies against N cadherin and E cadherin detect protein in all samples. These findings are consistent with the predicted absence of CDH12 expression by PC12 cells.

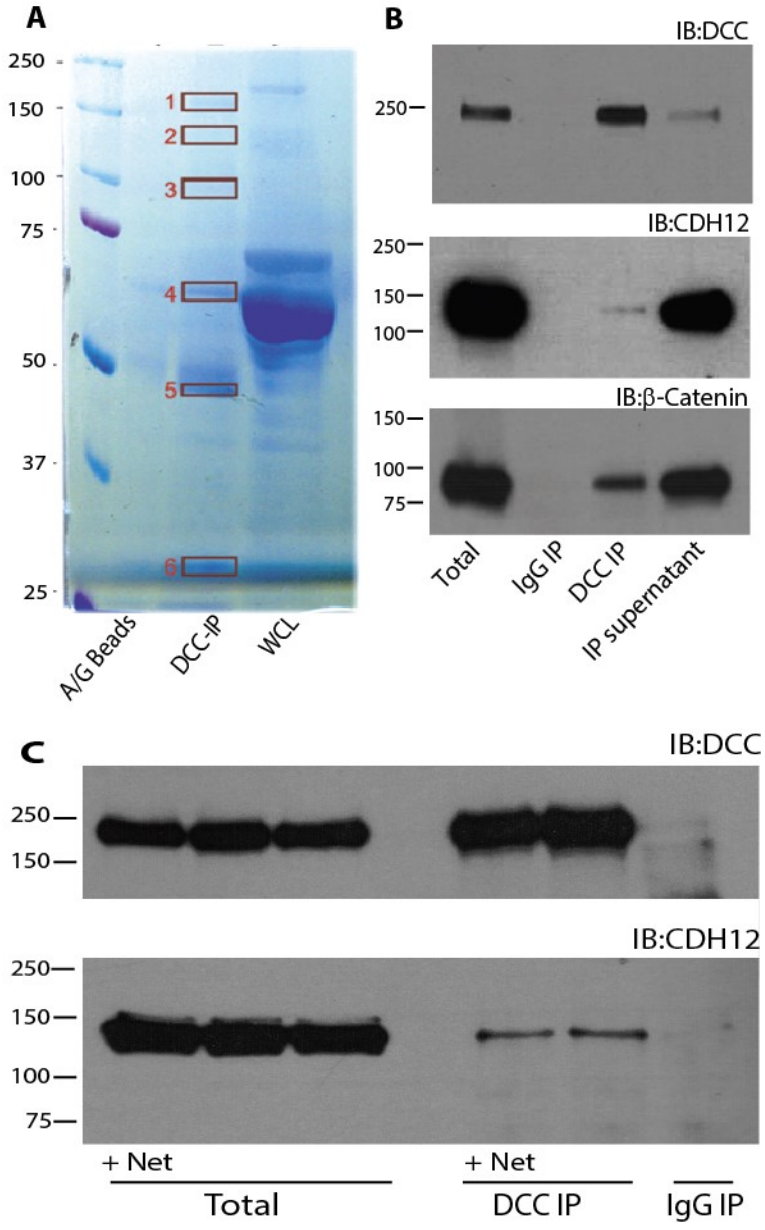

Figure 3.2: CDH12 is a possible DCC interacting protein. A: Analysis of proteins obtained from co-IP with DCC_{in} from homogenates of 2 DIV E13 rat embryonic spinal commissural neurons. Neurons were stimulated with netrin-1 for 15 min prior to IP with DCC_{in} antibody. Proteins in whole cell homogenates were then separated on a polyacrylamide gel and the highlighted bands excised and sent for mass spectrometry analysis. **B:** Western blots show DCC IP from whole E13 spinal cord. Total protein, IgG control IP, DCC IP, and IP supernatant samples are shown. DCC is enriched in the DCC IP and completely absent from the IgG control IP. CDH12 and β catenin are both present in DCC IP lanes and absent in IgG controls. **C:** Western blots showing DCC IP from cultured commissural neurons with or without 200 ng/ml netrin-1 treatment for 15 min. DCC is present in DCC IP lanes with and without netrin and absent in IgG controls. CDH12 is also present in DCC IP lanes and absent in IgG controls. Netrin-1 does not affect CDH12 co-IP with DCC.

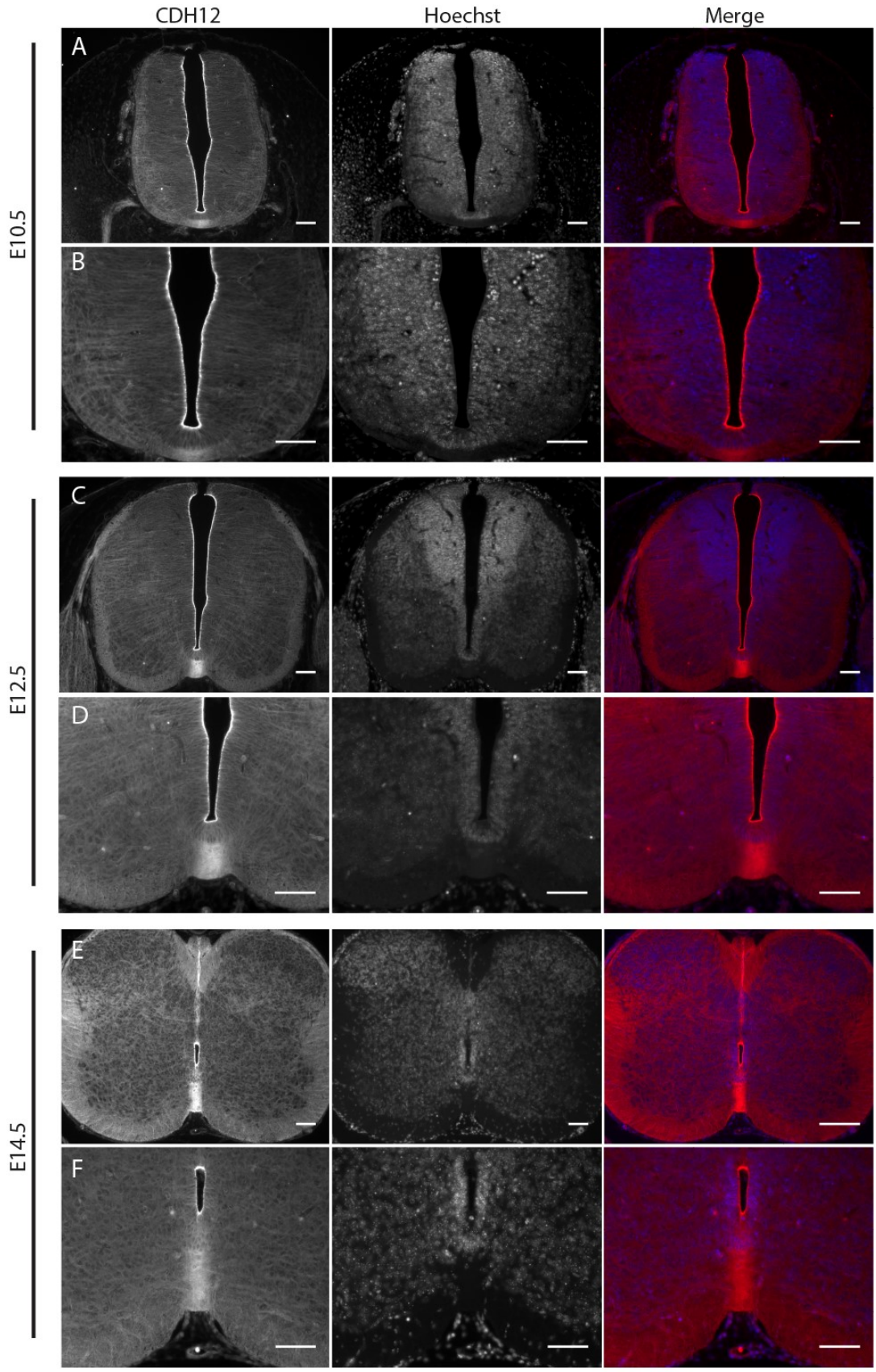
CDH12
Hoechst
Merge
A
B
C
D
E
F
E10.5
E12.5
E14.5
Scale bar = 100um

Figure 3.3: Immunohistochemical distribution of CDH12 in E10.5, E12.5, and E14.5 mouse spinal cord. Tissue sections were labeled with CDH12 (red) and Hoechst (blue). B, D and F are enlargements of the ventral spinal cord and floor plate of A, C and E respectively (scale bar = 100 μm).

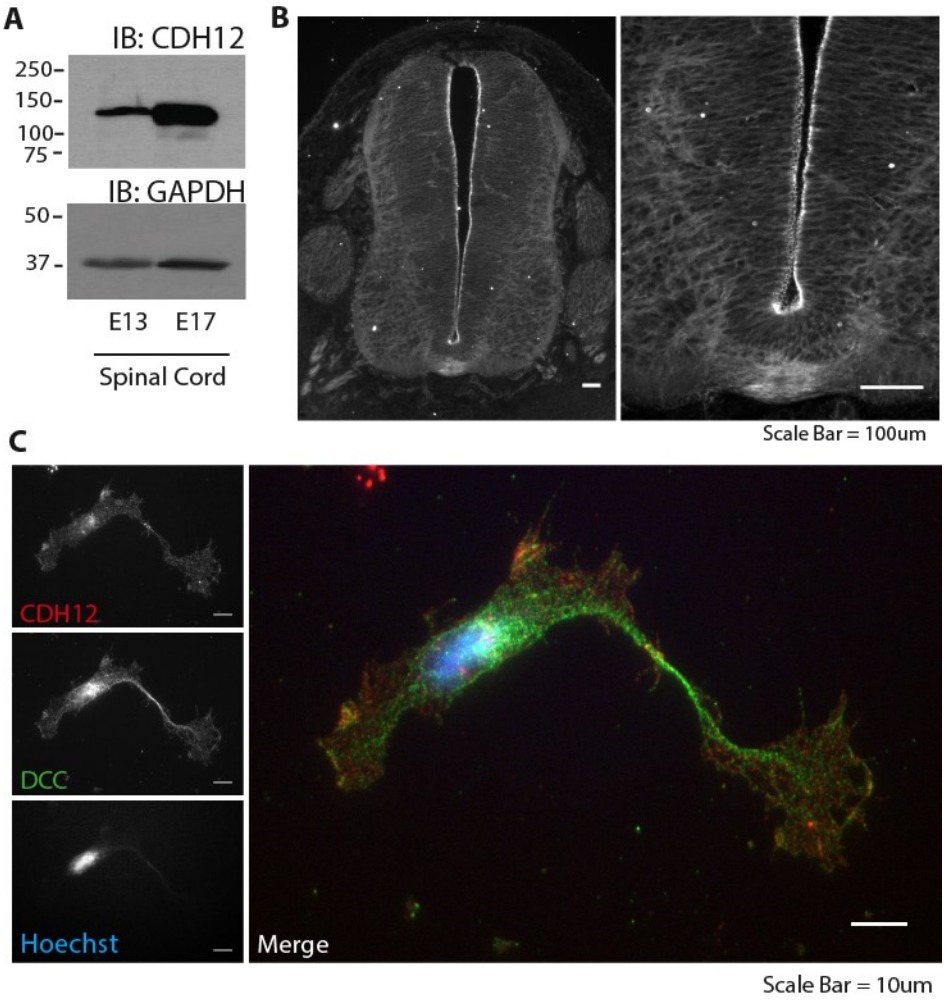

Figure 3.4: Distribution of CDH12 protein in embryonic rat spinal cord *in vivo* and embryonic spinal commissural neurons *in vitro*. A: Western blot illustrating CDH12 immunoreactivity in E13 and E17 spinal cord homogenates, with GAPDH as a loading control. **B:** Section of E13 rat spinal cord shows the distribution of CDH12 immunoreactivity. CDH12

immunoreactivity delineates the edges of neuroepithelial cells, floor plate cells and commissural axons (scale bar = 100 µm). **C:** Distribution of CDH12 immunocytochemistry in 2 DIV E13 rat spinal commissural neurons. CDH12 is labelled red, DCC green, and Hoechst blue (scale bar = 10 µm).

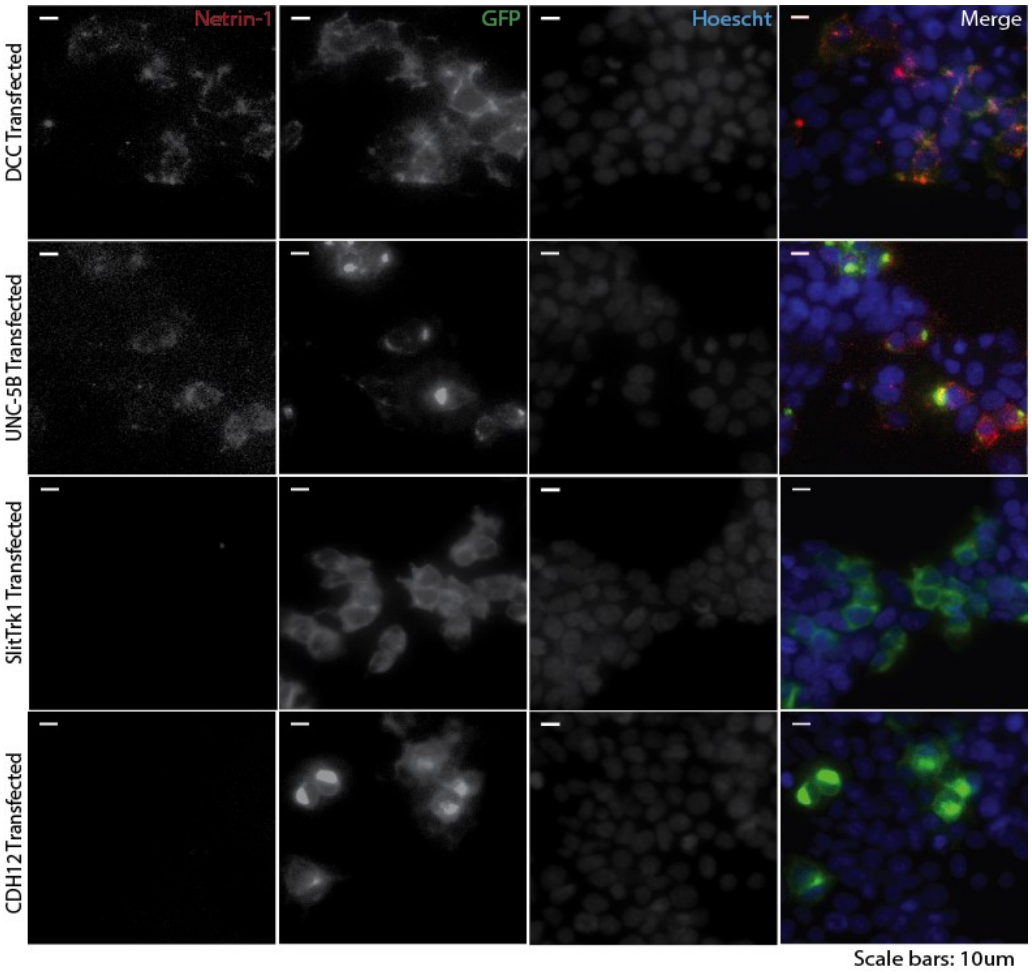

Figure 3.5: CDH12 does not bind netrin-1. HEK293T cells transfected to express DCC-GFP, Unc-5B-GFP, Slitrk1-GFP, or CDH12-GFP protein chimeras. Netrin-1 binds to DCC and Unc-5B expressing HEK293T cells but not to Slitrk1 or CDH12 expressing cells. Netrin-1 is labeled red, GFP green, and Hoechst blue (scale bars = 10 µm).

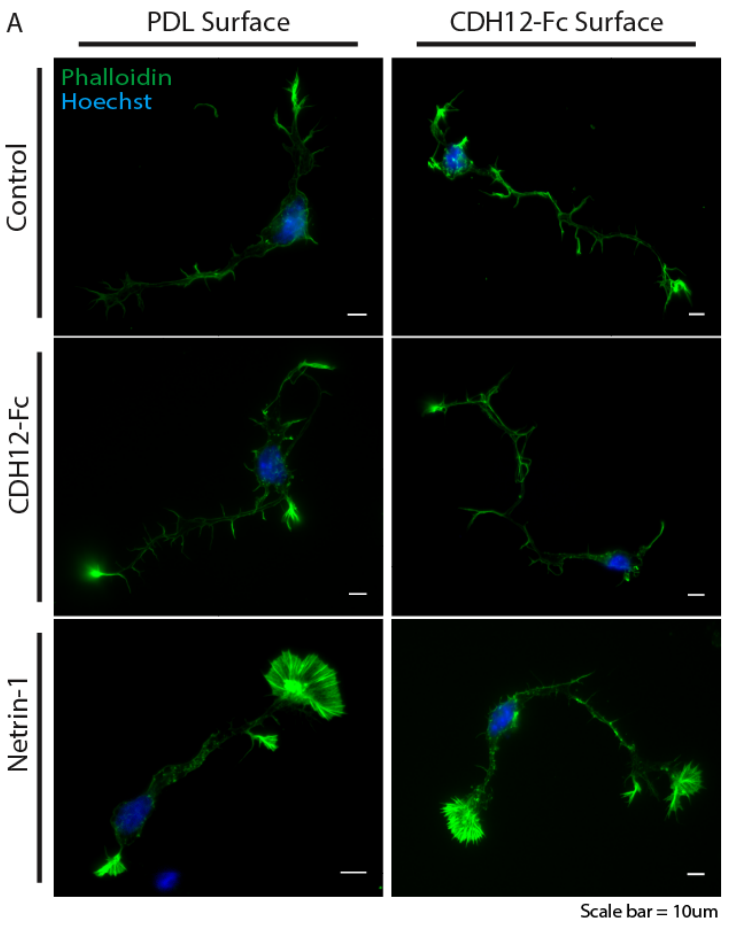
A
PDL Surface
CDH12-Fc Surface
Phalloidin
Hoechst
Control
CDH12-Fc
Netrin-1
Scale bar = 10um

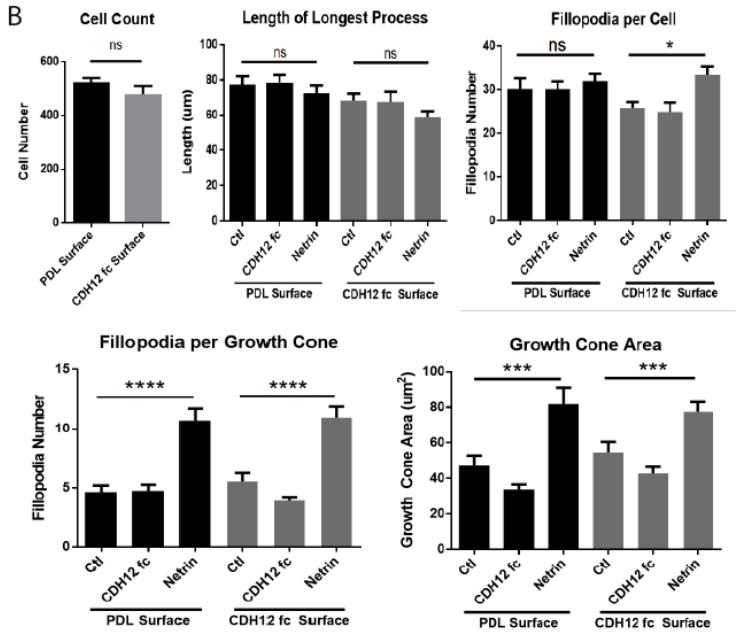
B
Cell Count
Cell Number
PDL Surface
CDH12 fc Surface
Length of Longest Process
Length (um)
Fillopodia per Cell
Fillopodia Number
Ctl
CDH12 fc
Netrin
Fillopodia per Growth Cone
Growth Cone Area
Growth Cone Area (um²)

Figure 3.6: CDH12 substrate enhances netrin-1 induced filopodia formation. Embryonic rat spinal commissural neurons were grown on glass coverslips coated with either PDL or PDL + CDH12-Fc. Neurons were then treated for 15 min with either CDH12-Fc, netrin-1 or left untreated as control. Representative images are shown. Quantification of cell number, length of the longest process, filopodia per cell, filopodia per growth cone, and growth cone area are shown in the histograms below. For cell counts, all conditions were grouped. No significant differences were detected in the number of cells or the length of the longest process in any condition. The total number of filopodia per cell was unchanged with the addition of netrin-1 to cells on the PDL surface. In contrast, on the CDH12-Fc coated surface treatment with netrin-1 significantly increased the number of filopodia per cell. The number of filopodia per growth cone, and the surface area of the growth cone, were both significantly increased following 15 min treatment with netrin-1 on both PDL and CDH12-Fc surfaces. Phalloidin labeled F-actin is green and Hoechst staining is blue (scale bar = 10 μm. One-way ANOVA with Tukey test. n = 30 neurons, 10 neurons from 3 coverslips per condition. **** $p<0.0001$, *** $p<0.001$, * $P<0.05$).

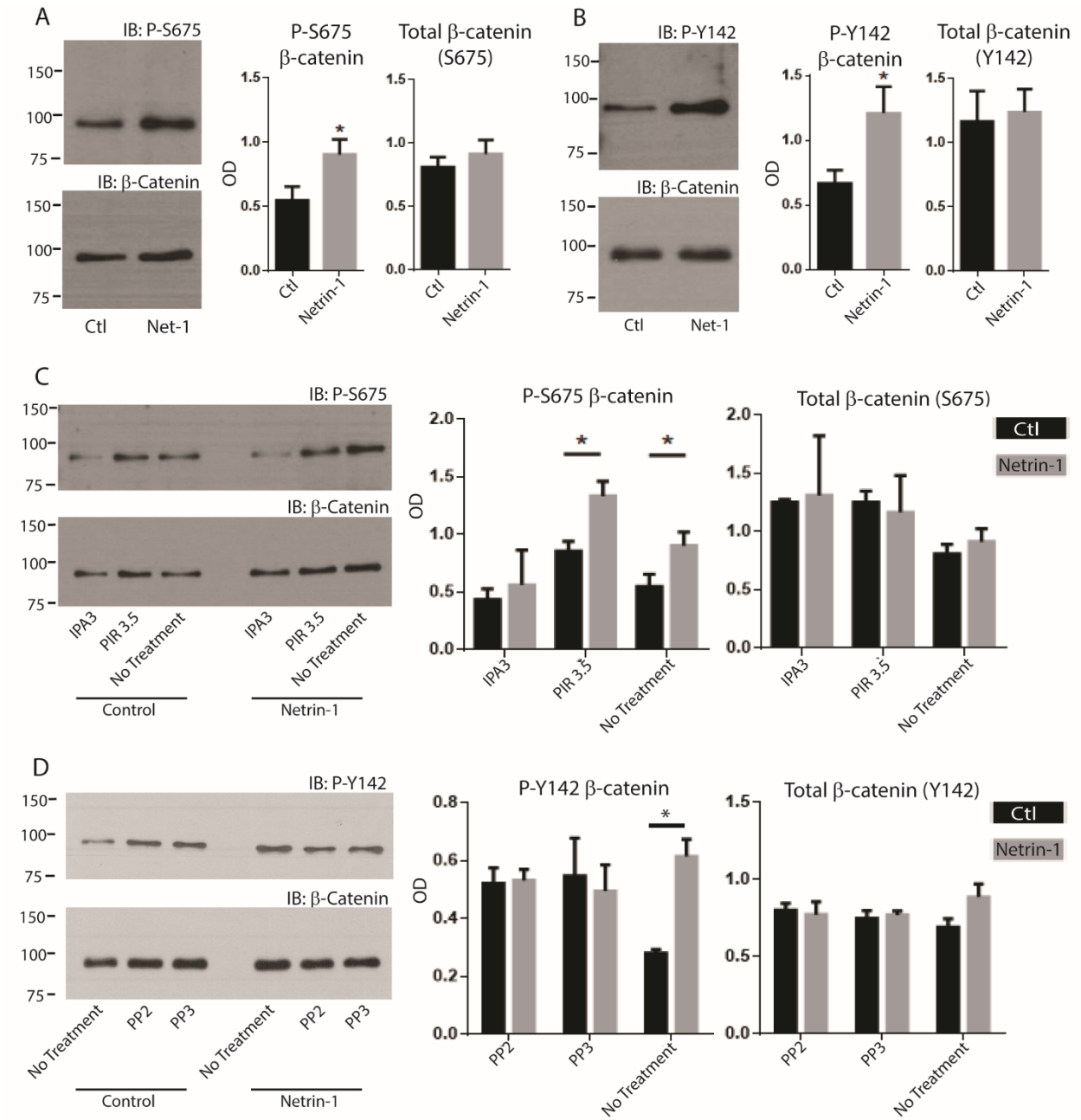

Figure 3.7: Increased phosphorylation of β-catenin following netrin-1 treatment. Cultured commissural neurons were treated with 200 ng/ml of netrin-1 for 15 min and phosphorylated β-catenin level assessed via western blot analysis. **A-B)** Antibodies detecting phosphorylation at serine 675 (S675) and tyrosine 142 (Y142) were used. Both sites increased phosphorylation following treatment with netrin-1. Total β-catenin levels were unchanged. **C)** Netrin-1 induced

phosphorylation at S675 is Pak1 dependant. Cultured commissural neurons were treated for 20 min with IPA3 a Pak inhibitor or PIR3.5 an inactive analog of IPA3 prior to treatment with netrin-1. Netrin-1 induced phosphorylation at S675 was blocked by IPA3 but was not affected by the control compound PIR3.5. Total β-catenin levels were not affected by either drug. **D)** Netrin-1 induced phosphorylation at Y142 in response to SFKs. Cultured commissural neurons were treated for 20 min with the SFK inhibitor PP2, or PP3 an inactive analog of PP2, prior to treatment with netrin-1. Either PP2 or PP3 increased baseline phosphorylation making it impossible to assess netrin-1 induced phosphorylation. Total β-catenin levels were not affected by either drug (unpaired two tailed t-test, n= 6 for Y142 and n=8 for S675 n=3 for IPA3 and PIR 3.5, n=4 for PP2 and PP3. $P<0.05$).

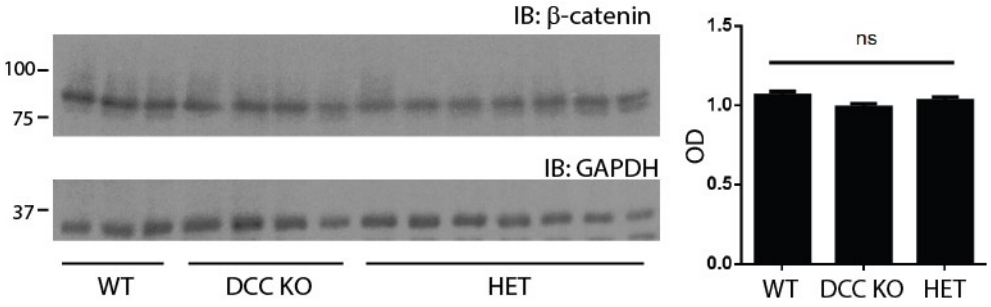

Figure 3.8: Unaltered β-catenin expression in DCC null embryonic mouse spinal cord. β-catenin immunoreactivity detected from homogenates of E14 spinal cord dissected from wildtype (WT), Heterozygous (HET), and DCC knockout (KO) mice. Western blot analysis of E14 spinal cord homogenates probed for β-catenin. GAPDH was used as a loading control. Quantification of optical density detected no difference in protein levels for any genotype.

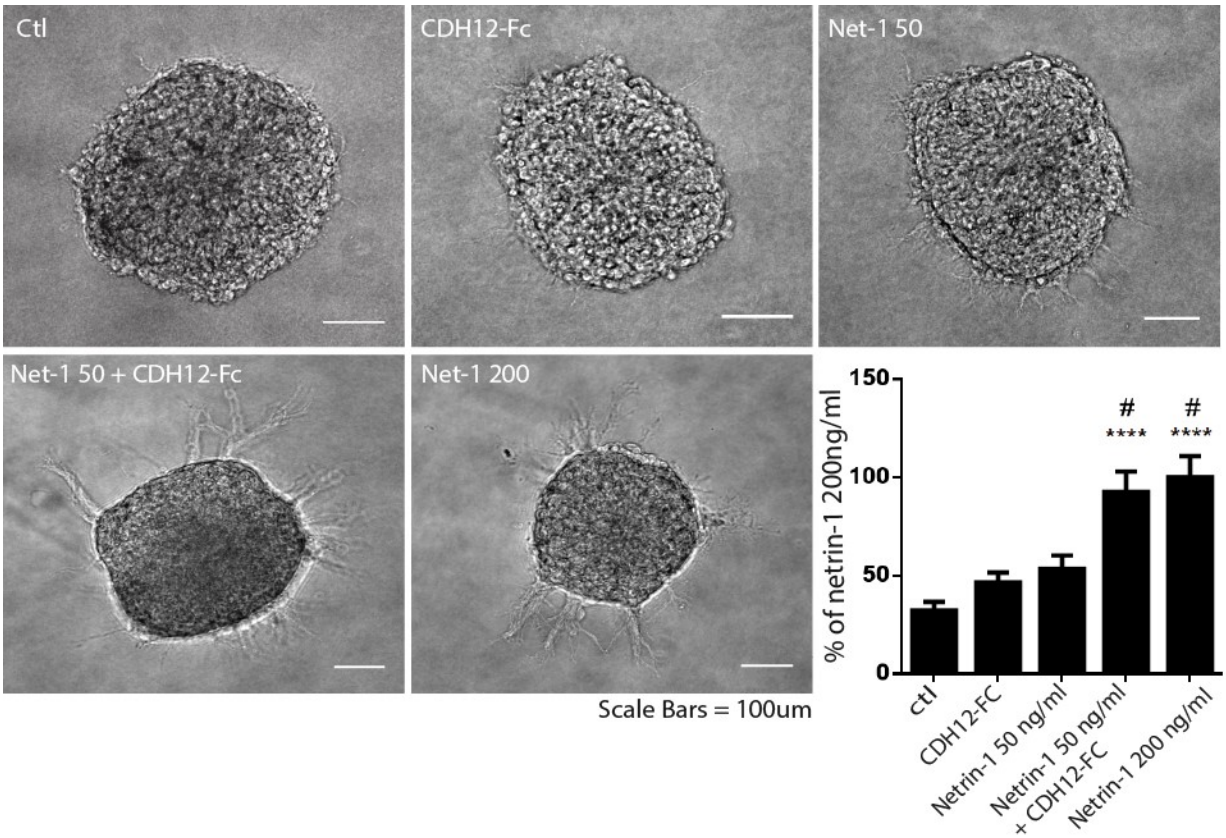

Figure 3.9: CDH12-Fc potentiates netrin-1 induced commissural axon outgrowth. Representative images of E13 embryonic rat dorsal spinal explants. Quantification of axon outgrowth from dorsal spinal explants is shown in the lower right, presented as the percentage of outgrowth compared to that evoked by 200 ng/ml netrin-1. (Scale bar = 100 μm. One-way ANOVA with Tukey test. n= 4-6 explants per litter from 3 litters. * compared to control, # compared to netrin-1 50 ng/ml. # $P<0.05$, **** $P<0.0001$).

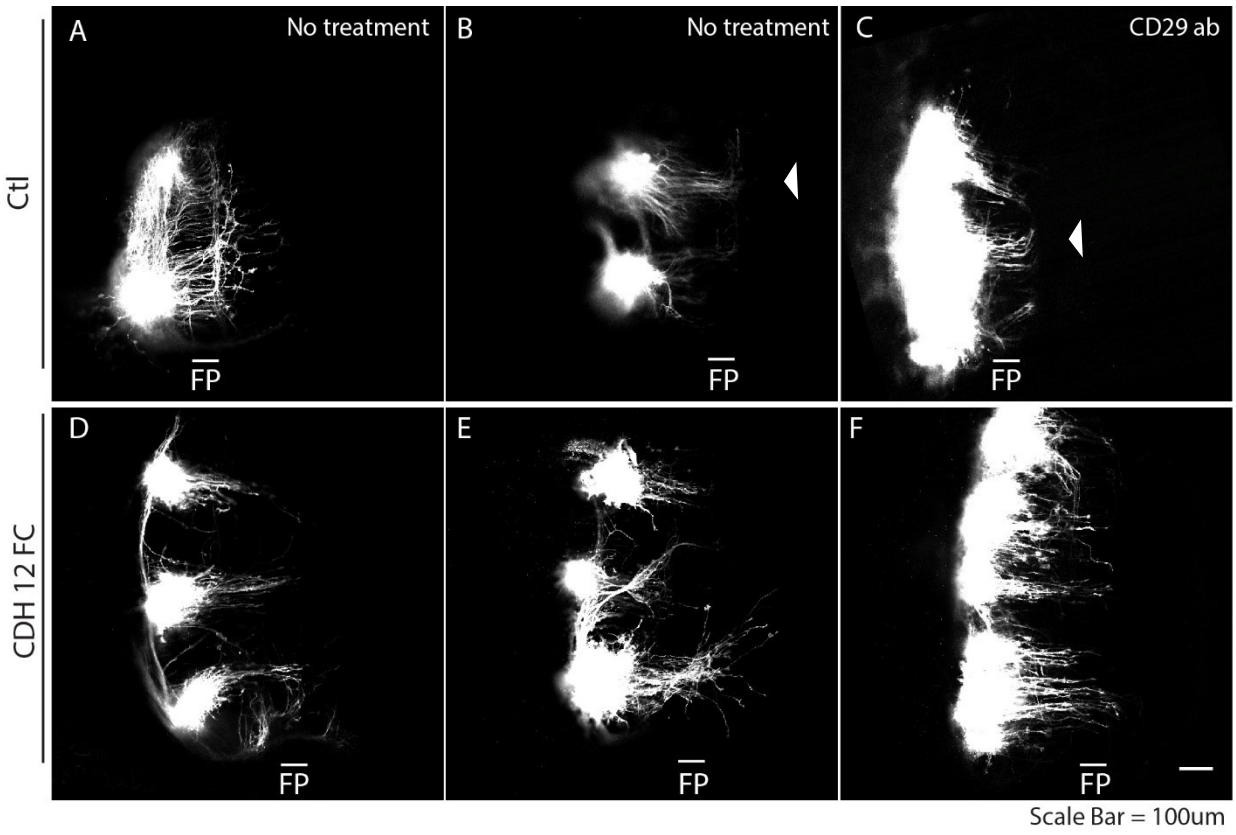

Figure 3.10: Competing CDH12-CDH12 binding with CDH12-Fc disrupts commissural axon guidance at the ventral midline. E11 rat spinal cords were micro dissected, opened along the dorsal midline and embedded in a collagen gel as an "open book assay". DiI was injected along the dorsal edge of the embryonic spinal cord open book explant, targeting the region enriched with commissural neuron cell bodies and allowing dye diffusion down axonal processes. Appropriate rostral turns after crossing the floor plate are highlighted with a white arrowhead in panels B and C. **A & B)** Untreated open book embryonic spinal cord preparations. Commissural neurons cross the midline and complete a rostral turn towards the head of the animal**. C)** Open book explanted embryonic spinal cords treated with a β-integrin antibody as a control for the CDH12-Fc domain. Commissural neurons successfully cross the midline and complete a rostral turn**. D-F)** Commissural neurons in open book explanted embryonic spinal

cords treated with CDH12-Fc cross the midline but fail to make the turn to extend rostrally. Some commissural axons stall in the floor plate and some continue to grow into the contralateral side of the spinal cord post crossing. FP indicates the floor plate (scale bar = 100 μm).

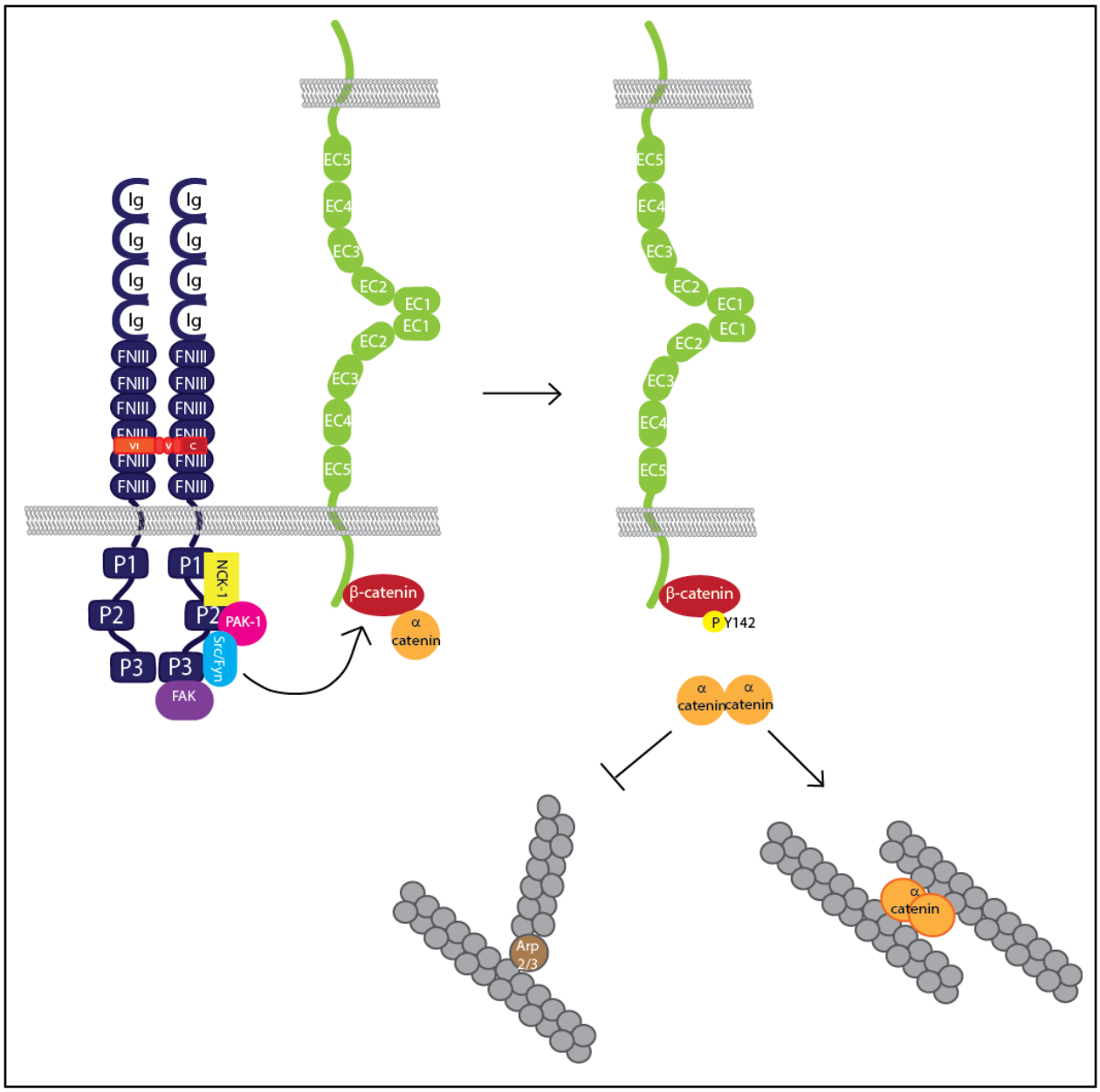

Figure 3.11: Model for cadherin function in commissural axon guidance. Netrin-1 binding to DCC activates Fyn which then phosphorylates β-catenin at Y142. This dissociates α-catenin from the cadherin-catenin adhesion complex. In the cytosol α-catenin forms dimers and binds to the F-actin cytoskeleton. α-catenin competes with the Arp2/3 binding site on F-actin preventing Arp2/3 from binding to F-actin. This favours actin bundle formation over branch formation leading to filopodia elongation and increased outgrowth.

Preface

In the previous chapter we identified and characterized an interaction between DCC and CDH12 in the developing spinal cord. The expression of several axon guidance cues, including netrin-1, have been found to persist in the adult animal and have been shown to play important roles in synapse function. Previous work in our lab has identified an important role for netrin-1 at glutamatergic synapses regulating dendritic spine morphology, recruitment of synaptic proteins, and LTP in the adult animal (Glasgow et al., 2018; Goldman et al., 2013; Horn et al., 2013). Similarly, cadherins have also been shown to regulate these synaptic processes (Bamji, 2005; Bozdagi et al., 2000). In this study we investigate the possibility that DCC and CDH12 interact in the brain, focusing on their function at the synapse. We show that netrin-1 influences DCC and CDH12 protein dynamics within the plasma membrane and leads to an increase in their cell surface localization. A manuscript of this chapter is in preparation for publication.

.

Chapter 4

DCC interacts with CDH12 in the rat brain and may influence synaptic function

Stephanie N. Harris*, Katherine E. Horn*, Angelica Gopal[#], Stephen D. Glasgow*, Paul Wiseman[#], Timothy E. Kennedy*

*Montreal Neurological Institute, Department of Neurology and Neurosurgery,

McGill University, Montreal, Quebec, Canada, H3A 2B4

[#] Montreal Neurological Institute, Department of Chemistry,

McGill University, Montreal, Quebec, Canada, H3A 2B4

I. ABSTRACT

Cell adhesion molecules are critical for synapse formation and function in the central nervous system. Cadherins in particular are implicated in mediating synaptic function, synapse specificity, and specifying the formation of neural circuits. Trans-synaptic cadherin binding constitutes a major adhesive force that stabilizes new synaptic contacts. Along with the signalling partner β – catenin, cadherins are important regulators of dendritic spine morphology and activity dependent plasticity, including long term potentiation (LTP). Netrin-1 and DCC are developmental axon guidance cues that are also expressed in the adult nervous system. They have recently been shown to regulate synapse function and LTP. In chapter 3, we provide evidence that DCC and CDH12, a type II classical cadherin, functionally interact during axon guidance in the embryonic spinal cord. Here we provide evidence for a similar interaction between DCC and CDH12 in the post-natal and adult brain. Our findings indicate that the application of exogenous netrin-1 is sufficient to increase the amount and co-localization of CDH12 and DCC in the neuronal plasma membrane. We show that DCC co-IPs with CDH12 and mass spectrometry analysis provides evidence for the intracellular adaptor protein Dlg5 binding DCC. Dlg5 regulates cadherin trafficking and stability and Dlg5 null mice exhibit significantly reduced cadherin protein at the cell surface. We hypothesize that DCC and CDH12 traffic to the neuronal plasma membrane in response to netrin-1 through a mechanism that may be regulated by Dlg5.

II. INTRODUCTION

In the nervous system, neurons communicate with one another through specialized junctions called synapses. Synapses form when two filopodia, one from the nascent presynaptic cell and one from the postsynaptic cell, come into contact and that contact is stabilized through adhesion. Cell adhesion molecules (CAMs) localized to the synaptic membrane stabilize and anchor the pre- and post-synapse in close proximity and trans-synaptic cadherin binding is thought to "link up and lock in" nascent synapses (Fannon & Colman, 1996). Synaptic junctions exhibit some similarities to adherens junctions and, as in adherens junctions, cadherins are central to their formation and maintenance (Fannon & Colman, 1996). Cadherins are a large superfamily of calcium-dependant CAMs comprised of five extracellular cadherin repeats, a transmembrane domain, and an intracellular domain (Shapiro & Weis, 2009). The extracellular domain mediates cadherin-cadherin binding, while the intracellular domain binds the catenin family of intracellular proteins that signal downstream of cadherins (S. T. Suzuki, 1996). Cadherins promote cell adhesion by binding *in trans,* often homophilically, to cadherins present on opposing cells (Weis, 1995). Cadherin – cadherin adhesive interactions are important for stabilizing the initial synaptic contact, while cadherin mediated intracellular signaling through catenins regulates cytoskeletal changes underlying synaptic structure (Bruses, 2006). N-cadherin knockouts have defects in many synaptic processes including transmission, vesicle recycling, and long term potentiation (LTP) (Bozdagi et al., 2000; Bozdagi et al., 2004; Jungling et al., 2006; Saglietti et al., 2007). β-catenin, a key downstream signalling partner of cadherins, also plays a key role in synaptic function and has differential effects at the pre and post synapse. At the pre synapse, β-catenin is required for synaptic vesicle clustering and neurotransmitter release while at the post synapse β-catenin regulates spine morphology (Arikkath & Reichardt, 2008).

Both the presynaptic and post synaptic functions of β-catenin are mediated through binding to PDZ domain containing proteins. Discs large 5 homolog (Dlg5) is a member of the membrane associated guanylate kinase (MAGUK) protein family and contains four PDZ domains (S.-H. J. Wang et al., 2014). Through direct interactions with β-catenin, Dlg5 regulates N-cadherin trafficking and stability (Nechiporuk, Fernandez, & Vasioukhin, 2007; S.-H. J. Wang et al., 2014). Dlg5 knockout mice have fewer dendritic spines on cortical neurons *in vitro* and have defects in synaptic transmission, both of which are attributed to significantly reduced level of N-cadherin in the neuronal plasma membrane (S.-H. J. Wang et al., 2014).

Several developmental axon guidance cues continue to be expressed in the adult brain and have been shown to contribute to synaptic function. In the developing and adult brain, netrin-1 and its receptor DCC are widely expressed by neurons and influence processes such as axon branching, filopodia formation, synapse formation, and synaptic plasticity (Glasgow et al., 2018; Goldman et al., 2013; Horn et al., 2013; Manitt et al., 2009). Beads coated with netrin-1 adhere to the processes of cortical neurons in cell culture and this local concentration of netrin-1 results in the recruitment of synaptic proteins to the site of bead-neurite contact (Goldman et al., 2013). In addition to an impact on synaptogenesis, netrin-1 and DCC also regulate synaptic transmission in the mature brain. Both netrin-1 and DCC are required for LTP, and the addition of exogenous netrin-1 alone is sufficient to potentiate the hippocampal Schaffer collateral synapse through recruitment of GluA1-containing α-amino-3-hydroxy-5-methyl-4-isoxazolepropionic acid glutamate receptors (AMPARs) (Glasgow et al., 2018; Horn et al., 2013).

In chapter 3 we provided evidence that DCC interacts with a type II classical cadherin, cadherin 12 (CDH12), to regulate axon guidance in the developing spinal cord. Here, we provide evidence that this interaction may also occur in postnatal brain and may play a role in trans-

synaptic adhesion. Additionally, we provide evidence that DCC may interact with Dlg5 and propose that DCC, CDH12, and Dlg5 may form a functional protein complex that regulates protein trafficking within the cell and in turn, influence synapse function.

III. METHODS

III.i. Animals

All procedures were performed in accordance with the Canadian Council on Animal Care guidelines for the use of animals in research and approved by the Montreal Neurological Institute Animal Care Committee and the McGill Animal Compliance Office. Sprague-Dawley rats were obtained from Charles Rivers Laboratory at various developmental stages (St-Constant, QC, Canada) (vaginal plug = E0).

III.ii. Antibodies and reagents

Antibodies: Rabbit anti CDH12 (abcam, EPR1792), mouse anti β-catenin (BD transduction laboratories, 610153), mouse anti DCCin (BD pharmingen, 554223); rabbit anti GAPDH (santa cruz biotechnology, sc-25778), monoclonal mouse anti β III tubulin clone TUB 2.1 (Sigma Aldrich, T4026), mouse anti synaptophysin (Sigma Aldrich, S5768), rabbit anti PSD95 (Cell Signalling, D27E11), chicken anti Map2 (GeneTex, GTX85455), Hoechst 33258 (Life Technologies)), peroxidase-conjugated donkey anti mouse IgG (Jackson Immuno Research, 715-035-150), peroxidase conjugated donkey anti rabbit (Jackson Immuno Research, 711-035-152), alexa fluor donkey anti rabbit (molecular probes, A31572 & A21206), alexa fluor goat anti mouse (molecular probes, A-11001), alexa fluor anti chicken (molecular probes A-21103), CDH12-Fc (R&D Systems 2240-CA-050).

III.iii. Immunohistochemistry

Floating sections were cut 40 µm thick using a microtome from PFA perfused P15 rat brains. Sections were blocked and permeabilized in 0.25% Triton-X 100 and 3% hiHS in PBS. Primary antibodies were diluted in a buffer of 0.1% Trition-X 100 and 1% hiHS in PBS and incubated overnight at 4^{o} C. sections were then washed in a buffer of 0.1% Triton-X 100 and 1% hiHS in PBS 3 x 10 min with rocking. Secondary antibodies were diluted in 1% hiHS in PBS for 2 hr at rt and then washed 3 x 10 min in PBS. Sections were transferred onto slides using a paintbrush and cover slipped using Fluoro-Gel with tris buffer (Electron Microscopy Sciences).

III.iv. Western blot analysis

Proteins were separated on an 8% poly acrylamide gel and then transferred by electroblotting onto nitrocellulose using a 350 mA current for 1 hr and 15 min. Nitrocellulose membranes were blocked in 5% skim milk powder in TBST for 1 hr. Primary antibodies were diluted in blocking buffer and incubated at 4^{o} C overnight. Membranes were then washed in blocking buffer 3 x 10 min. Secondary antibodies were diluted in blocking buffer and incubated for 1 hr at rt. Membranes were then washed 2 x 10 min in TBST and 2 x 10 min in TBS. The membrane was then incubated with Western Lightning ECL pro (Perkin-Elmer Inc.) and exposed to film.

III.v. Cell culture

Cortical and hippocampal neuron cultures were prepared from embryonic day 17 (E17) rat embryos (Charles River, Quebec). Cortices or hippocampi were dissected from embryos in cold Hank's Balanced Salt Solution without calcium or magnesium (Thermo Fisher) and then pooled for dissociation using 0.25% Trypsin and 0.05% DNAse I in warm minimal essential media for suspension cultures (Thermo Fisher) with 0.02 M HEPES pH7.4. Dissociated cells were washed

with Neurobasal (Thermo Fisher) supplemented with 10% fetal bovine serum and then triturated using flamed glass pipettes to obtain a single cell suspension. Neurons were plated on plasma treated coverslips or cell culture plastic both coated with 10 µg/ml of PDL. PDL coating was carried out for 1 hr at rt using a volume of 500 µl PDL per coverslip. PDL coated coverslips were then washed 3 times with ddH_2O and allowed to air dry. Neurons were grown in neurobasal supplemented with 1% B27, 1% penicillin-streptomycin, 0.5% N2, 0.25% glutamax, and 0.2 % fungizone. Cells were cultured at 37^o C with 5% CO_2.

III.vi. Immunocytochemistry

Cells were fixed using 4% para formaldehyde (PFA) for 20 min on ice. Cells were blocked and permeabilized in 0.25% Triton-X 100 and 3% hiHS in PBS. Primary antibodies were diluted in a buffer of 0.1% Trition-X 100 and 1% hiHS in PBS and incubated overnight at 4^o C. Cells were then washed in the primary antibody buffer 3 x 10 min with rocking. Secondary antibodies were diluted in 1% hiHS in PBS for 2 hr at rt and then washed 3 x 10 min in PBS. Cells were then rinsed once briefly in water and mounted on slides using Fluoro-Gel with tris buffer (Electron Microscopy Sciences).

III.vii. Subcellular fractionation

Brains were homogenized in 10 volumes of 10 mM HEPES, 320 mM sucrose buffer pH 7.4 with added protease inhibitors (Aprotinin 2 µg/ml, Leupeptin 5 µg/ml, EDTA 5 mM, PMSF 1 mM, and sodium orthovanadate 1 mM) and spun at 800 RCF in a JA-17 rotor for 10 min. One ml of the supernatant was kept as S1 and the pellet was resuspended in HEPES/sucrose buffer and kept as P1. S1 was then spun again at 11000 RCF in a JA-17 rotor for 15 min. One ml of the supernatant was kept as S2 and the pellet was resuspended in HEPES/sucrose buffer and kept as

P2. The resuspended P2 was then spun again at 13000 RCF in a JA-17 rotor for 15 min. The pellet was resuspended in water and homogenized and kept as P2*. The supernatant was discarded. The resuspended P2* was then spun at 31000 RCF in a JA-17 rotor for 20 min. One ml of the supernatant was kept as LS1 and the pellet was resuspended in HEPES/sucrose buffer and kept as LP1. LS1 and S2 were then both spun at 206000 RCF in a 70Ti rotor for 2 hr. The S2 pellet was resuspended in HEPES/sucrose buffer and kept as P3 and the supernatant kept as S3. The pellet of LS1 was resuspended in water and kept as LP2 and the supernatant kept as LS2.

Post synaptic density (PSD) fractionation was carried out the same as above until P2*. P2* was resuspended in 3 volumes of 40 mM Tris-HCl pH 8.0 and homogenized. Triton X-100 was added to a final concentration of 0.5% and the sample was then divided into 3 equal samples and spun at 31000 RCF in a JA-17 rotor for 20 min. The first pellet was resuspended in 40 mM Tris-HCl and kept as PSD1, the second pellet was resuspended in 40 mM Tris-HCl + 0.5% triton and labelled as PSD2, and the third pellet was resuspended in 40mM Tris-HCl + 3% sarcosyl and labelled as PSD3. PSD2 and PSD3 were then spun again at 200000 RCF in a TLA100.4 rotor for 1 hr. Both pellets were resuspended in 40 mM Tris-HCl and kept as their respective PSD2 and PSD3 samples.

III.viii. ICCS

Cortical neurons were cultured as described above for 6 DIV before being fixed with 4% PFA on ice for 20 min. Neurons were then immunostained as described above. Images were taken using total internal reflection fluorescence (TIRF) microscopy and analysed for image cross correlation spectroscopy (ICCS) as previously described (Gopal et al., 2017).

III.ix. Biotinylation of surface proteins

Cortical neurons were cultured as described above. All steps were carried out on ice unless specified. Cells were washed with 1 mM $MgCl_2$, 0.1 mM $CaCl_2$ in PBS for 2 x 5 min. One mg/ml biotin solution (Sulfo-NHS-LC-Biotin; ThermoScientific) in 1 mM $MgCl_2$, 0.1 mM $CaCl_2$ in PBS was added to the plate and agitated in the dark for 30 min. Biotin reaction was quenched by washing twice with 10 mM glycine in PBS. Cells were lysed in 1 mL of phosphate buffered radio immunoprecipitation assay buffer (PB-RIPA: 10 mM phosphate buffer [pH 7.2], 150 mM NaCl, 1% NP-40, 0.5% sodium deoxycholate, and 0.1% SDS) with protease inhibitors (Aprotinin 2 µg/ml, Leupeptin 5 µg/ml, EDTA 5 mM, PMSF 1 mM, and sodium orthovanadate 1 mM) and spun down at 13793 RCF at 4^o C for 5 min (Eppendorf 5415 C centrifuge). Sixty µl was collected and kept as a measure of starting protein. Immunopure immobilized streptavidin (ThermoScientific) was added to the supernatant and tubes rotated for 2 hr at 4^o C. Samples were spun at 5000RPM for 20 s to pellets beads. The beads were then washed 2 times with 1mL PB-RIPA. Laemmli buffer (Laemmli, 1970) diluted in PB-RIPA was then added to the beads to elute all associated proteins and the samples were boiled for 5 min. The supernatants were then analysed via western blot.

III.x. Co-Immunoprecipitation

Cortical neuron cultures were treated with 200 ng/ml netrin-1 for 15 min and then lysed in ice-cold 3% Triton-X 100 lysis buffer (50 mM HEPES [pH 7.4], 150 mM NaCl, 2 mM EGTA [pH 8], 15mM $MgCl_2$, 0.1% glycerol, 3% Triton X-100) or 1% Triton X-100 lysis buffer (50 mM HEPES [pH 7.4], 150 mM NaCl, 2 mM EGTA [pH 8], 15mM $MgCl_2$, 0.1% glycerol, 1% Triton X-100), both with added protease inhibitors (Aprotinin 2 µg/ml, Leupeptin 5 µg/ml, EDTA 5 mM, PMSF 1 mM, sodium orthovanadate 1 mM, and sodium fluoride 10 mM). Lysis buffer was

added, and the cells were collected into tubes and placed on ice for 20 min. The samples were then spun at 13793 RCF at 4^{o} C for 15 min (Eppendorf 5415 C centrifuge). The supernatant was then used for immunoprecipitation and the pellet was discarded. Samples were pre-cleared by adding protein A/G beads to the sample for 1 hr at 4^{o} C. The beads were then pelleted, and the supernatant was transferred to a new tube. 2 µg of DCC_{in} antibody was added and incubated for 1 hr at 4^{o} C. Controls were left untreated but were also incubated at 4^{o} C for 1 hr. Protein A/G beads were added to all samples and incubated for 1 hr at 4^{o} C. Beads were then pelleted and washed 3 times with 1 mL of 3% Triton-X 100 lysis buffer, or 1% Triton-x 100 lysis buffer, both with protease inhibitors. Laemmli buffer (Laemmli, 1970) was then added to the beads to elute all associated proteins and the samples were boiled for 5 min. The supernatants were then analysed via western blot.

III.xi. Mass spectrometry

As described in Chapter 3.

III.xii. Electrophysiological recordings

Whole-cell patch clamp electrophysiological recordings were made from E17 rat hippocampal neurons (14 DIV), prepared as described above. Neurons were plated on glass coverslips at high density (2.5-4 x 10^5). Individual coverslips were transferred to an upright microscope (SliceScope 2000; Scientifica), and continuously perfused with artificial cerebrospinal fluid (ACSF) containing (in mM): 135 NaCl, 3.5 KCl, 1.2 $MgCl_2$, 2 $CaCl_2$, 10 HEPES, and 20 D-Glucose (pH: 7.4, 300 mOsm). Borosilicate glass pipettes (Sutter Instruments) were pulled with resistances of 4–8MΩ, and filled with an intracellular solution containing (in mM): 120 $CsMeSO_3$, 20 CsCl, 10 HEPES, 7 di-tris phosphocreatine, 2 $MgCl_2$, 0.2 EGTA, 4 Na_2ATP, and 0.3 Tris-GTP (pH 7.2-7.26, 280-290 mOsm). Access resistance was monitored throughout the

recording (<20 MΩ), and recordings were discarded if values increased by >20%. Voltage-clamp recordings were sampled at 10 kHz and filtered at 2 kHz using pClamp (v10.4, Molecular Devices).

Miniature excitatory postsynaptic currents (mEPSCs) were recorded in voltage-clamp mode at a holding potential of −70 mV in the presence of picrotoxin (100 μM; PTX) and tetrodotoxin (1 μM; TTX) to block gamma-Aminobutyric acid $(GABA)_A$-mediated synaptic currents and sodium currents, respectively. α-amino-3-hydroxy-5-methyl-4-isoxazolepropionic acid glutamate receptor (AMPAR)-mediated currents were analyzed using MiniAnalysis (Synaptosoft), and events were detected using a threshold of 5 pA. Cumulative distribution plots were generated using an equal number of randomly-selected events per condition (100 events/cell per condition), which were subsequently rank-ordered and averaged across each condition.

IV. RESULTS

IV.i. Cadherin 12 protein distribution in the brain

To assess the distribution of CDH12 protein in brain, sections of P15 rat brain were immunostained for CDH12 using a validated monoclonal antibody (Chapter 3, Figure 3.1). CDH12 immuno-positive neurons were readily detected throughout the cortex and hippocampus (Figure 4.1A). Western blot analysis of whole brain homogenates confirmed detection of CDH12 in brain from E13 to adult (Figure 4.1B). Intense CDH12 staining was detected in the CA1-CA3 pyramidal neurons of the hippocampal gyrus, accompanied by a striking absence of staining in the dentate gyrus (DG) (Figure 4.1A). Differential expression of cadherins has previously been

shown to contribute to a synaptic code that specifies connections formed during developmental synaptogenesis. Specifically, CDH9 mediates the specificity of synaptic connections between DG and CA3 neurons (Williams et al., 2011). This spatially distinct distribution of CDH12 suggests a similar possible function regulating synapse specificity, particularly the Schaffer collateral synapse between CA3 and CA1 neurons.

We then examined the distribution of CDH12 in dispersed neuronal cultures. We cultured cortical and hippocampal neurons and visualized CDH12 staining in both neuron types. Cultures were immunostained for CDH12, Map2, and β-tubulin. Map2 specifically localizes to dendrites (Caceres, Banker, Steward, Binder, & Payne, 1984). In 14 DIV cortical neurons CDH12 immunoreactivity was detected overlapping with both Map2 and β-tubulin positive processes, suggesting localization in both axons and dendrites. In 33 DIV hippocampal cultures CDH12 immunoreactivity was largely overlapping with Map2 positive processes suggesting that CDH12 distribution may be relatively more enriched in dendrites in aged hippocampal cultures (Figure 4.2). CDH12 staining was also strongly punctate in both cultures, suggesting that CDH12 may be localized to dendritic spines.

IV.ii. Subcellular localization of cadherin 12

To further investigate the subcellular distribution of CDH12 protein relative to synapses, we carried out subcellular fractionation. Brain homogenates from P14 rat were divided into eight fractions; H, P1, P2, P2*, S3, P3, LP1, and LP2 which are shown schematically in figure 4.3A. CDH12 and DCC are both enriched in the LP1 and LP2 fractions, consistent with being present on the synaptic plasma membrane and in cargo vesicles in the synaptic compartment (Figure 4.3B). While these findings provide evidence that DCC and CDH12 are enriched at synapses, it

is important to note that this fractionation technique does not differentiate between the pre- and post-synaptic compartments.

To determine if DCC and CDH12 might be associated with the PSD, a different method of fractionation was applied. We used adult rat brain to assess mature synapses with well developed PSDs and fractionated it as before up to P2. Fraction P2, the crude synaptosomal fraction, was then further partitioned into three fractions enriched for the PSD. PSD1, PSD2, and PSD3 are extracted from P2 using increasingly harsh detergent conditions. PSD1; tris resistant post synaptic density, PSD2; Triton resistant post synaptic density, PSD3; sarcosyl resistant post synaptic density (Fallon et al., 2002). CDH12 and DCC are both highly enriched in the PSD fractions obtained from adult rat brain (Figure 4.4C). CDH12 protein is most enriched in the tris resistant PSD1 fraction with a large amount of protein still present in the Triton resistant PSD2 fraction. This is consistent with fractionation of N-cadherin which has previously been show to be enriched in the PSD1 and PSD2 fractions (Liu et al., 2016).

IV.iii. Netrin-1 promotes aggregation and co-localization of CDH12 and DCC

To determine if netrin-1 dynamically influences the distributions of CDH12 and DCC proteins in the plasma membrane of cultured cortical neurons we employed Total Internal Reflection Fluorescence (TIRF) microscopy with image cross correlation spectroscopy (ICCS) analysis. TIRF microscopy illuminates a very thin optical slice, a few hundred nanometres, directly proximal to the cover glass. This technique allows the visualization of proteins specifically at the cell membrane without exciting fluorophores bound to proteins inside the cell (Fish, 2009). ICCS can be used to determine the cluster density (CD), degree of aggregation (DA) and the interaction fraction of various proteins in fixed neuronal tissue (Gopal et. al 2017). Briefly, CD is a measure of the number of particles detected per beam area where particles can be present as a

monomer or as a multimer. DA measures the extent of particle aggregation and is related to both fluorescent intensity and CD (Figure 4.4A). A higher number indicates that particles are more highly aggregated. Finally, the interaction fraction is a measure of co-localization between two fluorophores of a different colour. The number of co-localized particles is related to the total number of particles and the two interaction fractions, one for each fluorophore, are then averaged to give a measure of co – localization. A simplified schematic of these measures is shown in Figure 4.4A and 4.4C.

We treated 6 DIV cultured embryonic cortical neurons with 200 ng/ml netrin-1 for 15 minutes. Following treatment neurons were fixed in 4% PFA and imaged using TIRF microscopy. Using ICCS analysis we then compared CD, DA, and the interaction fraction of DCC and CDH12 to untreated sister cultures. We found that application of netrin-1 resulted in a significant decrease in DCC CD, with a similar but non-significant trend for CDH12, while both CDH12 and DCC exhibited a significant increase in DA following netrin-1 application (Figure 4.4 A-C). These findings provide evidence that netrin-1 treatment promotes the aggregation of DCC and CDH12 proteins within neuronal plasma membrane and are consistent with previous results demonstrating increased aggregation of ectopically expressed DCC in HEK293 cells following netrin-1 application (Gopal et al., 2016). Netrin-1 application also resulted in an increase in the interaction fraction, measured from both fluorophores, supporting the conclusion that the co–localization of the two proteins increases following netrin-1 application (Figure 4.4 D-E). All images were taken using TIRF microscopy and thus represents what is occurring in the plasma membrane at the cell surface and not vesicle membranes inside in the cell. Therefore, we can conclude that netrin-1 causes increased aggregation and co-localization of DCC and CDH12 on the cell surface which may indicate a functional response to netrin-1.

IV.iv. Netrin-1 increases cell surface CDH12 and DCC

ICCS provided evidence for a netrin-1 induced increase in aggregation and co – localization of CDH12 and DCC on the cell surface. The netrin-1 induced increase in aggregation and co-localization seen could be due to lateral movement of existing protein within the cell membrane or insertion of protein into the membrane. To determine if netrin-1 increases the amount of cell surface CDH12 and DCC we treated 3 DIV cortical neuron cultures with 200 ng/ml netrin-1 for 0, 10, or 15 min prior to biotinylating cell surface proteins. Biotinylated proteins were isolated using streptavidin beads followed by extracting these beads from the total cell lysate. Western blot analysis of biotinylated proteins revealed that netrin-1 treatment results in a rapid increase of both CDH12 and DCC on the cell surface after 10 and 15 min of netrin-1 treatment (Figure 4.4F). Netrin-1 has been previously shown to recruit DCC to the neuronal plasma membrane via a tetanus toxin sensitive mechanism, suggesting that the mechanism requires VAMP2 dependent vesicle insertion (Bouchard et al., 2004). In the current study, we detect an increase in plasma membrane DCC and CDH12 and hypothesize it may be due to mobilization of cargo vesicles; however, additional studies will be required to determine if this is the case or if proteins are being stabilized in the plasma membrane with reduced endocytic internalization.

IV.v. DCC Co-IPs with CDH12

Since increased amounts of DCC and CDH12 are detected in neuronal plasma membrane and increased co-localization was also detected following netrin-1 treatment, we then aimed to determine if the two proteins may interact as a protein complex. We therefore carried out co-immunoprecipitation (co-IP) experiments from homogenates of P10 cortex homogenate and from 3DIV cultured cortical neurons. Whole cortex from P10 rat brain was homogenized and immunoprecipitated for DCC_{in} and samples analysed via western blot (Figure 4.5A). A CDH12

immunoreactive band was detected in the DCC IP sample but not in the beads only control, indicating co-IP of CDH12 with DCC. Notably, the capacity to co-IP CDH12 with DCC was detergent sensitive. No interaction was detected using a 1% triton lysis buffer, but co-IP was readily detected using 3% triton in the lysis buffer (Figure 4.5A). This may indicate that CDH12 and DCC are part of a relatively detergent resistant protein complex or perhaps a highly organized membrane domain, like a lipid raft, and that the standard 1% triton containing buffer is not sufficiently harsh to extract the complex. Consistent with this prediction, we detect DCC enriched in the insoluble pellet of whole cell homogenates that is typically discarded following the initial cell lysis (data not shown). As in the brain homogenates, DCC IP from 3 DIV cultured cortical neurons again were immunopositive for CDH12 in the DCC IP samples and not in the beads alone control (Figure 4.5B). These IPs were also probed for the cadherin downstream signaling partner, β-catenin, detecting a β-catenin immunopositive band in the DCC IP samples but not in beads only controls (Figure 4.5B). The capacity to co-IP DCC with CDH12 and β-catenin provides evidence for a heteromeric protein complex in cortical neurons that includes these proteins and is consistent with the results obtained in the embryonic spinal cord (Chapter 3).

An unbiased screen for DCC binding partners in spinal commissural neurons revealed CDH12 as a candidate DCC interacting protein (Chapter 3). That same screen also returned a hit for Dlg5, a known regulator of cadherin containing vesicle trafficking (Table 4.1) (Nechiporuk et al., 2007). Dlg5 regulates cell surface N-cadherin expression through direct interactions with β-catenin, regulating delivery of the cadherin/catenin complex to the cell surface and stabilizing the complex once inserted into the membrane (Nechiporuk et al., 2007). Further studies will be required, but this suggests that DCC, CDH12, and Dlg5 may be present in a signalling complex

within neurons. We hypothesize that Dlg5 may regulate trafficking of vesicles that contain DCC and CDH12. This may occur through interactions with the SNAP Receptor (SNARE) complex which is a large protein complex that mediates exocytosis. Notably, the syntaxin family of proteins, members of the SNARE complex, have been shown to interact with both DCC and Dlg5 (Cotrufo et al., 2012; Nechiporuk et al., 2007).

Table 4.1

Protein Description	Mass spec peptide sequence	Dlg5 sequence	Amino Acid Range
Discs Large 5 Homolog (Dlg5)	LAEVEPELSFK	LAEVEPELSFK	1612-1622

IV.vi. Functional significance of cadherin 12 in cortical neurons

While Dlg5 has been previously linked to synapse function, it remained unclear whether CDH12 contributes to excitatory synaptic transmission at cortical neuron synapses (S.-H. J. Wang et al., 2014). To begin to assess the possible contribution of CDH12 to excitatory synaptic transmission, we recorded AMPAR-mediated miniature excitatory postsynaptic currents (mEPSCs) from 14DIV cultured cortical neurons that had been treated with CDH12-Fc to disrupt cadherin-cadherin binding. Twenty-four-hour bath application of CDH12-Fc resulted in a significant increase in the mEPSC amplitude (16.6±2.0 pA in control cultures vs. 24.7±2.8 pA in CDH12-Fc, $p = 0.026$) (Figure 4.7). We did not detect a significant change in mEPSC frequency (3.6±0.9 Hz in control cultures vs. 7.6±2.1 Hz in CDH12-Fc, $p = 0.09$), however an intriguing trend towards an increase was present, suggesting that further investigation may be warranted. These findings suggest that CDH12-Fc may impact function of postsynaptic proteins involved in excitatory synaptic transmission.

V. DISCUSSION

Cell adhesion molecules play an important role regulating synapse formation and function in the mammalian CNS. Here we show that CDH12 interacts with DCC in the postnatal rat brain and both are PSD enriched. Additionally, our findings support the conclusion that application of netrin-1 to cortical neurons leads to an increase in aggregation and co-localization of DCC and CDH12 in the plasma membrane. Stimulation of neurons with netrin-1 also increased the amount of DCC and CDH12 on the cell surface, a process that we postulate may be mediated through Dlg5 regulated vesicle trafficking.

V.i. CDH12 expression in the brain

Both CDH12 and DCC are distributed throughout the rat brain, including high expression in the cortex and hippocampus (Figure 4.1, Allen Brain Atlas: http://mouse.brain-map.org/). Interestingly, CDH12 protein is abundant in both the CA1 and CA3 region of the hippocampus but is strikingly absent from the DG. This pattern of expression is consistent with a cadherin code for synapse specificity and circuit formation. A cadherin code suggests that differential combinations of cadherins are expressed by different subsets of neurons and neurons are directed to connect based on patterns of complementary cadherin expression (Fannon & Colman, 1996). This has previously been shown to be true for a number of cadherin family members, including the type II cadherins CDH6 and CDH9. Expression of CDH6 is important for correct formation of auditory tracts (S. C. Suzuki et al., 1997), while CDH9 is specifically important for DG – CA3 synapses in the hippocampus (Williams et al., 2011). While the specific function of CDH12 in circuit formation has yet to be determined, the pattern of expression detected suggests that it may help tune synapse specificity between CA1 - CA3 neurons.

In cultures of either cortical or hippocampal neurons a particularly punctate distribution of CDH12 was detected. CDH12 appears to be detected along axons and dendrites in 14 DIV cortical neurons and mainly associated with dendrites in 33DIV hippocampal cultures. The punctate nature of the staining also suggests CDH12 may be localized to dendritic spines. Consistent with this, we confirmed post synaptic localization of CDH12 to PSD using subcellular fractionation. CDH12 and DCC are both enriched in the LP1 and LP2 synaptic fractions and further into the post synaptic fractions isolated from whole brain homogenates, suggesting that both proteins may occupy the same or similar subcellular compartment where they could possibly interact to regulate synaptic function.

V.ii. DCC interacts with CDH12 and Dlg5 which may regulate function

Treating neuronal cultures with netrin-1 leads to aggregation and co-localization of DCC and CDH12 in the plasma membrane and cell surface expression of both CDH12 and DCC is increased in cortical neuron cultures following netrin-1 stimulation. Previous work demonstrated that netrin-1 fractionates into LP1 and LP2 synaptic fractions and is highly associated with excitatory synapses in the rat cortex (Goldman et al., 2013; Horn et al., 2013). Further, depolarization of cells through NMDARs causes release of netrin-1 from dendritic spines (Glasgow et al., 2018). Binding of netrin-1 to DCC has previously been shown to increase the amount of DCC at the cell surface (Moore et al., 2008). Therefore, we postulate that release of netrin-1 from depolarized spines could bind to plasma membrane DCC, leading to recruitment and insertion of DCC and CDH12 from a subcellular pool of vesicles. Trans synaptic binding of CDH12 could then contribute to stabilizing the synaptic contact at the site of netrin-1 release.

We show that DCC co-IPs with both CDH12 and results from mass spectrometry analysis suggests Dlg5 may also interact with DCC. Dlg5 fractionates with the PSD, placing it in the

appropriate compartment to interact with DCC and CDH12, possibly to mediate trafficking and insertion into the synaptic membrane (S.-H. J. Wang et al., 2014). Dlg5 is a MAGUK intracellular scaffolding protein that plays an important role in synapse function by regulating cell surface expression and stability of N-cadherin at the synapse (Nechiporuk et al., 2007; S.-H. J. Wang et al., 2014). Dlg5 binds directly to β-catenin and regulates trafficking of the cadherin cell adhesion complex to the cell surface through interactions with syntaxin 4 (S.-H. J. Wang et al., 2014). Trafficking and stabilization of the cadherin complex on the cell surface is important for determining cell polarity, regulating dendritic spine development, and synaptic function.

Disruption of CDH12 binding in mature cortical neuron cultures through the addition of CDH12-Fc receptor body led to an increase in mEPSC amplitude but failed to significantly alter mEPSC frequency or interevent interval. This was a somewhat unexpected result as the CDH12-Fc protein disrupts endogenous cadherin-cadherin interactions, which are thought to be important for synapse stability (Tanaka et al., 2000). However, this result is complimentary to what is seen in Dlg5 knockout cultures which also show an increase in mEPSC amplitude (S.-H. J. Wang et al., 2014). This further supports the idea that Dlg5 may regulate cadherin function at the cell surface which in turn affects synaptic function. While the mechanism impacted by Dlg5 or CDH12 that regulates mEPSC amplitude has yet to be determined, our data suggest that CDH12 and Dlg5 may be components of a heteromeric protein complex, that may also include DCC, and that this complex may regulate synapse function in cortical neurons.

VI. FIGURES

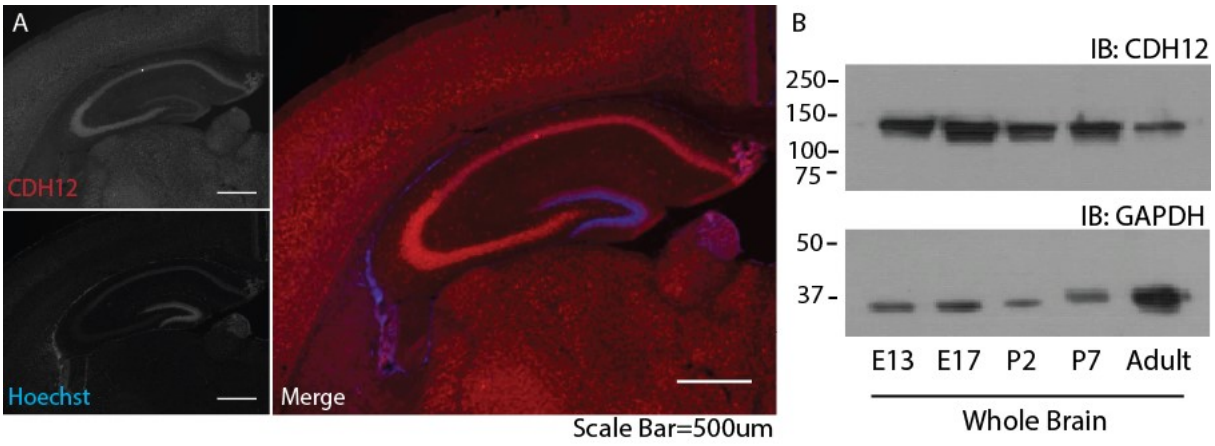

Figure 4.1: Characterization of the distribution of CDH12 protein in rat brain A: P15 rat brain section. CDH12 immunoreactivity is red and Hoechst staining to mark cell nuclei is blue (scale bar = 500 μm). **B:** Western blot showing relative levels of CDH12 protein in whole brain homogenates at E13, E17, P2, P7, and adult. GAPDH is presented as a loading control.

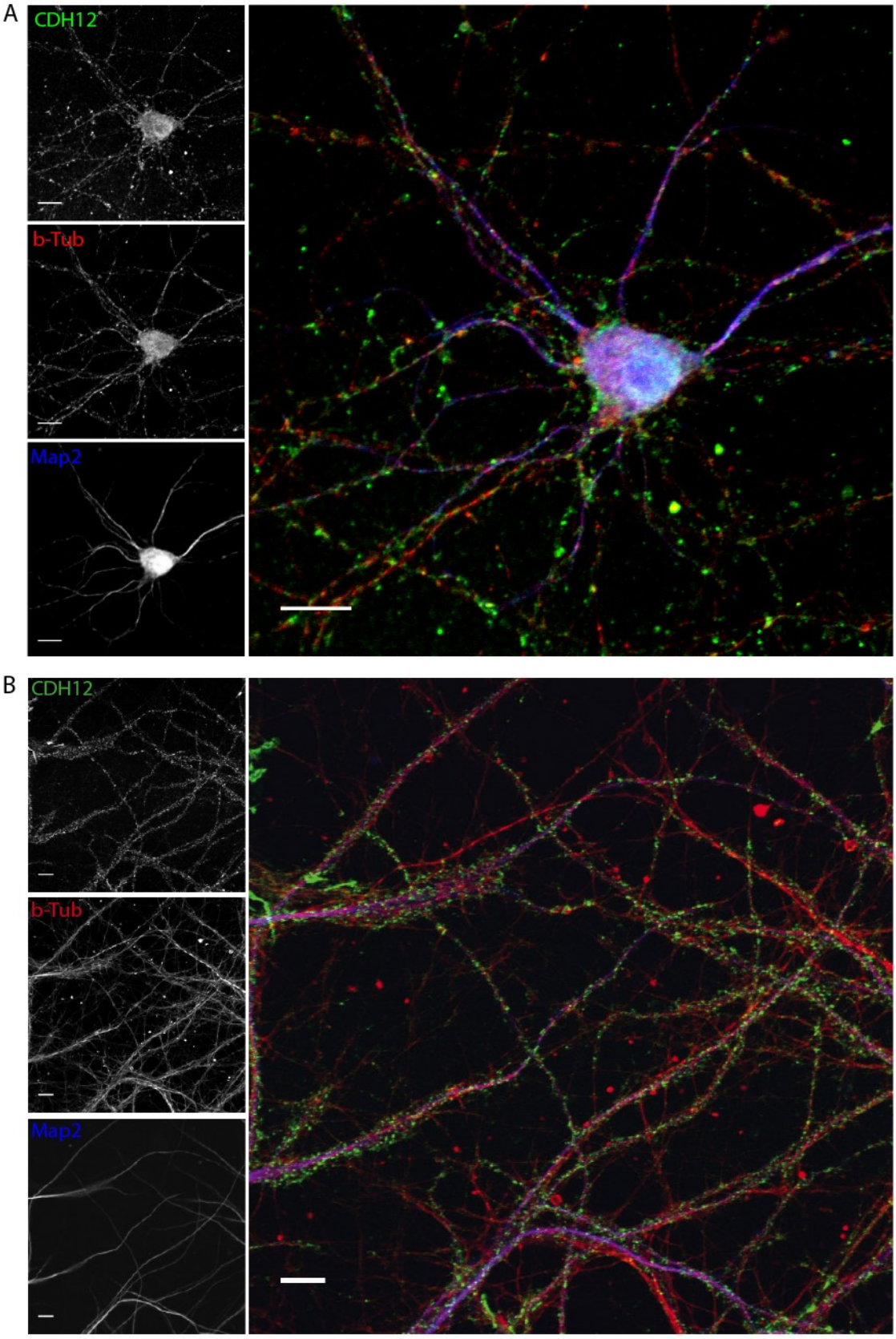
A
CDH12
b-Tub
Map2
B
CDH12
b-Tub
Map2
Scale Bar = 10um

Figure 4.2: CDH12 distribution in cultured rat neurons. A: 14 DIV cortical neuron cultures immunolabelled for CDH12 (green), β-tubulin (red), and Map2 (blue). CDH12 labelling localizes with both Map2 positive processes and β-tubulin positive processes. **B:** 33 DIV hippocampal neuron cultures immunolabelled for CDH12 (green), β-tubulin (red), and Map2 (blue). CDH12 staining is punctate in nature and largely localized with Map2 positive processes which suggests it may be distributing to dendritic spines (scale bar = 10 µm).

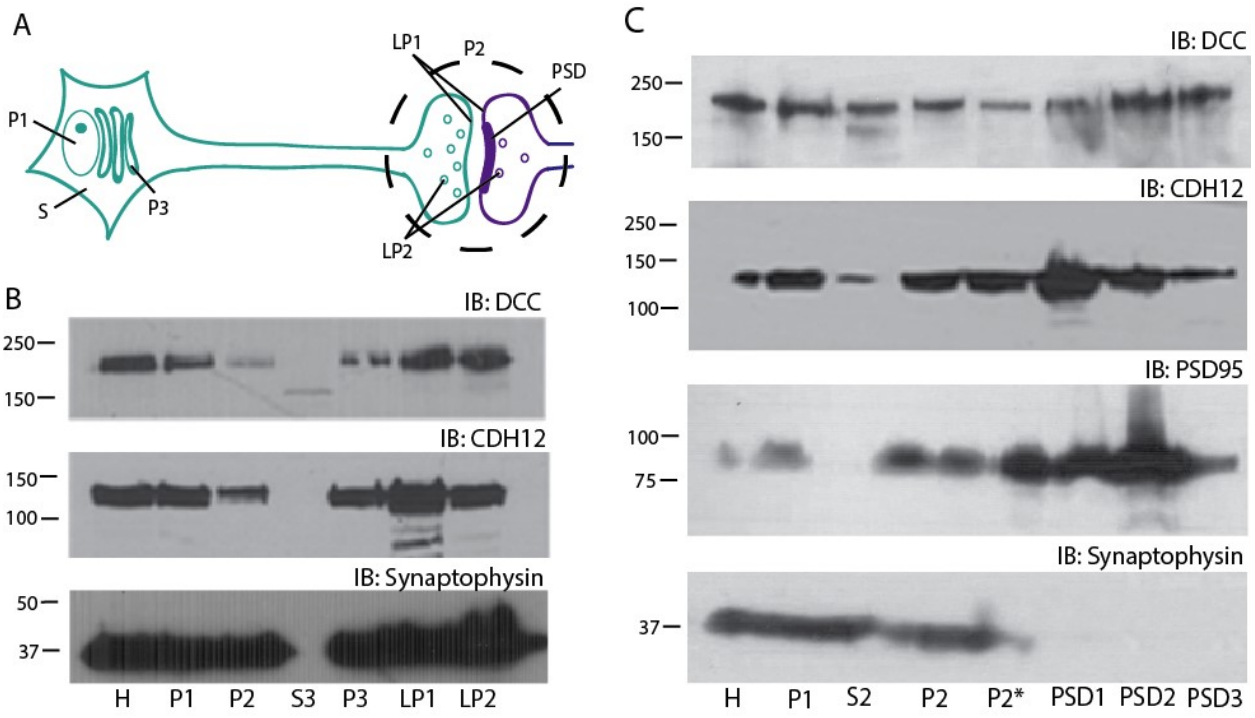

Figure 4.3: Subcellular fractionation to address the distribution of DCC and CDH12. A: Schematic representation of a neuron and its partitioning into different subcellular fractions. H; whole cell contents, P1; nuclei and cellular debris, P2; mitochondria, synaptosomes, synaptic vesicle membranes, P2*; synaptosomes, synaptic vesicle membranes, P3; Golgi, endoplasmic

reticulum, internal membrane, LP1; terminal membrane, LP2; synaptic vesicles and microsomes (Huttner, Schiebler, Greengard, & De Camilli, 1983). **B:** Subcellular fractionation of P14 rat brain detects DCC and CDH12 in all fractions except S3, which corresponds to soluble proteins. DCC and CDH12 are both present in the LP1 and LP2 fractions, which are enriched for synaptic plasma membranes and synaptic vesicles, respectively. The presynaptic, synaptic vesicle protein, Synaptophysin is included as a control. This method of fractionation does not separately enrich for pre- and post-synaptic proteins. **C:** Fractionation to selectively enrich for post-synaptic density shows both DCC and CDH12 are detected and enriched in the post-synaptic density. PSD95 and Synaptophysin immunoreactivities are used as markers of the post and pre-synaptic compartments, respectively. PSD1; tris resistant, PSD2; Triton resistant, PSD3; sarcosyl resistant.

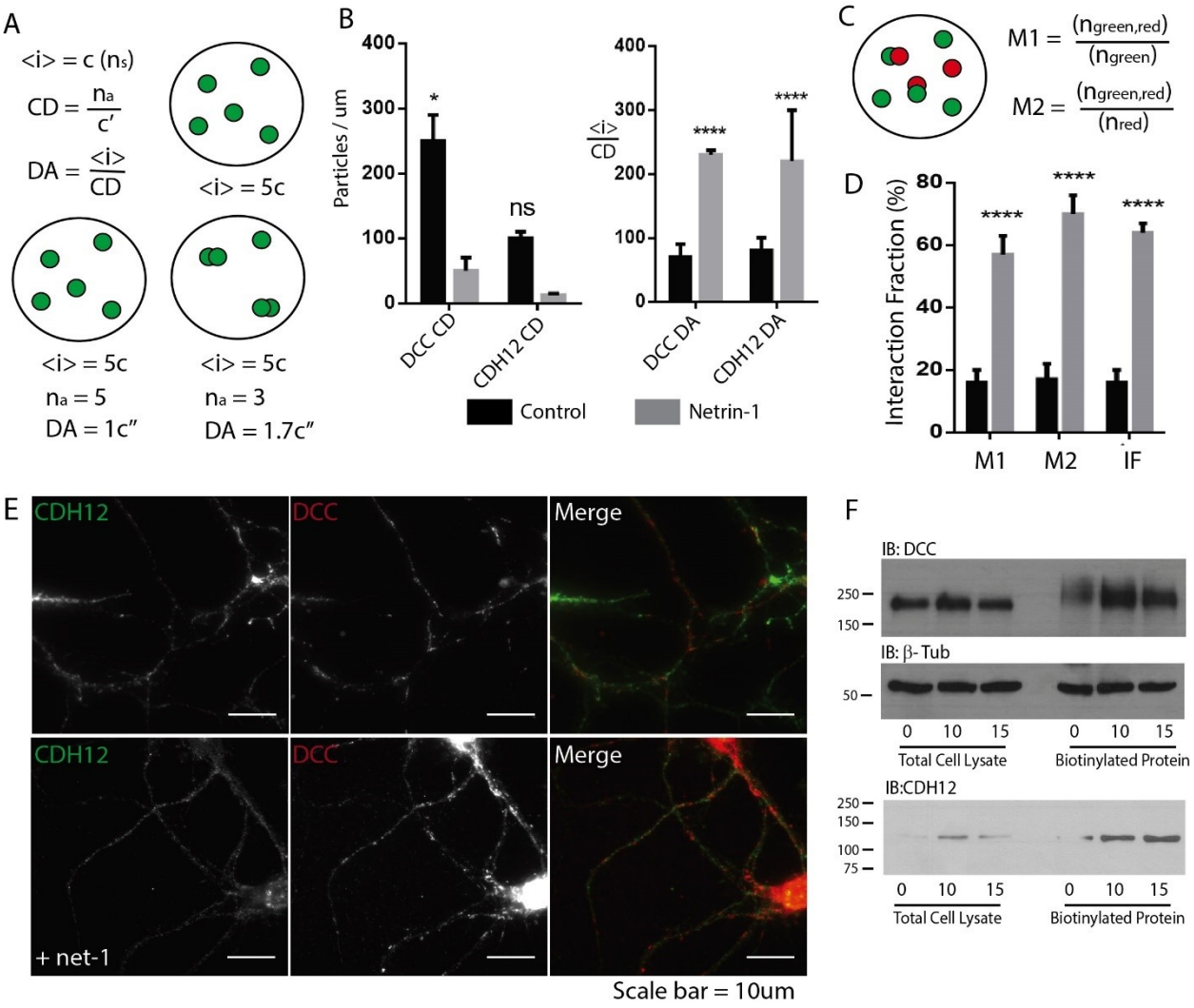

Figure 4.4: ICCS supports interaction of DCC and CDH12 in cortical neurons. A-E: ICCS measurements of DCC and CDH12 in 6DIV cortical neurons +/- netrin-1 for 15 min and imaged using TIRF microscopy. **A:** Schematic representation of cluster density (CD) and degree of aggregation (DA) calculations. <i> is intensity, n_a is number of aggregates, and c, c', and c'' are constants. **B:** Quantification of CD and DA for CDH12 and DCC in cultured cortical neurons (Un-paired two tailed t test. n=9 ROIs. * P<0.05, **** P<0.0001). **C:** Schematic representation of interaction fraction calculations. The interaction fraction is a measure of co-localization. $n_{green,red}$ is the number of co-localized particles, n_{red} is the total number of red particles, and n_{green}

is the total number of green particles. **D:** Quantification of the interaction fraction for CDH12 and DCC in cultured cortical neurons (Un-paired two tailed t test. n=9 ROIs. **** P<0.0001). **E:** Representative images of cortical neurons +/- netrin-1. CDH12 immunoreactivity is shown as green and DCC immunoreactivity as red (scale bar = 10 μm). **F:** Cell surface distribution of DCC and CDH12. 3 DIV mouse cortical neurons were stimulated with 200ng/ml netrin-1 for 0, 10, or 15 min. Cell lysates and biotinylated samples were visualized using western blot. After 10 and 15 min of netrin stimulation increased levels of both DCC and CDH12 proteins were detected on the cell surface.

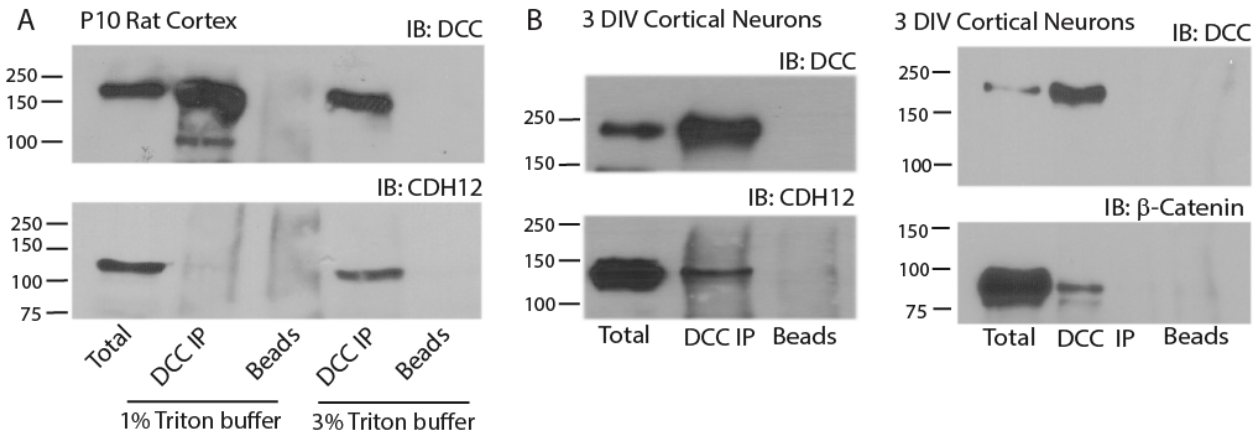

Figure 4.5: DCC, CDH12, and β-catenin co-IP. A: Western blots showing DCC immunoprecipitation from P10 rat cortex homogenate. Total protein, DCC IP and beads control are shown. DCC is enriched in the DCC IP and completely absent in beads control. CDH12 and β-catenin are both present in DCC IP lanes and absent in beads controls. DCC IPs were done with both a 1 % triton X-100 lysis buffer and 3 % triton X-100 buffer. Co-IP of CDH12 is detergent sensitive and only able to IP with DCC using a 3 % triton lysis buffer. **B:** Western blots showing DCC immunoprecipitation from cultured cortical neurons. DCC is present in DCC

IP lanes and absent in beads control. CDH12 is also present in DCC IP lanes and absent in beads controls. β-catenin is also present in DCC IP lanes and absent in beads controls. All IP's from cultured neurons were done using 3% triton X-100 lysis buffer.

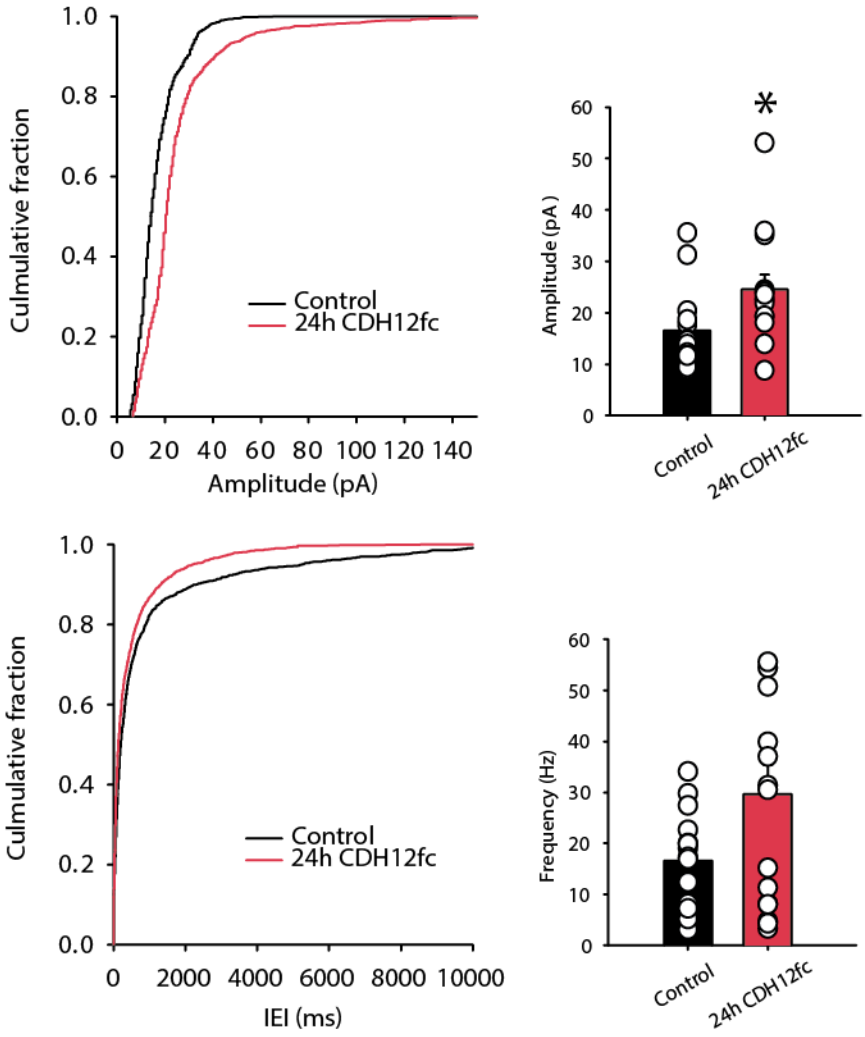

Figure 4.6: Electrophysiological recordings from 14 DIV cortical neuron cultures. Cultures were left untreated or treated with CDH12-Fc for 24 hr prior to recording from cells. Treatment with CDH12-Fc resulted in an increase in amplitude of mini EPSCs but no significant change in inter-event interval (IEI) or frequency of events (un-paired two tailed t test, n=100 events per cell, 15-16 cells, $P<0.05$).

Preface

Netrin-1 is a secreted axon guidance cue, however, the distribution of the protein detected in the embryonic spinal cord suggests that it is not freely diffusible. Proteoglycans are ECM proteins widely expressed in all organisms. HSPGs are particularly abundant in the developing spinal cord and expressed in a similar distribution to netrin-1 (Ivins et al., 1997). Netrin-1 has been previously shown to bind to heparin, a highly sulfated HSPG, making HSPGs ideal candidates to bind netrin-1 in the developing spinal cord. Further, work done in *C. elegans* identified an interaction between DCC and glypicans which was critical for appropriate axon guidance (Blanchette et al., 2015). In this chapter we investigate the interaction between netrin-1 and HSPGs in the developing spinal cord. We identify the netrin-1 C-domain as a critical GAG binding domain and show that GAGs can potentiate netrin-1 induced commissural axon outgrowth *in vitro.* Additionally, we show that perturbed expression of glypican-1, a member of the HSPG family, leads to mis guided commissural axon growth *in vivo*. A manuscript corresponding to this chapter is in preparation for publication.

Chapter 5

Proteoglycan binding regulates the distribution and function of netrin-1 in the embryonic spinal cord: identification of a GAG binding site in the netrin-1 C-terminal domain

Stephanie N. Harris*[!], Ian V. Beamish*[!], Celina Cheung*[!], Lynda Djerbal[#], Nathalie Marcal*[!], Daryan Chitsaz*[!], Chao Chang[##], K. Adam Baker*, Michael J. Landry[%!], Simon Moore*[!], Mahmoud Moussa*, Christopher J. Barrett[%!], Claire Y. Benard[++], Artur Kania[##,&], Ralf Richter[#], Jessica C.F. Kwok[#,Σ], Timothy E. Kennedy*[!]

[!]McGill Program in Neuroengineering

*Department of Neurology and Neurosurgery, Montreal Neurological Institute, McGill University, Montreal, Quebec, Canada, H3A 2B4

[%]Department of Chemistry, McGill University, Montreal, Quebec, Canada, *H3A 0B8*

[++]Département des Sciences Biologiques, Université du Québec à Montréal, Montréal, Québec, Canada, H2X 1Y4

[##] Institut de Recherches Cliniques de Montréal (IRCM), Montréal, Québec, Canada, H2W 1R7

[&]Department of Anatomy and Cell Biology, Division of Experimental Medicine, McGill University, Montréal, Quebec, Canada, H3A 2B2

[+]Cambridge Centre for Brain Repair, University of Cambridge, Cambridge, United Kingdom

[#]School of Biomedical Sciences, University of Leeds, Leeds, United Kingdom

[Σ] Institute of Experimental Medicine, Czech Academy of Science, Prague, Czechia

I. ABSTRACT

Axons may travel long distances to reach their targets during development. Netrin-1 is a secreted multi-functional axon guidance cue that is essential for normal embryonic neural development. Commissural neurons, with cell bodies in the dorsal embryonic spinal cord, express the netrin receptor Deleted in Colorectal Cancer (DCC) and require netrin-1 to extend axons to the ventral midline. Secreted netrins are ~75 kDa proteins composed of three major domains; amino terminal domains VI and V that are homologous to laminins and contain known netrin-receptor binding sites, and a carboxyl terminal NTR-like C-domain of unknown function. Here we provide evidence that netrin-1 is localized and anchored within the extracellular matrix (ECM) of the developing CNS via specific interactions between the C-domain and ECM proteoglycan glycosaminoglycans (GAGs). Our findings identify interactions between netrin-1 and specific Heperan Sulfate Proteoglycans (HSPG) isolated from developing rat CNS, and that HSPGs increase axon outgrowth in response to netrin-1. Specifically, glypican binding to netrin-1 enhances axon outgrowth and ectopic expression of glypican-1 leads to guidance defects in the developing spinal cord. A previous study demonstrated that LON-2 (glypican) is required for responses to netrin in *C. elegans*, suggesting that the interaction between GAGs, netrins and netrin receptors is a highly conserved axon guidance mechanism.

II. INTRODUCTION

Commissural axons in the embryonic spinal cord pioneer a circumferential trajectory to the ventral midline of the neural tube in response to multiple extracellular cues (Colamarino & Tessier-Lavigne, 1995; Kolodkin & Tessier-Lavigne, 2011). In the absence of netrin-1 the vast majority of commissural axons deviate from their normal path and do not reach the floor plate at the ventral midline (Bin et al., 2015; Nishitani et al., 2017; Serafini et al., 1996). The distribution of netrin-1 as a gradient in the early neural tube is thought to be critical to direct axon extension by either attracting commissural axons or repelling motor axons (Colamarino & Tessier-Lavigne, 1995; Kennedy et al., 1994; Kennedy et al., 2006). How the graded distribution of netrin-1 protein is initially established and maintained within the spinal cord is not known. Netrin-1 is a secreted protein; however, immunohistochemical and biochemical analyses indicate that the majority of netrin-1 is not freely soluble *in vivo* but is instead immobilized on cell surfaces or bound to extracellular matrix (ECM) in the neural epithelium (Baker et al., 2006; Kennedy, 2000).

Netrins were initially purified from a high salt extract of homogenized embryonic CNS, in part, using heparin affinity chromatography which is characteristic of membrane associated proteins (Serafini et al., 1994). Netrin-1 binds heparan sulfate (HS) and chondroitin sulfate (CS) glycosaminoglycans (GAGs) with high affinity, suggesting that it likely binds heparan sulfate proteoglycans (HSPGs) and chondroitin sulfate proteoglycans (CSPGs) (Kappler et al., 2000; Serafini et al., 1994; Shipp & Hsieh-Wilson, 2007). Proteoglycans, including the HSPGs: glypicans and syndecans, and the CSPGs: aggrecan, neurocan, versican, brevican, and phosphocan, along with hyaluronan, form specialized extracellular matrices around neurons and neural epithelial cells in the developing and mature nervous system (Bandtlow & Zimmermann,

2000; Cui, Freeman, Jacobson, & Small, 2013). Like netrin-1, HSPGs and CSPGs can promote or inhibit axon growth in the mammalian nervous system (Fawcett, 2009) and blocking GAG synthesis during development severely disrupts axon guidance, including the formation of midline commissures (Inatani et al., 2003). Further, digesting GAGs with chondroitinase ABC (ChABC) in the mature CNS increases axon regeneration, enhances synaptic plasticity, prolongs memory, and can re-open critical periods of synaptic plasticity (Fawcett, 2009; Galtrey et al., 2007; N. G. Harris et al., 2013; Pizzorusso et al., 2002; Romberg et al., 2013; D. Wang et al., 2011). Due to their potential clinical importance, it is essential to understand the molecular mechanisms that underlie GAG function in the CNS. Although no specific netrin-proteoglycan interaction has yet been demonstrated in vertebrate species, a recent genetic study in *C. elegans* reported that the core protein of the nematode glypican LON-2 interacts with UNC40, the *C. elegans* homologue of the netrin receptor DCC, and is required for axon guidance in response to the netrin UNC6 (Blanchette et al., 2015).

Our findings reveal a close physical and functional interaction between GAGs and netrin-1 in the developing neural epithelium. We propose that following secretion *in vivo*, netrin-1 is captured by GAG binding sites that immobilize and present netrin-1 in the ECM and on cell surfaces or that netrin-1 may be co-secreted bound to GAGs. We demonstrate that netrin-1 binds to GAGs isolated from the embryonic spinal cord, and that the distribution of netrin-1 largely, if not entirely, overlaps with the distribution of GAGs. In particular, our findings reveal an interaction with the glypican family of HSPGs in the mammalian embryonic spinal cord, and we demonstrate that this interaction promotes commissural axon outgrowth. Our results suggest that the immobilization and presentation of netrin-1 by glypican in the embryonic spinal cord is a

highly conserved functional analogue of the requirement for LON-2 in UNC6 mediated axon guidance in *C. elegans* (Blanchette et al., 2015).

III. METHODS

III.i. Animals

All procedures were performed in accordance with the Canadian Council on Animal Care guidelines for the use of animals in research and approved by the Montreal Neurological Institute Animal Care Committee and the McGill Animal Compliance Office. Sprague-Dawley rats were obtained from Charles Rivers Laboratory at various developmental stages (St-Constant, QC, Canada) (vaginal plug = E0).

III.ii. Antibodies and reagents

Antibodies: Rabbit anti netrin-1 (abcam, EPR5428), rabbit anti myc (abcam , ab9106), mouse anti HS 10E4 (amsbio, clone F58-10E4, 370155-1), mouse anti CS (Sigma, clone CS-56, C 8035) , mouse anti GST (B-14) (Santa Cruz, SC-138), mouse anti glypcan-1 (QED Biosciences, 34029), peroxidase-conjugated donkey anti mouse IgG (Jackson Immuno Research, 715-035-150) alexa flour donkey anti rabbit (molecular probes, A31572 & A21206), alexa fluor goat anti mouse (molecular probes, A-11003, A-11001, & A-21042).

Reagents: Chondroitinase ABC (Sigma, C3667-5UN), Heparinase III (Sigma, H8891-5UN), HS I, II, & III (Iduron, GAG-HSI, GAG-HSII, GAG-HSIII), recombinant human glypican 1-6 (R&D systems, 4250-GP-050, 2304-GP-050, 2119-GP-050/CF, 9195-GP-050, 2607-G5-050, 2845-GP-050) , recombinant human syndecan 1-4 (R&D systems, 2780-SD-050, 2965-SD-050, 3539-SD-050, 2918-SD-050 , sulfated β-cyclodextrin (Sigma #389153-5G).

III.iii. Generation of recombinant netrin-1 C terminal domain protein fragments

Purified recombinant full-length netrin-1 and the netrin VI-V peptide were generated from constitutively expressing HEK293 cells as described (Kennedy et al., 2006). The DNA construct encoding the netrin-1 C-domain was generated using the polymerase chain reaction (PCR) from a plasmid encoding chick netrin-1 using primers flanking the 5' and 3' ends of the C-domain (5' AAG ATC CCC GCC GCG CC; 3' CTC GAG CTA CGC CTT CCT ACA CTT CC). Compared to human netrin-1, the netrin-1 C-domain amino acid sequence is 88% identical in chick, 96% identical in rat, and 98% identical in mouse (Figure 5.1). A cDNA construct encoding the putative GAG binding domain found at the end of the C-domain, ARRLRKFQQREKKGKCRKA (100% identical in rat, mouse, and human) was generated as an oligomer (GGA TCC GCA CGG CGG CTG CGG AAG TTC CAG CAG AGG GAG AAG AAG GGG AAG TGT AGG AAG GCG TAG CTC GAG) which was annealed to obtain a double stranded DNA sample. Both the netrin-1 C-domain and the putative GAG binding domain cDNA constructs were then subcloned into a PGEX 4TI vector (GE Healthcare), which encodes a 5' glutathione S transferase (GST) tag.

Plasmids encoding the netrin-1 C-domain GST fusion proteins and the pGEX 4TI vector alone (GE Healthcare) were transformed into BL21 *E.coli* (Invitrogen) and grown to an optical density of 0.5 at 600 nm absorbance. Protein expression was then induced with 1M isopropyl-β-d-1-thiogalactopyranoside (IPTG) (Sigma Aldrich). Bacteria cultures were incubated for an additional 3 hr following induction, and bacteria then pelleted at 4000 x RCF for 30 min at 4^{o} C (Beckman Coulter Avanti J-E).

Recombinant proteins were purified using GST sepharose column chromatography. Protein was isolated from bacteria by sonication in 1% NP40, 150 mM NaCl, 50 mM Tris-HCl

pH 7.4 lysis buffer and then centrifuged at 15000 x RCF to remove cell debris. The supernatant was filtered and loaded onto the column at 0.3 ml/min. The column was washed with PBS plus 5 mM EDTA and 0.15 mM PMSF followed by a second wash with PBS plus 5 mM EDTA. Protein was then eluted using a buffer composed of 20 mM Hepes, 10mM L-glutathione reduced at pH 8.3.

III.iv. Heparin batch binding assay

Purified recombinant GST-protein chimeras corresponding to 500 µg of GST linked to either the full-length netrin-1 C-domain, only the putative GAG binding site, or GST alone, were added to 300 µl of 1% NP40, 150 mM NaCl, 50 mM Tris-HCl pH 7.4 lysis buffer with protease inhibitors *(*Aprotinin 1 µg/mL, Leupeptin 1 µg/mL, 1 mM DTT, 1 mM PMSF, DNAse I 4 mg/mL, and lysozyme 0.2 mg/mL). A 10% "input" sample was taken from this solution and 30 µl of a 50% heparin agarose bead (Sigma-Aldrich) slurry in PBS added to the remaining protein. Proteins and beads were incubated, rotating, for 1 hr at 4^{o} C, and then rapidly pelleted using a quick spin in an Eppendorf 5415 C centrifuge. Thirty µl of supernatant was saved and the rest discarded. Beads were then washed five times with 1 mL of 1% NP40 lysis buffer with protease inhibitors (as described above). Beads were then pelleted as above and resuspended in Laemmli buffer (Laemmli, 1970).

III.v. Cell surface binding assay

HEK293T Cells were grown on plasma treated coverslips (Circular 12 mm diameter, No. 0, Deckglaser) coated with 10 µg/ml of poly-D-lysine (PDL). PDL coating was carried out for 1 hr at room temp using a volume of 500 µl PDL per coverslip. PDL coated coverslips were then washed 3 times with ddH_2O and allowed to air dry. HEK293T cells were cultured for 24 hr to reach 80% confluency prior to assessing surface binding. Cells were grown in DMEM (Thermo

Fisher) supplemented with 10% heat inactivated FBS, and 1% P/S and cultured at 37^{o} C with 5% CO_2. To assess binding 1 μg/ml of protein in 10% BSA and 0.1% sodium azide was incubated with cells for 90 min at rt. Cells were washed 3 times with PBS at rt and then fixed with methanol at -20^{o} C in a freezer for 15 min and washed with PBS before staining.

III.vi. Immunocytochemistry

Cells were blocked and permeabilized in 0.25% Triton-X 100 and 3% heat inactivated horse serum in PBS. Primary antibodies were diluted in a buffer of 0.1% Triton-X 100 and 3 % heat inactivated horse serum in PBS and incubated overnight at 4^{o} C. Cells were then washed in PBS 3 x 10 min with rocking. Secondary antibodies were diluted in 0.1% Triton-x 100 and 3% heat inactivated horse serum in PBS for 1 hr at rt and then washed 3 x 10 min in PBS. Coverslips were then rinsed once in water and mounted on slides using Fluoro-Gel with tris buffer (Electron Microscopy Sciences).

III.vii. Immunohistochemistry

Whole embryos were dissected out of the uterus and fixed by submersion in Carnoy's solution, 60% ethanol, 10% acetic acid, 30% chloroform, for 2 hr at rt. Embryos were then washed twice with 100% ethanol for 20 min and cleared in toluene for 1 hr before being embedded in paraffin (Fisher Scientific). Sections, 10 μm thick, were cut with a microtome and mounted on SuperFrost Plus Slides (Fisher Scientific). Tissue sections on slides were dewaxed and rehydrated prior to staining as follows. Excess wax was removed by melting in an oven at 50^{o} C. Sections were then moved through a series of Xylene, 100% ethanol, 95% ethanol, 70% ethanol, and rehydrated in PBS, for 2 x 3 min in each solution.

Sections stained with antibodies against HS or CS were treated with either 2.5 U/ml of heparinase III (Sigma) in a buffer of 0.1 M sodium acetate and 0.1 mM calcium acetate pH 7.0 or

0.2 U/ml chondroitinase ABC (Sigma) in a buffer of 0.1 M ammonium acetate pH 8 for 2 hr at 37^{o} C. Slides were washed in TBS with 0.2% Triton-X 100 and then treated for antigen retrieval by boiling in 10 mM citrate buffer at pH 6 for 20 min in a microwave oven, as described (Kennedy et al., 2006). Slides were cooled in buffer for an additional 15 min before being washed 2 x 5 minutes in TBS. Slides were then blocked and permeabilized in 0.2% Triton-X 100 and 5% heat inactivated calf serum in TBS. Primary antibodies were diluted in a buffer of 0.2% Triton-X 100 and 5% heat inactivated calf serum in TBS and incubated overnight at 4^{o} C. Sections were then washed in TBS for 3 x 10 min with rocking. Secondary antibodies were diluted in 0.2% Triton-X 100 and 5% heat inactivated calf serum in TBS for 1 hr at rt and then washed 3 x 10 min in TBS. Slides were then rinsed once in water and cover slipped using Fluoro-Gel with tris buffer (Electron Microscopy Sciences).

III.viii. Glycan isolation from embryonic neural tissue

Whole brain or whole spinal cord were micro dissected from E11 and E13 Sprague Dawley rats in ice cold HBSS with calcium and magnesium (Thermo Fisher). Following dissection, tissue was transferred to a tube on ice without media for GAG isolation. Tissue was homogenized on ice in a buffer of 0.1 M Tris and 10 mM calcium acetate at pH 7.8. Pronase (Roche #11459643001) was then added to the sample at a weight ratio of 1 mg of enzyme for every 100 mg of sample and incubated overnight at 4^{o} C. The sample was centrifuged at 13793 x RCF for 15 min at 4^{o} C after which the supernatant was collected and cooled on ice. Ice cold trichloroacetic acid (TCA) was added to a final concentration of 5% and samples kept on ice for 1 hr. Samples were centrifuged at 8161 x RCF for 30 min at 4^{o} C, the supernatant collected, and the pellet then washed twice with 5% ice cold TCA. All supernatants were pooled and washed 5 times with diethyl ether. Following ether evaporation, samples were neutralized with sodium

bicarbonate to pH 7.0-7.5. Sodium acetate was then added to a final concentration of 5% w/v. Ice cold ethanol was then added to a final concentration of 75% ethanol in the sample and kept overnight at 4° C. Samples were then spun at 735 x RCF for 15 min at 4° C. Supernatants were discarded, and pellets washed twice with ice cold 100% ethanol. Pellets were then dried at rt and dissolved in water.

Glycan concentrations were measured using a cetylpyridinium chloride (CPC) turbidimetry assay. Samples were mixed 1:1 with a solution of 0.05% CPC and 33.25 mM $MgCl_2$. The absorbance of the resulting mixture was read at 405 nm and compared to a standard curve to determine final glycan concentration. Glycans were recovered from the turbidimetry assay by precipitation with 0.5 % CPC overnight at 4° C. Samples were then centrifuged at 13793 x RCF at 4° C for 30 min. The pellet was dissolved in butanol and 4 volumes of sodium acetate saturated ethanol added and incubated at 4° C overnight. Samples were then centrifuged at 13793 RCF at 4° C for 30 min and pellets washed twice with 100 % ethanol. Samples were then dried, and pellets dissolved in water.

III.ix. Biotinylation of isolated GAGs

Glycans were biotinylated using 50 mM EZ-link hydrazide biotins (Thermo Fisher Scientific) in dimethyl sulfoxide (DMSO) and 100 mg/ml 1-Ethyl-3-(3-dimethylaminopropyl)carbodiimide (EDC) (Thermo Fisher Scientific) in 0.1 M 2-(N-morpholino)-ethane sulfonic acid (MES) at pH 5.5. One µg of glycans was biotinylated with 2.5 µl of EDC solution, and 5 µl of biotin solution brought to a final volume of 1 ml with 0.1 M MES buffer at pH 5.5. Samples were protected from light and rotated for 16 hr at rt. Following biotinylation, residual chemicals and biotin were removed by dialysis with 3.5 kDa molecular weight cut-off dialysis cassettes (Thermo Fisher Scientific), against 3 L of PBS at 4° C for 16 hr. Samples were then removed from the

cassettes and stored at -20° C at a final concentration of 0.02 µg/µl. The degree of biotinylation was determined using a biotin quantitation kit (Vector Labs), according to the manufacturer's instruction.

III.x. GAG ELISA assay

A high bind 96 well plate (Greiner) was coated with protein at a concentration of 10 µg/ml in PBS without potassium (PBS-K) overnight at 4° C. The plate was washed 3 times with PBS-K with 0.1 % Triton-X 100 and then blocked with 10 % bovine serum albumin (BSA) for 1 hr at rt. The plate was then washed again as above and biotinylated GAGs, 0.8 ng/µl, added to each well for 1 hr at rt. The plates were again washed as before and a 1:1000 dilution of streptavidin alkaline phosphatase (ab 136224, abcam) added to the wells for 1 hr at rt. The wells were then washed as before and PNPP (Thermo Scientific) added to each well. Plates were incubated for 30 min and absorbance read at 405 nm using a spectrophotometer (Biorad).

III.xi. Embryonic dorsal spinal cord explants

Brachial spinal cord segments were micro dissected from E13 rat embryos and dorsal explants, ~200 µm x ~200 µm, embedded in a 3D collagen matrix as described (Moore & Kennedy, 2008). Immediately following embedding, explants were treated as described in the figure legends. Sixteen hr after treatment explants were fixed in 4% PFA for 1 hr on ice. Explants were imaged using bright field phase contrast microscopy (Zeiss Axiovert S100TV, 20x objective, MagnaFire CCD camera and MagnaFire 4.1C imaging software (Optronics, Goleta, USA).

III.xii. Surface plasmon resonance

Surface plasmon resonance (SPR) was carried out using Biacore 3000 and Biacore T200 instruments (GE Healthcare) and CM4 sensor chips (GE Healthcare) were generated as described

(Djerbal et al., 2019). Briefly, sensor chips were coated with biotinylated HS at a level of ~60 RU or left untreated as a control. Prior to use, chips were injected with HBS buffer containing 2 M NaCl and then washed with HBS-P buffer (10 mM HEPES, 0.15 M NaCl, 0.05% P20, pH 7.4). A range of netrin-1 full length and netrin-1 VI-V concentrations between 0 nM and 100 nM were injected at 25^{o}C at a speed of 30 µl/min over the defined surfaces. Surfaces were then regenerated with a pulse of 2M NaCl. Control readings were then subtracted from GAG readings. Both association and dissociation phases were fitted using a Langmuir 1:1 binding model with mass transfer (BIAevaluation 3.1 software, GE Healthcare).

III.xiii. Chick *in ovo* electroporation

Chick spinal cord electroporation was performed as previously described (Croteau, Kao, & Kania, 2019). Briefly, chicken embryos at Hamburger–Hamilton (HH) stage 15/16 were electroporated with glypican-1-myc expression plasmids in a 5:1 weight ratio with pN2-eGFP plasmids or pN2-eGFP plasmids alone as controls. Embryos were incubated at 39℃ until harvesting at HH stage 24/25.

IV. RESULTS

IV.i. The netrin-1 NTR-like C-domain contains GAG binding sequences

Although its functional significance is not clear, the amino acid sequence of the netrin-1 carboxyl terminal NTR-like C-domain is remarkably highly conserved across many species, including mammals, birds, amphibians, and fish (Figure 5.1A). The high degree of conservation suggests an important role, however, no function for the netrin-1 C-domain has so far been reported. Short sequences of amino acids within the C-domain that are 100% conserved in all vertebrate netrin-1s examined include a series of basic amino acids that encode putative GAG

binding sites (Figure 5.1B). Consensus amino acid sequences for GAG binding sites are XBBXBX and XBBBXXBX where B is the basic amino acid R or K, and X any amino acid (Cardin & Weintraub, 1989). In addition to two potential GAG binding sequences found in the C-domain, scanning the amino acid sequence of netrin-1 revealed four additional putative GAG binding sequences, one in domain VI and three in domain V (Figure 5.1B). Netrin-1 is known to bind heparin, and salt elution demonstrates that full-length netrin-1 binds to a heparin affinity column with substantially higher affinity than a truncated netrin-1 variant that lacks the C-domain, referred to as the VI-V peptide. Elution of full-length netrin-1 from a heparin affinity column requires ~1.6 M NaCl solution while purifying the VI-V peptide requires only ~0.6 M NaCl, supporting the possibility that the C-domain is important for GAG binding. The amount of salt required to extract recombinant full-length netrin-1 and the netrin-1 VI-V peptide from constitutively expressing HEK293 cells also indicates a role for the C-domain in cell surface binding, which we hypothesize is GAG binding dependent. Extraction of recombinant full-length netrin-1 from the surface of HEK293 cells utilizes 1.2 M NaCl, while netrin-1 VI-V may be purified directly from the conditioned media without salt extraction.

Netrin-1 binding to HEK293 cells may be mediated through an interaction with cell surface GAGs which led us to test the capacity of purified full-length netrin-1 and netrin-1 VI-V to bind to the cell surface. HEK293T cells express RNA encoding all members of the glypican and syndecan HSPG families to varying levels, with the highest expression being syndecan 2 (proteinatlas.org). When added to cells in culture, exogenous recombinant full-length netrin-1 was rapidly captured on the surface of HEK293T cells; however, the netrin-1 VI-V peptide exhibited a much lower level of binding, indicated by quantification of fluorescence intensity (Figure 5.1C). Pre-incubation of HEK293T cells for 2 hr with 2.5 U/ml heparinase III to digest

cell surface HSPG GAG chains resulted in substantially reduced binding of full-length netrin-1 to the cell surface (Figure 5.1C). These results provide evidence that HSPGs mediate netrin-1 binding to the extracellular face of the plasma membrane of HEK293T cells via the netrin-1 C-domain and suggest the possibility of a direct interaction between the C-domain and GAGs.

IV.ii. HSPGs and CSPGs in embryonic spinal cord

To visualize the overall distribution of HSPGs and CSPGs in the embryonic spinal cord we used antibodies that bind either HS or CS GAG chains to detect all HSPG or CSPG family members, respectively. Sections of E13 rat spinal cord were immunolabelled for HS or CS and colabelled for netrin-1 (Figure 5.2). HS immunoreactivity was enriched in the ventral region of the spinal cord with particularly strong axonal staining in the ventral commissure itself. Blood vessels and ventral funiculi composed of axons running longitudinally were also HS immunopositive, as previously reported (Halfter et al., 1997; Laurie, Leblond, & Martin, 1983). A substantial degree of overlap between netrin-1 and HS is apparent, particularly in the ventral commissure; however, HS was notably absent from floor plate cells, which express and secrete high levels of netrin-1 (Figure 5.2A). A medially enriched band of strong CS immunoreactivity was associated with mid-level neural epithelial cells and roof plate cells. In contrast to the distribution of HS, little overlap between CS and netrin-1 was detected (Figure 5.2B).

IV.iii. Netrin- C-domain mediates GAG binding

To further investigate the sequence specificity of GAG binding by the netrin-1 C-domain we generated two different recombinant netrin-1 peptides, the complete netrin-1 C-domain and a peptide composed of only the 20 most C-terminal amino acids that encode the putative GAG binding domain (Figure 5.3). PGEX 4TI plasmids were generated encoding each of these peptides as a GST fusion protein for production in *E.coli*. The capacity of these netrin-1 C-

domain peptides to bind heparin was then tested using a batch binding assay with heparin coated beads. The GST-fusion proteins were incubated with heparin coated beads and bound proteins separated by SDS-PAGE and identified by western blotting. Both the full-length C-domain GST peptide and the GAG binding domain GST peptide readily bound to the heparin coated beads. A small amount of the full-length C-domain GST peptide was detected in the supernatant while all of the GAG binding domain GST peptide was bound to the heparin beads (Figure 5.3). GST-alone was readily washed from the beads indicating heparin binding was due to the C-domain and not the GST tag. These results demonstrate that the 20 C-terminal amino acids of netrin-1 are sufficient for netrin-1 to bind heparin (Figure 5.3).

IV.iv. Netrin-1 binds GAGs expressed in the embryonic CNS

The sulfation pattern of GAG chains is tightly regulated throughout development and varies depending on age and tissue expression (Bulow & Hobert, 2006; Turnbull et al., 2001). As a result, GAGs may exhibit different sulfation patterns in different tissues and at different developmental time points. A small GAG chain of eight sugars has over a million different potential sulfation patterns and changes in sugar sulfation can alter the capacity of netrin-1 to bind heparin (Sasisekharan & Venkataraman, 2000; Shipp & Hsieh-Wilson, 2007). Therefore, it is important to investigate the capacity of netrin-1 to bind GAGs isolated from the embryonic CNS, in particular, GAGs isolated from the developing spinal cord, where they may influence netrin-1 function.

To investigate netrin-1 binding to endogenous GAGs, spinal cords were micro-dissected from E11 and E13 rat embryos and homogenized. Protein content was degraded and precipitated to remove protein from the sample. GAGs were then precipitated in ethanol and recovered as a pellet before being resuspended in water. E11 and E13 spinal cords were chosen since these are

ages during which spinal commissural axons are actively extending to the ventral midline and the ventral commissure is forming (Holley, 1982; Silos-Santiago & Snider, 1992; Wentworth, 1984). Significantly more full-length netrin-1, compared to the VI-V peptide, was bound to the isolated GAGs at both ages tested, further highlighting the importance of the C-domain for netrin-1 GAG binding. Netrin-1 binding was also significantly higher for GAGs isolated from E13 compared to E11 spinal cord (Figure 5.4A).

While isolation from tissue generates GAGs with potential physiological relevance, the GAGs isolated are a mixture of several proteoglycan families (Deepa et al., 2006). To determine which families of GAG chains are responsible for netrin-1 binding, we selectively digested HSPGs using heparinase III and CSPGs using chondroitinase ABC in material derived from E11 and E13 spinal cord and then examined netrin-1 GAG binding. At both E11 and E13, digestion with chondroitinase ABC had no effect on GAG binding suggesting CSPGs are not major binding partners for netrin-1 in the embryonic spinal cord (Figure 5.4B). In contrast, digestion with heparinase III altered GAG binding at both ages. Intriguingly, in the GAGs isolated from E11 spinal cord, heparinase III digestion increased nerin-1 binding. Heparinase III digests GAGs at the linkage between hexosamines and glucuronic acid while leaving linkages between hexosamines and iduronic acid intact (Wei, Lyon, & Gallagher, 2005). Depending on the composition of the GAG chains, this could result in differing degrees of chain digestion. As a result, digestion of E11 GAGs with Heparinase III may only digests a portion of the GAG chain and possibly expose additional binding sites for netrin-1. Heparinase III digestion of GAGs isolated from E13 spinal cord resulted in a significant decrease in netrin-1 binding, revealing that bindings sites change as the cord matures, and indicating that HSPGs are major GAG binding partners for netrin-1 in the E13 spinal cord (Figure 5.4B).

IV.v. HSPGs are required for netrin-1 induced axon outgrowth

Netrin-1 evokes robust commissural axon outgrowth from explants of embryonic dorsal spinal cord and this is a well-established assay of netrin-1 function (Kennedy et al., 1994; Tessier-Lavigne et al., 1988). Here, we used this assay to assess how GAGs might influence the capacity of netrin-1 to promote axon outgrowth from explants of E13 rat spinal cord (Figure 5.5). To remove HSPGs from the explant we included heparinase III in the culture medium and saw significantly reduced axon outgrowth in response to the addition of purified recombinant netrin-1. This finding demonstrates that endogenous HSPGs made by cells within the explant, either by commissural neurons, neuroepithelium, or both, are required for netrin-1 mediated outgrowth. This result is consistent with previous findings demonstrating that genetic knockout of exostosin-1 (EXT1) resulted in severe defects in commissural axon guidance and ventral commissure formation. EXT1 is an enzyme essential for elongation of the HSPG GAG chains and was deleted from the dorsal portion of the spinal cord, a region which contains commissural neuron cell bodies (Matsumoto et al., 2007).

To determine whether the addition of exogenous heparin could modulate commissural axon outgrowth evoked by netrin-1 we carried out a dose-response analysis. Application of 200 ng/ml netrin-1 evokes maximal levels of commissural axon outgrowth from E13 dorsal spinal explants, while application of 50 ng/ml netrin-1 results in approximately half the maximal level (Figure 5.5A). Addition of exogenous heparin alone did not increase axon outgrowth from explants treated with 200 ng/ml netrin-1 (Figure 5.5B). However, addition of heparin to explants treated with a sub-maximal level of netrin-1 (50 ng/ml) resulted in a dose dependent increase in axon outgrowth (Figure 5.5B). Addition of a DCC function blocking monoclonal antibody (Keino-Masu et al., 1996) blocked the outgrowth seen with the addition of heparin, supporting

the conclusion that the heparin-induced increase in outgrowth modulates netrin-1 DCC signaling and does not function as a secondary additive effect on outgrowth (Figure 5.5B).

Application of the netrin-1 VI-V peptide did not promote axon outgrowth from dorsal spinal explants, consistent with previous findings demonstrating that this truncated fragment of netrin-1 retains chemorepulsive but not chemoattractive function (Bin et al., 2013). Further, the addition of heparin had no effect on the capacity of the netrin-1 VI-V peptide to evoke axon outgrowth, with only background levels of outgrowth recorded (Figure 5.5B). These findings are consistent with a direct interaction between the netrin-1 C-domain and GAGs that facilitate netrin-1 function, and is reminiscent of the mechanism of FGF and FGFR function, in which heparin is a required co-factor for ligand receptor binding and signaling (Ornitz et al., 1992; Rapraeger et al., 1991; Spivak-Kroizman et al., 1994; Yayon et al., 1991).

GAGs are highly charged molecules, composed of long polymers of negatively charged sugar residues. We therefore investigated the possibility that an interaction with any negatively charged polymer might be sufficient to promote netrin-1 mediated axon outgrowth. Using the same axon outgrowth assay, we replaced heparin with sulfonated polystyrene, a highly sulfonated, negatively-charged synthetic polymer. Addition of sulfonated polystyrene had no impact, negative or positive, on axon outgrowth at any of the tested concentrations. This finding indicates that simply including a negatively-charged sulfate rich polymer is not sufficient to modulate netrin-1 function (Figure 5.5C). In an attempt to more closely emulate GAGs, we tested sulfated β-cyclodextrin, a highly charged cyclic oligosaccharide that has previously been used to mimic heparin function in angiogenesis (Baumann & Rys, 1999; Folkman & Shing, 1992). Similar to heparin, sulfated β-cyclodextrin significantly potentiated axon outgrowth in response to netrin-1. Although sulfonated polystyrene and sulfated β-cyclodextrin are both

polymers rich in negatively charged sulfate ions, our findings indicate that polymeric-charge alone is not sufficient to potentiate netrin-1 function (Figure 5.5C). Sulfonated polystyrene is an unbranched charged polymer that contains a rigid aromatic carbon ring structure that is not present in sugar molecules, which have a flexible carbon ring. Sulfated β-cyclodextrin is composed of an unbranched chain of flexible sugars that form a helical structure with a hydrophobic core, similar to that formed by HSPG GAG chains. The flexibility of sulfated β-cyclodextrin and GAGs is thought to be critical for ligand binding (Gandhi & Mancera, 2008). These results provide evidence that structure, along with charge, are essential for netrin-1 binding, and suggests that different GAG structures may differentially interact with netrin-1.

IV.vi. Netrin-1 binds glypicans and syndecans

Glypicans and syndecans are the two major families of HSPGs expressed in the CNS. There are 6 glypican family members, glypican 1 through 6, and 4 syndecan family members, syndecan 1 through 4. Amino acid sequence identity across the glypican and syndecan families is illustrated in figure 5.6A. Using an ELISA binding assay with recombinant purified netrin-1 protein bound to the plate, we examined binding to recombinant glypicans 1 - 6 and syndecans 1 – 4. In all cases, with the notable exception of glypican-5, full-length netrin-1 exhibited significantly higher binding than the netrin VI-V peptide, which lacks the C-domain (Figure 5.6B). For all glypicans and syndecans the degree of full-length netrin-1 binding was high; however, while all syndecan family members exhibited a relatively consistent level of binding to netrin-1, the binding of different glypican family members was more variable (Figure 5.6B). We also examined netrin-1 binding to isolated HS chains with varying degrees of sulfation, where HS1 is the least sulfated and HS3 is the most sulfated (Figure 5.6B). Binding of full-length netrin-1 was high for all HS chains and significantly higher than the VI-V peptide for binding to HS1 and HS2. Interestingly,

binding of the VI-V peptide to HS3 was significantly higher than to HS1 or HS2 (Figure 5.6B). This indicates that changes in the degree of sulfation can alter the ability of netrin-1 to bind GAGs and may account for the high degree of binding seen between netrin-1 VI-V and glypican 5. We then used surface plasmon resonance (SPR) to determine the equilibrium dissociation constant (K_D) of netrin-1 binding to highly sulfated HS GAG chains (Table 5.1, Figure 5.6C). Consistent with our ELISA binding data we saw tight binding of both full-length netrin-1 and netrin VI-V to the highly sulfated HS chain with a K_D in the pM range (Table 5.1, Figure 5.6C).

Table 5.1

	Ligand	k_a (1/Ms)	k_d (1/s)	K_D (M)	Average K_D (M)
Netrin-1 FL	HS	2.39×10^{6}	2.06×10^{-5}	8.61×10^{-12}	1.87×10^{-11}
		2.39×10^{6}	6.93×10^{-5}	2.89×10^{-11}	
Netrin-1 VI-V	HS	4.84×10^{5}	8.92×10^{-6}	1.84×10^{-11}	2.18×10^{-10}
		5.28×10^{5}	2.21×10^{-4}	4.18×10^{-10}	

IV.vii. Glypicans modulate netrin-1 induced axon outgrowth

Studies in *C. elegans* and *Drosophila* have identified functional roles for glypicans in axon guidance, while syndecan function in the nervous system has largely focused on synapse formation and function (Blanchette et al., 2015; Ivins et al., 1997; Karthikeyan et al., 1994; Rawson et al., 2005; Yamaguchi, 2002). Because of this we chose to focus on the glypican family of HSPGs in relation to netrin-1 function in the developing spinal cord. A recent genetic and biochemical study identified a required function for the *C. elegans* glypican, LON-2, in netrin-1 mediated axon guidance, demonstrating that the LON-2 core protein interacts in cis with the DCC homologue UNC40 (Blanchette et al., 2015). Glypican-1 is highly expressed in the embryonic mammalian spinal cord during commissural axon extension toward the ventral midline (Karthikeyan et al., 1994). Immunohistochemical analysis using a well characterized glypican-1 antibody (Karthikeyan et al., 1994) revealed remarkably similar distributions of

glypican-1 and netrin-1 in sections of E13 rat spinal cord (Figure 5.7H). Glypican-2 is also expressed in the E14 rat spinal cord in a distribution similar to netrin-1 protein (Ivins et al., 1997).

We tested the impact of recombinant mouse and human glypican proteins on commissural axon outgrowth in E13 rat spinal cord explants (Figure 5.7). All glypican family members evoked a dose dependent potentiation of axon outgrowth in response to the 50 ng/ml submaximal concentration of netrin-1 (Figure 5.7), a result similar to that evoked by the addition of heparin to dorsal spinal explants (Figure 5.5). Addition of any glypican to 200 ng/ml of netrin-1 did not significantly increase outgrowth and the addition of any glypican alone, without netrin-1, induced no outgrowth (Figure 5.7).

Glypican 5 was the only family member to exhibit significant binding to the netrin-1 VI-V peptide (Figure 5.6B). We speculated that binding to glypican 5 might be sufficient to multimerize the netrin-1 VI-V peptide and would thus promote axon outgrowth by cross-linking DCC to initiate downstream signaling (Stein et al., 2001). However, despite its capacity to bind to the netrin-1 VI-V peptide, addition of glypican 5 to explants treated with netrin-1 VI-V produced no significant increase in outgrowth (Figure 5.7G). While glypican 5 likely multimerizes the netrin-1 VI-V peptide, in the absence of the C-domain this is predicted to occur through one of the putative GAG binding sites in domain VI or domain V. The first GAG binding site in domain V, ARRCRF, highlighted in red in figure 5.1B, includes amino acids that are critical for DCC binding to netrin-1 (Finci et al., 2014). Mutation of R349 and R351 in netrin-1, which correspond to the second and third arginine residues in the predicted GAG binding domain, are essential for DCC binding netrin-1 and chemoattractive function (Finci et al., 2014). These findings raise the intriguing possibility of competitive binding between

glypican-5 and DCC at this site in domain VI of netrin-1. DCC binding may displace glypican-5 from this site, or glypican-5 may have the capacity to competitively inhibit DCC binding to netrin-1, both of which may disrupt netrin-1 function.

We then went on to assess the effect of ectopic glypican-1 expression on commissural axon extension *in vivo*. Chick spinal cords were co-electroporated with myc tagged glypican-1 and GFP or with GFP alone and immunohistochemistry used to assess axon growth (Figure 5.8). Expression of GFP alone did not affect the trajectory of commissural axons. In glypican-1 electroporated spinal cords some commissural axons were deflected by glypican-1 expressing GFP positive cells and deviated from their normal trajectory, as indicated by the arrowhead in figure 5.8C. Further, the axons of neurons that ectopically express glypican-1 did not follow the normal growth trajectory. Glypican-1 positive axons were detected appearing to grow dorsally towards the roof plate, or laterally towards the ventricle as indicated by the arrowheads in figure 5.8D. These findings provide evidence that ectopic mis-expression of glypicans can modulate netrin-1 dependent commissural axon outgrowth and support the conclusion that this interaction is functionally significant *in vivo*.

V. DISCUSSION

V.i. Netrin-1 interacts with GAGs via C-domain interactions

Here we provide evidence that netrin-1 and GAGs interact in the developing nervous system and co-operate to guide spinal commissural axon extension during embryonic development. Previous findings have demonstrated that for chemoattractant function netrin-1 must be bound to a substrate so that mechanical force can pull the extending axon forward (Moore, Zhang, Lynch, & Sheetz, 2012). Our findings support the conclusion that following secretion, netrin-1 is anchored to the immobilized ECM through GAG interactions and that this contributes to generating the

graded extracellular distribution that directs axon extension. GAGs are abundantly expressed in the embryonic spinal cord and the distribution of HSPGs is remarkably similar to the distribution of netrin-1 (Figure 5.2 & 5.7H). Findings from our ELISA binding studies indicate that netrin-1 binds to multiple different GAGs, including GAGs isolated directly from embryonic spinal cord tissue. This suggests that the distribution of netrin-1 protein in the embryonic CNS may be influenced by its binding to GAGs which could function to stabilize a gradient of immobilized netrin-1 protein in the path of extending commissural axons (Kennedy et al., 2006).

Importantly, our findings demonstrate that netrin-1/GAG binding is functionally significant. The addition of HSPGs increases axon outgrowth evoked by sub maximal concentrations of netrin-1. Further, we show that GAG dependent enhancement of netrin-1 function occurs via a mechanism dependent on DCC signaling. These findings are supported by previous studies demonstrating that commissural axon guidance requires the enzyme EXT1, which catalyzes an essential step in GAG chain elongation (Matsumoto et al., 2007). Specifically, our findings reveal a critical role for the netrin-1 C-domain in GAG binding. The results shown here support the conclusion that HSPGs in the developing spinal cord function to cross link netrin-1 via C-domain dependent interactions that influence the spatial distribution of netrin-1 protein.

V.ii. Multimerization of netrin-1 activates DCC

Our findings support the conclusion that cross linking netrin-1 via GAG binding facilitates DCC multimerization, which is required for function (Figure 5.9) (Stein et al., 2001). Addition of heparin or HSPGs to E13 rat dorsal spinal cord explant assays resulted in dose dependent increases in axon outgrowth evoked by submaximal levels of netrin-1. In contrast, no potentiation of outgrowth was found in response to maximal doses of 200 ng/ml netrin-1. Our

findings also indicate that GAG potentiation of netrin-1 induced axonal outgrowth is entirely DCC dependent. Our working model suggests that GAG binding cross-links multiple netrin-1 monomers to facilitate DCC multimerization. We reason that axon outgrowth to 200 ng/ml netrin-1 is not further potentiated by GAG addition since all available DCC will already be bound. Further, the dose dependence of heparin or GAG enhanced axon outgrowth followed a bell-shaped curve, with inhibition of axon outgrowth at the highest concentrations of applied GAGs. This is consistent with GAG dependent ligand multimerization, as the surplus of GAG binding sites at high concentrations will result in single netrin-1 molecules being bound by single GAG chains, thereby inhibiting ligand multimerization and function. This model of GAGs binding netrin-1 to promote function is similar to how HSPGs cross-link monomeric FGF to multimerize and activate FGFR signaling (Ornitz et al., 1992; Spivak-Kroizman et al., 1994; Yayon et al., 1991).

Activation of DCC signaling requires netrin-1 binding and DCC multimerization (Stein et al., 2001). Netrin-1 binds to DCC through amino acid motifs in domains VI and V, however, in two different studies investigating the structure of netrin-1 binding to DCC, the netrin-1 C-domain was excluded from the crystal structure (Finci et al., 2014; K. Xu et al., 2014). Curiously, these crystal structures indicate that during crystal formation netrin-1 VI-V is sufficient to dimerize DCC. However, previous work demonstrated that the netrin-1 VI-V peptide failed to multimerize DCC in an *in vitro* binding assay (Bin et al., 2013). Further, netrin-1 VI-V was unable to oligomerize DCC in HEK293T cells as measured by image cross correlation spectroscopy (ICCS) and total internal reflection microscopy (Gopal et al., 2016). Functionally, the netrin-1 VI-V peptide maintains chemorepellent but not the chemoattractive activities of full-length netrin-1, suggesting that the monomeric netrin-1 VI-V peptide is

sufficient to activate the UNC-5 homologues, but unable to activate DCC, in spite of the capacity of VI-V to bind DCC (Keino-Masu et al., 1996; Leonardo et al., 1997). While the netrin-1 VI-V peptide alone does not induce commissural axon outgrowth in E13 dorsal spinal explants (Figure 5.5B), a VI-V-Fc protein chimera, which dimerizes netrin-1 VI-V and thereby cross links DCC, evokes levels of commissural axon outgrowth similar to full-length netrin-1 (Keino-Masu et al., 1996). These findings support the conclusion that multimerization of both netrin-1 and DCC are required to activate chemoattraction and our findings reveal the critical importance of the netrin-1 C-domain in multimerizing netrin-1 to support chemoattractive signaling (Figure 5.9).

V.iii. Structural specificity of GAG function

The capacity of HSPGs to potentiate netrin-1 axon outgrowth is not simply the result of pairing netrin with a negatively charged polymer. The GAG binding sequence in netrin-1 consists of a high concentration of positively charged amino acids and we speculated that other negatively charged polymers would be capable of binding and cross-linking netrin-1. In contrast, we found that sulfonated polystyrene did not potentiate netrin-1 function while sulfated β-cyclodextrin, a known heparin mimic, did potentiate netrin-1 induced axon outgrowth, revealing specificity of GAG chain function. While both these molecules are unbranched, negatively charged, and rich in sulfate ions, their structure is quite different from one another. Sulfonated polystyrene is composed of a rigid carbon backbone with sulfonated aromatic rings as side groups, whereas sulfated β-cyclodextrin consists of hexamide sugar molecules linked as a relatively flexible polymer chain (Figure 5.5C). The flexibility of the carbon ring structure within the GAG chain facilitates GAG-protein interactions and it has been argued that a change in conformation is required for GAGs to bind certain proteins (Gandhi & Mancera, 2008). The aromatic rings in sulfonated polystyrene would not be able to undergo the conformational

changes required for GAG protein binding. Additionally, sulfated is different from sulfonated. Sulfated molecules are based on a carbon – oxygen – sulfur bond while in sulfonates the sulfur is bound directly to the carbon atom. This difference in bond structure effects the stability of the molecule as the sulfur – oxygen bond is more readily hydrolyzed and could therefore alter its ability to bind netrin-1 (Knaggs & Nepras, 2005). These results indicate that while charge is likely an important factor in GAG netrin-1 binding, additional structural features contribute to the specificity of functional netrin-1/GAG binding.

The glypican family of HSPGs mediates netrin-1 induced axon guidance in *C. elegans* via binding of the glypican core protein to the netrin-1 receptor UNC40 (DCC) (Blanchette et al., 2015). In mammals there are 6 members of the glypican protein family, glypican 1-6, all of which are expressed in the mammalian nervous system. Glypican-1 and -2 proteins exhibit remarkably similar distributions compared to netrin-1 in the developing spinal cord (Figure 5.7H) (Ivins et al., 1997). Our functional studies indicate that all 6 glypicans have the capacity to increase netrin-1 induced axon outgrowth in response to submaximal levels of netrin-1. We also examined the truncated netrin-1 VI-V peptide in combination with glypican 5. Despite glypican 5 showing a particularly high degree of binding to the truncated VI-V protein there was no increase in commissural neuron outgrowth. We propose that this is due to competition between the GAG chain and DCC as both bind the same sequence in domain V of netrin-1.

V.iv. Netrin Synergizing Activity

The initial purification of netrins also revealed a secondary membrane associated factor, termed netrin synergizing activity (NSA), that has a significant impact on netrin-1 induced axon outgrowth (Serafini et al., 1994). In functional assays, netrin-1 purified from embryonic chick brain exhibited substantially reduced commissural axon outgrowth promoting activity from E11

rat dorsal spinal cord explants compared to E13 rat dorsal spinal cord explants. During the purification protocol, netrin-1 was retained by a heparin column, and the column flow through contained no axon outgrowth promoting activity. Remarkably, re-mixing the inactive column flow through with the eluent, or with purified netrin-1 protein, enhanced axon outgrowth from E11 rat spinal cord explants, while having no significant effect on outgrowth from E13 explants (Serafini et al., 1994). The identity of NSA is still a mystery, yet, because heparin can bind strongly to netrin-1, HSPGs have been suggested as candidates to be NSA (Kappler et al., 2000; Serafini et al., 1994). However, subsequent studies have provided evidence against this, demonstrating that the NSA is a heparin binding protein and not an HSPG itself, possibly a metalloproteinase (Galko & Tessier-Lavigne, 2000). In agreement, several of our findings suggest that a glypican is unlikely to be the NSA. First, the functional assays carried out here, demonstrating that inclusion of a glypican strongly enhances netrin-1 induced axon outgrowth, utilized E13 rat dorsal spinal cord explants, on which NSA exerted little to no effect (Serafini et al., 1994). Additionally, partial enrichment and characterization of NSA supports a molecular weight between 25-35 kDa (Galko & Tessier-Lavigne, 2000), while glypican core proteins are closer to 65kDa, and glycosylated glypicans are much larger. Although our findings indicate that HSPGs strongly facilitate netrin-1 function, we conclude that NSA is unlikely to be a glypican family member.

V.v. Conserved heparin binding function of the NTR domain

The netrin-1 C-domain is the founding member of the NTR domain family. Our findings concur with a body of literature demonstrating that HSPGs potentiate protein function through NTR domain binding. Procollagen-protinase enhancers (PCPE) contain a C-terminal NTR domain that interacts with heparin. Bekhouche et al., (2010) demonstrated that PCPE-1 binds to both heparin

and BMP-1 through NTR domain interactions and while PCPE-1 can stimulate BMP-1 function without heparin, the effect is significantly enhanced when heparin is also bound to PCPE-1 in *vitro* (Bekhouche et al., 2010).

The Amyloid precursor protein (APP) has been proposed to regulate netrin-1 mediated commissural axon outgrowth (Rama et al., 2012). Interestingly, APP must be bound to an HSPG for it to promote neurite outgrowth (Small et al., 1994). In the presence of β-D-xyloside, an inhibitor of protein glycanation, APP induced neurite outgrowth was severely inhibited demonstrating the requirement for GAG chains (Williamson et al., 1996). These findings raise the possibility that DCC, netrin-1, APP and a proteoglycan, such as glypican, may form a complex that is required for commissural axon extension in the embryonic spinal cord.

Axon guidance cues also appear to interact with proteoglycans in the adult CNS. Semaphorin 3A directs axon guidance in the developing nervous system, and has recently been shown to be a component of perineuronal nets (PNNs), GAG rich structures in the brain that influence critical period closure during maturation as well as learning and memory in adults (de Winter et al., 2016; Dick et al., 2013; Vo et al., 2013). Netrin-1 has recently been found to regulate synapse formation during maturation and synaptic plasticity in the adult mammalian brain raising the interesting possibility that netrin-1 may also interact with GAGs in the adult CNS to regulate synapse function (Glasgow et al., 2018; Goldman et al., 2013).

Netrin-1 and HSPGs are widely expressed throughout the nervous system both in the developing animal and in the adult and both execute a wide range of functions. Understanding the interaction between netrin-1 and GAGs in the embryonic spinal cord will provide important insight into how these two families of proteins interact and how they may function in other contexts.

VI. FIGURES

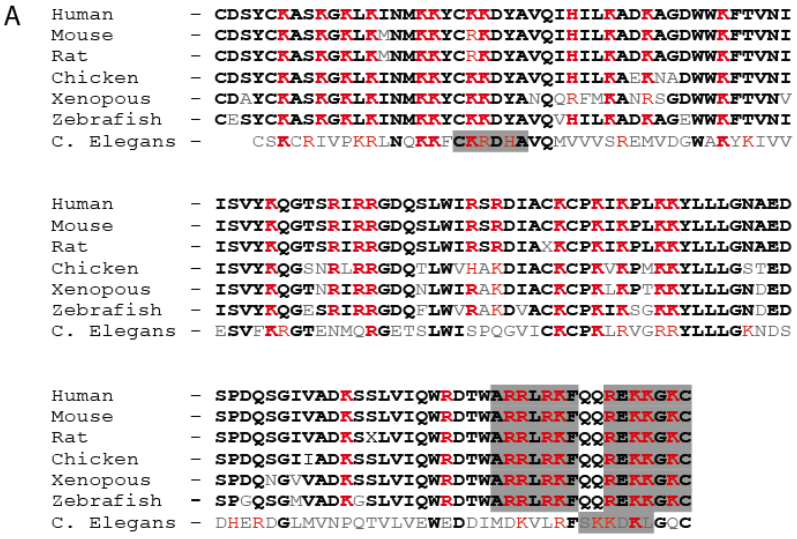
A
Human
Mouse
Rat
Chicken
Xenopous
Zebrafish
C. Elegans

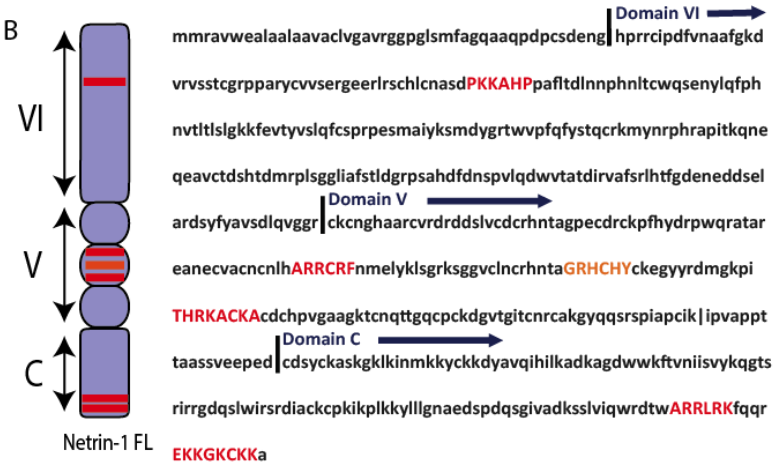
B
VI
V
C
Netrin-1 FL
Domain VI
Domain V
Domain C

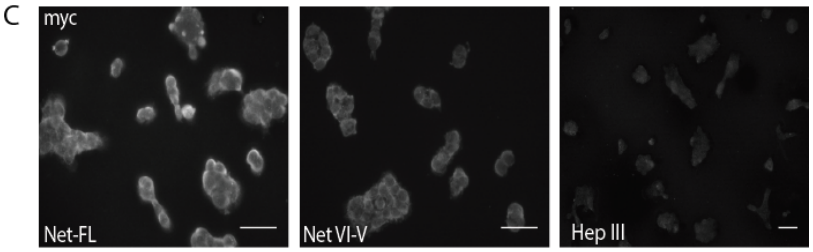
C
myc
Net-FL
Net VI-V
Hep III

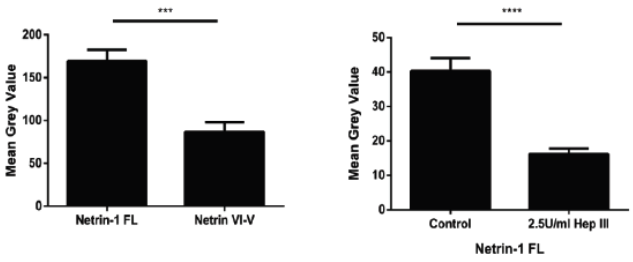
Mean Grey Value
Netrin-1 FL
Netrin VI-V
Control
2.5U/ml Hep III
Netrin-1 FL

Figure 5.1: Netrin-1 C-domain Alignment and HEK293 cell binding A) Alignment of the netrin c-domain from various species. **Bold** indicates a conserved amino acid to human, red a basic amino acid, and grey background a potential GAG binding site. **B)** Schematic showing the domain structure of human netrin-1 protein and the amino acid sequence (uniprot.org). Matches for consensus GAG binding sequences are highlighted in red capital letters within the amino acid sequence and represented as red bars in the schematic. An additional possible GAG binding sequence is highlighted in orange. This sequence fits the consensus rules for GAG binding, but the basic residues are histidine rather than lysine and arginine which is a rarely seen in GAG binding. **C)** Cell surface binding of netrin-1 to HEK293T cells. Left image shows full length netrin-1-myc binding, middle image shows netrin VI-V myc binding, and right image shows full length netrin-1-myc binding to the surface of HEK293T cells treated with 2.5U/ml heparinase III (scale bars = 50um). Quantification of the mean grey value is shown below (unpaired two tailed t-test, $p<0.002$, n=3 coverslips with 3 measures per coverslip).

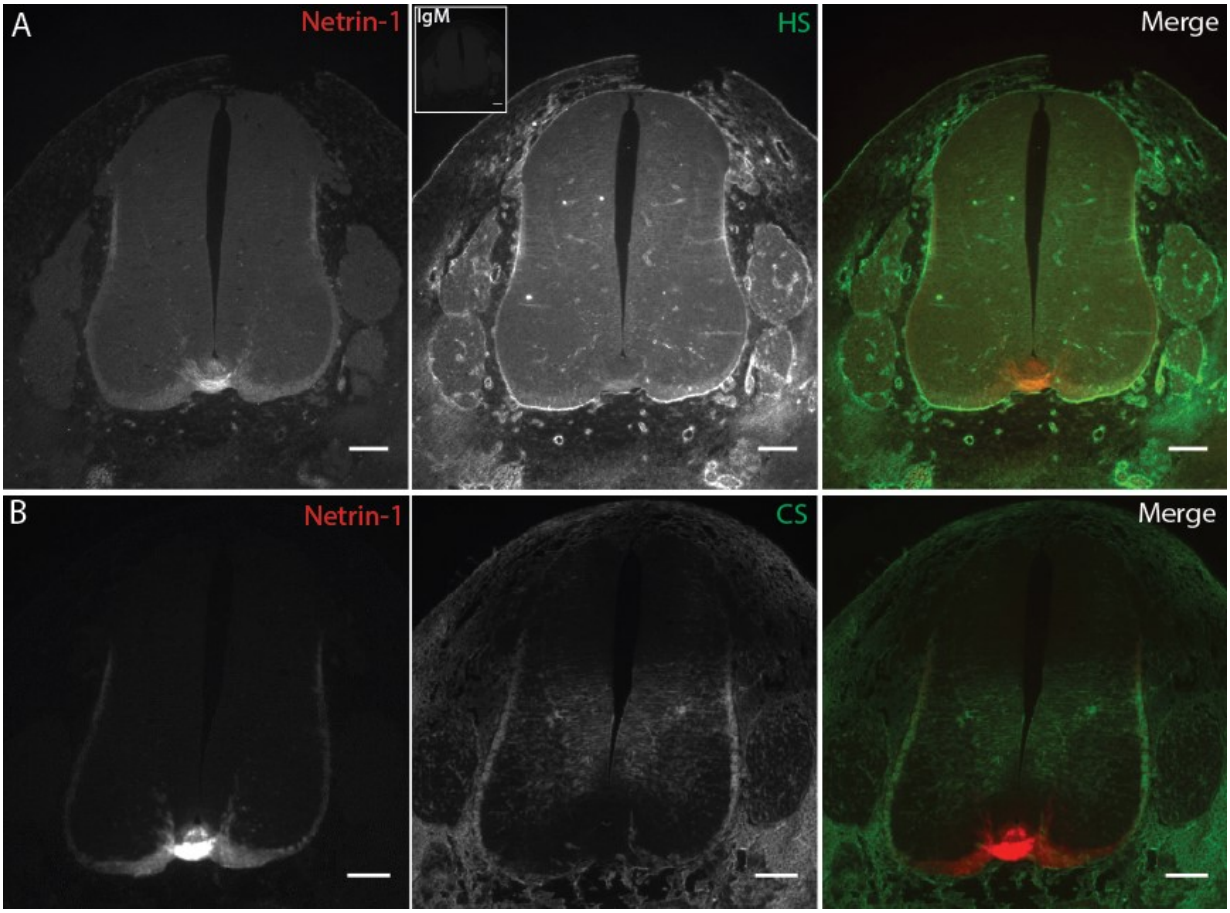

Figure 5.2: Distribution of HS and CS in rat E13/14 rat spinal cord. **A)** Sections stained for netrin-1 (red) and HS (green). IgM Secondary antibody alone is shown inlaid on HS stain. **B)** Sections stained for netrin-1 (red) and CS (green, scale bars = 100um).

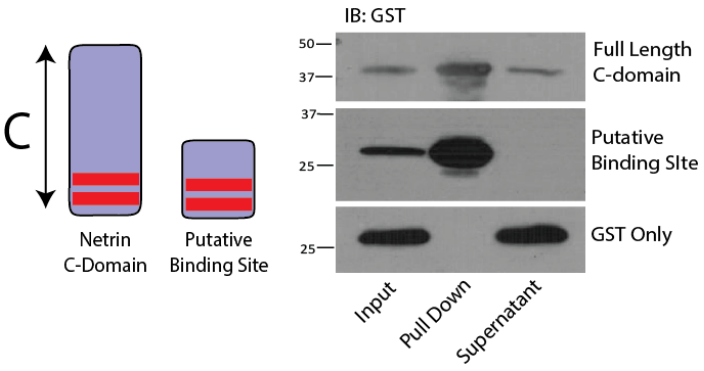

Figure 5.3: Heparin batch binding assay. Schematic illustrating chick netrin-1 C-domain deletion constructs. The "netrin C-domain" construct corresponds to the full-length C-domain and the "putative binding site" construct is composed of the 20 most C-terminal amino acids of the C-domain. Both constructs are GST tagged. Full length C-domain, putative binding site construct, or GST alone were incubated with heparin coated beads in a heparin batch binding assay. Input, heparin pull down, and the supernatant were analyzed by western blot. Membranes were immunoblotted with a GST antibody to detect the tagged constructs. Both netrin-1 C-domain and putative binding site constructs bound heparin coated beads while GST was found in the supernatant only indicating that the 20 amino acid netrin-1 putative GAG binding site in the C-domain is sufficient to bind heparin coated beads.

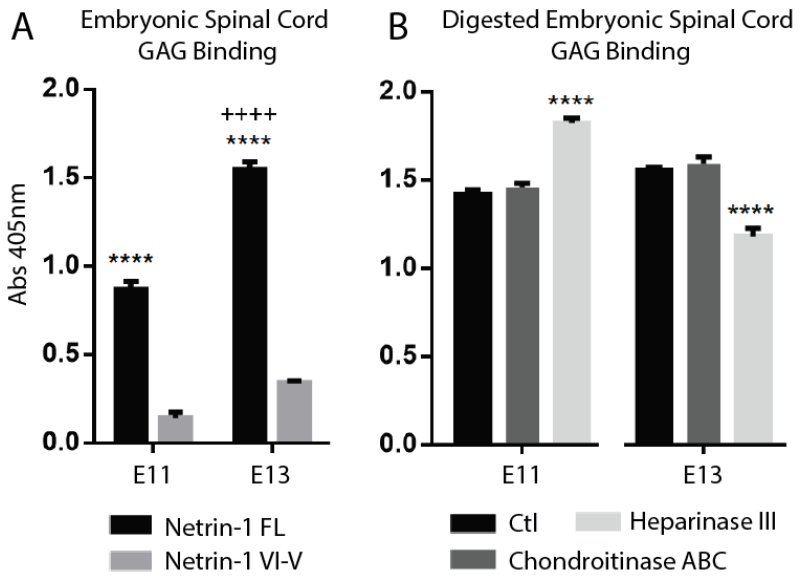

Figure 5.4: ELISA assay of netrin-1 binding to GAGs isolated from embryonic rat CNS. **A)** GAGs isolated from E11 spinal cord and E13 rat spinal cord binding to full length netrin-1 and netrin VI-V. In all samples full length netrin-1 binding was significantly higher than netrin VI-V binding. Binding of full-length netrin-1 to E13 spinal cord was significantly higher than E11 spinal cord. Netrin VI-V binding is not significantly different across samples (ordinary two-way ANOVA with Tukey test, n=3, $P<0.0001$. * compared to VI-V, + compared to E11). **B)** GAGs isolated from E11 and E13 rat spinal cord were digested with heparinase III or chondroitinase ABC to specifically removes one family of GAGs prior to analyzing full length netrin-1 binding. Chondroitinase ABC treated samples are not significantly different from undigested control samples. Heparinase III treated samples are significantly higher in E11 spinal cord and significantly lower in E13 spinal cord (two-way ANOVA with Tukey test n=3, $P<0.0001$. * compared to control).

A

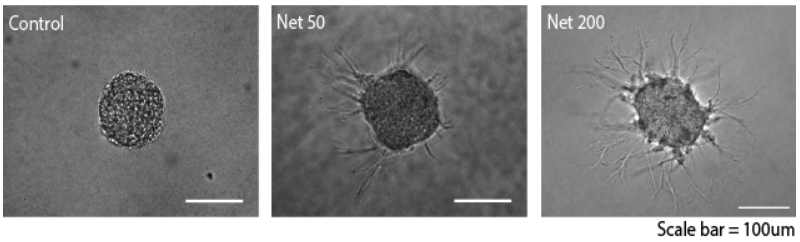
Control
Net 50
Net 200
Scale bar = 100um

B

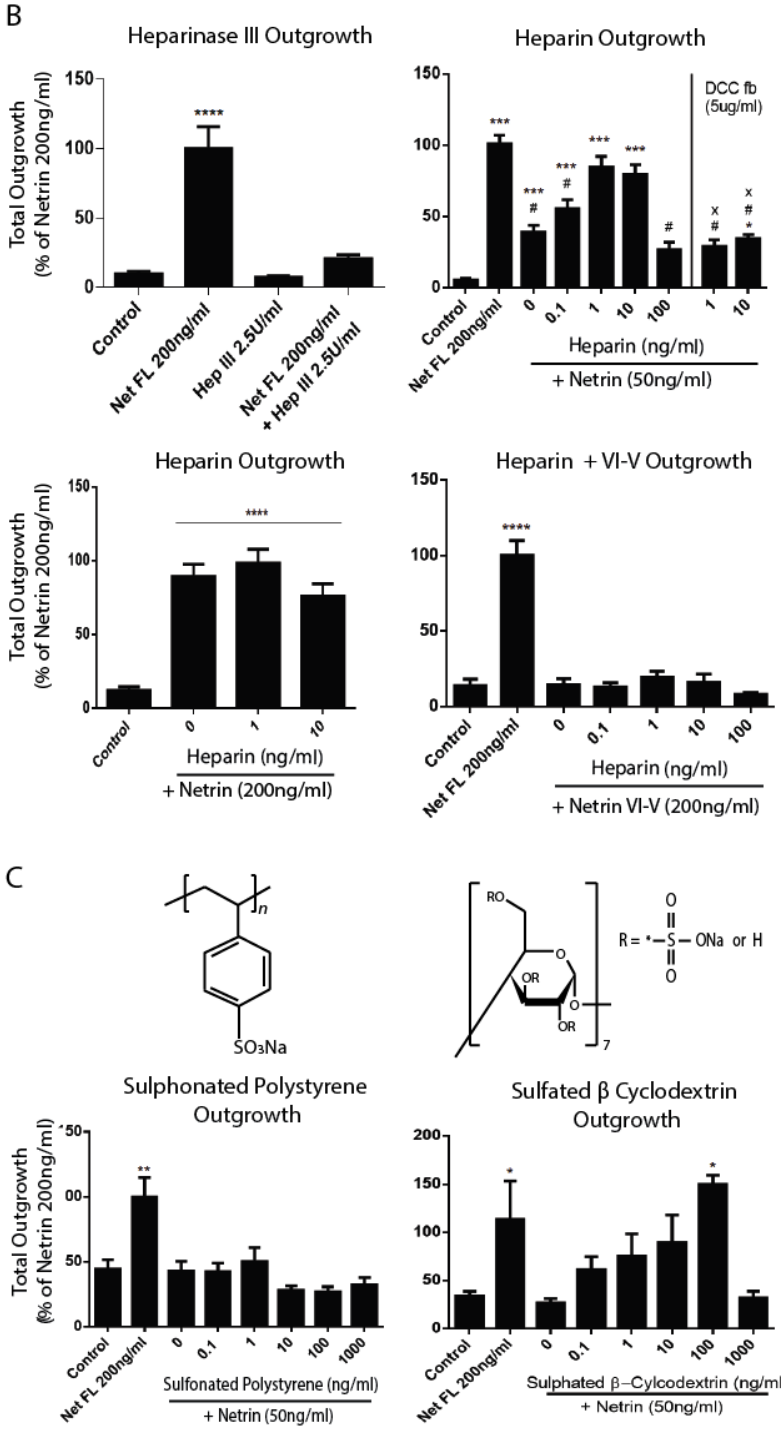
Heparinase III Outgrowth
Total Outgrowth (% of Netrin 200ng/ml)
Control
Net FL 200ng/ml
Hep III 2.5U/ml
Net FL 200ng/ml + Hep III 2.5U/ml
Heparin Outgrowth
DCC fb (5ug/ml)
Heparin (ng/ml)
+ Netrin (50ng/ml)
Heparin Outgrowth
Heparin (ng/ml)
+ Netrin (200ng/ml)
Heparin + VI-V Outgrowth
Heparin (ng/ml)
+ Netrin VI-V (200ng/ml)

C

SO3Na
RO
OR
R = -S-ONa or H
Sulphonated Polystyrene Outgrowth
Total Outgrowth (% of Netrin 200ng/ml)
Sulfonated Polystyrene (ng/ml)
+ Netrin (50ng/ml)
Sulfated β Cyclodextrin Outgrowth
Sulphated β–Cylcodextrin (ng/ml)
+ Netrin (50ng/ml)

Figure 5.5: Dorsal spinal explant assay with heparin and synthetic polymers. A) Examples of dorsal spinal explants. Outgrowth shown in control, 50ng/ml netrin-1, and 200ng/ml netrin-1 conditions. Explants in all experiments looked similar to the ones shown but with varying degrees outgrowth depending on treatment condition. **B)** Top left: Heparan sulphate is required for netrin-1 induced axon outgrowth. Degradation of HS in dorsal spinal explants using 2.5U/ml of heparinase III completely abolishes netrin-1 induced axon outgrowth using 200ng/ml of netrin-1. Top right: Heparin potentiates netrin-1 induced axon outgrowth using 50ng/ml concentrations of netrin-1. This effect is blocked using a DCC function blocking antibody (DCC fb). Bottom left: Heparin has no effect on netrin-1 induced outgrowth at 200ng/ml of netrin-1. Bottom right: Netrin VI-V does not induce axonal outgrowth in dorsal spinal explants and addition of heparin has no effect on netrin VI-V outgrowth (*'s represent comparison to ctl, #'s represent comparison to net FL 200ng/ml, x represents comparison to the same conditions without DCC fb antibody. One-way ANOVA, n=3 litters with 4-6 explants per litter. **** $p<0.0001$, #### $p<0.0001$, *** $p<0.001$, * $P<0.05$, # $P<0.05$, x $p<0.05$). **C)** Left: Sulfonated polystyrene has no effect on netrin-1 induced outgrowth in dorsal spinal explants. Sulfonated polystyrene was generated in house with an average molecular weight of 70 KDa and the chemical structure as shown. Addition of sulfonated polystyrene to dorsal explants treated with 50ng/ml netrin-1 had no effect on the total axonal outgrowth. Right: Sulfated β cyclodextrin potentiates netrin-1 induced outgrowth in dorsal spinal explants. Sulfated β cyclodextrin was purchased from Sigma with a sulfation labelling of 12-15 mol per mol of sulfated β cyclodextrin and a chemical structure as shown. Addition of sulfated β cyclodextrin to dorsal explants treated with 50ng/ml netrin-1 potentiated outgrowth in a dose dependent manner. Quantification is

shown in the graphs (one-way ANOVA, n=3 litters with 4-6 explants per litter. ** p<0.01, * P<0.05 compared to control).

A

	Glypican-1	Glypican-2	Glypican-3	Glypican-4	Glypican-5
Glypican-2	41				
Glypican-3	26	23			
Glypican-4	44	42	26		
Glypican-5	27	26	45	28	
Glypican-6	50	45	28	65	28

	Syndecan-1	Syndecan-2	Syndecan-3
Syndecan-2	55		
Syndecan-3	61	64	
Syndecan-4	38	43	73

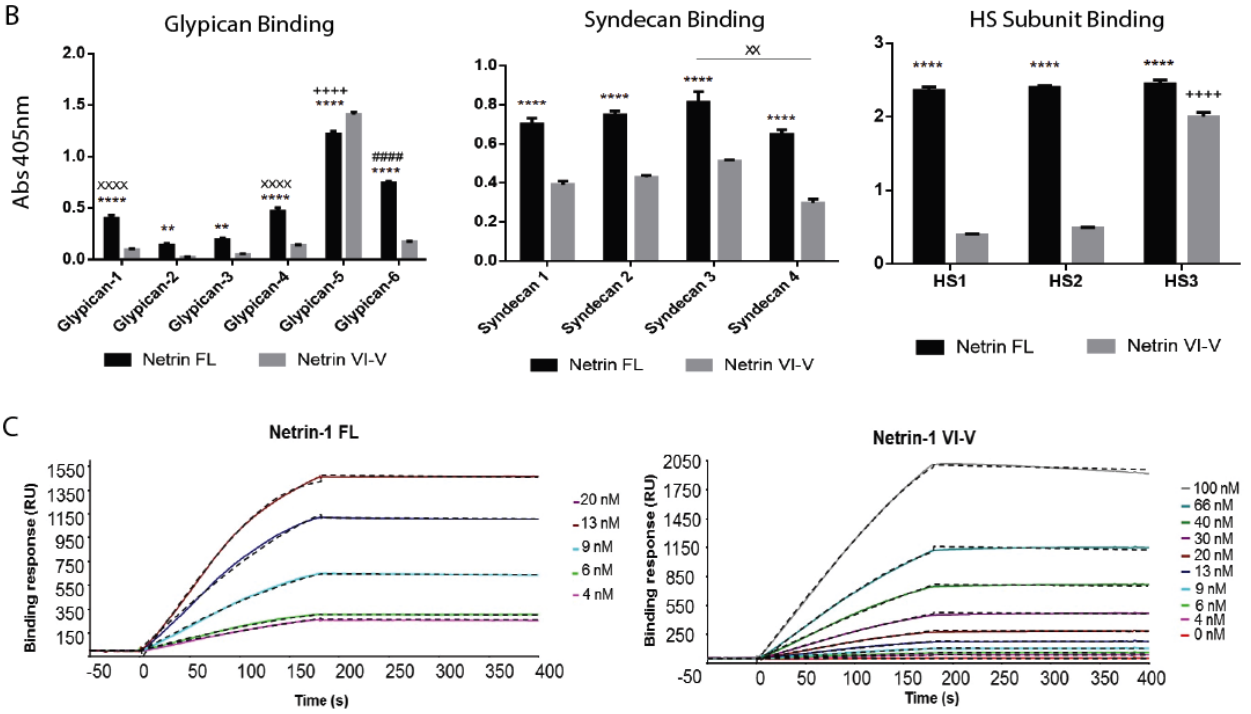

Figure 5.6: Glypican and syndecan ELISA and SPR. A) Protein sequence identity between different members of the glypican and syndecan protein families. All sequences are from homo sapiens and compared using NCBI protein BLAST. **B)** ELISA assay of netrin-1 binding to GAGs. Left: Glypicans 1-4 and 6 have significantly higher binding to full length netrin-1 while glypican 5 has significantly higher binding to netrin VI-V. Glypicans 1 and 4 have significantly higher binding than 2 and 3. Glypican 6 has higher binding than glypicans 1-4 and glypican 5 has the highest binding of all the members (*'s represent comparison between netrin-1 FL and VI-V,

x's represent comparison between glypican 1 and 4 to glypican 2 and 3, # represents comparison of glypican 6 to glypican 1-4, and + represents comparison of glypican 5 to all other glypicans). Middle: all syndecan family members have significantly higher binding to netrin-1 FL over VI-V. Syndecan 3 has significantly higher binding than syndecan 4, and there is no significant difference between other family members (*'s represent comparison between netrin-1 FL and VI-V, x's represent comparison between syndecan 3 and syndecan 4). Right: binding of differentially sulfated HS to netrin-1. HS1 is the least sulfated while HS3 is the most sulfated. In all cases full length netrin-1 has significantly higher binding to HS than netrin VI-V. Highly sulfated HS3 has significantly higher binding to netrin VI-V than the less sulfated HS2 and HS1 (two-way ANOVA with Tukey test, n=3, **** $p<0.0001$, ++++ $p<0.0001$, #### $p<0.0001$, xxxx $p<0.0001$, ** $p<0.01$, xx $p<0.01$). **C)** Surface plasmon resonance measures to determine K_D of full-length netrin-1 and netrin-1 VI-V binding to heavily sulfated HS chains.

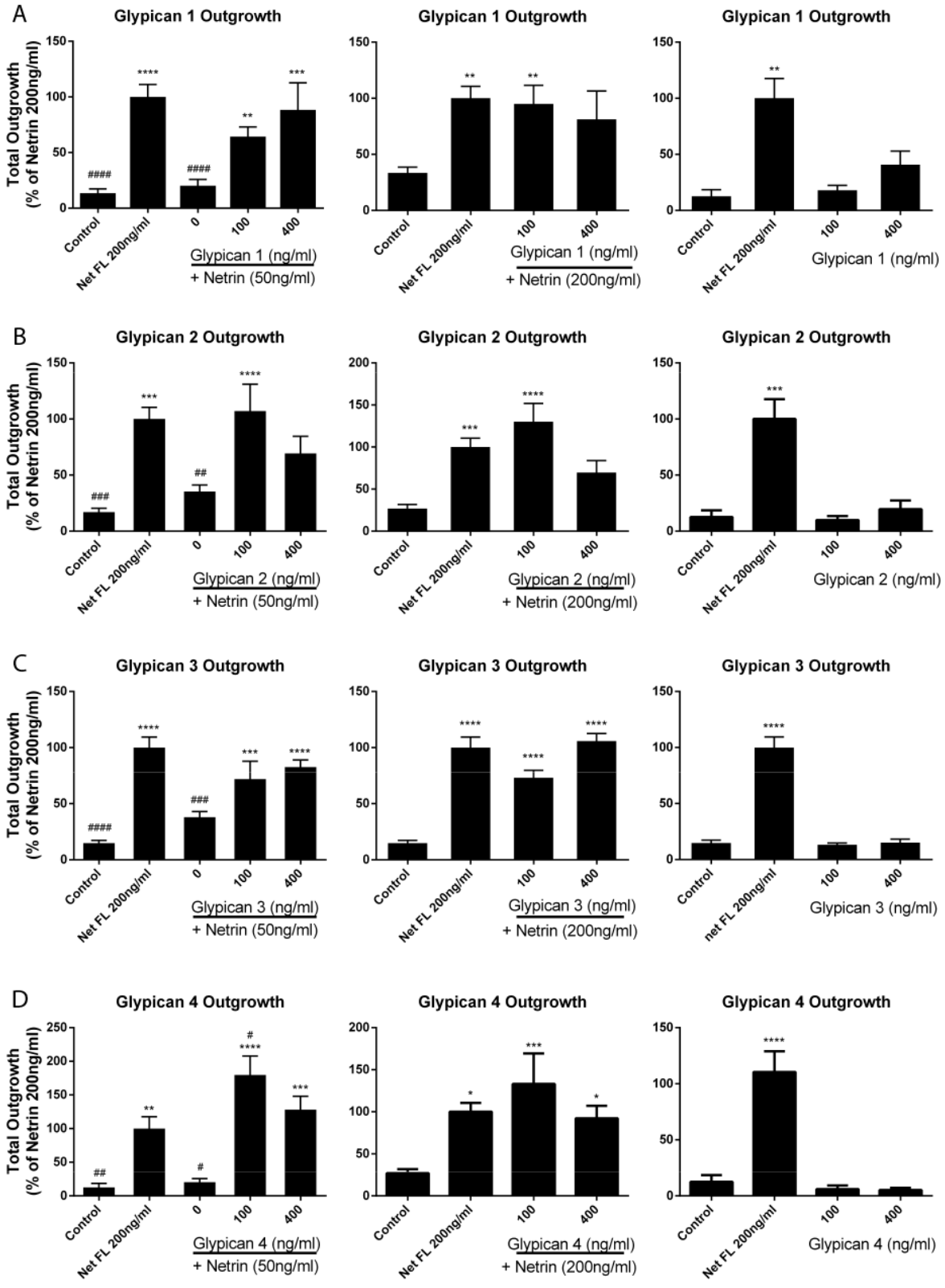
A
Glypican 1 Outgrowth
Total Outgrowth (% of Netrin 200ng/ml)
Control
Net FL 200ng/ml
0
100
400
Glypican 1 (ng/ml)
+ Netrin (50ng/ml)
Glypican 1 Outgrowth
Control
Net FL 200ng/ml
100
400
Glypican 1 (ng/ml)
+ Netrin (200ng/ml)
Glypican 1 Outgrowth
Control
Net FL 200ng/ml
100
400
Glypican 1 (ng/ml)
B
Glypican 2 Outgrowth
Total Outgrowth (% of Netrin 200ng/ml)
Control
Net FL 200ng/ml
0
100
400
Glypican 2 (ng/ml)
+ Netrin (50ng/ml)
Glypican 2 Outgrowth
Control
Net FL 200ng/ml
100
400
Glypican 2 (ng/ml)
+ Netrin (200ng/ml)
Glypican 2 Outgrowth
Control
Net FL 200ng/ml
100
400
Glypican 2 (ng/ml)
C
Glypican 3 Outgrowth
Total Outgrowth (% of Netrin 200ng/ml)
Control
Net FL 200ng/ml
0
100
400
Glypican 3 (ng/ml)
+ Netrin (50ng/ml)
Glypican 3 Outgrowth
Control
Net FL 200ng/ml
100
400
Glypican 3 (ng/ml)
+ Netrin (200ng/ml)
Glypican 3 Outgrowth
Control
net FL 200ng/ml
100
400
Glypican 3 (ng/ml)
D
Glypican 4 Outgrowth
Total Outgrowth (% of Netrin 200ng/ml)
Control
Net FL 200ng/ml
0
100
400
Glypican 4 (ng/ml)
+ Netrin (50ng/ml)
Glypican 4 Outgrowth
Control
Net FL 200ng/ml
100
400
Glypican 4 (ng/ml)
+ Netrin (200ng/ml)
Glypican 4 Outgrowth
Control
Net FL 200ng/ml
100
400
Glypican 4 (ng/ml)

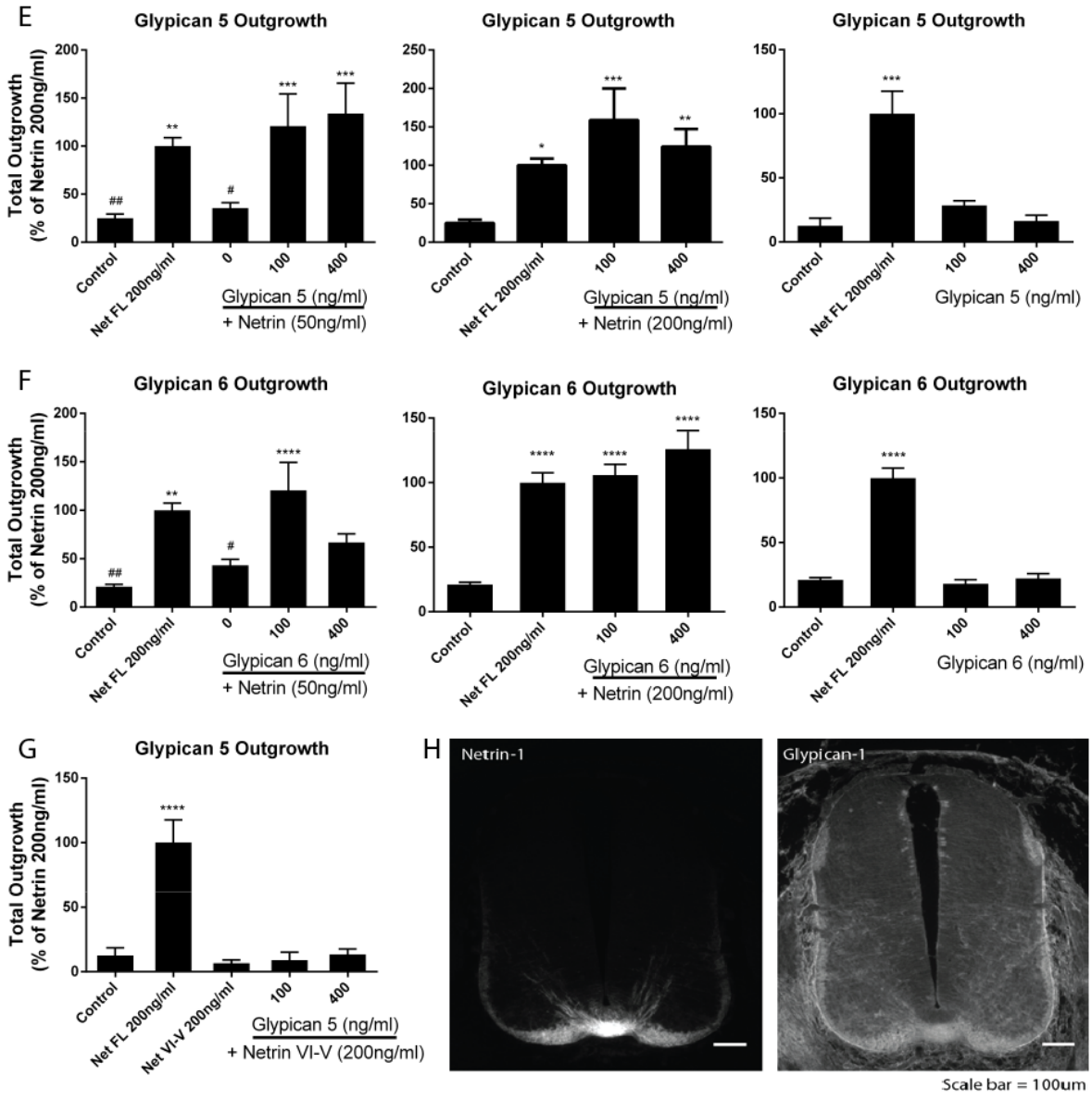

Figure 5.7: Glypican induced axon outgrowth. Left: Axon outgrowth using 50ng/ml netrin-1. Middle: Axon outgrowth using 200ng/ml netrin-1. Right: Axon outgrowth with glypicans alone. **A:** Glypican-1 induced outgrowth. **B:** Glypican-2 induced outgrowth. **C:** Glypican-3 induced outgrowth. **D:** Glypican-4 induced outgrowth. **E:** Glypican-5 induced outgrowth. **F:** Glypican-6 induced outgrowth. **G:** Glypican-5 induced outgrowth with netrin VI-V. * compared to control, # compared to Net FL 200ng/ml for all graphs (one way ANOVA n=3, **** $p<0.0001$, ***

$p<0.001$, , ** $p<0.01$, * $p<0.05$. Same p values for hashtags). **H:** E13 rat spinal cords stained for netrin-1 (left) and glypican-1 (right, scale bar = 100μm).

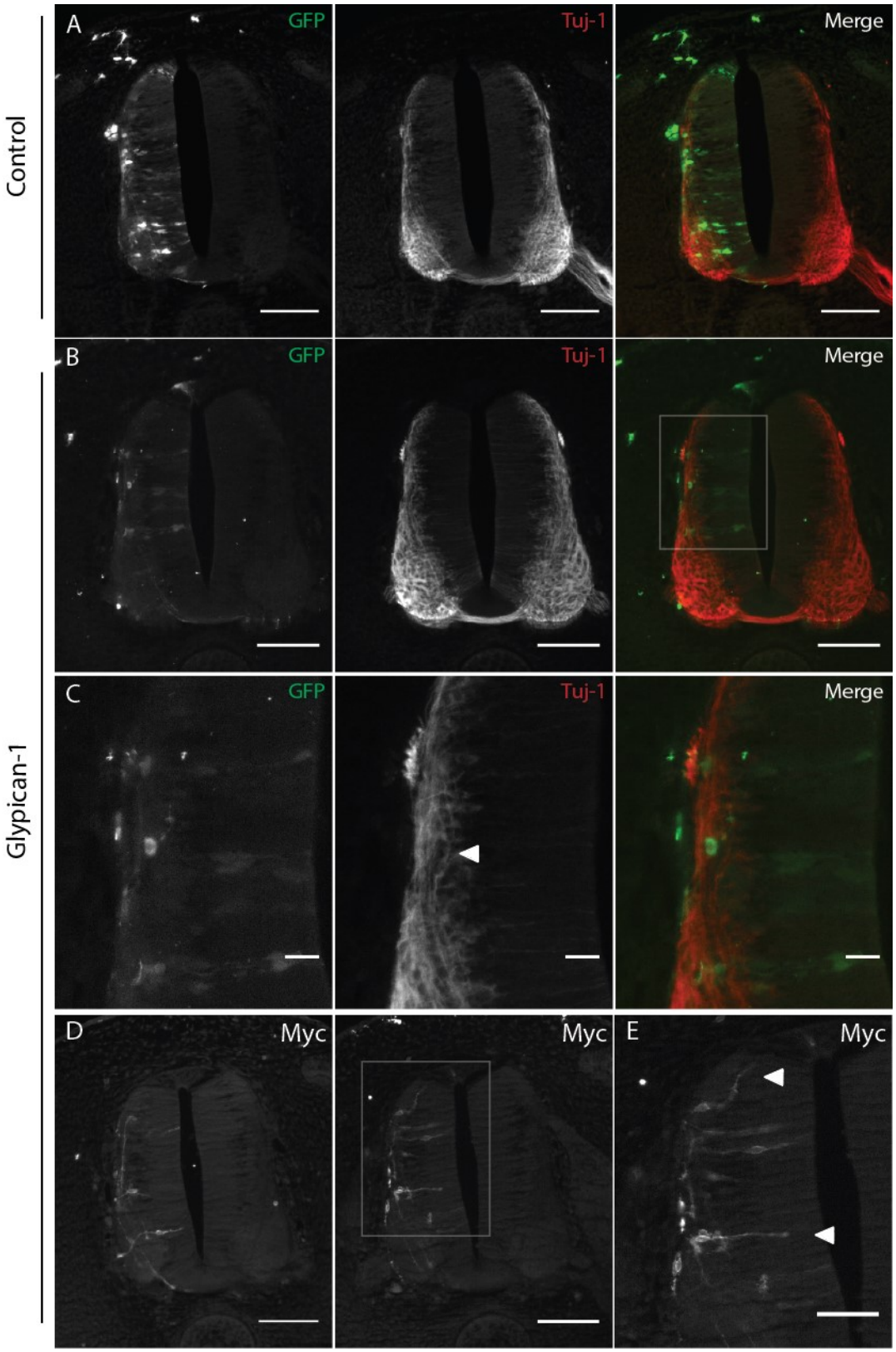
Control
Glypican-1
A
GFP
Tuj-1
Merge
B
GFP
Tuj-1
Merge
C
GFP
Tuj-1
Merge
D
Myc
Myc
E
Myc

Figure 5.8: Glypican-1 electroporated chick spinal cords. **A)** GFP electroporated spinal cords. **B-D)** Myc tagged glypican-1 co-electroporated with GFP. **C)** Enlargement of the area in B indicated by the grey box in the merge image. **E)** Enlargement of the area indicated by the grey box in D (scale bar = 100µm in A, B, &D and 50µm in C & E).

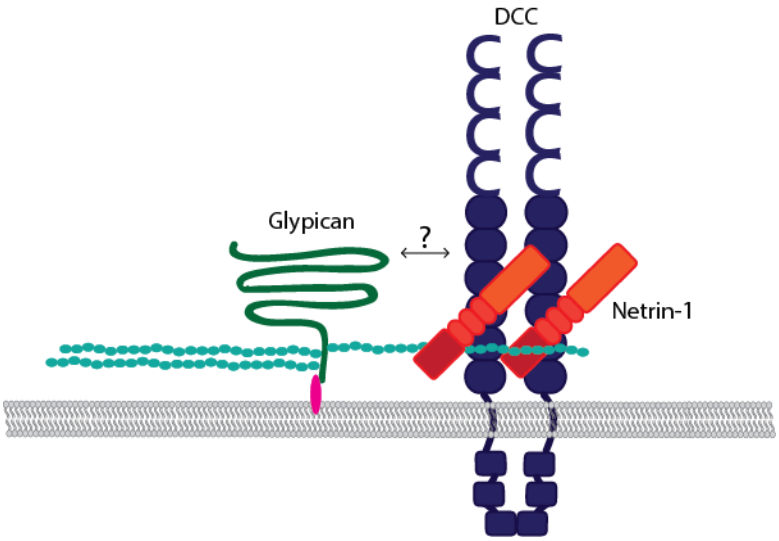

Figure 5.9: Model of HSPG multimerization of netrin-1.

Preface

In the previous chapter we investigated a role for netrin binding to GAGs in the developing spinal cord. As previously discussed, persistent netrin-1 expression in the adult regulates synaptic function (Glasgow et al., 2018; Goldman et al., 2013; Horn et al., 2013). Guidance cues in the adult have also been shown to interact with PNNs, a specialized GAG structure critical for regulating synaptic plasticity (de Winter et al., 2016). In this chapter we show that netrin-1 binds to PNN GAGs through interactions between the netrin-1 C-domain and the CS-E subunit of CSPGs. Netrin-1 binding to CSPG GAGs alters the physical properties of GAG films and may translate to regulation of synaptic plasticity. A manuscript of this chapter is in preparation for publication.

Chapter 6

Netrin-1 is associated with perineuronal nets in the adult rodent brain

Stephanie N. Harris*, Lynda Djerbal[#], Heleen M. van't Spijker[+], Ralf Richter[#], James W. Fawcett[+,Σ], Jessica C.F. Kwok[#,Σ], Timothy E. Kennedy*

*Department of Neurology and Neurosurgery, Montreal Neurological Institute,

McGill University, Montreal, Quebec, Canada, H3A 2B4

[#]School of Biomedical Sciences, University of Leeds, Leeds, United Kingdom

[+]Cambridge Centre for Brain Repair, University of Cambridge, Cambridge, United Kingdom

[Σ] Institute of Experimental Medicine, Czech Academy of Science, Prague, Czechia

I. ABSTRACT

Perineuronal nets (PNNs) are a specialized elaboration of extracellular matrix that forms around a subset of neurons in the adult central nervous system (CNS) and regulates synaptic plasticity. PNNs mainly surround parvalbumin (PV) expressing interneurons, however, recent work has shown that excitatory neurons in the hippocampus may also be surrounded by PNNs. The axon guidance cue netrin-1 has recently been shown to be a key regulator of synaptic plasticity in the hippocampus. Here we show that PNN surrounded neurons in the adult rat neocortex may express netrin-1 and that netrin-1 protein binds to PNN glycosaminoglycans (GAGs). Specifically, netrin-1 is bound most tightly to CS-E, a chondroitin sulfate subunit enriched in PNNs, and that netrin-1 bindings results in the softening of GAG films.

II. INTRODUCTION

Perineuronal nets (PNNs) are a specialized extracellular matrix structure found in the mature brain that surrounds the cell bodies and proximal dendrites of a subset of neurons throughout various brain structures (Bozzelli et al., 2018). PNNs mainly surround fast spiking parvalbumin (PV) positive neurons however, they are not limited to inhibitory interneurons. Subsets of excitatory neurons in the hippocampus and visual cortex are also known to be surrounded by PNNs (Bozzelli et al., 2018; Lensjø et al., 2017). PNNs are composed of the glycosaminoglycan hyaluronan (HA), proteoglycans, tenascins, and link proteins and provide important structural and functional support to neurons (Deepa et al., 2006). Chondroitin sulfate proteoglycans (CSPGs) from the lectican family, HA, tenascin-r, and the link proteins HAPLN 1,2 and 4 are major PNN components and are produced either by the neuron they surround or by nearby glia cells (C. Lander et al., 1997; Maleski & Hockfield, 1997). The precise ratio of the lecticans; aggrecan, versican, brevican, and neurocan, varies depending on neuron type and brain region, which generates heterogeneity among PNN structures (Bozzelli et al., 2018; Deepa et al., 2006; Irvine & Kwok, 2018). Proteoglycans are important co-receptors for many molecules in the CNS and may form a co-receptor complex to facilitate ligand/receptor function. CSPGs in PNNs regulate the function of various proteins by acting as an intermediary between proteins and neurons surrounded by PNNs. In this way, PNNs can create a physical barrier blocking certain proteins from the neuron or, alternatively, locally concentrating proteins in proximity to neurons (Frischknecht et al., 2009; van 't Spijker & Kwok, 2017). Proteoglycans also bind and regulate the function of many developmental cues during embryogenesis (Holt & Dickson, 2005). Interestingly, these developmental cues often continue to be expressed in the adult animal and mediate a variety of functions in the adult CNS (Bouzioukh et al., 2006; Glasgow et al., 2018;

Goldman et al., 2013; Horn et al., 2013; Manitt et al., 2009). One example of this is the repellent axon guidance cue semaphorin 3a (Sema3a) that has been shown to be a constituent of PNNs and is localized to the PNN by binding CSPGs, specifically binding via CS-E residues (Dick et al., 2013; Vo et al., 2013). These findings led us to question if other developmental axon guidance cues, specifically netrin-1, may also be localized to the PNN. Netrin-1 is a bi-functional axon guidance cue that is essential for normal neural development (Bin et al., 2015; Serafini et al., 1996). Following embryogenesis, netrin-1 is widely expressed at a relatively high level by neocortical neurons during post-natal maturation, and neuronal expression of netrin-1 continues in the adult nervous system, influencing synapse formation and function (Glasgow et al., 2018; Goldman et al., 2013; Horn et al., 2013). In many biological contexts, netrins and semaphorins function together, as a 'ying and yang', appearing to exert opposing functions that are thought to generate a balance point within the system. We hypothesised that this may be the case in the PNN. Here we demonstrate that PNNs surround netrin-1 positive neurons in the adult rat brain and provide evidence for an interaction between netrin-1 and CSPGs in the PNN.

III. METHODS

III.i. Animals

All procedures were performed in accordance with the Canadian Council on Animal Care guidelines for the use of animals in research and approved by the Montreal Neurological Institute Animal Care Committee and the McGill Animal Compliance Office. Sprague-Dawley rats were obtained from Charles Rivers Laboratory (St-Constant, QC, Canada).

III.ii. Antibodies and reagents

Antibodies: Rabbit anti Netrin-1 (abcam, EPR5428), Goat anti Sema3a (C17) (Santa Cruz, SC-1146), goat anti HAPLN1 (R&D Systems, AF2608), rabbit anti myc (abcam, ab9106), goat anti semaphorin 3a C-17 (Santa Cruz Biotechnology, sc-1146), peroxidase-conjugated donkey anti goat IgG (Jackson Immuno Research, 705-035-147), peroxidase conjugated donkey anti rabbit (Jackson Immuno Research, 711-035-152), alexa fluor donkey anti rabbit (molecular probes, A31572, A21206, & A31573), alexa fluor donkey anti goat (molecular probes, A21432), wisteria floribunda agglutinin (WFA) (Sigma, L1516-2MG), streptavidin alex fluor (molecular probes, S11223)

Reagents: Chondroitinase ABC (Sigma, C3667-5UN), Heparinase III (Sigma, H8891-5UN), heparitinase I (EC 4.2.2.7) and III (EC 4.2.2.8) from *Flavobacterium heparinum* (Sigma), Hyaluronidase (EC 4.2.2.1) from *Streptomyces hyalurolyticus* (Sigma), EndoHf (NEB, P0703S), CS subunits (Seikagaku Corporation, Tokyo, Japan).

III.iii. Immunohistochemistry

Adult rat cortices were dissected and fixed by submersion in Carnoy's solution (60% ethanol, 10% acetic acid, 30% chloroform) for 2 hr at rt. Cortices were then washed twice with 100% ethanol for 20 min and cleared in toluene for 1 hr before being embedded in paraffin (Fisher Scientific). Sections, 10 μm thick, were cut with a microtome and mounted on SuperFrost Plus Slides (Fisher Scientific). Tissue sections on slides were dewaxed and rehydrated prior to staining as follows. Excess wax was removed by melting in an oven at 50^{o} C. Sections were then moved through a series of Xylene, 100% ethanol, 95% ethanol, 70% ethanol, and rehydrated in PBS, for 2 x 3 min in each solution.

Slides were washed in TBS with 0.2% Triton-X 100 and then treated for antigen retrieval by boiling in 10 mM citrate buffer at pH 6.0 for 20 min in a microwave oven, as described (Kennedy et al., 2006). Slides were cooled in citrate buffer for an additional 15 min before being washed 2 x 5 min in TBS. Slides were then blocked and permeabilized in 0.2% Triton-X 100 and 5% heat inactivated calf serum in TBS. Primary antibodies were diluted in a buffer of 0.2% Triton-X 100 and 5% heat inactivated calf serum in TBS and incubated overnight at 4^{o} C. Sections were then washed in TBS for 3 x 10 min with rocking. Slides were then incubated with WFA for 1 hr and then washed 3 x 10 min in TBS prior to secondary antibody. Secondary antibodies were diluted in 0.2% Triton-X 100 and 5% heat inactivated calf serum in TBS for 1 hr at rt and then washed 3 x 10 min in TBS. Slides were rinsed once in water and cover slipped using Fluoro-Gel with tris buffer (Electron Microscopy Sciences).

III.iv. Biochemical fractionation of whole brain

Fractionation of the glycan content in whole brain was carried out as described (Deepa et al., 2006; Foscarin et al., 2017). Briefly, adult rat brains were homogenized and centrifuged through a series of buffers. Brains were homogenized in buffer 1 and spun down at 15000 rpm at 4^{o} C for 30 min. The supernatant was collected, and the pellet re-extracted with the same buffer two more times. The procedure was repeated for three extractions with each buffer and supernatants for each fraction pooled together. Buffer 1: 50 mM TBS pH 7.0 with protease inhibitors. Buffer 2: buffer 1 plus 0.5% Triton X-100. Buffer 3: buffer 2 plus 1 M NaCl. Buffer 4: Buffer 2 plus 6 M urea.

III.v. Isolation of glycans from fractions

Whole brains were dissected from adult Sprague Dawley rats in cold HBSS with calcium and magnesium (Thermo Fisher). Briefly, tissue was homogenized into fractions as described above

and dialyzed against PBS. Pronase (Roche #11459643001) was then added to the sample at a weight ratio of 1 mg of enzyme for every 100 mg of sample and incubated overnight at 37^{o} C. The sample was centrifuged at 13793 RCF for 15 min at 4^{o} C after which the supernatant was collected and cooled on ice. Ice cold trichloroacetic acid (TCA) was added to a final concentration of 5% and samples kept on ice for 1 hr. Samples were centrifuged at 8161 x RCF for 30 min at 4^{o} C, the supernatant collected, and the pellet then washed twice with 5% ice cold TCA. All supernatants were pooled and washed 5 times with diethyl ether. Following ether evaporation, samples were neutralized with sodium bicarbonate to pH 7.0-7.5. Sodium acetate was then added to a final concentration of 5% w/v. Ice cold ethanol was then added to a final concentration of 75% ethanol in the sample and kept overnight at 4^{o} C. Samples were then spun at 735 x RCF for 15 min at 4^{o} C. Supernatants were discarded, and pellets washed twice with ice cold 100% ethanol. Pellets were then dried at rt and dissolved in water.

Glycan concentrations were measured using a cetylpyridinium chloride (CPC) turbidimetry assay. Samples were mixed 1:1 with a solution of 0.05% CPC and 33.25 mM $MgCl_2$. The absorbance of the resulting mixture was read at 405 nm and compared to a standard curve to determine final glycan concentration.

III.vi. Biotinylation of isolated GAGs

One μg of isolated glycans were biotinylated using 0.25 mM EZ-link hydrazide biotins (Thermo Fisher Scientific) in dimethyl sulfoxide (DMSO) and 0.25 mg/ml 1-Ethyl-3-(3-dimethylaminopropyl)carbodiimide (EDC) (Thermo Fisher Scientific) in 0.1 M 2-(N-morpholino)-ethane sulfonic acid (MES) at pH 5.5. Samples were protected from light and rotated for 16 hr at rt. Following biotinylation, residual chemicals and biotin were removed by dialysis with 3.5 kDa molecular weight cut-off dialysis cassettes (Thermo Fisher Scientific),

against 3 L of PBS at 4° C for 16 hr. Samples were then removed from the cassettes and stored at -20° C at a final concentration of 0.02 μg/μl. The degree of biotinylation was determined using a biotin quantification kit (Vector Labs), according to the manufacturer's instruction.

III.vii. GAG ELISA Assay

Full length netrin-1 and netrin-1 VI-V proteins were generated from constitutively expressing HEK293T cells as described (Kennedy et al., 2006). A high bind 96 well plate (Greiner) was coated with protein at a concentration of 10 μg/ml in PBS without potassium (PBS-K) overnight at 4° C. The plate was washed 3 times with PBS-K with 0.1% Triton-X 100 and then blocked with 10% bovine serum albumin (BSA) for 1 hr at rt. The plate was then washed again as above and biotinylated GAGs, 0.8 ng/μl, added to each well for 1 hr at rt. The plates were again washed as before and a 1:1000 dilution of streptavidin alkaline phosphatase (ab 136224, abcam) added to the wells for 1 hr at rt. The wells were then washed as before and PNPP (Thermo Scientific) added to each well. Plates were incubated for 30 min and absorbance read at 405 nm using a spectrophotometer (Biorad).

III.viii. Western blot analysis

Proteins were separated on an 8% polyacrylamide gel and then transferred by electroblotting onto a nitrocellulose membrane using a 350 mA current for 1 hr and 15 min. Nitrocellulose membrane was blocked in 5% skim milk powder or 3% bovine serum albumin (BSA), depending on the primary antibody specifications, in TBST for 1 hr. Primary antibodies were diluted in the blocking buffer and incubated at 4° C overnight. Membranes were then washed in blocking buffer 3 x 10 min. Secondary antibodies were diluted in blocking buffer and incubated for 1 hr at

rt. Membranes were then washed 2 x 10 min in TBST and 2 x 10 min in TBS. The membrane was then incubated with Western Lightning ECL pro (Perkin-Elmer Inc.) and exposed to film.

III.ix. Surface plasmon resonance

Surface plasmon resonance (SPR) was carried out using Biacore 3000 and Biacore T200 instruments (GE Healthcare) and CM4 sensor chips (GE Healthcare) that were generated as described (Djerbal et al., 2019). Briefly, sensor chips were coated with biotinylated CS-E or CS-D at a level of ~60 RU or left untreated as a control. Prior to use, chips were injected with HBS buffer containing 2 M NaCl and then washed with HBS-P buffer (10 mM HEPES, 0.15 M NaCl, 0.05% P20, pH 7.4). A range of netrin-1 full length and netrin-1 VI-V concentrations between 0 nM and 100 nM were injected at 25^{o} C at a speed of 30 µl/min over the defined surfaces. Surfaces were then regenerated with a pulse of 2M NaCl. Control readings were then subtracted from GAG readings. Both association and dissociation phases were fitted using a Langmuir 1:1 binding model with mass transfer (BIAevaluation 3.1 software, GE Healthcare).

III.x. Quartz crystal microbalance with dissipation monitoring

Quartz crystal microbalance with dissipation monitoring (QCM-D) was carried using a Q-Sense E4 system (Biolin Scientifica, Sweden) as described (Djerbal et al., 2019). Briefly, biotinylated GAGs were captured on sensors and anchored via their reducing ends on a streptavidin monolayer on a supported lipid bilayer. Proteins were injected over the assembled film for 20 min at a rate of 20 µl/min. In between proteins films were washed with PBS. Shifts in frequency, Δf, and dissipation, ΔD, were recorded at six overtones (3, 5, 7, 9, 11 and 13). All values for Δf, and ΔD shown here are from the 3rd overtone. All other overtones showed qualitatively similar responses.

IV. RESULTS

IV.i. Netrin-1 associates with PNNs

To investigate whether netrin-1 localizes to PNNs, we used a netrin-1 specific monoclonal antibody (abcam, EPR1791-4) to examine the distribution of netrin-1 protein in the young adult rat brain. We co-labelled adult rat brain sections using a fluorescently labeled lectin, *Wisteria floribunda* agglutinin (WFA), a common PNN marker which binds to the N-acetylgalactosamine moiety of the CS GAGs (Hilbig, Bidmon, Blohm, & Zilles, 2001). At low magnification netrin-1 and WFA are detected colocalized on cells throughout the neocortex (Figure 6.1A). Using high magnification confocal microscopy we further investigated the relationship of netrin-1 to PNNs and additionally examined the distribution of netrin-1 in relation to Sema3a, an axon guidance cue present in PNNs (Vo et al., 2013). We detected neurons immunoreactive for both netrin-1 and Sema3a that were also surrounded by a PNN (Figure 6.1B). Sema3a largely co-localizes with the staining for WFA that surrounds the neuron, consistent with previous studies demonstrating it is a component of PNNs (Vo et al., 2013). Some co-localization of netrin-1 with WFA was detected, however, the large majority of netrin-1 staining is present just below the WFA positive layer, possibly on the cell membrane or inside the cell in a cytoplasmic pool of vesicles (Figure 6.1B). We then used Zeiss Airyscan microscopy to visualise the distribution of netrin-1 in relation to WFA at the cell surface. Examining the maximum projection image, netrin-1 immunoreactivity is clearly visible within holes in the WFA staining, as indicated by the white arrows (Figure 6.1C). These results suggest that while both Sema3a and netrin-1 are associated with neurons surrounded with PNNs, Sema3a appears to be integrated into the meshwork of the PNN while netrin-1 is enriched in the holes in the PNN where synapses are thought to locate.

IV.ii. Netrin-1 binds PNN GAGs

Neuronal ECM is not uniform and can be broken down into three subtypes, loose, membrane associated, and PNN, depending on molecular composition and organisation (Bozzelli et al., 2018; Sorg et al., 2016). Loose ECM is composed mainly of HA and CS, and fills the majority of the extracellular space in the CNS (Happel & Frischknecht, 2016). Membrane associated ECM is a more condensed form of ECM bound to the cell membrane of all CNS cell types and can be easily remodelled following injury (Bozzelli et al., 2018). PNN ECM is highly specialized and structured, and surrounds only the cell bodies and proximal dendrites of a subset of neurons (Celio & Blumcke, 1994). Through a series of buffer extractions and differential centrifugation, adult mammalian brain homogenate can be separated into 4 fractions which are differentially enriched with these different types of ECM and the proteins associated with them (Deepa et al., 2006; Foscarin et al., 2017). Fraction 1 is enriched for soluble ECM GAGs, fraction 2 and 3 for membrane bound ECM GAGs, and fraction 4 contains PNN ECM GAGs. We separated whole adult rat brain into these four fractions and used western blot analysis to determine which GAG fraction endogenous netrin-1 is associated with (Figure 6.2). For simplicity, fractions 2 and 3 were pooled to combine all membrane associated GAGs into one sample. Netrin-1 was detected in all GAG fractions, with the majority being split between the soluble fraction 1 and the PNN associated fraction 4 (Figure 6.2A). As a control to validate the fractionation, the western blots were also probed for hyaluronan and proteoglycan binding link protein 1 (HAPLN1), as it is enriched in PNNs (Kwok et al., 2010) (Figure 6.2A). Interestingly, the netrin-1 immunoreactive band detected in fraction 4 is shifted to a slightly lower apparent molecular weight than the netrin-1 immunoreactive bands in fractions 1-3 (Figure 6.2A). The estimated molecular weight of netrin-1 in fraction 1 is 76 kDa while in fraction 4 the weight shifted down to approximately

65 kDa. A similar shift to a lower apparent molecular weight of netrin-1 has been previously detected during rat spinal cord maturation, with the shift in molecular weight occurring at age ~P14 (Manitt et al., 2001). The molecular weight shift detected may be due to differential post-translational modifications, as netrins are glycosylated proteins and there are no known alternative splice variants of netrin-1. To test this idea, we used Endo H digestion to remove all N-linked glycosylation contained in these fractions. Following Endo H digestion, the estimated molecular weight of netrin-1 shifted down to ~60 kDa in all fractions. We also examined a full-length purified recombinant myc tagged chick netrin-1 and detected a similar downshift in apparent molecular weight following Endo H digestion (Figure 6.2C). These results demonstrate that netrin-1 is post-translationally glycosylated and that the netrin-1 in the PNN is glycosylated differently than netrin-1 in membrane bound or loose ECM (Figure 6.2B).

After determining the relative enrichment of netrin-1 within the different GAG fractions, we then examined the capacity of netrin-1 to directly bind GAGs isolated from the four brain fractions using a modified ELISA assay (Figure 6.2D) (Dick et al., 2013; Vo et al., 2013). We examined binding of both recombinant purified full-length netrin-1 (FL) and netrin-1 VI-V, which is a truncated variant of netrin-1 that lacks the C-terminal domain. Our previous studies identified a critical GAG binding domain within the C-domain (Chapter 5). In all fractions, the binding of netrin-1 FL was significantly higher than netrin-1 VI-V, further demonstrating the importance of the netrin-1 C-domain for GAG binding. Netrin-1 binding to GAGs was also significantly higher in fractions 2, 3 and 4 than binding to the soluble GAGs enriched in fraction 1.

Since GAGs isolated from adult brain tissue contain a mixture of different GAG families we investigated which GAGs contribute to netrin-1 binding in the adult rat brain (Deepa et al.,

2006). To determine the GAG binding specificity of netrin-1, we systematically digested GAGs from the brain fractions using specific GAG degrading enzymes, thereby removing them from the sample. We used this approach to digest HA, CSs, and HSs using hyaluronidase, chondroitinase ABC, and heparitinase, respectively. We focused on fraction 1 and fraction 4 due to their different capacities to bind netrin-1 when undigested and because netrin-1 is relatively enriched in these fractions, as revealed by western blot analysis (Figure 6.2A). Digestion of fraction 1 with hyaluronidase had no effect on netrin-1 binding, while chondroitinase ABC decreased netrin-1 binding, and heparitinase digestion increased netrin-1 binding (Figure 6.2E). The detected increase in netrin-1 binding following heparitinase digestion is strikingly similar to what we found when E11 spinal cord GAGs were digested with heparinase and netrin-1 binding assessed (Chapter 5). HSs are particularly abundant in fraction 1 and digesting them may unmask other GAG binding partners that are then able to interact with netrin-1. Further, if these interactions are of a higher affinity than the digested HSs, this could account for the increased netrin-1 binding. The decrease in binding following chondroitinase ABC digestion suggests netrin-1 is binding to CSs in fraction 1. Digestion of fraction 4, the PNN associated GAG fraction, with any one of the three enzymes resulted in decreased binding, consistent with all three GAG families contributing to netrin-1 binding in fraction 4 (Figure 6.2E). Digestion of fraction 4 with chondroitinase ABC resulted in the greatest loss of binding, suggesting that CSs are the major binding partner for netrin-1 in this fraction. CSs are the main GAG component of PNNs and netrin-1 binding to CSs may be important to localize netrin-1 within the PNN.

CS GAG chains are comprised of five common sugar disaccharide subunits, CS -A, -B, -C, -D, and -E (Sugahara et al., 2003) (Figure 6.3A-E). The subunit composition of CS GAG chains changes throughout development and varies between cell types and in different tissues

(Bulow & Hobert, 2006). During embryogenesis, CS-C is the most abundant subunit in the GAG chain, while in the adult animal, CS-A becomes the most abundant (Djerbal, Lortat-Jacob, & Kwok, 2017). GAG composition of the different ECM fractions in the brain is also variable. Loose extracellular matrix is rich in CS-A while more compact structures, such as the PNN, are rich in di-sulfate CS subunits, particularly CS-E (Deepa et al., 2006; Djerbal et al., 2017). The accumulation of CS-A decreases by 6% from fraction 1 to fraction 4 while the accumulation of CS-E increases by 20% from fraction 1 to fraction 4 (Deepa et al., 2006). We therefore wanted to examine the capacity of netrin-1 to bind different CS subunits which might influence its spatial localization within the ECM. We again used netrin-1 FL and netrin-1 VI-V and as before detected significantly higher binding of the full-length protein across all subunits. Additionally, distinct differences in binding between netrin-1 FL and the different CS subunits were detected. CS-C and CS-D exhibited the weakest binding, followed by CS-A and CS-B with moderate binding, and finally CS-E with significantly higher binding to netrin-1 than all other subunits. These findings demonstrate that while netrin-1 is capable of binding to all CS subunits, it exhibits significantly higher affinity binding to CS-E and this may be responsible for localizing netrin-1 to PNNs.

To further quantify netrin-1 binding to CS subunits we used surface plasmon resonance (SPR) to determine the equilibrium dissociation constant (K_D) of netrin-1 binding (Table 6.1, Figure 6.4). We examined netrin-1 FL and netrin-1 VI-V binding to both CS-E and CS-D subunits. Consistent with our ELISA binding data we saw no binding of netrin-1 VI-V to CS-D and weak binding to CS-E. Netrin-1 FL bound tightly to both CS-D and CS-E with a K_D in the pM range (Table 6.1, Figure 6.4).

Table 6.1	Ligand	k_a (1/Ms)	k_d (1/s)	K_D (M)	Average K_D (M)
Netrin-1 VI-V	CS-D	No Binding			N/A
		No Binding			
	CS-E	5.3×10^5	5.4×10^{-3}	1.03×10^{-8}	9.52×10^{-9}
		7.12×10^5	6.22×10^{-3}	8.74×10^{-9}	
Netrin-1 FL	CS-D	4.29×10^6	1.45×10^{-4}	3.39×10^{-11}	2.07×10^{-11}
		2.18×10^6	1.63×10^{-5}	7.46×10^{-12}	
	CS-E	5.64×10^6	8.85×10^{-5}	1.57×10^{-11}	1.57×10^{-11}
		5.36×10^6	8.35×10^{-5}	1.56×10^{-11}	

IV.iii. Netrin-1 softens CS GAG films

We next aimed to determine the effect of netrin-1 binding on the physical properties of GAG films. A quartz crystal microbalance with dissipation monitoring (QCM-D) device was used to measure ligand binding and GAG film stiffness. We tested films made from chains of CS-D or CS-E and assessed the physical changes resulting from netrin-1 addition. We also examined Sema3a as a control, since addition of Sema3a has been previously shown to cause stiffening of the GAG films (Djerbal et al., 2019). A decrease in frequency after ligand application indicates binding to the GAG film while changes in dissipation indicate alterations to the viscoelastic properties of the film. An increase in dissipation indicates thickening and softening while a decrease indicates thinning and stiffening. Application of netrin-1 FL to both CS-D and CS-E films caused a decrease in frequency, indicating ligand binding. The largest decrease in frequency was seen with the CS-E film indicating very tight binding which is consistent with the K_D binding data (Figure 6.5). Netrin-1 application also increased the dissipation when applied to both CS-D and CS-E films indicating that netrin-1 causes a softening of the GAG films. In contrast to Sema3a, which stiffens the films, these findings suggest that netrin-1 acts to open the PNN while Sema3a tightens it, fitting with the 'ying and yang' actions of these two proteins.

V. DISCUSSION

The persistent expression of developmental axon guidance cues in the adult animal suggests that they have a role beyond guiding axons to appropriate targets during embryogenesis. Previous studies have demonstrated that Sema3a is a constituent of PNNs in the adult brain and the findings we report here compliment this and demonstrate that netrin-1 is also associated with PNNs (Dick et al., 2013; Vo et al., 2013). While both proteins are well characterized for their function in axon guidance they also have effects on synaptic plasticity in the adult CNS (Bouzioukh et al., 2006; Glasgow et al., 2018; Horn et al., 2013; Luo, Raible, & Raper, 1993; Serafini et al., 1996; Q. Wang et al., 2017). In hippocampal slices, the addition of exogenous Sema3a leads to a decrease in field excitatory post synaptic currents (EPSC) in the CA1 region (Bouzioukh et al., 2006). Sema3a also has an inhibitory effect on the outgrowth of DRG neurons, an effect that is amplified in the presence of PNN proteins (Dick et al., 2013). In contrast, netrin-1 has been demonstrated to promote synapse formation during post-natal maturation and enhance plasticity in the adult mammalian brain (Glasgow et al., 2018; Goldman et al., 2013; Horn et al., 2013). Addition of netrin-1 to hippocampal slices results in a prolonged increase in EPSCs in CA1 hippocampal neurons and activity dependant release of netrin-1 from dendrites is required for LTP (Glasgow et al., 2018; Horn et al., 2013).

PNNs are key regulators of synaptic plasticity and PNNs are generally thought to “lock in” neuronal circuitry and limit synaptic plasticity, with the appearance of PNNs coinciding with the closure of developmental critical periods (Bozzelli et al., 2018). CSPGs are generally thought to be inhibitory in nature. Consistent with this, digesting GAGs in the mature CNS with chondroitinase ABC increases axon regeneration, enhances plasticity, and can enhance memory function (Fawcett, 2009; Galtrey et al., 2007; N. G. Harris et al., 2013; Romberg et al., 2013; D.

Wang et al., 2011). PNNs have also been shown to regulate the strength of existing synapses by limiting the lateral mobility of AMPA receptors on the surface of the neuron (Frischknecht et al., 2009). Degradation of the PNN leads to lateral diffusion of AMPARs away from synaptic sites, which leads to a weakening of synaptic strength (Frischknecht et al., 2009). Recent work from the Kennedy lab has demonstrated that netrin-1 drives the insertion of GluA1 receptor subunit containing AMPARs at hippocampal synapses (Glasgow et al., 2018). The observation that netrin-1 is enriched in the holes in PNNs that correspond to synapses suggest that netrin-1 and PNNs may function together to strengthen specific active synapses within a neural circuit, with netrin-1 promoting synaptic insertion of AMPARs and the PNN itself fencing in AMPAR lateral movement, leading to a coordinated strengthening of the synapse.

Here, we have identified a subset of netrin-1 positive neurons that are enclosed by PNNs in the adult rat neocortex, with netrin-1 enriched in the holes in the mesh structure of the PNN. Additionally, netrin-1 binds tightly to GAGs isolated from the PNN, with particularly high affinity for CS-E, the CSPG subunit that is preferentially segregated into PNNs. Netrin-1 binding to GAG films also alters the physical properties of the film, leading to a softening which may correlate with an "opening" of the PNN and a subsequent increase in synaptic plasticity. While the specific function(s) of PNN associated netrin-1 remains to be elucidated, we speculate that it may promote synapse strengthening or maintenance of synapse function. The presence of netrin-1 in the PNN may also act to balance an inhibitory influence of Sema3a. Both Sema3a and netrin-1 are secreted proteins whose release is regulated by neuronal activity (de Wit, Toonen, Verhaagen, & Verhage, 2006; Glasgow et al., 2018). Regulated release could adjust the balance of netrin-1 and Sema3a in the PNN, which would then result in changes to PNN softness, or "openness", with the potential to tune synapse structure and function. Increased Sema3a in the

PNN would produce a more rigid and less plastic PNN while increased netrin-1 would soften the PNN and allow for increased synaptic plasticity. While this remains to be proven, we propose that Sema3a and netrin-1 function in conjunction with the PNN to balance synapse number, structure and function in the adult brain.

VI. FIGURES

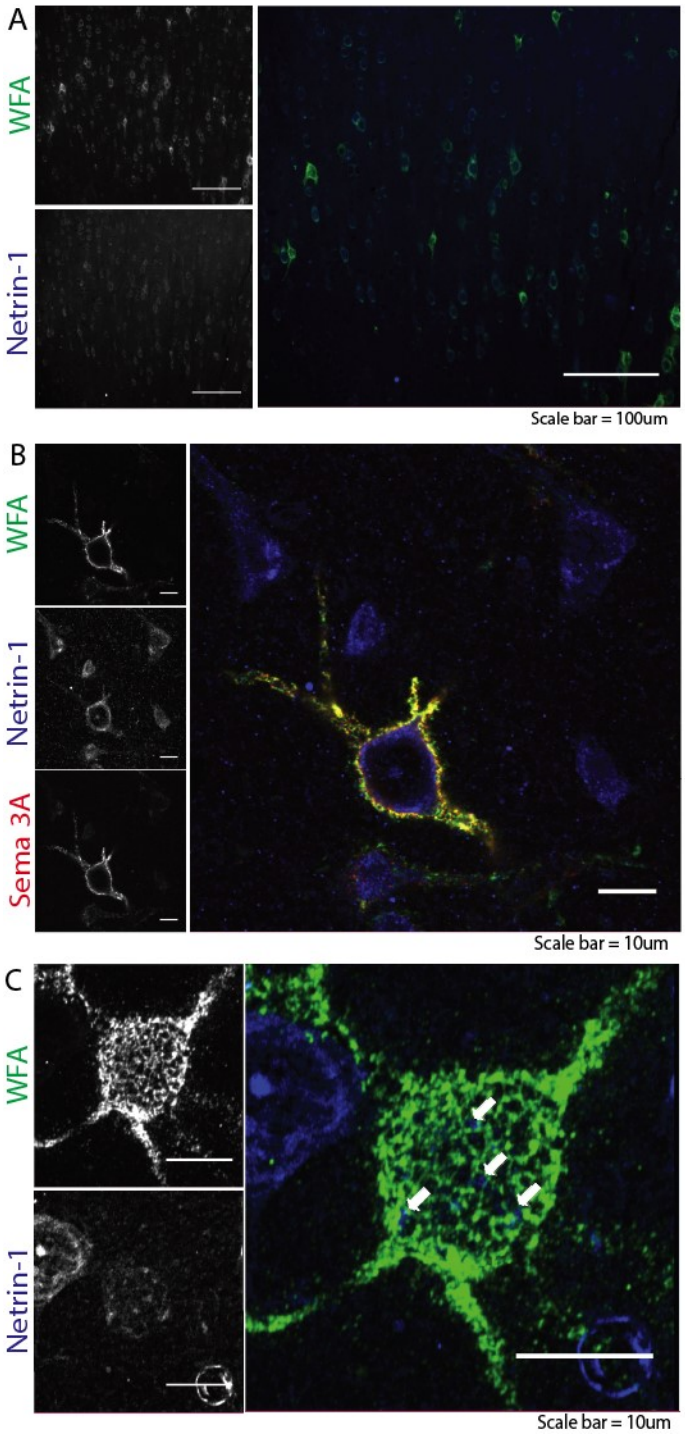
A
WFA
Netrin-1
Scale bar = 100um
B
WFA
Netrin-1
Sema 3A
Scale bar = 10um
C
WFA
Netrin-1
Scale bar = 10um

Figure 6.1: PNN staining in adult rat brain. A: Low magnification image of adult rat cortex stained for WFA (green) to mark PNNs and netrin-1 (blue, scale bars = 100 μm). **B:** High magnification image of adult rat cortex stained for WFA (green), netrin-1 (blue), and semaphorin 3a (red, scale bars = 10 μm). **C:** Maximum projection of a neuron stained for WFA (green) and netrin-1 (blue). Netrin-1 is visible in the holes of the WFA staining as indicated by white arrow heads (scale bars = 10 μm).

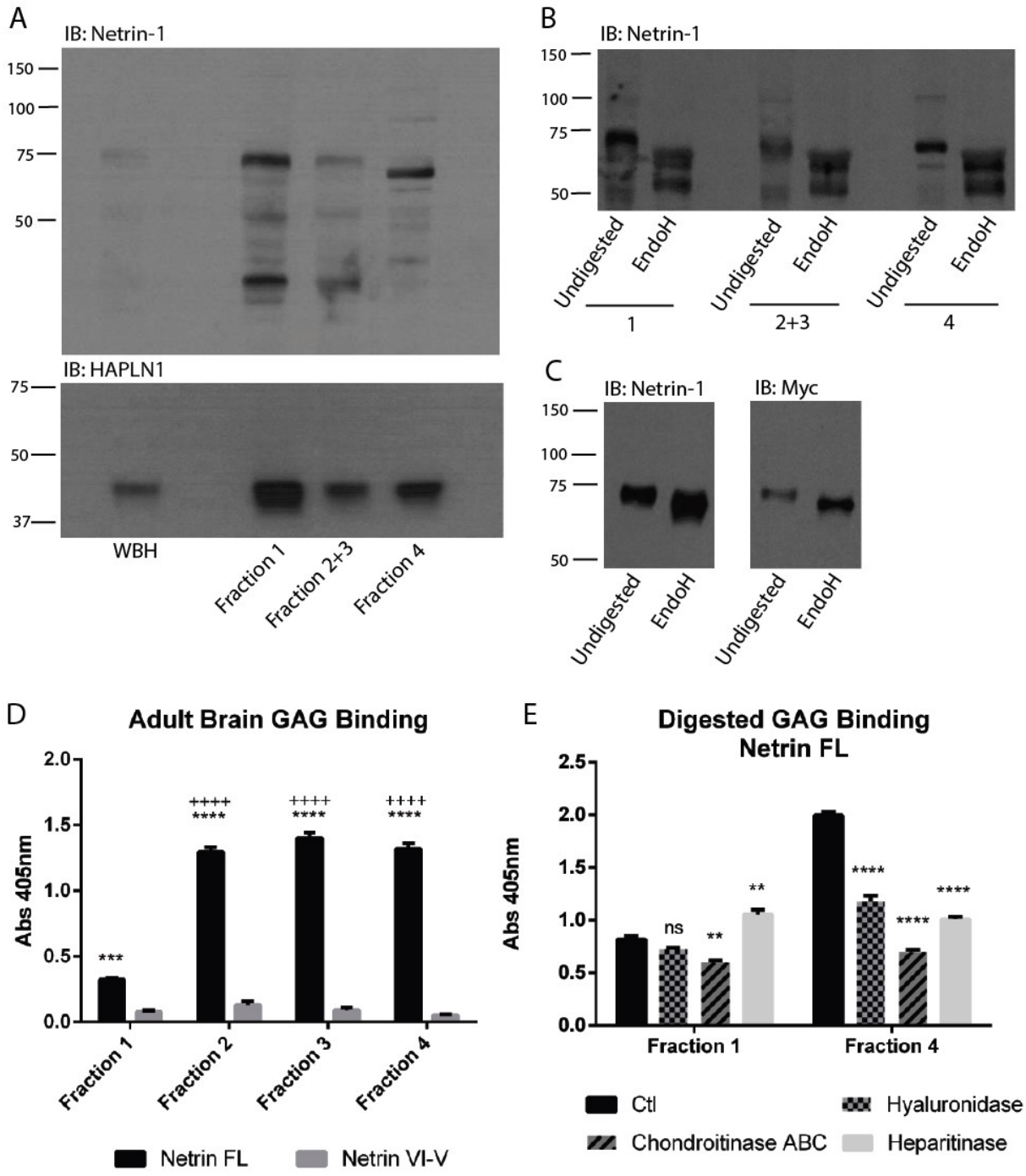

Figure 6.2: Adult GAG binding to netrin-1. A: Netrin-1 protein is present in all four GAG fractions in adult rat brain. Fraction 1: Soluble GAGs, fractions 2 and 3: Membrane bound GAGs, fraction 4: PNN associated GAGs. HAPLN1 is a link protein found in high

concentrations in PNNs and used as a fractionation control. Estimated molecular weight of netrin-1: fraction 1 76 kDa, fraction 2/3 74 kDa, fraction 4 65 kDa. **B:** PNN fractions after digestion with Endo H to remove N-linked glycosylation. Estimated molecular weight of netrin-1: fraction 1 62 kDa, fraction 2/3 61 kDa, fraction 4 60 kDa. **C:** Full length myc tagged chick netrin-1 before and after Endo H digestion. **D:** ELISA binding assay for GAGs isolated from adult rat brain to netrin-1. GAGs are divided into the four fractions. In all fractions full length netrin-1 binding is significantly higher than netrin VI-V binding. Fraction 1 binding is significantly lower than fractions 2-4 (*'s represent comparison between full length and VI-V, +'s represent comparison to fraction 1. Two-way ANOVA with Tukey test, n=3, $p<0.0001$). **E:** ELISA binding assay of digested GAG fractions 1 and 4 to netrin-1. GAGs isolated from adult rat brain were digested with heparitinase, chondroitinase ABC, or hyaluronidase prior to analysing full length netrin-1 binding. In fraction 1 digestion with chondroitinase ABC caused a significant decrease in GAG binding while digestion with heparitinase caused a significant increase in GAG binding. In fraction 4 digestion with all three enzymes caused a significant decrease in GAG binding with the largest decrease seen after chondroitinase ABC digestion (*'s represent comparison to undigested fraction. One-way ANOVA with Tukey test, n=3, **** $p<0.0001$, ** $p<0.01$).

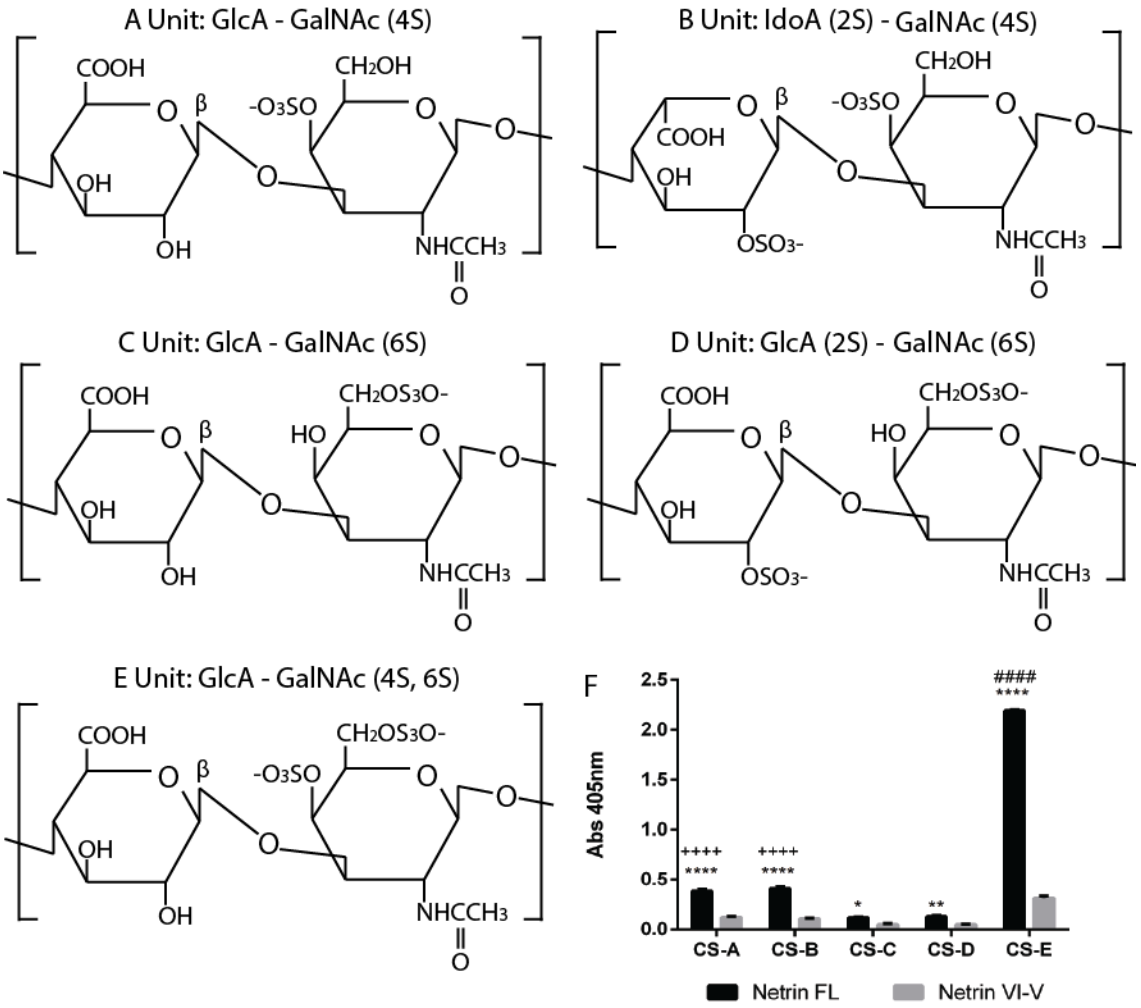

Figure 6.3: A-E: CS subunit structure F: Binding of different CS subunits to netrin-1. In all cases full length netrin-1 has significantly higher binding to CS subunits than netrin VI-V. CS-A and CS-B have significantly higher binding than CS-C and CS-D. The CS-E subunit has the highest binding to netrin-1 (*'s compared to VI-V, +'s compared to CS-C and CS-D, #'s compared to all other subunits. Two-way ANOVA with Tukey test, n=3, **** $p<0.0001$, ++++ $p<0.0001$, #### $p<0.0001$).

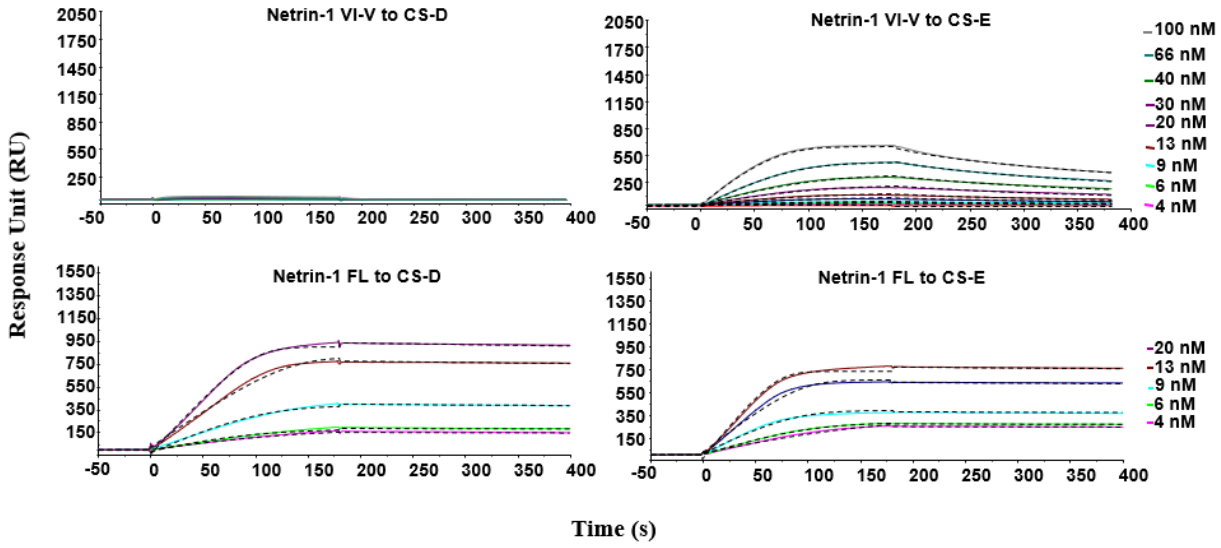

Figure 6.4: Surface plasmon resonance measurements for the interaction between netrin-1 and CS subunits D and E. There is no apparent binding between netrin-1 VI-V and CS-D (top left). Netrin-1 VI-V binding to CS-E has an average K_D of 9.52 nM (top right). Netrin-1 FL binding to CS-D has an average K_D of 20.68 pM (bottom left). Netrin-1 FL binding to CS-E has an average K_D of 15.65 pM (bottom right).

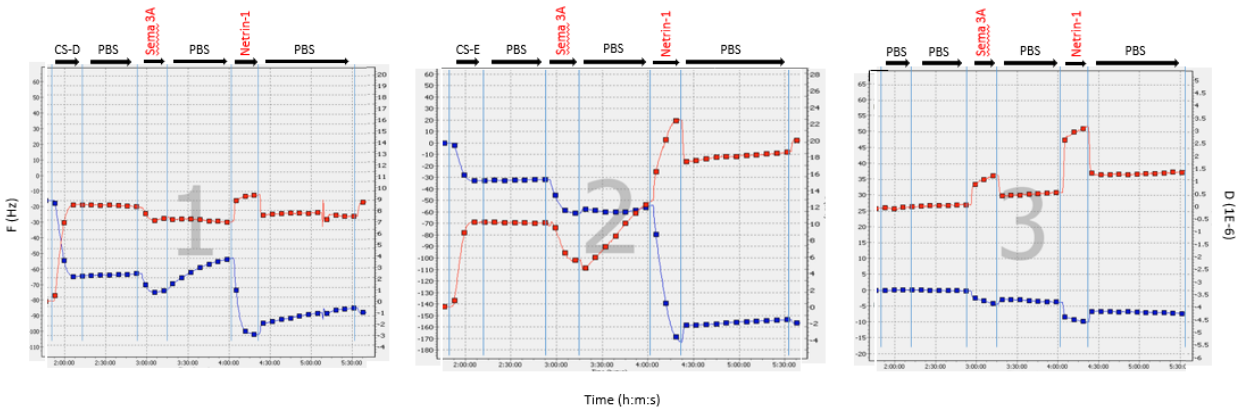

Figure 6.5: QCM-D data for netrin-1. Left: CS-D, Middle: CS-E, Right: Control. Netrin-1 binds tightly to CS-E and CS-D polymer films and leads to a softening of the film. This effect is opposite of Sema3a. Blue lines represent frequency and red lines dissipation. A decrease in frequency represents binding and an increase in dissipation indicates the film is softening.

DISCUSSION

Preface

In this chapter the results obtained in the previous data chapters will be discussed and integrated into two new models, one for axon guidance, and one for synapse function.

Chapter 7

General Discussion and Concluding Remarks

I. Integrated Model of Commissural Axon Guidance

Guiding embryonic spinal commissural axons from their origin in the dorsal spinal cord to the ventral midline and across requires multiple coordinated signalling events. One of the most studied axon guidance cues in this process is netrin-1, a secreted protein that binds to its receptor DCC on the surface of commissural axons. Netrin-1 binding to DCC elicits an attractive response, leading to actin polymerization and filopodia formation at the leading edge of the growth cone (Lai Wing Sun et al., 2011). While the requirement for netrin-1 and DCC for guidance to the midline is clear, much remains unknown about its interactions with other molecules in the spinal cord and their underlying signalling mechanisms (Bin et al., 2015; Keino-Masu et al., 1996; Serafini et al., 1996). In this thesis, we demonstrate that netrin-1 and DCC interact with cadherins and proteoglycans to regulate commissural axon outgrowth in the developing spinal cord. Based on the results obtained, we propose an integrated model for commissural axon guidance (Figure 7.1). We propose that HSPGs bind and localize netrin-1 in the ECM of the embryonic spinal cord and this binding to GAGs facilitates binding of netrin-1 to DCC (Chapter 5). This then activates kinases downstream of DCC which phosphorylate β-catenin and initiate the formation of linear actin bundles, a process required for filopodia formation and growth cone expansion (Chapter 3).

Netrin-1 is traditionally described as a chemotropic axon guidance molecule, however, while it is a secreted molecule, it has been reported that in order to function and direct extending

commissural axons, netrin-1 must be bound to a substrate or matrix (Moore, Biais, & Sheetz, 2009; Moore et al., 2012). It has been demonstrated that netrin-1 bound to the surface of an immobilized polystyrene micro-bead is sufficient to induce growth cone turning. Conversely, netrin-1 bound to a bead that is free to move does not direct growth. These findings provided strong evidence that netrin-1 must be immobilized on a surface in order to direct commissural axon outgrowth, growth cone expansion, and axon attraction (Moore et al., 2009; Moore et al., 2012). However, how netrin-1 is immobilized *in vivo* following secretion is not known. HSPGs are abundant in ECM of the developing spinal cord and are a good candidate molecule for binding netrin-1. Previous work demonstrated the importance of EXT1, an enzyme required for the elongation of HSPG GAG side chains, in the formation of the spinal commissure (Inatani et al., 2003). In Chapter 5 we show that netrin-1 binds tightly to HSPGs through interactions with the C-domain, a domain for which a clear function was previously unknown (Figure 5.4 & 5.6). Further, we show that this interaction can potentiate netrin-1 induced commissural axon outgrowth in a DCC-dependent manner (Figure 5.5 & 5.7). Our working model proposes that HSPGs bind and aggregate netrin-1 in the ECM which then multimerizes DCC to initiate downstream signalling within the neuron (Figure 7.1).

DCC activation leads to the recruitment and activation of numerous signalling molecules. While it is well established that DCC activation through netrin-1 leads to the re-organisation of the actin cytoskeleton, the exact molecular mechanisms underlying this remain unknown (Shekarabi & Kennedy, 2002; Shekarabi et al., 2005). In Chapter 3 we provide evidence that DCC interacts with the type II classical cadherin CDH12 and its signalling partner β-catenin (Figure 3.2). The cadherin/catenin complex is known to regulate cytoskeletal dynamics and has a direct impact on actin filament formation (Yamada, Pokutta, Drees, Weis, & Nelson, 2005).

More specifically, phosphorylation of β-catenin at Y142, which we show here is regulated by netrin-1 (Figure 3.7), has a direct impact on the ability of α-catenin to interact with actin filaments (Piedra et al., 2003).

Integrating the results obtained in Chapter 3 and Chapter 5 provides a new working model for the mechanisms underlying commissural axon guidance in the developing spinal cord (Figure 7.1). We propose that netrin-1 in the spinal cord is bound and immobilized in the ECM through interactions between HSPGs and the netrin-1 C-domain. The GAG chains aggregate netrin-1 which in turn binds and multimerizes DCC. Both netrin-1 and DCC multimerization are required for proper function (Keino-Masu et al., 1996; Stein et al., 2001). Netrin-1 binding to DCC then activates downstream signalling, including activation of SFKs and PAK1 (Lai Wing Sun et al., 2011). SFKs and PAK1 can then phosphorylate β-catenin which is in a signalling complex with CDH12 and DCC (Figure 3.2 & 3.7). Phosphorylation of β-catenin at Y142 results in α-catenin dissociating from the cadherin adhesion complex. Free α-catenin homodimerizes and binds to actin filaments, ultimately inhibiting the arp2/3 complex and shifting actin polymerization away from branched sheets towards linear bundles (Piedra et al., 2003) (Figure 7.1). The revised model links together multiple signalling pathways and provides new insight into how these proteins may function together during commissural axon guidance.

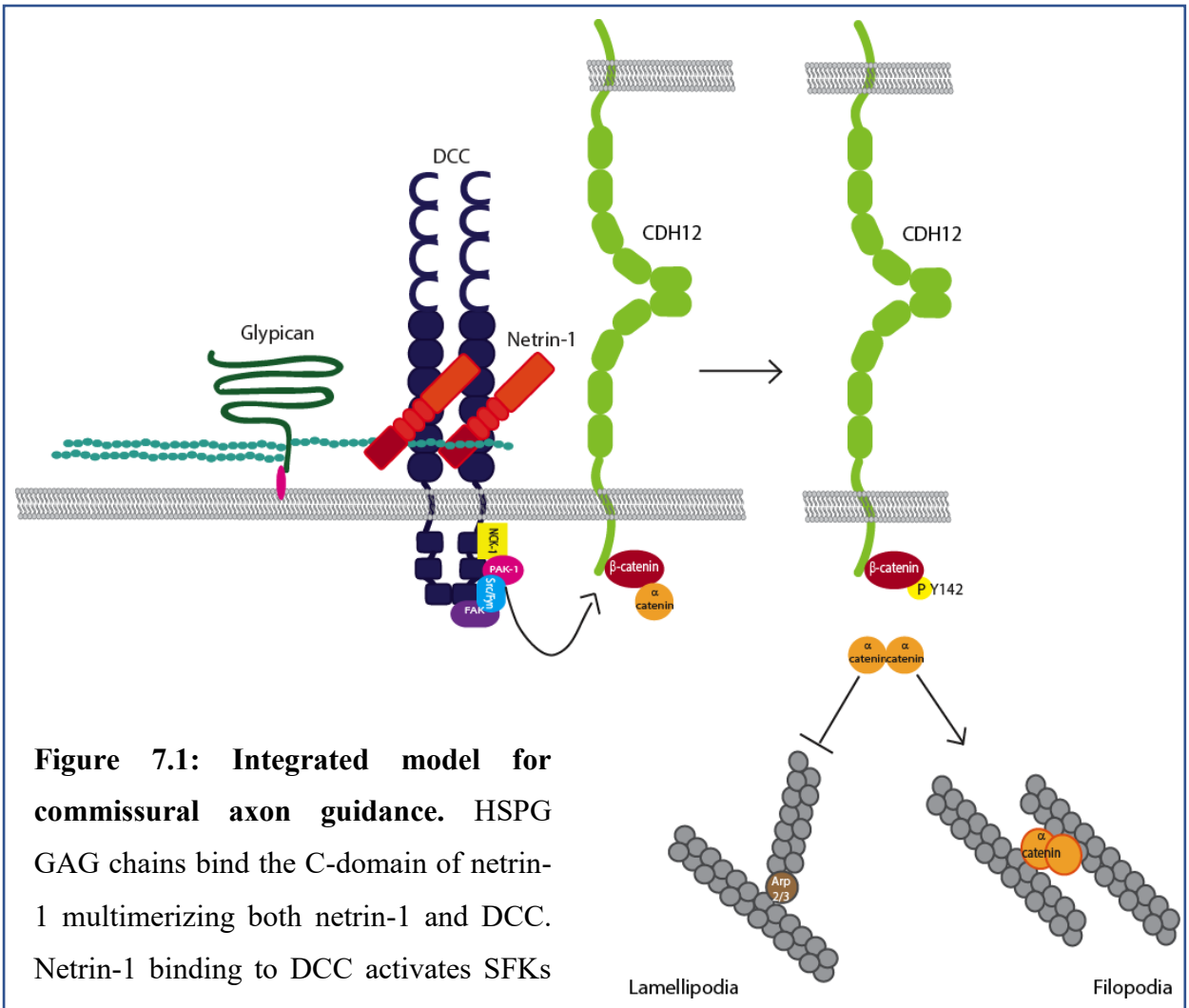

Figure 7.1: Integrated model for commissural axon guidance. HSPG GAG chains bind the C-domain of netrin-1 multimerizing both netrin-1 and DCC. Netrin-1 binding to DCC activates SFKs and Pak1 downstream of DCC leading to the phosphorylation of β-catenin. Phosphorylation of Y142 on β-catenin causes the dissociation of α-catenin which then forms homodimers that bind to actin filaments promoting filopodia formation.

II. Integrated Model for Synapse Function

PNNs are critical regulators of synaptic plasticity. More specifically, they are thought to limit plasticity and "lock in" neuronal circuits. Despite PNNs restricting synaptic plasticity, synaptic potentiation still occurs in the adult brain. Therefore, there must be a mechanism to modulate

PNNs and allow for plasticity in the adult brain. In this thesis we demonstrate that netrin-1 binds CSPGs in the adult brain, and that netrin-1 binding to CS subunits can alter the physical properties of GAG films (Chapter 6). We also show that netrin-1 regulates DCC and CDH12 aggregation and co-localization in the plasma membrane, and that netrin-1 treatment increases the cell surface distribution of both of these proteins (Chapter 4). Integrating these findings, we suggest a model for synaptic function in which netrin-1 binds to CSPGs in the PNN and modulates the physical properties of the PNN to promote synaptic plasticity in the adult brain (Figure 7.2). Our findings suggest that netrin-1 release at depolarized dendritic spines will increase the plasma membrane insertion of DCC, CDH12, and AMPARs which mediate synaptic function and plasticity (Figure 7.2).

Digesting the PNN with chondroitinase ABC has been shown to re-open critical periods and increase the number of synapses (Lensjo et al., 2017; Pyka et al., 2011). This is consistent with the idea that PNNs restrict synaptic plasticity. However, chondroitinase ABC digestion also results in synapses with reduced function, providing evidence that the PNN also plays an important role in maintaining synaptic function (van 't Spijker & Kwok, 2017). This observed decrease in synaptic function is thought to be due to increased lateral mobility of AMPAR subunits in the cell membrane away from the region of synaptic contact (Frischknecht et al., 2009). The proposed model consolidates these two observations and suggests that localized opening of the PNN, specifically at sites of netrin-1 release, regulates synaptic plasticity. In Chapter 6 we show that a subset of netrin-1 positive cells in the neocortex are surrounded by PNNs (Figure 6.1). We show that netrin-1 binds to the CS-E subunit of CSPGs through interactions with the netrin-1 C-domain, and netrin-1 binding alters the physical properties of GAG films, causing the film to soften (Figure 6.5). This softening may be correlated with an

"opening" of the PNN. Importantly, in this model, the PNN outside the area of netrin-1 release would remain "closed", thus preventing the lateral diffusion of the newly inserted synaptic proteins.

Previous work from the Kennedy lab has demonstrated that netrin-1 and DCC promote synapse function in the adult brain (Glasgow et al., 2018; Goldman et al., 2013; Horn et al., 2013). Depolarization of neurons or NMDAR activation resulted in the rapid local release of netrin-1 from dendritic spines and application of exogenous netrin-1 recruits AMPARs to the synaptic membrane to potentiate glutamatergic synapses onto hippocampal CA1 pyramidal neurons. (Glasgow et al., 2018). Depolarization of cortical neurons was also previously shown to cause an increase in the amount of DCC in the neuronal plasma membrane (Bouchard et al., 2008). In Chapter 4 we show that netrin-1 regulates DCC and CDH12 distribution within cortical neurons. Treatment of embryonic cortical neurons in cell culture with netrin-1 increased in the amounts of both DCC and CDH12 in the plasma membrane (Figure 4.5). We hypothesize that DCC, CDH12 and β-catenin may be contained within the same population of vesicles, or alternatively that different pools of cargo vesicles may be co-recruited, and that the MAGUK protein Dlg5 could regulate their trafficking within the cell. Therefore, netrin-1 may be functioning to trigger a positive feedback loop where neuronal activity causes netrin-1 release, which then leads to increased cell surface expression of DCC, CDH12, and AMPARs, resulting in enhanced synaptic potentiation at the site of netrin-1 release.

Integrating the results obtained in Chapter 4 and Chapter 6, we propose a working model for netrin-1 and DCC function at synapses (Figure 7.2). In the proposed model, neuronal activity and dendritic spine depolarization stimulates netrin-1 release which then binds to CSPGs in the PNN. This contributes to localized "opening" of the PNN, facilitating the insertion of new

proteins into the synaptic membrane and the expansion of dendritic spine volume. Netrin-1 release drives the insertion of DCC and CDH12 from a subcellular pool of vesicles. Following insertion, cadherins are predicted to bind across the synapse to stabilize and strengthen the synaptic contact. Netrin-1 is sufficient to trigger the insertion of AMPARs into the post-synaptic membrane to enhance potentiation and the unopened surrounding PNN would prevent lateral diffusion away from the synaptic site. Our model provides a mechanism that permits spatially localized synaptic plasticity in response to neuronal activity within neuronal circuits that have been "locked in" by PNNs.

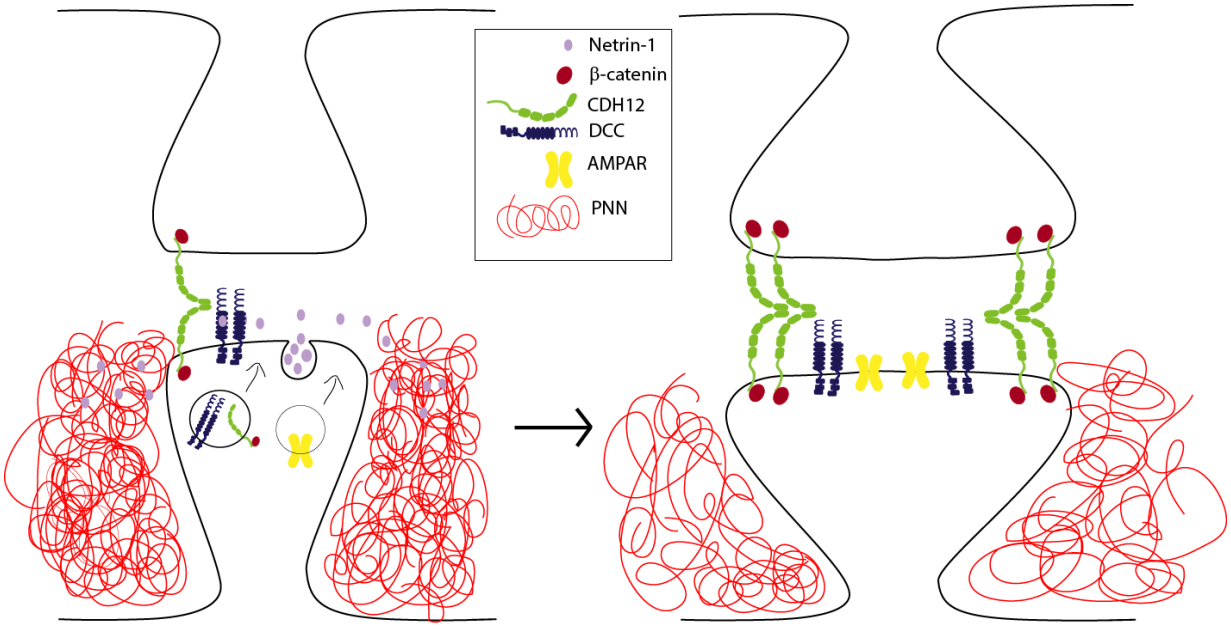

Figure 7.2: Integrated model for synapse function: Depolarization of the synapse causes netrin-1 release from the dendritic spine. Netrin-1 binding to the PNN causes the PNN to "open" allowing for synapse maturation and expansion. Release of netrin-1 leads to insertion of DCC and CDH12 into the membrane from vesicles. AMPARs are also inserted into the synaptic membrane and lateral diffusion away from the synaptic site is prevented by the un-opened surrounding PNN.

III. Concluding Remarks

Netrin-1 is a well studied axon guidance molecule that functions in many cellular processes within the nervous system. While much is known about how netrin-1 interacts with DCC to mediate axon guidance and synaptic function, not much is known about how netrin-1 interacts with other molecules in the CNS. Understanding how different signaling pathways integrate to regulate the coordinated function of the nervous system is important as neurons are not isolated cells. The findings in this thesis provide new insights into how known signalling pathways integrate and work together to mediate axon guidance and synapse function in the CNS. Ultimately, these findings contribute to our knowledge of how mechanisms of signal transduction are functionally integrated rather than operating as isolated signalling pathways within cells.

BIBLIOGRAPHY

Publications

1. Landry, M. J., Kaien, G., **Harris, S. N.,** Al Alwan, L., Gutsin, L., Di Biasio, D., Jiang, B., Nakamura, D. S., Corkery, T. C., Kennedy, T. E., Barrett, C. J. (2018). Tunable Engineered Extracellular Matrix: Polyelectrolyte Multilayers Promote Improved Neural Cell Growth and Survival. *Biomaterials* (submitted)

2. Glasgow, S. D., S. Labrecque, I. V. Beamish, S. Aufmkolk, J. Gibon, D. Han, **S. N. Harris,** P. Dufresne, P. W. Wiseman, R. A. McKinney, P. Seguela, P. De Koninck, E. Ruthazer and T. E. Kennedy (2018). Activity-dependent netrin-1 secretion drives synaptic insertion of GluA1-containing AMPA receptors in the hippocampus. bioRxiv. doi:10.1101/330688

3. Gopal, A. A., Ricoult, S. G., **Harris, S. N**., Juncker, D., Kennedy, T. E., & Wiseman, P. W. (2017). Spatially Selective Dissection of Signal Transduction in Neurons Grown on Netrin-1 Printed Nanoarrays via Segmented Fluorescence Fluctuation Analysis. *ACS Nano, 11*(8), 8131-8143. doi:10.1021/acsnano.7b03004

4. Bin, J. M., **Harris, S. N**. and Kennedy, T. E. (2016), The oligodendrocyte-specific antibody 'CC1' binds Quaking 7. J. Neurochem., 139: 181–186. doi:10.1111/jnc.13745

5. Goldman, J. S., Ashour, M. A., Magdesian, M. H., Tritsch, N. X., **Harris, S. N**., Christofi, N., . . . Kennedy, T. E. (2013). Netrin-1 Promotes Excitatory Synaptogenesis between Cortical Neurons by Initiating Synapse Assembly. *The Journal of Neuroscience, 33*(44), 17278-17289. doi:10.1523/jneurosci.1085-13.2013

References

Aberle, H., Schwartz, H., Hoschuetzky, H., & Kemler, R. (1996). Single amino acid substitutions in proteins of the armadillo gene family abolish their binding to alpha-catenin. *J Biol Chem, 271*(3), 1520-1526.

Allen, N. J., Bennett, M. L., Foo, L. C., Wang, G. X., Chakraborty, C., Smith, S. J., & Barres, B. A. (2012). Astrocyte glypicans 4 and 6 promote formation of excitatory synapses via GluA1 AMPA receptors. *Nature, 486*(7403), 410-414. doi:10.1038/nature11059

Araque, A., Parpura, V., Sanzgiri, R. P., & Haydon, P. G. (1999). Tripartite synapses: glia, the unacknowledged partner. *Trends Neurosci, 22*(5), 208-215. doi:10.1016/s0166-2236(98)01349-6

Arikkath, J., & Reichardt, L. F. (2008). Cadherins and catenins at synapses: roles in synaptogenesis and synaptic plasticity. *Trends Neurosci, 31*(9), 487-494. doi:10.1016/j.tins.2008.07.001

Augsburger, A., Schuchardt, A., Hoskins, S., Dodd, J., & Butler, S. (1999). BMPs as mediators of roof plate repulsion of commissural neurons. *Neuron, 24*(1), 127-141. doi:10.1016/s0896-6273(00)80827-2

Aviles, E. C., & Stoeckli, E. T. (2016). Canonical wnt signaling is required for commissural axon guidance. *Dev Neurobiol, 76*(2), 190-208. doi:10.1002/dneu.22307

Bain, J., McLauchlan, H., Elliott, M., & Cohen, P. (2003). The specificities of protein kinase inhibitors: an update. *Biochem J, 371*(Pt 1), 199-204. doi:10.1042/bj20021535

Baker, K. A., Moore, S. W., Jarjour, A. A., & Kennedy, T. E. (2006). When a diffusible axon guidance cue stops diffusing: roles for netrins in adhesion and morphogenesis. *Curr Opin Neurobiol, 16*(5), 529-534. doi:10.1016/j.conb.2006.08.002

Bamji, S. X. (2005). Cadherins: actin with the cytoskeleton to form synapses. *Neuron, 47*(2), 175-178. doi:10.1016/j.neuron.2005.06.024

Bamji, S. X., Shimazu, K., Kimes, N., Huelsken, J., Birchmeier, W., Lu, B., & Reichardt, L. F. (2003). Role of beta-catenin in synaptic vesicle localization and presynaptic assembly. *Neuron, 40*(4), 719-731. doi:10.1016/s0896-6273(03)00718-9

Bandtlow, C. E., & Zimmermann, D. R. (2000). Proteoglycans in the developing brain: new conceptual insights for old proteins. *Physiol Rev, 80*(4), 1267-1290. doi:10.1152/physrev.2000.80.4.1267

Bashaw, G. J., & Klein, R. (2010). Signaling from axon guidance receptors. *Cold Spring Harb Perspect Biol, 2*(5), a001941. doi:10.1101/cshperspect.a001941

Baumann, R., & Rys, P. (1999). Metachromatic activity of beta-cyclodextrin sulfates as heparin mimics. *Int J Biol Macromol, 24*(1), 15-18.

Beaubien, F., Raja, R., Kennedy, T. E., Fournier, A. E., & Cloutier, J.-F. (2016). Slitrk1 is localized to excitatory synapses and promotes their development. *Scientific reports, 6*, 27343-27343. doi:10.1038/srep27343

Bekhouche, M., Kronenberg, D., Vadon-Le Goff, S., Bijakowski, C., Lim, N. H., Font, B., . . . Moali, C. (2010). Role of the Netrin-like Domain of Procollagen C-Proteinase Enhancer-1 in the Control of Metalloproteinase Activity. *285*(21), 15950-15959. doi:10.1074/jbc.M109.086447

Bin, J. M., Han, D., Lai Wing Sun, K., Croteau, L. P., Dumontier, E., Cloutier, J. F., . . . Kennedy, T. E. (2015). Complete Loss of Netrin-1 Results in Embryonic Lethality and Severe Axon Guidance Defects without Increased Neural Cell Death. *Cell Rep, 12*(7), 1099-1106. doi:10.1016/j.celrep.2015.07.028

Bin, J. M., Rajasekharan, S., Kuhlmann, T., Hanes, I., Marcal, N., Han, D., . . . Kennedy, T. E. (2013). Full-length and fragmented netrin-1 in multiple sclerosis plaques are inhibitors of oligodendrocyte precursor cell migration. *Am J Pathol, 183*(3), 673-680. doi:10.1016/j.ajpath.2013.06.004

Blanchette, C. R., Perrat, P. N., Thackeray, A., & Bénard, C. Y. (2015). Glypican Is a Modulator of Netrin-Mediated Axon Guidance. *PLOS Biology, 13*(7), e1002183. doi:10.1371/journal.pbio.1002183

Blockus, H., & Chedotal, A. (2016). Slit-Robo signaling. *Development, 143*(17), 3037-3044. doi:10.1242/dev.132829

Bouchard, J. F., Horn, K. E., Stroh, T., & Kennedy, T. E. (2008). Depolarization recruits DCC to the plasma membrane of embryonic cortical neurons and enhances axon extension in response to netrin-1. *J Neurochem, 107*(2), 398-417. doi:10.1111/j.1471-4159.2008.05609.x

Bouchard, J. F., Moore, S. W., Tritsch, N. X., Roux, P. P., Shekarabi, M., Barker, P. A., & Kennedy, T. E. (2004). Protein kinase A activation promotes plasma membrane insertion of DCC from an intracellular pool: A novel mechanism regulating commissural axon extension. *J Neurosci, 24*(12), 3040-3050. doi:10.1523/jneurosci.4934-03.2004

Bourikas, D., Pekarik, V., Baeriswyl, T., Grunditz, A., Sadhu, R., Nardo, M., & Stoeckli, E. T. (2005). Sonic hedgehog guides commissural axons along the longitudinal axis of the spinal cord. *Nat Neurosci, 8*(3), 297-304. doi:10.1038/nn1396

Bouzioukh, F., Daoudal, G., Falk, J., Debanne, D., Rougon, G., & Castellani, V. (2006). Semaphorin3A regulates synaptic function of differentiated hippocampal neurons. *Eur J Neurosci, 23*(9), 2247-2254. doi:10.1111/j.1460-9568.2006.04783.x

Bovolenta, P., & Dodd, J. (1990). Guidance of commissural growth cones at the floor plate in embryonic rat spinal cord. *Development, 109*(2), 435-447.

Bozdagi, O., Shan, W., Tanaka, H., Benson, D. L., & Huntley, G. W. (2000). Increasing numbers of synaptic puncta during late-phase LTP: N-cadherin is synthesized, recruited to synaptic sites, and required for potentiation. *Neuron, 28*(1), 245-259. doi:10.1016/s0896-6273(00)00100-8

Bozdagi, O., Valcin, M., Poskanzer, K., Tanaka, H., & Benson, D. L. (2004). Temporally distinct demands for classic cadherins in synapse formation and maturation. *Mol Cell Neurosci, 27*(4), 509-521. doi:10.1016/j.mcn.2004.08.008

Bozzelli, P. L., Alaiyed, S., Kim, E., Villapol, S., & Conant, K. (2018). Proteolytic remodeling of perineuronal nets: Effects on synaptic plasticity and neuronal population dynamics. *Neural Plasticity, 2018*.

Braisted, J. E., Catalano, S. M., Stimac, R., Kennedy, T. E., Tessier-Lavigne, M., Shatz, C. J., & O'Leary, D. D. (2000). Netrin-1 promotes thalamic axon growth and is required for proper development of the thalamocortical projection. *J Neurosci, 20*(15), 5792-5801.

Brakebusch, C., Seidenbecher, C. I., Asztely, F., Rauch, U., Matthies, H., Meyer, H., . . . Fassler, R. (2002). Brevican-deficient mice display impaired hippocampal CA1 long-term potentiation but show no obvious deficits in learning and memory. *Mol Cell Biol, 22*(21), 7417-7427. doi:10.1128/mcb.22.21.7417-7427.2002

Brose, K., Bland, K. S., Wang, K. H., Arnott, D., Henzel, W., Goodman, C. S., . . . Kidd, T. (1999). Slit proteins bind Robo receptors and have an evolutionarily conserved role in repulsive axon guidance. *Cell, 96*(6), 795-806. doi:10.1016/s0092-8674(00)80590-5

Bruses, J. L. (2006). N-cadherin signaling in synapse formation and neuronal physiology. *Mol Neurobiol, 33*(3), 237-252. doi:10.1385/mn:33:3:237

Bulow, H. E., & Hobert, O. (2006). The molecular diversity of glycosaminoglycans shapes animal development. *Annu Rev Cell Dev Biol, 22*, 375-407. doi:10.1146/annurev.cellbio.22.010605.093433

Bülow, H. E., & Hobert, O. (2004). Differential Sulfations and Epimerization Define Heparan Sulfate Specificity in Nervous System Development. *Neuron, 41*(5), 723-736. doi:https://doi.org/10.1016/S0896-6273(04)00084-4

Butler, S. J., & Dodd, J. (2003). A role for BMP heterodimers in roof plate-mediated repulsion of commissural axons. *Neuron, 38*(3), 389-401. doi:10.1016/s0896-6273(03)00254-x

Caceres, A., Banker, G., Steward, O., Binder, L., & Payne, M. (1984). MAP2 is localized to the dendrites of hippocampal neurons which develop in culture. *Brain Res, 315*(2), 314-318. doi:10.1016/0165-3806(84)90167-6

Cardin, A. D., & Weintraub, H. J. (1989). Molecular modeling of protein-glycosaminoglycan interactions. *Arteriosclerosis, 9*(1), 21-32.

Carey, D. J. (1997). Syndecans: multifunctional cell-surface co-receptors. *Biochemical Journal, 327*(1), 1. doi:10.1042/bj3270001

Carstens, K. E., Phillips, M. L., Pozzo-Miller, L., Weinberg, R. J., & Dudek, S. M. (2016). Perineuronal Nets Suppress Plasticity of Excitatory Synapses on CA2 Pyramidal Neurons. *The Journal of Neuroscience, 36*(23), 6312. doi:10.1523/JNEUROSCI.0245-16.2016

Celio, M. R., & Blumcke, I. (1994). Perineuronal nets — a specialized form of extracellular matrix in the adult nervous system. *Brain Research Reviews, 19*(1), 128-145. doi:https://doi.org/10.1016/0165-0173(94)90006-X

Celio, M. R., Spreafico, R., De Biasi, S., & Vitellaro-Zuccarello, L. (1998). Perineuronal nets: past and present. *Trends in Neurosciences, 21*(12), 510-515. doi:https://doi.org/10.1016/S0166-2236(98)01298-3

Chan, S. S., Zheng, H., Su, M. W., Wilk, R., Killeen, M. T., Hedgecock, E. M., & Culotti, J. G. (1996). UNC-40, a C. elegans homolog of DCC (Deleted in Colorectal Cancer), is required in motile cells responding to UNC-6 netrin cues. *Cell, 87*(2), 187-195. doi:10.1016/s0092-8674(00)81337-9

Chanana, B., Steigemann, P., Jäckle, H., & Vorbrüggen, G. (2009). Reception of Slit requires only the chondroitin–sulphate-modified extracellular domain of Syndecan at the target cell surface. *Proceedings of the National Academy of Sciences, 106*(29), 11984. doi:10.1073/pnas.0901148106

Charron, F., Stein, E., Jeong, J., McMahon, A. P., & Tessier-Lavigne, M. (2003). The morphogen sonic hedgehog is an axonal chemoattractant that collaborates with netrin-1 in midline axon guidance. *Cell, 113*(1), 11-23. doi:10.1016/s0092-8674(03)00199-5

Chen, X. L., Nam, J.-O., Jean, C., Lawson, C., Walsh, C. T., Goka, E., . . . Schlaepfer, D. D. (2012). VEGF-induced vascular permeability is mediated by FAK. *Developmental cell, 22*(1), 146-157. doi:10.1016/j.devcel.2011.11.002

Chen, Z., Gore, B. B., Long, H., Ma, L., & Tessier-Lavigne, M. (2008). Alternative splicing of the Robo3 axon guidance receptor governs the midline switch from attraction to repulsion. *Neuron, 58*(3), 325-332. doi:10.1016/j.neuron.2008.02.016

Cho, K. R., Oliner, J. D., Simons, J. W., Hedrick, L., Fearon, E. R., Preisinger, A. C., . . . Vogelstein, B. (1994). The DCC gene: structural analysis and mutations in colorectal carcinomas. *Genomics, 19*(3), 525-531. doi:10.1006/geno.1994.1102

Clement, A. M., Nadanaka, S., Masayama, K., Mandl, C., Sugahara, K., & Faissner, A. (1998). The DSD-1 Carbohydrate Epitope Depends on Sulfation, Correlates with Chondroitin Sulfate D Motifs, and Is Sufficient to Promote Neurite Outgrowth. *273*(43), 28444-28453. doi:10.1074/jbc.273.43.28444

Clement, A. M., Sugahara, K., & Faissner, A. (1999). Chondroitin sulfate E promotes neurite outgrowth of rat embryonic day 18 hippocampal neurons. *Neurosci Lett, 269*(3), 125-128. doi:https://doi.org/10.1016/S0304-3940(99)00432-2

Colamarino, S. A., & Tessier-Lavigne, M. (1995). The axonal chemoattractant netrin-1 is also a chemorepellent for trochlear motor axons. *Cell, 81*(4), 621-629. doi:10.1016/0092-8674(95)90083-7

Cotrufo, T., Andres, R. M., Ros, O., Perez-Branguli, F., Muhaisen, A., Fuschini, G., . . . Soriano, E. (2012). Syntaxin 1 is required for DCC/Netrin-1-dependent chemoattraction of migrating neurons from the lower rhombic lip. *Eur J Neurosci, 36*(9), 3152-3164. doi:10.1111/j.1460-9568.2012.08259.x

Couchman, J. R., & Pataki, C. A. (2012). An introduction to proteoglycans and their localization. *The journal of histochemistry and cytochemistry : official journal of the Histochemistry Society, 60*(12), 885-897. doi:10.1369/0022155412464638

Croteau, L. P., Kao, T. J., & Kania, A. (2019). Ephrin-A5 potentiates netrin-1 axon guidance by enhancing Neogenin availability. *Sci Rep, 9*(1), 12009. doi:10.1038/s41598-019-48519-0

Cruciat, C.-M. (2014). Casein kinase 1 and Wnt/β-catenin signaling. *Current Opinion in Cell Biology, 31*, 46-55. doi:https://doi.org/10.1016/j.ceb.2014.08.003

Cui, H., Freeman, C., Jacobson, G. A., & Small, D. H. (2013). Proteoglycans in the central nervous system: role in development, neural repair, and Alzheimer's disease. *IUBMB Life, 65*(2), 108-120. doi:10.1002/iub.1118

Daugherty, R. L., & Gottardi, C. J. (2007). Phospho-regulation of Beta-catenin adhesion and signaling functions. *Physiology (Bethesda), 22*, 303-309. doi:10.1152/physiol.00020.2007

de la Torre, J. R., Hopker, V. H., Ming, G. L., Poo, M. M., Tessier-Lavigne, M., Hemmati-Brivanlou, A., & Holt, C. E. (1997). Turning of retinal growth cones in a netrin-1 gradient mediated by the netrin receptor DCC. *Neuron, 19*(6), 1211-1224. doi:10.1016/s0896-6273(00)80413-4

De Vries, M., & Cooper, H. M. (2008). Emerging roles for neogenin and its ligands in CNS development. *J Neurochem, 106*(4), 1483-1492. doi:10.1111/j.1471-4159.2008.05485.x

de Winter, F., Kwok, J. C., Fawcett, J. W., Vo, T. T., Carulli, D., & Verhaagen, J. (2016). The Chemorepulsive Protein Semaphorin 3A and Perineuronal Net-Mediated Plasticity. *Neural Plast, 2016*, 3679545. doi:10.1155/2016/3679545

de Wit, J., Toonen, R. F., Verhaagen, J., & Verhage, M. (2006). Vesicular trafficking of semaphorin 3A is activity-dependent and differs between axons and dendrites. *Traffic, 7*(8), 1060-1077. doi:10.1111/j.1600-0854.2006.00442.x

Deacon, S. W., Beeser, A., Fukui, J. A., Rennefahrt, U. E., Myers, C., Chernoff, J., & Peterson, J. R. (2008). An isoform-selective, small-molecule inhibitor targets the autoregulatory mechanism of p21-activated kinase. *Chem Biol, 15*(4), 322-331. doi:10.1016/j.chembiol.2008.03.005

Deepa, S. S., Carulli, D., Galtrey, C., Rhodes, K., Fukuda, J., Mikami, T., . . . Fawcett, J. W. (2006). Composition of perineuronal net extracellular matrix in rat brain: a different disaccharide composition for the net-associated proteoglycans. *J Biol Chem, 281*(26), 17789-17800. doi:10.1074/jbc.M600544200

Dent, E. W., Gupton, S. L., & Gertler, F. B. (2011). The growth cone cytoskeleton in axon outgrowth and guidance. *Cold Spring Harb Perspect Biol, 3*(3). doi:10.1101/cshperspect.a001800

Dhoot, G. K., Gustafsson, M. K., Ai, X., Sun, W., Standiford, D. M., & Emerson, C. P. (2001). Regulation of Wnt Signaling and Embryo Patterning by an Extracellular Sulfatase. *Science, 293*(5535), 1663. doi:10.1126/science.293.5535.1663

Dick, G., Tan, C. L., Alves, J. N., Ehlert, E. M., Miller, G. M., Hsieh-Wilson, L. C., . . . Kwok, J. C. (2013). Semaphorin 3A binds to the perineuronal nets via chondroitin sulfate type E motifs in rodent brains. *J Biol Chem, 288*(38), 27384-27395. doi:10.1074/jbc.M111.310029

Djerbal, L., Lortat-Jacob, H., & Kwok, J. (2017). Chondroitin sulfates and their binding molecules in the central nervous system. *Glycoconj J, 34*(3), 363-376. doi:10.1007/s10719-017-9761-z

Djerbal, L., Vives, R. R., Lopin-Bon, C., Richter, R. P., Kwok, J. C. F., & Lortat-Jacob, H. (2019). Semaphorin 3A binding to chondroitin sulfate E enhances the biological activity of the protein, and cross-links and rigidifies glycosaminoglycan matrices. *bioRxiv*, 851121. doi:10.1101/851121

Domanitskaya, E., Wacker, A., Mauti, O., Baeriswyl, T., Esteve, P., Bovolenta, P., & Stoeckli, E. T. (2010). Sonic hedgehog guides post-crossing commissural axons both directly and indirectly by regulating Wnt activity. *J Neurosci, 30*(33), 11167-11176. doi:10.1523/jneurosci.1488-10.2010

Dominici, C., Moreno-Bravo, J. A., Puiggros, S. R., Rappeneau, Q., Rama, N., Vieugue, P., . . . Chedotal, A. (2017). Floor-plate-derived netrin-1 is dispensable for commissural axon guidance. *Nature, 545*(7654), 350-354. doi:10.1038/nature22331

Drees, F., Pokutta, S., Yamada, S., Nelson, W. J., & Weis, W. I. (2005). Alpha-catenin is a molecular switch that binds E-cadherin-beta-catenin and regulates actin-filament assembly. *Cell, 123*(5), 903-915. doi:10.1016/j.cell.2005.09.021

Duan, X., Krishnaswamy, A., De la Huerta, I., & Sanes, J. R. (2014). Type II cadherins guide assembly of a direction-selective retinal circuit. *Cell, 158*(4), 793-807. doi:10.1016/j.cell.2014.06.047

Dutt, S., Cassoly, E., Dours-Zimmermann, M. T., Matasci, M., Stoeckli, E. T., & Zimmermann, D. R. (2011). Versican V0 and V1 Direct the Growth of Peripheral Axons in the Developing Chick Hindlimb. *The Journal of Neuroscience, 31*(14), 5262. doi:10.1523/JNEUROSCI.4897-10.2011

Erskine, L., & Herrera, E. (2007). The retinal ganglion cell axon's journey: insights into molecular mechanisms of axon guidance. *Dev Biol, 308*(1), 1-14. doi:10.1016/j.ydbio.2007.05.013

Ethell, I. M., & Yamaguchi, Y. (1999). Cell surface heparan sulfate proteoglycan syndecan-2 induces the maturation of dendritic spines in rat hippocampal neurons. *J Cell Biol, 144*(3), 575-586.

Evans, T. A., & Bashaw, G. J. (2010). Axon guidance at the midline: of mice and flies. *Curr Opin Neurobiol, 20*(1), 79-85. doi:10.1016/j.conb.2009.12.006

Fallon, L., Moreau, F., Croft, B. G., Labib, N., Gu, W. J., & Fon, E. A. (2002). Parkin and CASK/LIN-2 associate via a PDZ-mediated interaction and are co-localized in lipid rafts and postsynaptic densities in brain. *J Biol Chem, 277*(1), 486-491. doi:10.1074/jbc.M109806200

Fannon, A. M., & Colman, D. R. (1996). A model for central synaptic junctional complex formation based on the differential adhesive specificities of the cadherins. *Neuron, 17*(3), 423-434. doi:10.1016/s0896-6273(00)80175-0

Fawcett, J. (2009). Molecular control of brain plasticity and repair. *Prog Brain Res, 175*, 501-509. doi:10.1016/S0079-6123(09)17534-9

Fazeli, A., Dickinson, S. L., Hermiston, M. L., Tighe, R. V., Steen, R. G., Small, C. G., . . . Weinberg, R. A. (1997). Phenotype of mice lacking functional Deleted in colorectal cancer (Dcc) gene. *Nature, 386*(6627), 796-804. doi:10.1038/386796a0

Fearon, E. R., Cho, K. R., Nigro, J. M., Kern, S. E., Simons, J. W., Ruppert, J. M., . . . et al. (1990). Identification of a chromosome 18q gene that is altered in colorectal cancers. *Science, 247*(4938), 49-56. doi:10.1126/science.2294591

Filmus, J., Capurro, M., & Rast, J. (2008). Glypicans. *Genome biology, 9*(5), 224-224. doi:10.1186/gb-2008-9-5-224

Finci, L. I., Kruger, N., Sun, X., Zhang, J., Chegkazi, M., Wu, Y., . . . Meijers, R. (2014). The crystal structure of netrin-1 in complex with DCC reveals the bifunctionality of netrin-1 as a guidance cue. *Neuron, 83*(4), 839-849. doi:10.1016/j.neuron.2014.07.010

Fish, K. N. (2009). Total internal reflection fluorescence (TIRF) microscopy. *Curr Protoc Cytom, Chapter 12*, Unit12.18. doi:10.1002/0471142956.cy1218s50

Folkman, J., & Shing, Y. (1992). Angiogenesis. *J Biol Chem, 267*(16), 10931-10934.

Forcet, C., Stein, E., Pays, L., Corset, V., Llambi, F., Tessier-Lavigne, M., & Mehlen, P. (2002). Netrin-1-mediated axon outgrowth requires deleted in colorectal cancer-dependent MAPK activation. *Nature, 417*(6887), 443-447. doi:10.1038/nature748

Foscarin, S., Raha-Chowdhury, R., Fawcett, J. W., & Kwok, J. C. F. (2017). Brain ageing changes proteoglycan sulfation, rendering perineuronal nets more inhibitory. *Aging, 9*(6), 1607-1622. doi:10.18632/aging.101256

Foster, M., & Sherrington, C. S. (1897). A textbook of physiology. With C.S. Sherrington. Part 3. The central nervous system. Retrieved from https://archive.org/details/b21271458

Frantz, C., Stewart, K. M., & Weaver, V. M. (2010). The extracellular matrix at a glance. *Journal of Cell Science, 123*(24), 4195. doi:10.1242/jcs.023820

Frischknecht, R., Heine, M., Perrais, D., Seidenbecher, C. I., Choquet, D., & Gundelfinger, E. D. (2009). Brain extracellular matrix affects AMPA receptor lateral mobility and short-term synaptic plasticity. *Nat Neurosci, 12*(7), 897-904. doi:10.1038/nn.2338

Fuerer, C., Habib, S. J., & Nusse, R. (2010). A study on the interactions between heparan sulfate proteoglycans and Wnt proteins. *Developmental Dynamics, 239*(1), 184-190. doi:10.1002/dvdy.22067

Galko, M. J., & Tessier-Lavigne, M. (2000). Biochemical characterization of netrin-synergizing activity. *J Biol Chem, 275*(11), 7832-7838. doi:10.1074/jbc.275.11.7832

Galtrey, C. M., Asher, R. A., Nothias, F., & Fawcett, J. W. (2007). Promoting plasticity in the spinal cord with chondroitinase improves functional recovery after peripheral nerve repair. *Brain, 130*(Pt 4), 926-939. doi:10.1093/brain/awl372

Gandhi, N. S., & Mancera, R. L. (2008). The structure of glycosaminoglycans and their interactions with proteins. *Chem Biol Drug Des, 72*(6), 455-482. doi:10.1111/j.1747-0285.2008.00741.x

Garner, C. C., Zhai, R. G., Gundelfinger, E. D., & Ziv, N. E. (2002). Molecular mechanisms of CNS synaptogenesis. *Trends Neurosci, 25*(5), 243-251. doi:10.1016/s0166-2236(02)02152-5

Glasgow, S. D., Labrecque, S., Beamish, I. V., Aufmkolk, S., Gibon, J., Han, D., . . . Kennedy, T. E. (2018). Activity-Dependent Netrin-1 Secretion Drives Synaptic Insertion of GluA1-Containing AMPA Receptors in the Hippocampus. *Cell Rep, 25*(1), 168-182.e166. doi:10.1016/j.celrep.2018.09.028

Glickstein, M. (2006). Golgi and Cajal: The neuron doctrine and the 100th anniversary of the 1906 Nobel Prize. *Curr Biol, 16*(5), R147-151. doi:10.1016/j.cub.2006.02.053

Goldman, J. S., Ashour, M. A., Magdesian, M. H., Tritsch, N. X., Harris, S. N., Christofi, N., . . . Kennedy, T. E. (2013). Netrin-1 promotes excitatory synaptogenesis between cortical neurons by initiating synapse assembly. *J Neurosci, 33*(44), 17278-17289. doi:10.1523/jneurosci.1085-13.2013

Gopal, A. A., Rappaz, B., Rouger, V., Martyn, I. B., Dahlberg, P. D., Meland, R. J., . . . Wiseman, P. W. (2016). Netrin-1-Regulated Distribution of UNC5B and DCC in Live Cells Revealed by TICCS. *Biophysical journal, 110*(3), 623-634. doi:10.1016/j.bpj.2015.12.022

Gopal, A. A., Ricoult, S. G., Harris, S. N., Juncker, D., Kennedy, T. E., & Wiseman, P. W. (2017). Spatially Selective Dissection of Signal Transduction in Neurons Grown on Netrin-1 Printed Nanoarrays via Segmented Fluorescence Fluctuation Analysis. *ACS Nano, 11*(8), 8131-8143. doi:10.1021/acsnano.7b03004

Gorla, M., Santiago, C., Chaudhari, K., Layman, A. A. K., Oliver, P. M., & Bashaw, G. J. (2019). Ndfip Proteins Target Robo Receptors for Degradation and Allow Commissural Axons to Cross the Midline in the Developing Spinal Cord. *Cell Rep, 26*(12), 3298-3312.e3294. doi:10.1016/j.celrep.2019.02.080

Goutebroze, L., Carnaud, M., Denisenko, N., Boutterin, M.-C., & Girault, J.-A. J. B. N. (2003). Syndecan-3 and syndecan-4 are enriched in Schwann cell perinodal processes. *4*(1), 29. doi:10.1186/1471-2202-4-29

Gul, I. S., Hulpiau, P., Saeys, Y., & van Roy, F. (2017). Evolution and diversity of cadherins and catenins. *Exp Cell Res, 358*(1), 3-9. doi:10.1016/j.yexcr.2017.03.001

Hagihara, K., Watanabe, K., Chun, J., & Yamaguchi, Y. (2000). Glypican-4 is an FGF2-binding heparan sulfate proteoglycan expressed in neural precursor cells. *Developmental Dynamics, 219*(3), 353-367. doi:10.1002/1097-0177(2000)9999:9999<::AID-DVDY1059>3.0.CO;2-#

Halfter, W., Schurer, B., Yip, J., Yip, L., Tsen, G., Lee, J. A., & Cole, G. J. (1997). Distribution and substrate properties of agrin, a heparan sulfate proteoglycan of developing axonal pathways. *Journal of Comparative Neurology, 383*(1), 1-17. doi:10.1002/(SICI)1096-9861(19970623)383:1<1::AID-CNE1>3.0.CO;2-5

Hanke, J. H., Gardner, J. P., Dow, R. L., Changelian, P. S., Brissette, W. H., Weringer, E. J., . . . Connelly, P. A. (1996). Discovery of a novel, potent, and Src family-selective tyrosine kinase inhibitor. Study of Lck- and FynT-dependent T cell activation. *J Biol Chem, 271*(2), 695-701. doi:10.1074/jbc.271.2.695

Happel, M., & Frischknecht, R. (2016). Neuronal Plasticity in the Juvenile and Adult Brain Regulated by the Extracellular Matrix. In (pp. 143-158).

Harris, N. G., Nogueira, M. S., Verley, D. R., & Sutton, R. L. (2013). Chondroitinase enhances cortical map plasticity and increases functionally active sprouting axons after brain injury. *J Neurotrauma, 30*(14), 1257-1269. doi:10.1089/neu.2012.2737

Harris, R., Sabatelli, L. M., & Seeger, M. A. (1996). Guidance cues at the Drosophila CNS midline: identification and characterization of two Drosophila Netrin/UNC-6 homologs. *Neuron, 17*(2), 217-228. doi:10.1016/s0896-6273(00)80154-3

Hartmann, U., & Maurer, P. (2001). Proteoglycans in the nervous system — the quest for functional roles in vivo. *Matrix Biology, 20*(1), 23-35. doi:https://doi.org/10.1016/S0945-053X(00)00137-2

Helms, A. W., & Johnson, J. E. (2003). Specification of dorsal spinal cord interneurons. *Curr Opin Neurobiol, 13*(1), 42-49. doi:10.1016/s0959-4388(03)00010-2

Herbst, R., & Burden, S. J. (2000). The juxtamembrane region of MuSK has a critical role in agrin-mediated signaling. *Embo j, 19*(1), 67-77. doi:10.1093/emboj/19.1.67

Hilbig, H., Bidmon, H. J., Blohm, U., & Zilles, K. (2001). Wisteria floribunda agglutinin labeling patterns in the human cortex: a tool for revealing areal borders and subdivisions in parallel with immunocytochemistry. *Anat Embryol (Berl), 203*(1), 45-52.

Holley, J. A. (1982). Early development of the circumferential axonal pathway in mouse and chick spinal cord. *Journal of Comparative Neurology, 205*(4), 371-382. doi:10.1002/cne.902050406

Holt, C. E., & Dickson, B. J. (2005). Sugar codes for axons? *Neuron, 46*(2), 169-172. doi:10.1016/j.neuron.2005.03.021

Hong, K., Hinck, L., Nishiyama, M., Poo, M. M., Tessier-Lavigne, M., & Stein, E. (1999). A ligand-gated association between cytoplasmic domains of UNC5 and DCC family receptors converts netrin-induced growth cone attraction to repulsion. *Cell, 97*(7), 927-941. doi:10.1016/s0092-8674(00)80804-1

Horn, K. E., Glasgow, S. D., Gobert, D., Bull, S. J., Luk, T., Girgis, J., . . . Kennedy, T. E. (2013). DCC expression by neurons regulates synaptic plasticity in the adult brain. *Cell Rep, 3*(1), 173-185. doi:10.1016/j.celrep.2012.12.005

Huttner, W. B., Schiebler, W., Greengard, P., & De Camilli, P. (1983). Synapsin I (protein I), a nerve terminal-specific phosphoprotein. III. Its association with synaptic vesicles studied in a highly purified synaptic vesicle preparation. *J Cell Biol, 96*(5), 1374. doi:10.1083/jcb.96.5.1374

Hylin, M. J., Orsi, S. A., Moore, A. N., & Dash, P. K. (2013). Disruption of the perineuronal net in the hippocampus or medial prefrontal cortex impairs fear conditioning. *Learning & memory (Cold Spring Harbor, N.Y.), 20*(5), 267-273. doi:10.1101/lm.030197.112

Iglesias, B. V., Centeno, G., Pascuccelli, H., Ward, F., Peters, M. G., Filmus, J., . . . de Kier Joffe, E. B. (2008). Expression pattern of glypican-3 (GPC3) during human embryonic and fetal development. *Histol Histopathol, 23*(11), 1333-1340. doi:10.14670/hh-23.1333

Inatani, M., Irie, F., Plump, A. S., Tessier-Lavigne, M., & Yamaguchi, Y. (2003). Mammalian brain morphogenesis and midline axon guidance require heparan sulfate. *Science, 302*(5647), 1044-1046. doi:10.1126/science.1090497

Irvine, S. F., & Kwok, J. C. F. (2018). Perineuronal Nets in Spinal Motoneurones: Chondroitin Sulphate Proteoglycan around Alpha Motoneurones. *Int J Mol Sci, 19*(4). doi:10.3390/ijms19041172

Ishii, N., Wadsworth, W. G., Stern, B. D., Culotti, J. G., & Hedgecock, E. M. (1992). UNC-6, a laminin-related protein, guides cell and pioneer axon migrations in C. elegans. *Neuron, 9*(5), 873-881. doi:10.1016/0896-6273(92)90240-e

Islam, S. M., Shinmyo, Y., Okafuji, T., Su, Y., Naser, I. B., Ahmed, G., . . . Tanaka, H. (2009). Draxin, a repulsive guidance protein for spinal cord and forebrain commissures. *Science, 323*(5912), 388-393. doi:10.1126/science.1165187

Ivins, J. K., Litwack, E. D., Kumbasar, A., Stipp, C. S., & Lander, A. D. (1997). Cerebroglycan, a developmentally regulated cell-surface heparan sulfate proteoglycan, is expressed on developing axons and growth cones. *Dev Biol, 184*(2), 320-332. doi:10.1006/dbio.1997.8532

Jen, Y.-H. L., Musacchio, M., & Lander, A. D. (2009). Glypican-1 controls brain size through regulation of fibroblast growth factor signaling in early neurogenesis. *Neural development, 4*, 33-33. doi:10.1186/1749-8104-4-33

Johnson, K. G., Ghose, A., Epstein, E., Lincecum, J., O'Connor, M. B., & Van Vactor, D. (2004). Axonal Heparan Sulfate Proteoglycans Regulate the Distribution and Efficiency of the Repellent Slit

during Midline Axon Guidance. *Current Biology, 14*(6), 499-504. doi:https://doi.org/10.1016/j.cub.2004.02.005

Jungling, K., Eulenburg, V., Moore, R., Kemler, R., Lessmann, V., & Gottmann, K. (2006). N-cadherin transsynaptically regulates short-term plasticity at glutamatergic synapses in embryonic stem cell-derived neurons. *J Neurosci, 26*(26), 6968-6978. doi:10.1523/jneurosci.1013-06.2006

Kaksonen, M., Pavlov, I., Võikar, V., Lauri, S. E., Hienola, A., Riekki, R., . . . Rauvala, H. (2002). Syndecan-3-Deficient Mice Exhibit Enhanced LTP and Impaired Hippocampus-Dependent Memory. *Molecular and Cellular Neuroscience, 21*(1), 158-172. doi:https://doi.org/10.1006/mcne.2002.1167

Kam, Y., & Quaranta, V. (2009). Cadherin-bound beta-catenin feeds into the Wnt pathway upon adherens junctions dissociation: evidence for an intersection between beta-catenin pools. *PLoS One, 4*(2), e4580-e4580. doi:10.1371/journal.pone.0004580

Kantor, D. B., Chivatakarn, O., Peer, K. L., Oster, S. F., Inatani, M., Hansen, M. J., . . . Kolodkin, A. L. (2004). Semaphorin 5A is a bifunctional axon guidance cue regulated by heparan and chondroitin sulfate proteoglycans. *Neuron, 44*(6), 961-975. doi:10.1016/j.neuron.2004.12.002

Kappler, J., Franken, S., Junghans, U., Hoffmann, R., Linke, T., Müller, H. W., & Koch, K.-W. (2000). Glycosaminoglycan-Binding Properties and Secondary Structure of the C-Terminus of Netrin-1. *Biochemical and Biophysical Research Communications, 271*(2), 287-291. doi:https://doi.org/10.1006/bbrc.2000.2583

Karthikeyan, L., Flad, M., Engel, M., Meyer-Puttlitz, B., Margolis, R. U., & Margolis, R. K. (1994). Immunocytochemical and in situ hybridization studies of the heparan sulfate proteoglycan, glypican, in nervous tissue. *Journal of Cell Science, 107*(11), 3213. Retrieved from http://jcs.biologists.org/content/107/11/3213.abstract

Kastenhuber, E., Kern, U., Bonkowsky, J. L., Chien, C.-B., Driever, W., & Schweitzer, J. (2009). Netrin-DCC, Robo-Slit, and Heparan Sulfate Proteoglycans Coordinate Lateral Positioning of Longitudinal Dopaminergic Diencephalospinal Axons. *The Journal of Neuroscience, 29*(28), 8914. doi:10.1523/JNEUROSCI.0568-09.2009

Kearns, A. E., Vertel, B. M., & Schwartz, N. B. (1993). Topography of glycosylation and UDP-xylose production. *268*(15), 11097-11104. Retrieved from http://www.jbc.org/content/268/15/11097.abstract

Keino-Masu, K., Masu, M., Hinck, L., Leonardo, E. D., Chan, S. S., Culotti, J. G., & Tessier-Lavigne, M. (1996). Deleted in Colorectal Cancer (DCC) encodes a netrin receptor. *Cell, 87*(2), 175-185. doi:10.1016/s0092-8674(00)81336-7

Keleman, K., Rajagopalan, S., Cleppien, D., Teis, D., Paiha, K., Huber, L. A., . . . Dickson, B. J. (2002). Comm sorts robo to control axon guidance at the Drosophila midline. *Cell, 110*(4), 415-427. doi:10.1016/s0092-8674(02)00901-7

Kennedy, T. E. (2000). Cellular mechanisms of netrin function: long-range and short-range actions. *Biochem Cell Biol, 78*(5), 569-575.

Kennedy, T. E., Serafini, T., de la Torre, J. R., & Tessier-Lavigne, M. (1994). Netrins are diffusible chemotropic factors for commissural axons in the embryonic spinal cord. *Cell, 78*(3), 425-435. doi:10.1016/0092-8674(94)90421-9

Kennedy, T. E., Wang, H., Marshall, W., & Tessier-Lavigne, M. (2006). Axon guidance by diffusible chemoattractants: a gradient of netrin protein in the developing spinal cord. *J Neurosci, 26*(34), 8866-8874. doi:10.1523/jneurosci.5191-05.2006

Kent, C. B., Shimada, T., Ferraro, G. B., Ritter, B., Yam, P. T., McPherson, P. S., . . . Fournier, A. E. (2010). 14-3-3 proteins regulate protein kinase a activity to modulate growth cone turning responses. *J Neurosci, 30*(42), 14059-14067. doi:10.1523/jneurosci.3883-10.2010

Kidd, T., Bland, K. S., & Goodman, C. S. (1999). Slit is the midline repellent for the robo receptor in Drosophila. *Cell, 96*(6), 785-794. doi:10.1016/s0092-8674(00)80589-9

Kidd, T., Brose, K., Mitchell, K. J., Fetter, R. D., Tessier-Lavigne, M., Goodman, C. S., & Tear, G. (1998). Roundabout controls axon crossing of the CNS midline and defines a novel subfamily of

evolutionarily conserved guidance receptors. *Cell, 92*(2), 205-215. doi:10.1016/s0092-8674(00)80915-0

Knaggs, E. A., & Nepras, M. J. (2005). Sulfonation and Sulfation. In *Van Nostrand's Encyclopedia of Chemistry*.

Ko, J. (2012). The leucine-rich repeat superfamily of synaptic adhesion molecules: LRRTMs and Slitrks. *Molecules and Cells, 34*(4), 335-340. doi:10.1007/s10059-012-0113-3

Kolodkin, A. L., & Tessier-Lavigne, M. (2011). Mechanisms and molecules of neuronal wiring: a primer. *Cold Spring Harb Perspect Biol, 3*(6). doi:10.1101/cshperspect.a001727

Kolodziej, P. A., Timpe, L. C., Mitchell, K. J., Fried, S. R., Goodman, C. S., Jan, L. Y., & Jan, Y. N. (1996). frazzled encodes a Drosophila member of the DCC immunoglobulin subfamily and is required for CNS and motor axon guidance. *Cell, 87*(2), 197-204. doi:10.1016/s0092-8674(00)81338-0

Kostetskii, I., Li, J., Xiong, Y., Zhou, R., Ferrari, V. A., Patel, V. V., . . . Radice, G. L. (2005). Induced deletion of the N-cadherin gene in the heart leads to dissolution of the intercalated disc structure. *Circ Res, 96*(3), 346-354. doi:10.1161/01.RES.0000156274.72390.2c

Kwok, J. C., Carulli, D., & Fawcett, J. W. (2010). In vitro modeling of perineuronal nets: hyaluronan synthase and link protein are necessary for their formation and integrity. *J Neurochem, 114*(5), 1447-1459. doi:10.1111/j.1471-4159.2010.06878.x

Kwok, J. C., Dick, G., Wang, D., & Fawcett, J. W. (2011). Extracellular matrix and perineuronal nets in CNS repair. *Developmental neurobiology, 71*(11), 1073-1089. doi:10.1002/dneu.20974

Laemmli, U. K. (1970). Cleavage of structural proteins during the assembly of the head of bacteriophage T4. *Nature, 227*(5259), 680-685. doi:10.1038/227680a0

Lai Wing Sun, K., Correia, J. P., & Kennedy, T. E. (2011). Netrins: versatile extracellular cues with diverse functions. *Development, 138*(11), 2153-2169. doi:10.1242/dev.044529

Lander, C., Kind, P., Maleski, M., & Hockfield, S. (1997). A family of activity-dependent neuronal cell-surface chondroitin sulfate proteoglycans in cat visual cortex. *J Neurosci, 17*(6), 1928-1939.

Lander, C., Zhang, H., & Hockfield, S. (1998). Neurons Produce a Neuronal Cell Surface-Associated Chondroitin Sulfate Proteoglycan. *The Journal of Neuroscience, 18*(1), 174. doi:10.1523/JNEUROSCI.18-01-00174.1998

Laurie, G. W., Leblond, C. P., & Martin, G. R. (1983). Light microscopic immunolocalization of type IV collagen, laminin, heparan sulfate proteoglycan, and fibronectin in the basement membranes of a variety of rat organs. *American Journal of Anatomy, 167*(1), 71-82. doi:10.1002/aja.1001670107

Le, T. L., Yap, A. S., & Stow, J. L. (1999). Recycling of E-Cadherin. *J Cell Biol, 146*(1), 219. doi:10.1083/jcb.146.1.219

Lensjø, K. K., Christensen, A. C., Tennøe, S., Fyhn, M., & Hafting, T. (2017). Differential Expression and Cell-Type Specificity of Perineuronal Nets in Hippocampus, Medial Entorhinal Cortex, and Visual Cortex Examined in the Rat and Mouse. *eNeuro, 4*(3), ENEURO.0379-0316.2017. doi:10.1523/ENEURO.0379-16.2017

Lensjo, K. K., Lepperod, M. E., Dick, G., Hafting, T., & Fyhn, M. (2017). Removal of Perineuronal Nets Unlocks Juvenile Plasticity Through Network Mechanisms of Decreased Inhibition and Increased Gamma Activity. *J Neurosci, 37*(5), 1269-1283. doi:10.1523/jneurosci.2504-16.2016

Leonardo, E. D., Hinck, L., Masu, M., Keino-Masu, K., Ackerman, S. L., & Tessier-Lavigne, M. (1997). Vertebrate homologues of C. elegans UNC-5 are candidate netrin receptors. *Nature, 386*(6627), 833-838. doi:10.1038/386833a0

Li, W., Lee, J., Vikis, H. G., Lee, S. H., Liu, G., Aurandt, J., . . . Guan, K. L. (2004). Activation of FAK and Src are receptor-proximal events required for netrin signaling. *Nat Neurosci, 7*(11), 1213-1221. doi:10.1038/nn1329

Litwack, E. D., Ivins, J. K., Kumbasar, A., Paine-Saunders, S., Stipp, C. S., & Lander, A. D. (1998). Expression of the heparan sulfate proteoglycan glypican-1 in the developing rodent. *Developmental Dynamics, 211*(1), 72-87. doi:10.1002/(SICI)1097-0177(199801)211:1<72::AID-AJA7>3.0.CO;2-4

Liu, Y. T., Nian, F. S., Chou, W. J., Tai, C. Y., Kwan, S. Y., Chen, C., . . . Tsai, J. W. (2016). PRRT2 mutations lead to neuronal dysfunction and neurodevelopmental defects. *Oncotarget, 7*(26), 39184-39196. doi:10.18632/oncotarget.9258

Lodish, H., Berk, A., Kaiser, C. A., Matsudaira, P., Krieger, M., Darnell, J., . . . Zipursky, L. (2004). *Molecular Cell Biology*: Macmillan.

Long, H., Sabatier, C., Ma, L., Plump, A., Yuan, W., Ornitz, D. M., . . . Tessier-Lavigne, M. (2004). Conserved roles for Slit and Robo proteins in midline commissural axon guidance. *Neuron, 42*(2), 213-223. doi:10.1016/s0896-6273(04)00179-5

Lorentzen, Å. R., Melum, E., Ellinghaus, E., Smestad, C., Mero, I.-L., Aarseth, J. H., . . . Harbo, H. F. (2010). Association to the Glypican-5 gene in multiple sclerosis. *Journal of Neuroimmunology, 226*(1), 194-197. doi:https://doi.org/10.1016/j.jneuroim.2010.07.003

Luo, Y., Raible, D., & Raper, J. A. (1993). Collapsin: A protein in brain that induces the collapse and paralysis of neuronal growth cones. *Cell, 75*(2), 217-227. doi:https://doi.org/10.1016/0092-8674(93)80064-L

Lyuksyutova, A. I., Lu, C. C., Milanesio, N., King, L. A., Guo, N., Wang, Y., . . . Zou, Y. (2003). Anterior-posterior guidance of commissural axons by Wnt-frizzled signaling. *Science, 302*(5652), 1984-1988. doi:10.1126/science.1089610

Ma, J., Zhao, J., Lu, J., Wang, P., Feng, H., Zong, Y., . . . Lu, A. (2016). Cadherin-12 enhances proliferation in colorectal cancer cells and increases progression by promoting EMT. *Tumour Biol, 37*(7), 9077-9088. doi:10.1007/s13277-015-4555-z

Maleski, M., & Hockfield, S. (1997). Glial cells assemble hyaluronan-based pericellular matrices in vitro. *Glia, 20*(3), 193-202. doi:10.1002/(SICI)1098-1136(199707)20:3<193::AID-GLIA3>3.0.CO;2-9

Manabe, T., Togashi, H., Uchida, N., Suzuki, S. C., Hayakawa, Y., Yamamoto, M., . . . Chisaka, O. (2000). Loss of cadherin-11 adhesion receptor enhances plastic changes in hippocampal synapses and modifies behavioral responses. *Mol Cell Neurosci, 15*(6), 534-546. doi:10.1006/mcne.2000.0849

Manitt, C., Colicos, M. A., Thompson, K. M., Rousselle, E., Peterson, A. C., & Kennedy, T. E. (2001). Widespread expression of netrin-1 by neurons and oligodendrocytes in the adult mammalian spinal cord. *J Neurosci, 21*(11), 3911-3922.

Manitt, C., Nikolakopoulou, A. M., Almario, D. R., Nguyen, S. A., & Cohen-Cory, S. (2009). Netrin participates in the development of retinotectal synaptic connectivity by modulating axon arborization and synapse formation in the developing brain. *J Neurosci, 29*(36), 11065-11077. doi:10.1523/jneurosci.0947-09.2009

Maro, G. S., Klassen, M. P., & Shen, K. (2009). A beta-catenin-dependent Wnt pathway mediates anteroposterior axon guidance in C. elegans motor neurons. *PLoS One, 4*(3), e4690. doi:10.1371/journal.pone.0004690

Matsumoto, Y., Irie, F., Inatani, M., Tessier-Lavigne, M., & Yamaguchi, Y. (2007). Netrin-1/DCC signaling in commissural axon guidance requires cell-autonomous expression of heparan sulfate. *J Neurosci, 27*(16), 4342-4350. doi:10.1523/jneurosci.0700-07.2007

Matsunaga, M., Hatta, K., Nagafuchi, A., & Takeichi, M. (1988). Guidance of optic nerve fibres by N-cadherin adhesion molecules. *Nature, 334*(6177), 62-64. doi:10.1038/334062a0

Mayer, M., Bercsenyi, K., Geczi, K., Szabo, G., & Lele, Z. (2010). Expression of two type II cadherins, Cdh12 and Cdh22 in the developing and adult mouse brain. *Gene Expr Patterns, 10*(7-8), 351-360. doi:10.1016/j.gep.2010.08.002

McCrea, P. D., & Gu, D. (2010). The catenin family at a glance. *J Cell Sci, 123*(Pt 5), 637-642. doi:10.1242/jcs.039842

Ming, G. L., Song, H. J., Berninger, B., Holt, C. E., Tessier-Lavigne, M., & Poo, M. M. (1997). cAMP-dependent growth cone guidance by netrin-1. *Neuron, 19*(6), 1225-1235. doi:10.1016/s0896-6273(00)80414-6

Moon, L. D. F., Asher, R. A., Rhodes, K. E., & Fawcett, J. W. (2001). Regeneration of CNS axons back to their target following treatment of adult rat brain with chondroitinase ABC. *Nat Neurosci, 4*(5), 465-466. doi:10.1038/87415

Moore, S. W., Biais, N., & Sheetz, M. P. (2009). Traction on immobilized netrin-1 is sufficient to reorient axons. *Science, 325*(5937), 166. doi:10.1126/science.1173851

Moore, S. W., Correia, J. P., Lai Wing Sun, K., Pool, M., Fournier, A. E., & Kennedy, T. E. (2008). Rho inhibition recruits DCC to the neuronal plasma membrane and enhances axon chemoattraction to netrin 1. *Development, 135*(17), 2855-2864. doi:10.1242/dev.024133

Moore, S. W., & Kennedy, T. E. (2008). Dissection and culture of embryonic spinal commissural neurons. *Curr Protoc Neurosci, Chapter 3*, Unit 3.20. doi:10.1002/0471142301.ns0320s45

Moore, S. W., Zhang, X., Lynch, C. D., & Sheetz, M. P. (2012). Netrin-1 attracts axons through FAK-dependent mechanotransduction. *J Neurosci, 32*(34), 11574-11585. doi:10.1523/jneurosci.0999-12.2012

Moreno-Bravo, J. A., Roig Puiggros, S., Mehlen, P., & Chedotal, A. (2019). Synergistic Activity of Floor-Plate- and Ventricular-Zone-Derived Netrin-1 in Spinal Cord Commissural Axon Guidance. *Neuron, 101*(4), 625-634.e623. doi:10.1016/j.neuron.2018.12.024

Murakami, K., Tanaka, T., Bando, Y., & Yoshida, S. (2015). Nerve injury induces the expression of syndecan-1 heparan sulfate proteoglycan in primary sensory neurons. *Neuroscience, 300*, 338-350. doi:https://doi.org/10.1016/j.neuroscience.2015.05.033

Nakanishi, T., Kadomatsu, K., Okamoto, T., Ichihara-Tanaka, K., Kojima, T., Saito, H., . . . Muramatsu, T. (1997). Expression of syndecan-1 and -3 during embryogenesis of the central nervous system in relation to binding with midkine. *J Biochem, 121*(2), 197-205.

Nawabi, H., Briançon-Marjollet, A., Clark, C., Sanyas, I., Takamatsu, H., Okuno, T., . . . Castellani, V. (2010). A midline switch of receptor processing regulates commissural axon guidance in vertebrates. *Genes & development, 24*(4), 396-410. doi:10.1101/gad.542510

Nechiporuk, T., Fernandez, T. E., & Vasioukhin, V. (2007). Failure of Epithelial Tube Maintenance Causes Hydrocephalus and Renal Cysts in Dlg5−/− Mice. *Developmental cell, 13*(3), 338-350. doi:https://doi.org/10.1016/j.devcel.2007.07.017

Nishitani, A. M., Ohta, S., Yung, A. R., Del Rio, T., Gordon, M. I., Abraira, V. E., . . . Goodrich, L. V. (2017). Distinct functions for netrin 1 in chicken and murine semicircular canal morphogenesis. *Development, 144*(18), 3349-3360. doi:10.1242/dev.144519

Noren, N. K., Niessen, C. M., Gumbiner, B. M., & Burridge, K. (2001). Cadherin engagement regulates Rho family GTPases. *The Journal of biological chemistry, 276*(36), 33305-33308. doi:10.1074/jbc.C100306200

Okada, A., Charron, F., Morin, S., Shin, D. S., Wong, K., Fabre, P. J., . . . McConnell, S. K. (2006). Boc is a receptor for sonic hedgehog in the guidance of commissural axons. *Nature, 444*(7117), 369-373. doi:10.1038/nature05246

Okuda, T., Yu, L. M., Cingolani, L. A., Kemler, R., & Goda, Y. (2007). beta-Catenin regulates excitatory postsynaptic strength at hippocampal synapses. *Proc Natl Acad Sci U S A, 104*(33), 13479-13484. doi:10.1073/pnas.0702334104

Ornitz, D. M., Yayon, A., Flanagan, J. G., Svahn, C. M., Levi, E., & Leder, P. (1992). Heparin is required for cell-free binding of basic fibroblast growth factor to a soluble receptor and for mitogenesis in whole cells. *Molecular and Cellular Biology, 12*(1), 240. doi:10.1128/MCB.12.1.240

Patel, S. D., Chen, C. P., Bahna, F., Honig, B., & Shapiro, L. (2003). Cadherin-mediated cell-cell adhesion: sticking together as a family. *Curr Opin Struct Biol, 13*(6), 690-698. doi:10.1016/j.sbi.2003.10.007

Phan, K. D., Croteau, L. P., Kam, J. W., Kania, A., Cloutier, J. F., & Butler, S. J. (2011). Neogenin may functionally substitute for Dcc in chicken. *PLoS One, 6*(7), e22072. doi:10.1371/journal.pone.0022072

Piedra, J., Miravet, S., Castano, J., Palmer, H. G., Heisterkamp, N., Garcia de Herreros, A., & Dunach, M. (2003). p120 Catenin-associated Fer and Fyn tyrosine kinases regulate beta-catenin Tyr-142

phosphorylation and beta-catenin-alpha-catenin Interaction. *Mol Cell Biol, 23*(7), 2287-2297. doi:10.1128/mcb.23.7.2287-2297.2003

Pignata, A., Ducuing, H., & Castellani, V. (2016). Commissural axon navigation: Control of midline crossing in the vertebrate spinal cord by the semaphorin 3B signaling. *Cell Adh Migr, 10*(6), 604-617. doi:10.1080/19336918.2016.1212804

Pizzorusso, T., Medini, P., Berardi, N., Chierzi, S., Fawcett, J. W., & Maffei, L. (2002). Reactivation of ocular dominance plasticity in the adult visual cortex. *Science, 298*(5596), 1248-1251. doi:10.1126/science.1072699

Pratt, T., Conway, C. D., Tian, N. M., Price, D. J., & Mason, J. O. (2006). Heparan sulphation patterns generated by specific heparan sulfotransferase enzymes direct distinct aspects of retinal axon guidance at the optic chiasm. *J Neurosci, 26*(26), 6911-6923. doi:10.1523/jneurosci.0505-06.2006

Pratt, T., Davey, J. W., Nowakowski, T. J., Raasumaa, C., Rawlik, K., McBride, D., . . . Price, D. J. (2012). The expression and activity of beta-catenin in the thalamus and its projections to the cerebral cortex in the mouse embryo. *BMC Neurosci, 13*, 20. doi:10.1186/1471-2202-13-20

Price, S. R., De Marco Garcia, N. V., Ranscht, B., & Jessell, T. M. (2002). Regulation of motor neuron pool sorting by differential expression of type II cadherins. *Cell, 109*(2), 205-216. doi:10.1016/s0092-8674(02)00695-5

Pyka, M., Wetzel, C., Aguado, A., Geissler, M., Hatt, H., & Faissner, A. (2011). Chondroitin sulfate proteoglycans regulate astrocyte-dependent synaptogenesis and modulate synaptic activity in primary embryonic hippocampal neurons. *Eur J Neurosci, 33*(12), 2187-2202. doi:10.1111/j.1460-9568.2011.07690.x

Qu, C., Dwyer, T., Shao, Q., Yang, T., Huang, H., & Liu, G. (2013). Direct binding of TUBB3 with DCC couples netrin-1 signaling to intracellular microtubule dynamics in axon outgrowth and guidance. *Journal of Cell Science, 126*(Pt 14), 3070-3081. doi:10.1242/jcs.122184

Rajagopalan, S., Vivancos, V., Nicolas, E., & Dickson, B. J. (2000). Selecting a longitudinal pathway: Robo receptors specify the lateral position of axons in the Drosophila CNS. *Cell, 103*(7), 1033-1045. doi:10.1016/s0092-8674(00)00207-5

Rajasekharan, S., Baker, K. A., Horn, K. E., Jarjour, A. A., Antel, J. P., & Kennedy, T. E. (2009). Netrin 1 and Dcc regulate oligodendrocyte process branching and membrane extension via Fyn and RhoA. *Development, 136*(3), 415-426. doi:10.1242/dev.018234

Rajasekharan, S., & Kennedy, T. E. (2009). The netrin protein family. *Genome biology, 10*(9), 239. doi:10.1186/gb-2009-10-9-239

Rama, N., Goldschneider, D., Corset, V., Lambert, J., Pays, L., & Mehlen, P. (2012). Amyloid Precursor Protein Regulates Netrin-1-mediated Commissural Axon Outgrowth. *287*(35), 30014-30023. doi:10.1074/jbc.M111.324780

Rapraeger, A. C., Krufka, A., & Olwin, B. B. (1991). Requirement of heparan sulfate for bFGF-mediated fibroblast growth and myoblast differentiation. *Science, 252*(5013), 1705. doi:10.1126/science.1646484

Rawson, J. M., Dimitroff, B., Johnson, K. G., Rawson, J. M., Ge, X., Van Vactor, D., & Selleck, S. B. (2005). The Heparan Sulfate Proteoglycans Dally-like and Syndecan Have Distinct Functions in Axon Guidance and Visual-System Assembly in Drosophila. *Current Biology, 15*(9), 833-838. doi:https://doi.org/10.1016/j.cub.2005.03.039

Redies, C. (1995). Cadherin expression in the developing vertebrate CNS: from neuromeres to brain nuclei and neural circuits. *Exp Cell Res, 220*(2), 243-256. doi:10.1006/excr.1995.1313

Redies, C., Inuzuka, H., & Takeichi, M. (1992). Restricted expression of N- and R-cadherin on neurites of the developing chicken CNS. *J Neurosci, 12*(9), 3525-3534.

Redies, C., & Takeichi, M. (1996). Cadherins in the developing central nervous system: an adhesive code for segmental and functional subdivisions. *Dev Biol, 180*(2), 413-423. doi:10.1006/dbio.1996.0315

Reichardt, L. F., & Tomaselli, K. J. (1991). Extracellular matrix molecules and their receptors: functions in neural development. *Annual review of neuroscience, 14*, 531-570. doi:10.1146/annurev.ne.14.030191.002531

Ren, X. R., Ming, G. L., Xie, Y., Hong, Y., Sun, D. M., Zhao, Z. Q., . . . Xiong, W. C. (2004). Focal adhesion kinase in netrin-1 signaling. *Nat Neurosci, 7*(11), 1204-1212. doi:10.1038/nn1330

Reyes-Mugica, M., Meyerhardt, J. A., Rzasa, J., Rimm, D. L., Johnson, K. R., Wheelock, M. J., & Reale, M. A. (2001). Truncated DCC reduces N-cadherin/catenin expression and calcium-dependent cell adhesion in neuroblastoma cells. *Lab Invest, 81*(2), 201-210. doi:10.1038/labinvest.3780228

Rhiner, C., Gysi, S., Fröhli, E., Hengartner, M. O., & Hajnal, A. (2005). Syndecan regulates cell migration and axon guidance in <em>C. elegans</em&gt. *Development, 132*(20), 4621. doi:10.1242/dev.02042

Ridley, A. J. (2001). Rho GTPases and cell migration. *J Cell Sci, 114*(Pt 15), 2713-2722.

Rodrigues, S. (2011). *Signaling Mechanisms that Regulate Cytoskeletal Organization Downstream of Netrin-1 Mediated Axonal Chemoattraction* (Doctor of Philosophy). McGill University,

Romberg, C., Yang, S., Melani, R., Andrews, M. R., Horner, A. E., Spillantini, M. G., . . . Saksida, L. M. (2013). Depletion of perineuronal nets enhances recognition memory and long-term depression in the perirhinal cortex. *J Neurosci, 33*(16), 7057-7065. doi:10.1523/jneurosci.6267-11.2013

Ronca, F., Andersen, J. S., Paech, V., & Margolis, R. U. (2001). Characterization of Slit Protein Interactions with Glypican-1. *276*(31), 29141-29147. doi:10.1074/jbc.M100240200

Rönnberg, E., Melo, F. R., & Pejler, G. (2012). Mast cell proteoglycans. *The journal of histochemistry and cytochemistry : official journal of the Histochemistry Society, 60*(12), 950-962. doi:10.1369/0022155412458927

Ruoslahti, E. (1988). Structure and biology of proteoglycans. *Annu Rev Cell Biol, 4*, 229-255. doi:10.1146/annurev.cb.04.110188.001305

Sabatier, C., Plump, A. S., Le, M., Brose, K., Tamada, A., Murakami, F., . . . Tessier-Lavigne, M. (2004). The divergent Robo family protein rig-1/Robo3 is a negative regulator of slit responsiveness required for midline crossing by commissural axons. *Cell, 117*(2), 157-169. doi:10.1016/s0092-8674(04)00303-4

Saglietti, L., Dequidt, C., Kamieniarz, K., Rousset, M. C., Valnegri, P., Thoumine, O., . . . Passafaro, M. (2007). Extracellular interactions between GluR2 and N-cadherin in spine regulation. *Neuron, 54*(3), 461-477. doi:10.1016/j.neuron.2007.04.012

Sakai, N., Insolera, R., Sillitoe, R. V., Shi, S. H., & Kaprielian, Z. (2012). Axon sorting within the spinal cord marginal zone via Robo-mediated inhibition of N-cadherin controls spinocerebellar tract formation. *J Neurosci, 32*(44), 15377-15387. doi:10.1523/jneurosci.2225-12.2012

Salinas, P. C., & Price, S. R. (2005). Cadherins and catenins in synapse development. *Curr Opin Neurobiol, 15*(1), 73-80. doi:10.1016/j.conb.2005.01.001

Sarrazin, S., Lamanna, W. C., & Esko, J. D. (2011). Heparan sulfate proteoglycans. *Cold Spring Harb Perspect Biol, 3*(7). doi:10.1101/cshperspect.a004952

Sasisekharan, R., & Venkataraman, G. (2000). Heparin and heparan sulfate: biosynthesis, structure and function. *Current Opinion in Chemical Biology, 4*(6), 626-631. doi:https://doi.org/10.1016/S1367-5931(00)00145-9

Saunders, S., Paine-Saunders, S., & Lander, A. D. (1997). Expression of the Cell Surface Proteoglycan Glypican-5 Is Developmentally Regulated in Kidney, Limb, and Brain. *Dev Biol, 190*(1), 78-93. doi:https://doi.org/10.1006/dbio.1997.8690

Schaefer, L., & Schaefer, R. M. (2009). Proteoglycans: from structural compounds to signaling molecules. *Cell and Tissue Research, 339*(1), 237. doi:10.1007/s00441-009-0821-y

Selig, S., Lidov, H. G., Bruno, S. A., Segal, M. M., & Kunkel, L. M. (1997). Molecular characterization of Br-cadherin, a developmentally regulated, brain-specific cadherin. *Proc Natl Acad Sci U S A, 94*(6), 2398-2403. doi:10.1073/pnas.94.6.2398

Serafini, T., Colamarino, S. A., Leonardo, E. D., Wang, H., Beddington, R., Skarnes, W. C., & Tessier-Lavigne, M. (1996). Netrin-1 is required for commissural axon guidance in the developing vertebrate nervous system. *Cell, 87*(6), 1001-1014. doi:10.1016/s0092-8674(00)81795-x

Serafini, T., Kennedy, T. E., Galko, M. J., Mirzayan, C., Jessell, T. M., & Tessier-Lavigne, M. (1994). The netrins define a family of axon outgrowth-promoting proteins homologous to C. elegans UNC-6. *Cell, 78*(3), 409-424. doi:10.1016/0092-8674(94)90420-0

Shapiro, L., & Colman, D. R. (1999). The diversity of cadherins and implications for a synaptic adhesive code in the CNS. *Neuron, 23*(3), 427-430. doi:10.1016/s0896-6273(00)80796-5

Shapiro, L., & Weis, W. I. (2009). Structure and biochemistry of cadherins and catenins. *Cold Spring Harb Perspect Biol, 1*(3), a003053. doi:10.1101/cshperspect.a003053

Shekarabi, M., & Kennedy, T. E. (2002). The netrin-1 receptor DCC promotes filopodia formation and cell spreading by activating Cdc42 and Rac1. *Mol Cell Neurosci, 19*(1), 1-17. doi:10.1006/mcne.2001.1075

Shekarabi, M., Moore, S. W., Tritsch, N. X., Morris, S. J., Bouchard, J. F., & Kennedy, T. E. (2005). Deleted in colorectal cancer binding netrin-1 mediates cell substrate adhesion and recruits Cdc42, Rac1, Pak1, and N-WASP into an intracellular signaling complex that promotes growth cone expansion. *J Neurosci, 25*(12), 3132-3141. doi:10.1523/jneurosci.1920-04.2005

Shimoyama, Y., Tsujimoto, G., Kitajima, M., & Natori, M. (2000). Identification of three human type-II classic cadherins and frequent heterophilic interactions between different subclasses of type-II classic cadherins. *Biochem J, 349*(Pt 1), 159-167. doi:10.1042/0264-6021:3490159

Shipp, E. L., & Hsieh-Wilson, L. C. (2007). Profiling the sulfation specificities of glycosaminoglycan interactions with growth factors and chemotactic proteins using microarrays. *Chem Biol, 14*(2), 195-208. doi:10.1016/j.chembiol.2006.12.009

Silbert, J. E., & Sugumaran, G. (2002). Biosynthesis of chondroitin/dermatan sulfate. *IUBMB Life, 54*(4), 177-186. doi:10.1080/15216540214923

Silos-Santiago, I., & Snider, W. D. (1992). Development of commissural neurons in the embryonic rat spinal cord. *J Comp Neurol, 325*(4), 514-526. doi:10.1002/cne.903250405

Simpson, J. H., Bland, K. S., Fetter, R. D., & Goodman, C. S. (2000). Short-range and long-range guidance by Slit and its Robo receptors: a combinatorial code of Robo receptors controls lateral position. *Cell, 103*(7), 1019-1032. doi:10.1016/s0092-8674(00)00206-3

Sloan, T. F., Qasaimeh, M. A., Juncker, D., Yam, P. T., & Charron, F. (2015). Integration of shallow gradients of Shh and Netrin-1 guides commissural axons. *PLoS Biol, 13*(3), e1002119. doi:10.1371/journal.pbio.1002119

Small, D. H., Nurcombe, V., Reed, G., Clarris, H., Moir, R., Beyreuther, K., & Masters, C. L. (1994). A heparin-binding domain in the amyloid protein precursor of Alzheimer's disease is involved in the regulation of neurite outgrowth. *The Journal of Neuroscience, 14*(4), 2117. doi:10.1523/JNEUROSCI.14-04-02117.1994

Sorg, B. A., Berretta, S., Blacktop, J. M., Fawcett, J. W., Kitagawa, H., Kwok, J. C. F., & Miquel, M. (2016). Casting a Wide Net: Role of Perineuronal Nets in Neural Plasticity. *The Journal of Neuroscience, 36*(45), 11459. doi:10.1523/JNEUROSCI.2351-16.2016

Spivak-Kroizman, T., Lemmon, M. A., Dikic, I., Ladbury, J. E., Pinchasi, D., Huang, J., . . . Lax, I. (1994). Heparin-induced oligomerization of FGF molecules is responsible for FGF receptor dimerization, activation, and cell proliferation. *Cell, 79*(6), 1015-1024. doi:https://doi.org/10.1016/0092-8674(94)90032-9

Spreafico, R., De Biasi, S., & Vitellaro-Zuccarello, L. (1999). The Perineuronal Net: A Weapon for a Challenge. *Journal of the History of the Neurosciences, 8*(2), 179-185. doi:10.1076/jhin.8.2.179.1834

Spring, J., Paine-Saunders, S. E., Hynes, R. O., & Bernfield, M. (1994). Drosophila syndecan: conservation of a cell-surface heparan sulfate proteoglycan. *Proc Natl Acad Sci U S A, 91*(8), 3334-3338.

Stamos, J. L., & Weis, W. I. (2013). The beta-catenin destruction complex. *Cold Spring Harb Perspect Biol, 5*(1), a007898. doi:10.1101/cshperspect.a007898

Steigemann, P., Molitor, A., Fellert, S., Jäckle, H., & Vorbrüggen, G. (2004). Heparan Sulfate Proteoglycan Syndecan Promotes Axonal and Myotube Guidance by Slit/Robo Signaling. *Current Biology, 14*(3), 225-230. doi:https://doi.org/10.1016/j.cub.2004.01.006

Stein, E., & Tessier-Lavigne, M. (2001). Hierarchical organization of guidance receptors: silencing of netrin attraction by slit through a Robo/DCC receptor complex. *Science, 291*(5510), 1928-1938. doi:10.1126/science.1058445

Stein, E., Zou, Y., Poo, M., & Tessier-Lavigne, M. (2001). Binding of DCC by netrin-1 to mediate axon guidance independent of adenosine A2B receptor activation. *Science, 291*(5510), 1976-1982. doi:10.1126/science.1059391

Sudhof, T. C. (2018). Towards an Understanding of Synapse Formation. *Neuron, 100*(2), 276-293. doi:10.1016/j.neuron.2018.09.040

Sugahara, K., Mikami, T., Uyama, T., Mizuguchi, S., Nomura, K., & Kitagawa, H. (2003). Recent advances in the structural biology of chondroitin sulfate and dermatan sulfate. *Curr Opin Struct Biol, 13*(5), 612-620.

Suzuki, S. C., Inoue, T., Kimura, Y., Tanaka, T., & Takeichi, M. (1997). Neuronal circuits are subdivided by differential expression of type-II classic cadherins in postnatal mouse brains. *Mol Cell Neurosci, 9*(5-6), 433-447. doi:10.1006/mcne.1997.0626

Suzuki, S. T. (1996). Structural and functional diversity of cadherin superfamily: are new members of cadherin superfamily involved in signal transduction pathway? *J Cell Biochem, 61*(4), 531-542. doi:10.1002/(sici)1097-4644(19960616)61:4<531::aid-jcb6>3.0.co;2-p

Svensson, G., Awad, W., Hakansson, M., Mani, K., & Logan, D. T. (2012). Crystal structure of N-glycosylated human glypican-1 core protein: structure of two loops evolutionarily conserved in vertebrate glypican-1. *J Biol Chem, 287*(17), 14040-14051. doi:10.1074/jbc.M111.322487

Takeichi, M. (1991). Cadherin cell adhesion receptors as a morphogenetic regulator. *Science, 251*(5000), 1451-1455. doi:10.1126/science.2006419

Takeichi, M., & Abe, K. (2005). Synaptic contact dynamics controlled by cadherin and catenins. *Trends Cell Biol, 15*(4), 216-221. doi:10.1016/j.tcb.2005.02.002

Tanaka, H., Shan, W., Phillips, G. R., Arndt, K., Bozdagi, O., Shapiro, L., . . . Colman, D. R. (2000). Molecular modification of N-cadherin in response to synaptic activity. *Neuron, 25*(1), 93-107. doi:10.1016/s0896-6273(00)80874-0

Tang, L., Hung, C. P., & Schuman, E. M. (1998). A role for the cadherin family of cell adhesion molecules in hippocampal long-term potentiation. *Neuron, 20*(6), 1165-1175. doi:10.1016/s0896-6273(00)80497-3

Tanihara, H., Sano, K., Heimark, R. L., St John, T., & Suzuki, S. (1994). Cloning of five human cadherins clarifies characteristic features of cadherin extracellular domain and provides further evidence for two structurally different types of cadherin. *Cell Adhes Commun, 2*(1), 15-26. doi:10.3109/15419069409014199

Tessier-Lavigne, M., & Goodman, C. S. (1996). The molecular biology of axon guidance. *Science, 274*(5290), 1123-1133. doi:10.1126/science.274.5290.1123

Tessier-Lavigne, M., Placzek, M., Lumsden, A. G., Dodd, J., & Jessell, T. M. (1988). Chemotropic guidance of developing axons in the mammalian central nervous system. *Nature, 336*(6201), 775-778. doi:10.1038/336775a0

Tsien, R. Y. (2013). Very long-term memories may be stored in the pattern of holes in the perineuronal net. *Proceedings of the National Academy of Sciences, 110*(30), 12456. doi:10.1073/pnas.1310158110

Turnbull, J., Powell, A., & Guimond, S. (2001). Heparan sulfate: decoding a dynamic multifunctional cell regulator. *Trends in Cell Biology, 11*(2), 75-82. doi:https://doi.org/10.1016/S0962-8924(00)01897-3

Valenta, T., Hausmann, G., & Basler, K. (2012). The many faces and functions of beta-catenin. *Embo j, 31*(12), 2714-2736. doi:10.1038/emboj.2012.150

van 't Spijker, H. M., & Kwok, J. C. F. (2017). A Sweet Talk: The Molecular Systems of Perineuronal Nets in Controlling Neuronal Communication. *Front Integr Neurosci, 11*, 33. doi:10.3389/fnint.2017.00033

Varadarajan, S. G., Kong, J. H., Phan, K. D., Kao, T. J., Panaitof, S. C., Cardin, J., . . . Butler, S. J. (2017). Netrin1 Produced by Neural Progenitors, Not Floor Plate Cells, Is Required for Axon Guidance in the Spinal Cord. *Neuron, 94*(4), 790-799.e793. doi:10.1016/j.neuron.2017.03.007

Verheyen, E. M., & Gottardi, C. J. (2010). Regulation of Wnt/beta-catenin signaling by protein kinases. *Dev Dyn, 239*(1), 34-44. doi:10.1002/dvdy.22019

Vielmetter, J., Chen, X.-N., Miskevich, F., Lane, R. P., Yamakawa, K., Korenberg, J. R., & Dreyer, W. J. (1997). Molecular Characterization of Human Neogenin, a DCC-Related Protein, and the Mapping of Its Gene (NEO1) to Chromosomal Position 15q22.3–q23. *Genomics, 41*(3), 414-421. doi:https://doi.org/10.1006/geno.1997.4688

Vitellaro-Zuccarello, L., De Biasi, S., & Spreafico, R. (1998). One hundred years of Golgi's "perineuronal net": history of a denied structure. *Ital J Neurol Sci, 19*(4), 249-253.

Vo, T., Carulli, D., Ehlert, E. M., Kwok, J. C., Dick, G., Mecollari, V., . . . Verhaagen, J. (2013). The chemorepulsive axon guidance protein semaphorin3A is a constituent of perineuronal nets in the adult rodent brain. *Mol Cell Neurosci, 56*, 186-200. doi:10.1016/j.mcn.2013.04.009

Walz, A., Anderson, R. B., Irie, A., Chien, C. B., & Holt, C. E. (2002). Chondroitin sulfate disrupts axon pathfinding in the optic tract and alters growth cone dynamics. *J Neurobiol, 53*(3), 330-342. doi:10.1002/neu.10113

Wang, D., Ichiyama, R. M., Zhao, R., Andrews, M. R., & Fawcett, J. W. (2011). Chondroitinase combined with rehabilitation promotes recovery of forelimb function in rats with chronic spinal cord injury. *J Neurosci, 31*(25), 9332-9344. doi:10.1523/jneurosci.0983-11.2011

Wang, H., Katagiri, Y., McCann, T. E., Unsworth, E., Goldsmith, P., Yu, Z.-X., . . . Geller, H. M. (2008). Chondroitin-4-sulfation negatively regulates axonal guidance and growth. *Journal of Cell Science, 121*(18), 3083. doi:10.1242/jcs.032649

Wang, J. F., She, L., Su, B. H., Ding, L. C., Zheng, F. F., Zheng, D. L., & Lu, Y. G. (2011). CDH12 promotes the invasion of salivary adenoid cystic carcinoma. *Oncol Rep, 26*(1), 101-108. doi:10.3892/or.2011.1286

Wang, Q., Chiu, S. L., Koropouli, E., Hong, I., Mitchell, S., Easwaran, T. P., . . . Kolodkin, A. L. (2017). Neuropilin-2/PlexinA3 Receptors Associate with GluA1 and Mediate Sema3F-Dependent Homeostatic Scaling in Cortical Neurons. *Neuron, 96*(5), 1084-1098.e1087. doi:10.1016/j.neuron.2017.10.029

Wang, S.-H. J., Celic, I., Choi, S.-Y., Riccomagno, M., Wang, Q., Sun, L. O., . . . Kolodkin, A. L. (2014). Dlg5 Regulates Dendritic Spine Formation and Synaptogenesis by Controlling Subcellular N-Cadherin Localization. *The Journal of Neuroscience, 34*(38), 12745. doi:10.1523/JNEUROSCI.1280-14.2014

Wang, S., Ai, X., Freeman, S. D., Pownall, M. E., Lu, Q., Kessler, D. S., & Emerson, C. P. (2004). QSulf1, a heparan sulfate 6-O-endosulfatase, inhibits fibroblast growth factor signaling in mesoderm induction and angiogenesis. *Proc Natl Acad Sci U S A, 101*(14), 4833. doi:10.1073/pnas.0401028101

Wei, Z., Lyon, M., & Gallagher, J. T. (2005). Distinct Substrate Specificities of Bacterial Heparinases against N-Unsubstituted Glucosamine Residues in Heparan Sulfate. *280*(16), 15742-15748. doi:10.1074/jbc.M501102200

Weis, W. I. (1995). Cadherin structure: a revealing zipper. *Structure, 3*(5), 425-427. doi:10.1016/s0969-2126(01)00174-5

Weiss, T., Ricard-Blum, S., Moschcovich, L., Wineman, E., Mesilaty, S., & Kessler, E. (2010). Binding of procollagen C-proteinase enhancer-1 (PCPE-1) to heparin/heparan sulfate: properties and role

in PCPE-1 interaction with cells. *The Journal of biological chemistry, 285*(44), 33867-33874. doi:10.1074/jbc.M110.141366

Wentworth, L. E. (1984). The development of the cervical spinal cord of the mouse embryo. II. A Golgi analysis of sensory, commissural, and association cell differentiation. *Journal of Comparative Neurology, 222*(1), 96-115. doi:10.1002/cne.902220109

Williams, M. E., Wilke, S. A., Daggett, A., Davis, E., Otto, S., Ravi, D., . . . Ghosh, A. (2011). Cadherin-9 regulates synapse-specific differentiation in the developing hippocampus. *Neuron, 71*(4), 640-655. doi:10.1016/j.neuron.2011.06.019

Williamson, T. G., Mok, S. S., Henry, A., Cappai, R., Lander, A. D., Nurcombe, V., . . . Small, D. H. (1996). Secreted Glypican Binds to the Amyloid Precursor Protein of Alzheimer's Disease (APP) and Inhibits APP-induced Neurite Outgrowth. *271*(49), 31215-31221. doi:10.1074/jbc.271.49.31215

Witt, R. M., Hecht, M.-L., Pazyra-Murphy, M. F., Cohen, S. M., Noti, C., van Kuppevelt, T. H., . . . Segal, R. A. (2013). Heparan Sulfate Proteoglycans Containing a Glypican 5 Core and 2-O-Sulfo-iduronic Acid Function as Sonic Hedgehog Co-receptors to Promote Proliferation. *288*(36), 26275-26288. doi:10.1074/jbc.M112.438937

Wu, Z., Makihara, S., Yam, P. T., Teo, S., Renier, N., Balekoglu, N., . . . Tessier-Lavigne, M. (2019). Long-Range Guidance of Spinal Commissural Axons by Netrin1 and Sonic Hedgehog from Midline Floor Plate Cells. *Neuron, 101*(4), 635-647.e634. doi:10.1016/j.neuron.2018.12.025

Xu, K., Wu, Z., Renier, N., Antipenko, A., Tzvetkova-Robev, D., Xu, Y., . . . Nikolov, D. B. (2014). Neural migration. Structures of netrin-1 bound to two receptors provide insight into its axon guidance mechanism. *Science, 344*(6189), 1275-1279. doi:10.1126/science.1255149

Xu, S., Liu, Y., Li, X., Liu, Y., Meijers, R., Zhang, Y., & Wang, J. H. (2018). The binding of DCC-P3 motif and FAK-FAT domain mediates the initial step of netrin-1/DCC signaling for axon attraction. *Cell Discov, 4*, 8. doi:10.1038/s41421-017-0008-8

Yagi, T., & Takeichi, M. (2000). Cadherin superfamily genes: functions, genomic organization, and neurologic diversity. *Genes & development, 14*(10), 1169-1180.

Yamada, S., Pokutta, S., Drees, F., Weis, W. I., & Nelson, W. J. (2005). Deconstructing the cadherin-catenin-actin complex. *Cell, 123*(5), 889-901. doi:10.1016/j.cell.2005.09.020

Yamagishi, S., Yamada, K., Sawada, M., Nakano, S., Mori, N., Sawamoto, K., & Sato, K. (2015). Netrin-5 is highly expressed in neurogenic regions of the adult brain. *Frontiers in cellular neuroscience, 9*, 146-146. doi:10.3389/fncel.2015.00146

Yamaguchi, Y. (2002). Glycobiology of the synapse: the role of glycans in the formation, maturation, and modulation of synapses. *Biochim Biophys Acta, 1573*(3), 369-376.

Yamauchi, K., Varadarajan, S. G., Li, J. E., & Butler, S. J. (2013). Type Ib BMP receptors mediate the rate of commissural axon extension through inhibition of cofilin activity. *Development, 140*(2), 333-342. doi:10.1242/dev.089524

Yamauchi, K., Yamazaki, M., Abe, M., Sakimura, K., Lickert, H., Kawasaki, T., . . . Hirata, T. (2017). Netrin-1 Derived from the Ventricular Zone, but not the Floor Plate, Directs Hindbrain Commissural Axons to the Ventral Midline. *Sci Rep, 7*(1), 11992. doi:10.1038/s41598-017-12269-8

Yang, C., Li, X., Wang, C., Fu, S., Li, H., Guo, Z., . . . Lin, J. (2016). N-cadherin regulates beta-catenin signal and its misexpression perturbs commissural axon projection in the developing chicken spinal cord. *J Mol Histol, 47*(6), 541-554. doi:10.1007/s10735-016-9698-8

Yayon, A., Klagsbrun, M., Esko, J. D., Leder, P., & Ornitz, D. M. (1991). Cell surface, heparin-like molecules are required for binding of basic fibroblast growth factor to its high affinity receptor. *Cell, 64*(4), 841-848. doi:https://doi.org/10.1016/0092-8674(91)90512-W

Zhang, Y., Sivasankar, S., Nelson, W. J., & Chu, S. (2009). Resolving cadherin interactions and binding cooperativity at the single-molecule level. *Proc Natl Acad Sci U S A, 106*(1), 109-114. doi:10.1073/pnas.0811350106

Zhao, J., Li, P., Feng, H., Wang, P., Zong, Y., Ma, J., . . . Lu, A. (2013). Cadherin-12 contributes to tumorigenicity in colorectal cancer by promoting migration, invasion, adhersion and angiogenesis. *J Transl Med, 11*, 288. doi:10.1186/1479-5876-11-288

Zhu, G., Wang, Y., Huang, B., Liang, J., Ding, Y., Xu, A., & Wu, W. (2012). A Rac1/PAK1 cascade controls beta-catenin activation in colon cancer cells. *Oncogene, 31*(8), 1001-1012. doi:10.1038/onc.2011.294